FLUOROCARBENE, FLUOROALKYL, AND FLUORIDE COMPLEXES OF FIRST-ROW TRANSITION METALS

Graham Mark Lee

Thesis submitted to the

Faculty of Graduate and Postdoctoral Studies

University of Ottawa

In partial fulfillment of the requirements for the degree of

Doctor of Philosophy

Ottawa-Carleton Chemistry Institute

Faculty of Science

University of Ottawa

Abstract

Fluorinated organic compounds play important roles in our society, as these products range from life-saving pharmaceuticals and agrochemicals, to fluoropolymers with extremely high thermal and chemical stability. Although elemental fluorine (F_2) is the most reactive element, some fluoro-organic compounds are chemically inert. As such, controlled reactivity of fluorine or highly-fluorinated organic fragments is a considerable, yet important challenge for synthetic chemists.

Fluoro-organometallic chemistry has been studied for decades, as researchers attempt to maximize the potential of metal mediated/catalyzed processes for the synthesis of fluorinated organic molecules. Within this framework, metal fluorocarbene complexes are particularly interesting because of their highly tunable reactivity, and are proposed for use in important metathesis/polymerization reactions of perfluorinated alkenes. While considerable work is still needed to make these proposed reactions a reality, this thesis outlines contributions from our research group. We showed that cobalt fluorocarbene complexes $CpCo(=CFR^F)(PPh_2Me)$ (R^F = F, CF_3) undergo [2+2] cycloaddition reactions with tetrafluoroethylene (TFE) and phenylacetylene to form perfluorometallacyclobutane and partially fluorinated metallacyclobutene products, respectively. For both reactions, computational studies reveal a stepwise ring-closing mechanism, which proceeds through a singlet 1,4-diradical intermediate.

Next, the formation of $CpCo(=CF_2)(L)$ complexes is achieved via the direct addition of difluorocarbene, generated in situ, to a cobalt(I) precursor. Subsequent addition of CF_2 to cobalt fluorocarbene complexes results in [2+1] cycloaddition and formation of perfluorinated alkene complexes. The [2+1] addition is highly favored as the cobalt fluorocarbenes readily react with

electrophilic CF_2. A series of experiments provide evidence for the stepwise nature of fluoroalkene complex formation.

From Co(I) fluorocarbene complexes, the focus shifts to preparing metal fluorocarbenes with electrophilic-type reactivity. The synthesis of bis(perfluoroalkyl) complexes serve as precursors for preparation of perfluoroalkyl cobalt(III) fluorocarbenes, which undergo migratory insertion reactions of the fluorocarbene into the perfluoroalkyl ligand. Using a similar synthetic approach, nickel(II) and palladium(II) difluorocarbene complexes are prepared from their corresponding trifluoromethyl precursors.

The synthesis, characterization and reactivity of cobalt(III) fluoride complexes is also described, including the catalytic fluorination of acyl chlorides, demonstrating the first example of a cobalt(III) catalyzed fluorination reaction. The effects of the various ancillary ligands on these cobalt catalysts are investigated using high-throughput experimentation technology, and the scope of the reaction is expanded to include the synthesis of a variety of acyl fluoride compounds.

Finally, the results and learnings from this work will be summarized and highlighted. The future directions and novel research which could result from the continuation of these projects is discussed, with an emphasis placed on the areas believed to have the highest potential impact.

Acknowledgements

My Ph.D. work was made possible by my supervisor, Professor Tom Baker. Thank you for being an excellent mentor over the years, and for making grad school such a fun experience. You always made time for me, and gave me so many incredible opportunities which have changed my life for the better. I can't thank you enough, it's been a privilege to be a part of your research group, and I had a blast! To Dan Harrison, thank you for being a great friend and an incredible chemist. The work in this thesis was inspired to a great extent by conversations with you, and I appreciate your guidance and mentorship a tremendous amount.

To all the current and former members of the Baker research group, Christian, Kaitie, Matt, Alex, Nick, Uttam, Mehdi, it was a pleasure to work with all of you, and your friendship means so much. Thank you to the incredible staff at the University of Ottawa, who helped make this work possible, Ilia Korobkov, Serge Gorelsky, Glenn Facey, Eric Ye, and Roxanne Clément.

To my undergraduate supervisor, Professor Steve Westcott. Thanks for getting me this far, and for all the support and encouragement over the years. To my international supervisors, Professor Elena Fernandez and Dr. Don Bierer, thank you for the wonderful opportunity to work in your labs.

Thanks to all of my family and friends, I love you all so much. Mom and Dad, thanks for always supporting me, I couldn't have done it without you. Holly and Cole, thank you both for believing in me and supporting me. To Dave, Dan, Hamza and Nick, thanks for all the fun times.

To my beautiful wife Arianna, your love and support means everything to me.

Table of Contents

List of Figures

List of Schemes

List of Tables

Abbreviations

BDE	Bond dissociation energy
BTB	1,3-Bis(trifluoromethyl)benzene
CM	Cross metathesis
Cp	Cyclopentadienyl
Cp*	Pentamethylcyclopentadienyl
Cy	Cyclohexyl
DCE	1,2-Dichloroethane
DCM	Dichloromethane
DEE	Diethylether
DFT	Density functional theory
DMF	Dimethylformamide
DMSO	Dimethyl sulfoxide
EA	Elemental analysis
ESI-MS	Electrospray ionization mass spectrometry
equiv	Equivalents
FT-IR	Fourier transform infrared spectroscopy
FW	Formula weight
HTE	High-throughput experimentation
HOESY	Heteronuclear Overhauser effect spectroscopy
HOMO	Highest occupied molecular orbital
Hz	Hertz
IR	Infrared

MO	Molecular orbital
Mp	Melting point
MPA	Mulliken population analysis
MS	Mass spectroscopy
NHC	*N*-heterocyclic carbene
NMR	Nuclear magnetic resonance
NOESY	Nuclear Overhauser effect spectroscopy
ORTEP	Oak Ridge thermal ellipsoid plot
PET	Positron emission tomography
ppm	Parts per million
PTFE	Polytetrafluoroethylene
PXRD	Powder X-ray diffraction
py	Pyridine
R^F	Fluorine or perfluoroalkyl
RT	Room temperature
TFE	Tetrafluoroethylene
THF	Tetrahydrofuran
TMS	Trimethylsilyl
ToF	Time of flight
TON	Turnover number
UV	Ultraviolet
XRD	X-ray diffraction

.

Chapter 1

Introduction

1.1 Published Contributions

Sections of this chapter have been published:

1. Cobalt Fluorocarbene Complexes

Harrison, D. J.; Gorelsky, S. I.; Lee, G. M.; Korobkov, I.; Baker, R. T. *Organometallics*, **2013**, *32*, 12-15.

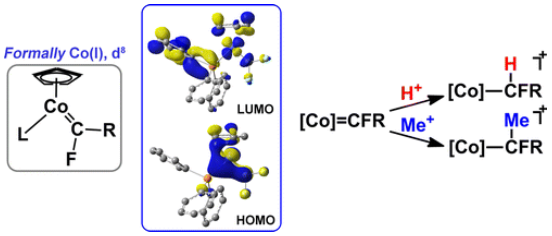

2. Cobalt Fluorocarbenes: Cycloaddition Reactions with Tetrafluoroethylene and Reactivity of the Perfluorometallacyclic Products

Harrison, D. J.; Lee, G. M.; Leclerc, M. C.; Korobkov, I.; Baker, R. T. *J. Am. Chem. Soc.*, **2013**, *135*, 18296-18299.

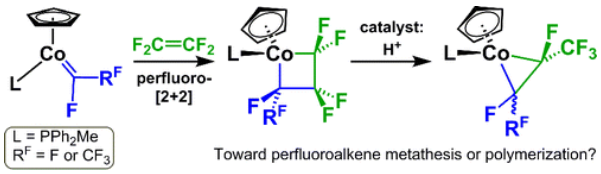

1.2 Fluorine in Organometallic Chemistry: Context for Research

1.2.1 Impetus for Studying Fluoro-Organometallic Chemistry

Carbon-fluorine (C-F) and carbon-fluoroalkyl (C-R^F) bond forming reactions which are either mediated or catalyzed by metal complexes are areas of research which have received increasing attention in recent years.[1–4] This is because organic molecules containing fluorine play an important role in our society. The

C-F bond confers unique and sometimes extreme properties to molecules which can be used to great advantage for pharmaceutical,[5] agrochemical,[6] and materials[7] applications seen in our daily life. Conversely, molecules containing C-F bonds can cause problems related to ozone degradation and environmental persistence,[8] and removal of fluorine from the environment via C-F activation by metal complexes is also a highly active area of research.[9] Fluorine is the most electronegative element (4.0 on the Pauling scale) and has three fairly non-polarizable lone pairs of electrons. The C-F bond, which is the strongest single bond to carbon (115 kcal/mol BDE for CH_3-F vs. 104.9 kcal/mol BDE for CH_3-H)[10], is highly polarized with δ^- at fluorine and δ^+ at carbon (the opposite of C-H). The extraordinary bond strength is attributed in part to the excellent energy match of the 2*s* and 2*p* orbitals of fluorine with those of carbon. While these properties can be highly desirable within target molecules, they also cause challenges for synthetic chemists trying to develop metal-based methods for the selective introduction of C-F containing fragments. This is partly because fluoro-organometallic complexes are often much more stable and less reactive than analogous hydrocarbon compounds. The firmly established organometallic reactions that relate to hydrocarbon transformations, including metal-catalyzed olefin polymerization/metathesis and cross-coupling reactions, are decidedly less developed for analogous fluorocarbon transformations. As such, improved approaches to synthesis and detailed understanding of the reactivity of fluoro-organometallic complexes are necessary for the growth of this field of research.

1.2.2 Overview of Fluoro-Organometallic Complexes

The purview of fluoro-organometallic chemistry in this thesis consists of the synthesis, characterization, and reactivity of metal complexes bearing fluorine or fluorocarbons as ligands. Examples of these complexes include metal fluorides, metal fluoroalkyls, metal fluorocarbenes, fluorinated metallacycles, and metal fluorovinyls. These fluoro-organometallic complexes are often related synthetically, as interconversion between the groups is common.[11–13] The work in this thesis is particularly focused on metal fluoroalkyl, metal fluorocarbene, and metal fluoride complexes (Figure 1.1).

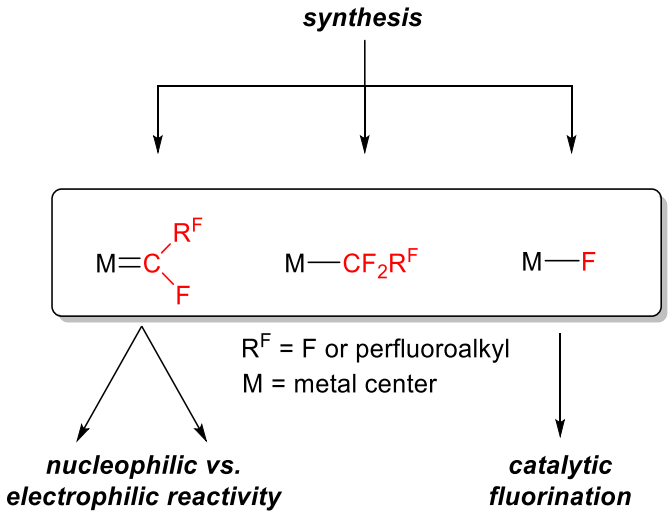

Figure 1.1. Scope of fluoro-organometallic chemistry explored in this work.

When it comes to studying fluoro-organometallic complexes, it is important to note a very useful quality of fluorine, which is its nuclear spin quantum number, I = ½, which is 100% naturally abundant and highly sensitive, making ^{19}F NMR spectroscopy an exceptionally convenient and powerful tool for characterizing fluoro-organometallic complexes, and fluorinated compounds in general. Depending on their chemical environment, ^{19}F resonances of fluorinated compounds cover a range of over 1100 ppm ($CFCl_3$ is typically used as a reference standard) (Figure 1.2).

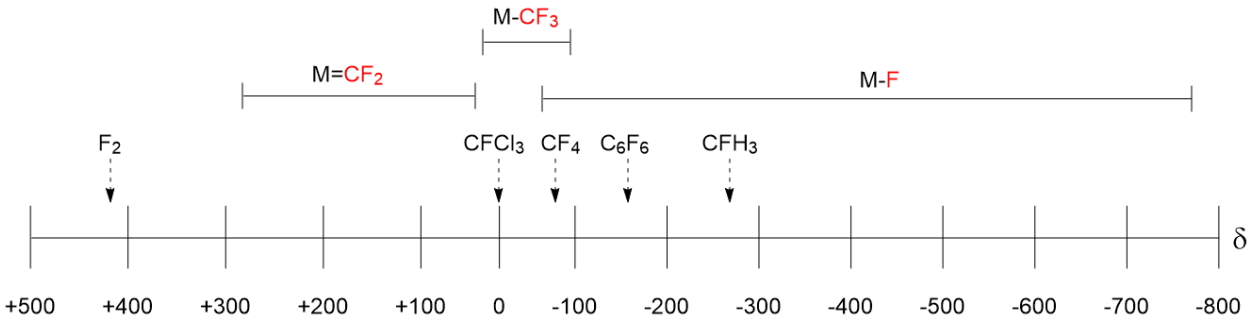

Figure 1.2.^{19}F NMR chemical shifts for different fluorochemicals and fluoro-organometallic complexes.

1.3 Metal Fluoroalkyl Complexes

Metal complexes with σ-bonded perfluoroalkyl ligands (i.e. CF_3, CF_2CF_3, etc.) are traditionally thought of as being much more stable and less reactive than their hydrocarbon counterparts, due in part to the strong inductive electron withdrawing effects of perfluoroalkyl groups compared to hydrocarbons. A clear example is that while $CH_3Mn(CO)_5$ undergoes insertion with CO at elevated pressures to form $CH_3COMn(CO)_5$, the trifluoromethyl analog $CF_3Mn(CO)_5$ does not react even when treated with 333 atm of CO at 200 °C.[14] This is also supported by the bond dissociation energy (BDE) obtained from microcalorimetry experiments and DFT calculations, for example, where $D[CF_3\text{-}Mn(CO)_5] = 172 \pm 7$ kJ/mol, and $D[CH_3\text{-}Mn(CO)_5] = 153 \pm 5$ kJ/mol.[15,16] Similarly, Vicic and coworkers showed that bis(perfluoroalkyl) complexes of nickel bipyridine exhibit high thermal stability relative to the dimethyl analog, which loses ethane upon gentle heating.[17] Computational studies reveal that there is a higher $M \leftarrow CX_3$ interaction for X = F than for X =H, and CF_3 can sometimes interact with a metal via C-F σ* orbitals, stabilizing the metal-based d orbitals.[18] Interestingly, while metal-carbon bonds for $M\text{-}CF_3$ are shorter than those of $M\text{-}CH_3$ in middle- and late-row metals, structural and computational studies show the opposite is true for group 4 metals.[19]

1.3.1 Synthesis of Metal Fluoroalkyls

Methods for making metal fluoroalkyls are diverse, with numerous approaches appearing in the literature over several decades. A few examples will be discussed here to illustrate the general approaches to metal fluoroalkyl synthesis, especially those relevant to future chapters.

1.3.1.1 Decarbonylation of Perfluoroacyl Ligands

Among the earliest examples of metal fluoroalkyl complexes are $(R^F)Mn(CO)_5$ and $(R^F)Co(CO)_4$, prepared via decarbonylation of $(R^F)COMn(CO)_5$ and $(R^F)COCo(CO)_4$ (Scheme 1.1).[20] This 1,1-deinsertion process requires no net change in the oxidation state of the metal center.

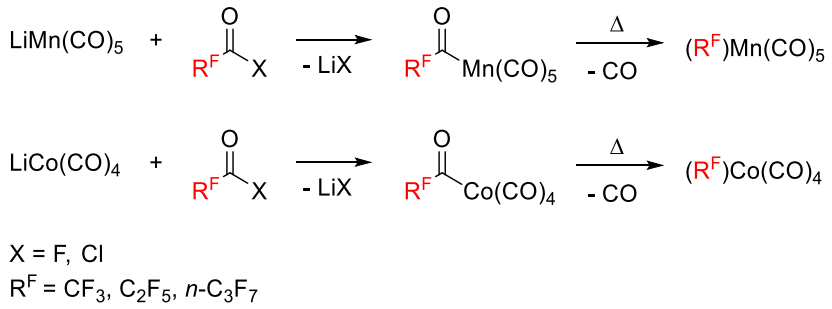

Scheme 1.1. Synthesis of $(R^F)Mn(CO)_5$ and $(R^F)Co(CO)_4$.

The decarbonylation pathway to metal fluoroalkyl formation was reported recently by Sanford and coworkers for the synthesis of nickel and palladium fluoroalkyl complexes, via oxidative addition of trifluoroacetic anhydride (TFAA) to the metal center, followed by facile decarbonylation of the resulting fluoroacyl ligand.[21] Finally, Karel and coworkers reported the synthesis of a series of iron perfluorometallacycles via decarbonylation of cyclic iron diacyl complexes.[22]

1.3.1.2 Oxidative Addition of R^F-I

One of the most direct methods for metal fluoroalkyl synthesis consists of oxidative addition of perfluoroalkyl iodides to a low valent metal center, via cleavage of the R^F-I bond. The oxidation state of the metal in the resulting perfluoroalkyl iodide complex is increased by two. In 1961, F. Gordon A. Stone studied the reactivity between perfluoroakyl iodides and iron pentacarbonyl, which resulted in the formation of perfluoroalkyl iron tetracarbonyl iodides.[23] In the same year, Stone and coworkers also reported on the reactivity of $CpCo(CO)_2$ (Cp = η^5-cyclopentadienyl) with perfluoroalkyl iodides, which gave $CpCo(CO)(I)(R^F)$ complexes (Scheme 1.2). Substitution of the carbonyl ligand by phosphines and phosphites was later reported by Baird and coworkers[24]

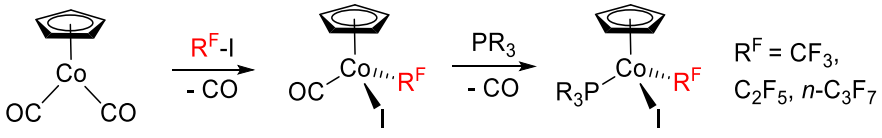

Scheme 1.2. Synthesis of cobalt(III) perfluoroalkyl iodide complexes.

This synthetic strategy has been shown to work particularly well with group 9 metals. Iridium(III) perfluoroalkyl iodide complexes were prepared first by Collman and coworkers,[25] while Efraty and coworkers and Hughes and coworkers each later reported Cp*Ir(L)(I)(R^F) (Cp* = η^5-pentamethylcyclopentadienyl) complexes.[26,27] Finally, Wilkinson and coworkers reported the synthesis of CpRh(CO)(I)(C_3F_7).[28] More recently, photo-initiated oxidative addition of ICF_3 to an aryl gold(I) complex, followed by silver-mediated aryl-CF_3 reductive elimination was described by Toste and coworkers[29]

1.3.1.3 From $Cd(CF_3)_2$ and $Hg(CF_3)_2$

Metal fluoroalkyl complexes can be prepared via metathesis of an M-X bond with bis-fluoroalkyl cadmium or mercury reagents, with no net change in oxidation state of the metal. The reagents typically used are $(CF_3)_2Cd$·glyme and $Hg(CF_3)_2$, with examples shown in Scheme 1.3. Morrison and coworkers reported the preparation of bis(trifluoromethyl) complex $CpCo(CO)(CF_3)_2$ from the reaction of $CpCo(CO)I_2$ with $(CF_3)_2Cd$·glyme.[30] The same group later used this method to prepare trifluoromethyl complexes of group 11 metals, such as $AuCF_3(PEt_3)$ and $AgCF_3(PMe_3)$, while $CuCF_3(PMe_3)$ could be observed in solution.[31] Finally, they reported the synthesis of $CpCr(NO)_2CF_3$ and $CpMo(NO)_2CF_3$ from their chloride precursors and $(CF_3)_2Cd$·glyme.[32] Brothers and coworkers reported that while $IrCl(CO)(PPh_3)_2$ did not react favorably with $Hg(CF_3)_2$, the hydride complex $IrH(CO)(PPh_3)_2$ reacted with $Hg(CF_3)_2$ to give the desired trifluoromethyl complex $Ir(CF_3)(CO)(PPh_3)_2$ in moderate yield.[33] While cadmium and mercury reagents have been employed successfully for the synthesis of metal fluoroalkyl complexes, handling of such toxic reagents is undesirable, and the development of safer alternatives has caused a decline in their use.

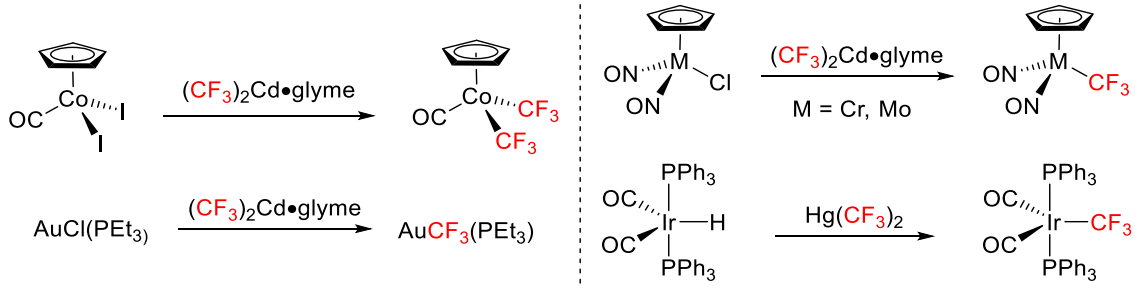

Scheme 1.3. Synthesis of metal fluoroalkyl complexes using cadmium and mercury reagents.

1.3.1.4 From Me_3SiCF_3

Trifluoromethyltrimethylsilane, Me_3SiCF_3, has been used extensively in nucleophilic trifluoromethylation reactions in organic chemistry.[34] Activation of Me_3SiCF_3, typically by catalytic or stoichiometric amounts of fluoride, results in the formation of pentacoordinated organosilicate species $[Me_3Si(CF_3)F]^-$ or $[Me_3Si(CF_3)_2]^-$, which then extrude trifluoromethanide anion $[CF_3]^-$.[35–37] The same process applies generally to R_3SiR^F, where R = Me or Et, and R^F = CF_2, C_2F_5, or *n*-C_3F_7, as one of the driving forces of this reaction is the formation of the strong Si-F bond in the byproduct R_3SiF. According to this, R_3SiR^F can be used to convert M-X to M-R^F (Scheme 1.4). In one of the earliest examples, Fuchikami reported the synthesis of Ar-R^F compounds mediated by CuI/KF and R_3SiR^F, where Cu-R^F species are believed to be key intermediates.[38] An important study by Grushin and coworkers reported that treatment of [(Xantphos)Pd(Ph)F] with Me_3SiCF_3 resulted in formation of [(Xantphos)Pd(Ph)CF_3], which when heated at 80 °C in C_6D_6 for 3 h underwent remarkably clean Ph-CF_3 reductive elimination.[39] Vicic and coworkers used Me_3SiCF_3 to prepare trifluoromethyl complexes of copper and nickel, and subsequently studied the magnitude of the electron-withdrawing effect of the CF_3 ligand, as well as their application in trifluoromethylation reactions.[40–42] Considering that Me_3SiCF_3 is commercially available, relatively inexpensive (~ $1/g), versatile, as well as a generally safe and easy to handle liquid, it has become the reagent of choice for the synthesis of metal trifluoromethyl complexes.

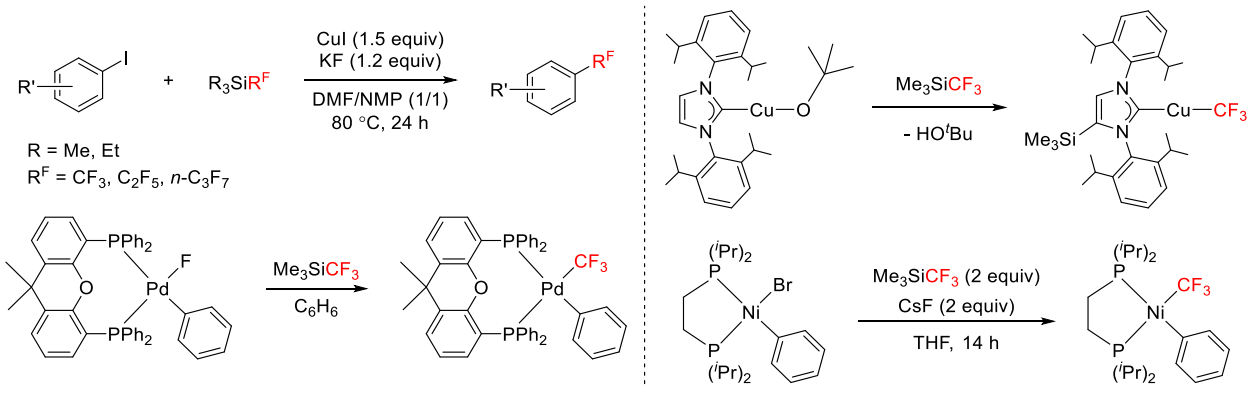

Scheme 1.4. Application of R_3SiR^F in metal fluoroalkyl synthesis.

1.3.2 Reactivity of Metal Fluoroalkyl Complexes

Despite the remarkable strength of M-R^F bonds, significant advances have recently been made with respect to catalytic reactivity.[43] For example, important metal-catalyzed trifluoromethylation reactions, utilizing both electrophilic and nucleophilic sources of CF_3, have surged in the past 10 years.[34,44,45] These reactions were developed in part by first systematically preparing M-CF_3 complexes, and determining which steric and electronic parameters favor key catalytic steps, such as reductive elimination of Ar-CF_3 groups.[39,46]

Another mode of reactivity of metal fluoroalkyl complexes involves activation of C-F bonds α to the transition metal, as these bonds have been shown to be weaker than normal C-F bonds. Spectroscopic evidence for this includes the C-F stretching bands in the IR spectra of $CpMo(CO)_3CF_3$ (1044, 1004, and 976 cm^{-1}) and $CpFe(CO)_2CF_3$ (1068, 1042, 1015, 985 cm^{-1}) being shifted to much lower frequencies when compared to the analogous trifluoroacetyl complexes $CpMo(CO)_3(COCF_3)$ (1175 cm^{-1}) and $CpFe(CO)_2(COCF_3)$ (1224 cm^{-1}).[15] The weakening of C-F bonds α to a transition metal is also revealed in X-ray crystal structures. For example, in $CpCo(n\text{-}C_3F_7)(PMe_3)[P(O)Ph(OMe)]$, the α-C-F bond distances (1.387(4) Å and 1.399(4) Å) are significantly longer than the β-C-F bond distances (1.342(4) Å and 1.356(4) Å) as well as the γ-C-F bond distances (1.292(5) Å, 1.310(5) Å, and 1.286(5) Å).[47] Carbon-fluorine bonds α to a transition metal can be activated using Lewis acids or alkali metals to furnish metal fluorocarbenes, and will be discussed in greater detail in section 1.4.

1.4 Metal Fluorocarbene Complexes

1.4.1 Overview of Metal Fluorocarbenes

Metal fluorocarbenes (M=CFR^F; R^F = F, perfluoroalkyl) are a distinct class of metal carbene which have received less attention than their hydrocarbon analogs and *N*-heterocyclic carbene complexes. The first metal fluorocarbenes were synthesized in 1978, and to date there are only approximately 30 metal fluorocarbene complexes reported, the structures of which are shown in Figure 1.3.

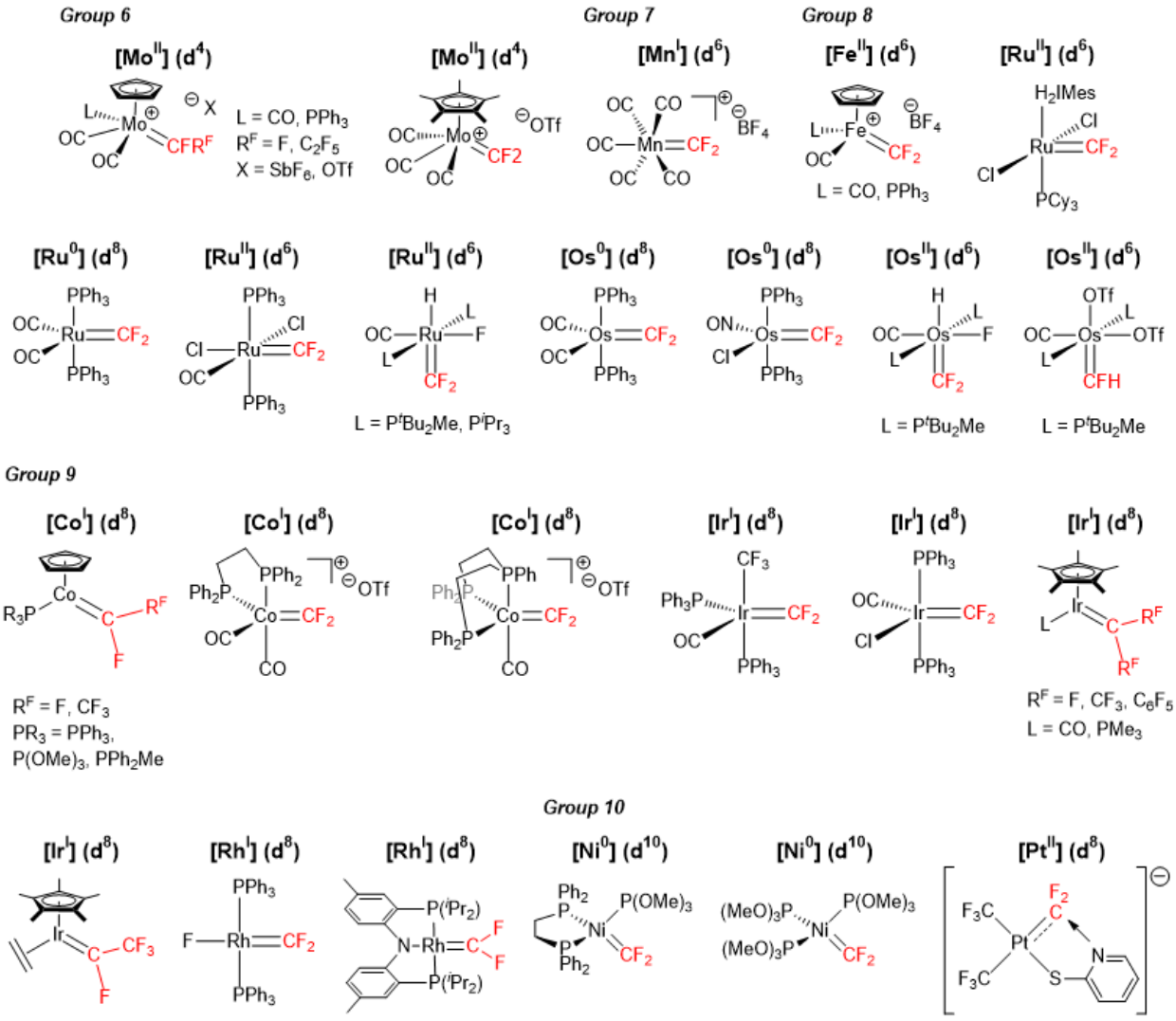

Figure 1.3. Structures of metal fluorocarbene complexes, with formal metal oxidation state and electronic configuration.

While a few examples of fluorocarbene complexes based on group 6 and 7 metals have been prepared, the majority of research has been focused on groups 8 and 9, with group 10 fluorocarbene complexes only recently being reported. Furthermore, the majority of metal fluorocarbene research has been focused on precious metals (Ru, Os, or Ir). Early reports of fluorocarbene complexes of first-row metals consisted of preparation of a manganese complex which was not isolated, as well as structural but very limited reactivity studies of iron difluorocarbenes.[48,49] Our group has contributed significantly to the research of first-row

metal fluorocarbenes, preparing the first examples of cobalt and nickel fluorocarbene complexes.[50–54] This section will feature detailed discussions of the bonding in metal fluorocarbenes, as well as their synthesis, characterization and reactivity.

1.4.2 Bonding in Metal Fluorocarbenes

Metal fluorocarbenes exhibit characteristics which transcend classical descriptions of "Fischer-type" and "Schrock-type" carbene complexes. According to these descriptions, the metal-ligand interactions of Fischer-type metal carbenes can be described as σ-donation from a singlet-carbene, with π-back-donation from the metal, whereas Schrock-type carbenes are better described as a covalent interaction between a triplet carbene and triplet metal (Figure 1.4).[55] Furthermore, Fischer-type carbenes typically react as electrophiles at the carbene carbon, and Schrock-type carbenes react as nucleophiles. This distinction has been shown to be an oversimplification, as there has been a spectrum of reactivity observed for metal carbenes. Variation of the metal and ancillary ligands of methylene complexes can alter the reactivity of the carbene carbon center from nucleophilic to electrophilic, and the same is true for metal fluorocarbene complexes.[56] In particular, the oxidation state of the metal can have a significant impact on the reactivity of metal fluorocarbenes (Section 1.4.4).

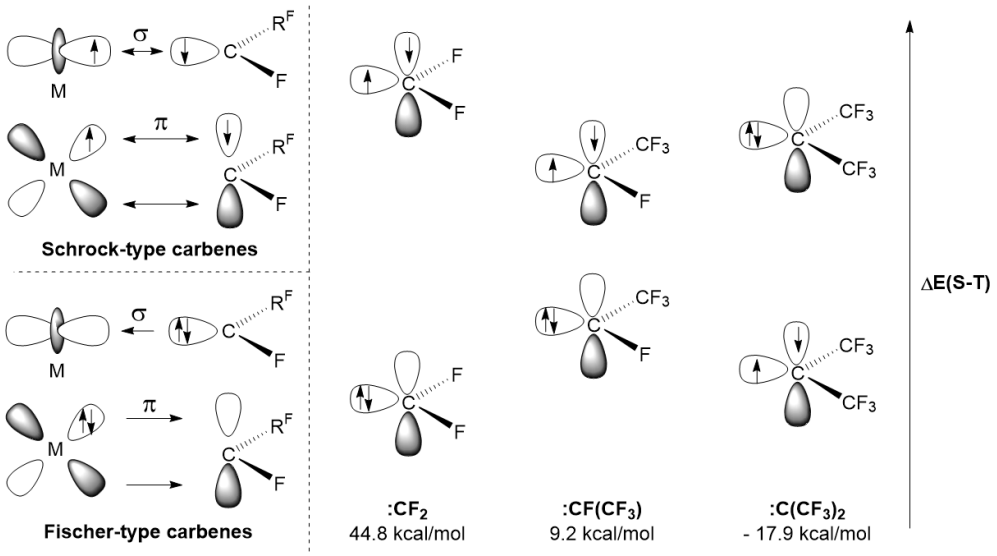

Figure 1.4. Schematic representations of the Dewar-Chatt-Duncanson donor-acceptor model of the dominant orbitals for Fischer-type and Schrock-type metal carbenes; singlet-triplet energy splitting for fluorinated carbenes.

In the case of metal fluorocarbenes, it is instructive to consider the electronic structure of various fluorocarbene ligands (Figure 1.4).[57] Difluorocarbene (CF_2) and fluoro(trifluoromethyl)carbene ($CF(CF_3)$) each have a singlet ground state, although CF_2 has a significantly larger singlet-triplet splitting ($\Delta E(S\text{-}T)$ = 44.8 kcal/mol) than for $CF(CF_3)$ ($\Delta E(S\text{-}T)$ = 9.2 kcal/mol). In contrast, bis(trifluoromethyl)carbene ($C(CF_3)_2$) has a triplet ground state, where $\Delta E(S\text{-}T)$ = -17.9 kcal/mol. This highlights the difference in π-donating ability of F and CF_3 substituents, with F being a significantly better π-donor and thus better at stabilizing the singlet ground state of CF_2 compared to $CF(CF_3)$. The singlet ground states for CF_2 and $CF(CF_3)$ suggest they will favor donor-acceptor bonding configurations with metals, while the triplet ground state of $C(CF_3)_2$ indicates a possible propensity for covalent metal bonding.

Modern DFT computational methods have provided deeper insight into metal fluorocarbene bonding. For example, first-row metal complexes M-CH_2, M-CHF, and M-CF_2 were studied using DFT, and the singlet ground state of CF_2 was shown to favor donor-acceptor bonding with metals.[58] A recent study from Ozerov and coworkers includes a comparison of the bonding of a (PNP)Rh fragment to CH_2 and CF_2 ligands.[13] In a report from our group, DFT computations were performed for $CpCo(=CF_2)(PPh_3)$ and $CpCo(=CF(CF_3))(PPh_3)$, at the PBE/TZVP level of theory.[50] The DFT results indicate donor–acceptor bonding between the metal and carbene fragments, as expected on the basis of the large singlet→triplet energy gaps for the CFR^F ligands (Figure 1.5). Three components in the cobalt–carbene bonding are identified from the fragment molecular orbital analysis: σ donation from the highest occupied fragment orbital (HOFO) of the carbene to the lowest unoccupied fragment orbital (LUFO) of $CpCo(PPh_3)$ (Figure 1.5A), π back-donation from the HOFO of $CpCo(PPh_3)$ to the LUFO of the carbene ligand (Figure 1.5B), and a second, weaker π interaction involving donation from HOFO-3 of $CpCo(PPh_3)$ to the CFR^F LUFO+1 (Figure 1.5C). The primary π component of the metal–carbene bonds, interaction B in

Figure 1.5, is stronger in CpCo(=CF(CF_3))(PPh_3), in comparison with CpCo(=CF_2)(PPh_3), as evidenced by the MPA-derived population of the carbene ligand LUFO (44% in CpCo(=CF(CF_3))(PPh_3) and 33% in CpCo(=CF_2)(PPh_3)). Replacing a carbene fluorine substituent with a CF_3 group results in stronger CpCo(PPh_3) HOFO→carbene LUFO interaction, consistent with the increased π-accepting abilities of the CF(CF_3) ligand relative to CF_2. This is manifested by the natural population analysis (NPA)-derived net charges of the carbene ligands (+0.109 au for [Co]=CF_2 vs -0.104 au for [Co]=CF(CF_3)), Mayer bond orders for metal carbon bonds (1.50 for [Co]=CF_2 vs 1.55 for [Co]=CF(CF_3)), and rotational free energy barriers for the carbene ligands ($\Delta G^{\ddagger}_{298\,K}$ = 14.1 kcal/mol for [Co]=CF_2 vs 17.6 kcal/mol for [Co]=CF(CF_3)).

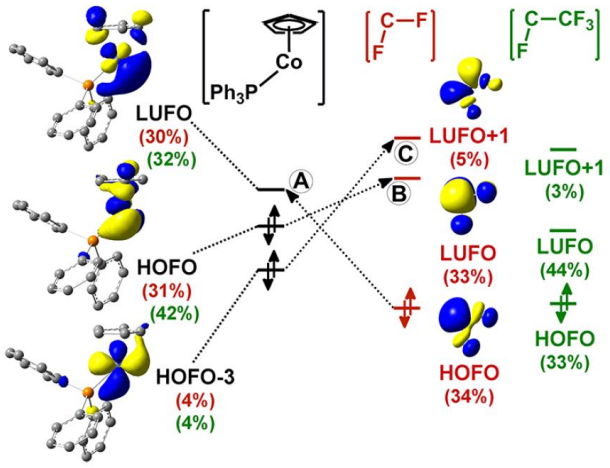

Figure 1.5. Interactions between fragment molecular orbitals (FOs) of CpCo(PPh_3) (left) and CF_2 (middle) or CF(CF_3) (right) in their singlet spin states, responsible for cobalt–carbene bonding (from PBE/TZVP calculations). The isosurface plots for the CF(CF_3) FOs (not shown) are generally similar to those displayed for CF_2. The significant σ (**A**) and π (**B** and **C**) donor/acceptor bonding interactions are labeled in the figure. The percentage values in parentheses represent changes in FO occupancies (decrease in the occupancy for occupied FOs and increase in the occupancy for unoccupied FOs) when the complex is formed from the CpCo(PPh_3) and carbene fragments.

1.4.3 Synthesis and Characterization of Metal Fluorocarbenes

There are various methods available for synthesizing metal fluorocarbene complexes, which are discussed in this section. When designing a synthetic procedure for a metal fluorocarbene, different methods might

be suitable depending on the structure and oxidation state of the targeted metal fluorocarbene product. Metal fluorocarbene research is limited by the availability of appropriate synthetic routes, as well as the proper precursor complexes, which are overwhelmingly metal fluoroalkyl complexes. Also discussed in this section are structural studies as well as the highly characteristic ^{19}F NMR spectra for metal fluorocarbene complexes.

1.4.3.1 Abstraction of α-C-F from a Metal Fluoroalkyl

The first metal fluorocarbenes were prepared by abstracting one fluoride from M-CF_2R^F (R^F = F, perfluoroalkyl) with a Lewis acid. This method can furnish cationic or neutral difluorocarbene complexes, without a net change in the oxidation state of the metal center. Treatment of $CpMoCF_2R^F(CO)_2(L)$ (R^F = F, C_2F_5; L = CO, PPh_3) with SbF_5 at low temperature furnished $[CpMo{=}CFR^F(CO)_2(L)][SbF_6]$,[59] and similar complexes $[Cp^RMo{=}CF_2(CO)_3][OTf]$ (Cp^R = Cp or Cp*) were later isolated using Me_3Si^+ (Me_3SiOTf) as a fluoride abstracting agent.[60] Similarly, manganese and iron complexes were prepared by abstracting a fluoride from M-CF_3 using BF_3, affording $[Mn{=}CF_2(CO)_5][BF_4]$ and $[CpFe{=}CF_2(CO)(L)][BF_4]$ (L = CO, PPh_3).[48,49] More recently, our group reported fluoride abstraction from cobalt(I) trifluoromethyl complexes using Me_3SiOTf to prepare $[Co{=}CF_2(DPPE)(CO)_2][OTf]$ (DPPE = $Ph_2PCH_2CH_2PPh_2$) and $[Co{=}CF_2(P_3)(CO)][OTf]$ (P_3 = $PhP(CH_2CH_2PPh_2)_2$).[53] Interestingly, a vacant coordination site on a metal center can act as an internal Lewis acid for fluoride abstraction (Scheme 1.5).

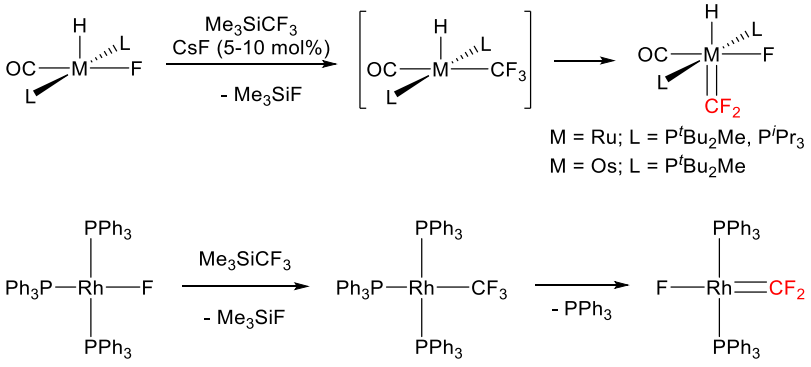

Scheme 1.5. Fluoride abstraction by unsaturated metal centers.

Caulton et al. reported octahedral ruthenium and osmium difluorocarbene complexes where fluoride elimination from M-CF_3 results in a fluoride ligand cis to CF_2.[11,61] This method was later used to prepare a square-planar rhodium difluorocarbene complex.[12]

1.4.3.2 Metathesis with 1,1-Difluoroethylene

While there has been a great interest in olefin metathesis reactions of fluorinated substrates,[62] perfluorinated alkane olefins and 1,1-disubstituted olefins have been classified in the past as generally inert to cross-metathesis (CM).[63] It was reported that reactions of Grubbs 2nd generation catalyst with 1,1-difluoroethylene result in the formation of a Ru=CF_2 complex, but this complex was inactive for further CM activity (Scheme 1.6).

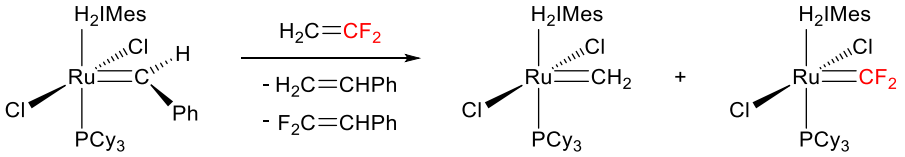

Scheme 1.6. Metathesis of Grubbs 2nd generation catalyst with 1,1-difluoroethylene.

Cross-metathesis involving tetrafluoroethylene (TFE) and dodecyl vinyl ether was later achieved, but the productive CM step is believed to not proceed via [Ru]=CF_2, which reacts with vinyl dodecyl ether to furnish only H_2C=CF_2 as the CM product.[64]

1.4.3.3 Difluorocarbene Complexes Derived from $Cd(CF_3)_2$·glyme

The cadmium reagent $Cd(CF_3)_2$·glyme has been recognized as a powerful ligand exchange reagent and low-temperature source of free difluorocarbene.[65] This reagent can also be used to effectively transfer CF_2 to a metal center, replacing a neutral L donor ligand, as demonstrated by Roper and coworkers in the preparation of Ru(0) and Os(0) difluorocarbene complexes (Scheme 1.7).[66,67] This strategy was also employed to

prepare Ir(=CF_2)(CF_3)(CO)(PPh_3)$_2$.[33] This synthetic approach is attractive as it does not require an isolated metal fluoroalkyl precursor, and there is no net change in metal oxidation state.

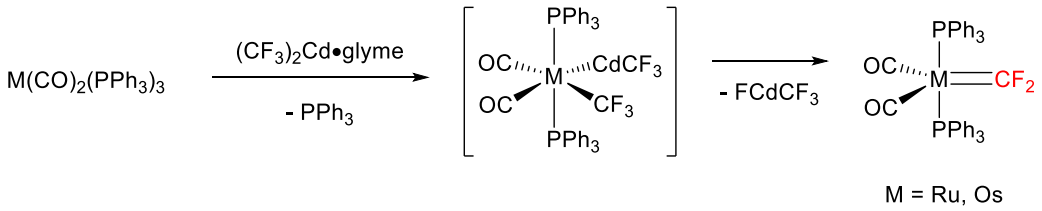

Scheme 1.7. Synthesis of difluorocarbene complexes using Cd(CF_3)$_2$·glyme.

1.4.3.4 Activation of C_α -F by Reduction

Metal fluoroalkyl complexes can be reduced using alkali metals, eliminating alkali metal fluorides and furnishing metal fluorocarbenes. Notably, this method typically results in a two-electron reduction at the metal center. This method was first demonstrated by Hughes and coworkers for the reduction of Ir(III) fluoroalkyl complexes Cp*Ir(PMe_3)(CF_2R^F)(I) (R^F = F, CF_3, C_6F_5) using excess potassium graphite (KC_8) to furnish Ir(I) fluorocarbenes Cp*Ir(=CFR^F)(PMe_3).[68] This method was extended to prepare the first example of a bis(trifluoromethyl) carbene complex, Cp*Ir(=C(CF_3)$_2$)(CO).[69] Our group has also used this approach to prepare the first fluorocarbene complexes of cobalt and nickel (Scheme 1.8).

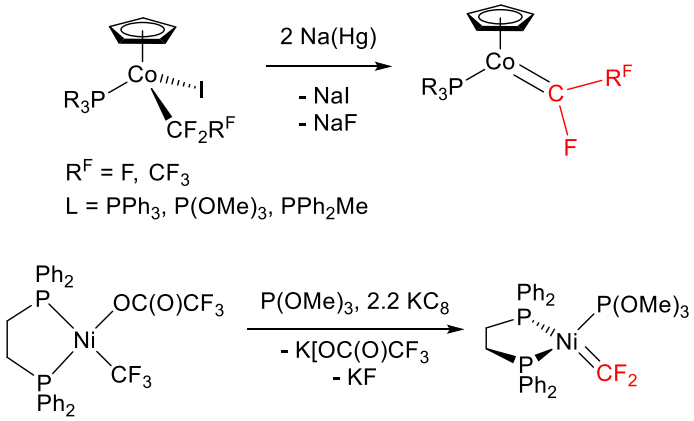

Scheme 1.8. Synthesis of cobalt and nickel fluorocarbene complexes by reduction.

Cobalt(III) perfluoroalkyl iodide complexes $CpCo(PR_3)(CF_2R^F)(I)$ (R^F = F, CF_3; L = PPh_3, $P(OMe)_3$, PPh_2Me) underwent two-electron reduction when treated with sodium-mercury amalgam to afford cobalt(I) fluorocarbenes $CpCo(=CFR^F)(PR_3)$.[50,51] Similarly, nickel(II) complex $Ni(DPPE)[OC(O)CF_3](CF_3)$ (DPPE = $Ph_2P(CH_2)_2PPh_2$) was reduced using KC_8 in the presence of $P(OMe)_3$ to afford nickel(0) fluorocarbene $Ni(=CF_2)(DPPE)[P(OMe)_3]$.[54] The unique reactivity of these cobalt and nickel fluorocarbene complexes will be discussed in section 1.4.4.

1.4.3.5 Direct transfer of Difluorocarbene

A desirable approach to metal fluorocarbene synthesis is the direct transfer of CF_2 to a metal center, similar to the result obtained from $Cd(CF_3)_2$·glyme, but preferably without using a toxic reagent. An established source of free difluorocarbene is Me_3SiCF_3, when activated by either F^- or I^-, as described by Prakash and coworkers for the synthesis of *gem*-difluorinated cyclopropanes from alkenes.[70] This method has apparently been applied by Ozerov and coworkers for the synthesis of (PNP)Rh=CF_2 (Scheme 1.9). When (PNP)Rh(TBE) (TBE = *tert*-butyl ethylene) was treated with TMS_3CF_3/CsF in benzene at 70 °C, (PNP)Rh=CF_2 and (PNP)Rh(TFE) were formed in 85% and 14% yield, respectively. It is not clear if (PNP)Rh(CF_3) is formed first, followed by fluoride abstraction, or if CF_2, which is formed in situ via decomposition of CF_3 into CF_2 and F^-, displaces TBE directly to furnish (PNP)Rh=CF_2. The side product (PNP)Rh(TFE) is proposed to result from TBE displacement by TFE, formed in situ by difluorocarbene dimerization.

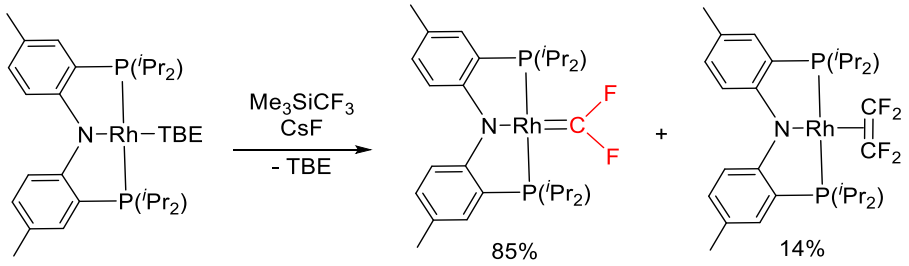

Scheme 1.9. Synthesis of (PNP)Rh=CF_2.

1.4.3.6 Characterization of Metal Fluorocarbenes

Crystallographic studies confirm that metal fluorocarbenes typically exhibit significantly shorter M-C bond distances than their metal fluoroalkyl analogs/precursors. For example, the Ir=CF_2 bond distance in Cp*Ir(=CF_2)(PMe_3) is 1.854(11) Å, while the Ir-CF_3 bond distance is 2.10(2) Å in Cp*Ir(PMe_3)(CF_3)(I).[68] The same holds true for molybdenum complexes, as the Mo=CF_2 bond distance in [Cp*Mo=CF_2(CO)$_3$][OTf] is 1.965(13) Å, while the Mo-CF_3 bond distance in Cp*Mo(CF_3)(CO)$_3$ is 2.248(5) Å.[60]

The ^{19}F NMR spectra for metal fluorocarbenes are highly characteristic, and typically feature positive chemical shifts. The ^{19}F NMR chemical shifts (ppm) for carbene-fluorine atoms of selected metal fluorocarbene complexes are shown in Figure 1.6.

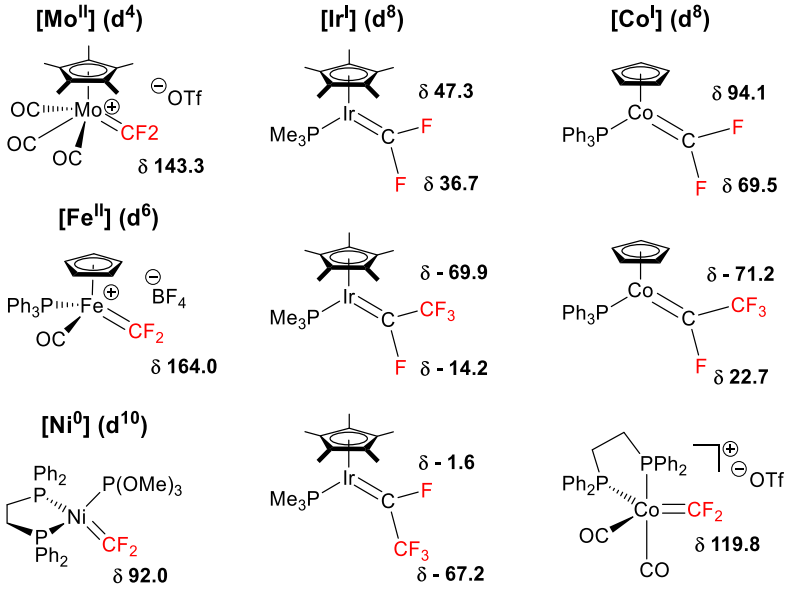

Figure 1.6. Selected metal fluorocarbenes and their ^{19}F NMR chemical shifts.

In general, a lower metal oxidation state and better electron-donating ability of ancillary ligands contribute to an upfield shift of the ^{19}F resonances for M=CF_2, while high metal oxidation states, cationic complexes, and electron-accepting ligands contribute to a downfield shift. Furthermore, the ^{19}F resonance(s) for M=CF_2 provides information about the barrier for rotation of the M=C bond. For example, CpCo(=CF_2)(PPh_3) has

non-equivalent fluorine environments (69.5 and 94.1 ppm), consistent with the calculated rotational free energy barrier for the carbene ligand ($\Delta G^{\ddagger}_{298\ K}$ = 14.1 kcal/mol for [Co]=CF_2).[50] In contrast, [CpFe=CF_2(CO)(PPh_3)][BF_4] has a single fluorocarbene resonance at 164.0 ppm, consistent with a low barrier to rotation.[49]

1.4.4 Reactivity of Metal Fluorocarbenes

Reactivity studies of isolated metal fluorocarbenes are very limited when compared to hydrocarbon analogs and metal-NHC complexes. In particular, involvement of metal fluorocarbenes in catalytic reactions are rare. Important early reports by Roper and coworkers established that changing the oxidation state of the metal center can switch the type of reactivity of metal fluorocarbenes from nucleophilic to electrophilic at the carbene carbon (Scheme 1.10).[66,71]

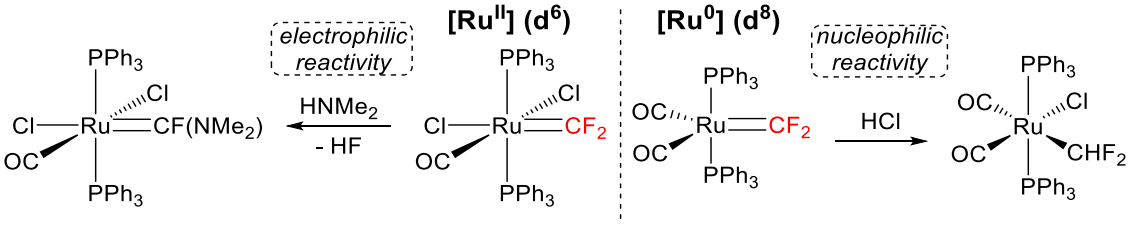

Scheme 1.10. Oxidation state control of reactivity of ruthenium fluorocarbene complexes.

Ruthenium(II) fluorocarbene Ru=CF_2(CO)$(Cl)_2$(PPh_3)$_2$ undergoes reactions with nucleophiles $HNMe_2$ and MeOH, eliminating HF and forming Ru(=$CFNMe_2$)(CO)(Cl_2)(PPh_3)$_2$ and Ru(=CFOMe)(CO)(Cl_2)(PPh_3)$_2$, respectively. In addition, Ru=CF_2(CO)$(Cl)_2$(PPh_3)$_2$ is highly susceptible to hydrolysis of the difluorocarbene ligand to carbonyl, eliminating 2 equiv HF and forming Ru$(CO)_2(Cl)_2$(PPh_3)$_2$. In contrast, ruthenium(0) fluorocarbene Ru=$CF_2$$(CO)_2$($PPh_3$)$_2$ is resistant to the same reactivity with nucleophiles, and can be crystallized from wet solvents. Furthermore, Ru=$CF_2$$(CO)_2$($PPh_3$)$_2$ reacts with electrophiles such as H^+, as the reaction with HCl furnishes Ru$(CF_2H)(CO)_2(Cl)$(PPh_3)$_2$. These results helped inform the design of metal fluorocarbenes to have either nucleophilic or electrophilic type character, aiding efforts toward

developing catalytic processes based on metal fluorocarbenes. Various examples of the known reactivity of fluorocarbene complexes are discusses below, including reactions involving transient metal fluorocarbenes.

1.4.4.1 Hydrolysis of $M=CF_2$

Metal fluorocarbenes which exhibit electrophilic-type reactivity typically have a metal center with an oxidation state ≥ +2, with $[Mn=CF_2(CO)_5][BF_4]$ being an exception. The most common reaction of electrophilic metal fluorocarbenes is hydrolysis of the fluorocarbene ligand to a carbonyl, with a strong driving force toward formation of two H-F bonds (568 kJ/mol) and a C-O triple bond. As such, these fluorocarbene complexes can only be handled in rigorously dried solvents, which still only mitigates their hydrolysis for a limited amount of time. This is likely responsible for the dearth of reactivity studies on electrophilic-type fluorocarbene complexes. In contrast, electron-rich cobalt and rhodium fluorocarbenes $CpCo(=CFR^F)(PR_3)$ and $(PNP)Rh=CF_2$ are resistant to hydrolysis, as deliberate attempts to hydrolyze these complexes were unsuccessful.

1.4.4.2 Fluoride Abstraction from $M=CF_2$

Ozerov and co-workers reported the abstraction of fluoride from $(PNP)Rh=CF_2$ using $[Et_3Si\text{-}H\text{-}SiEt_3][HCB_{11}Cl_{11}]$ to cleanly and reproducibly generate $[(PNP)Rh{\equiv}CF][HCB_{11}Cl_{11}]$.[13] This rhodium complex represents a rare example of an isolable metal fluorocarbyne. Hughes and coworkers previously reported the synthesis of group 6 complexes $Cp^RM{\equiv}CF(CO)_2$ (Cp^R = Cp, Cp*; M = Cr, Mo, W), via two-electron reduction of their trifluoromethyl precursors $Cp^RM(CF_3)(CO)_3$.[72,73]

1.4.4.3 Alkene Metathesis with Alkyl Vinyl Ethers

Despite ruthenium precatalysts having excellent tolerance toward diverse functional groups in olefin metathesis reactions, fluorinated alkenes are generally incompatible, as ruthenium fluorocarbene complexes

suffer from high thermodynamic stability and slow phosphine ligand dissociation, a plausible initiation step for catalytic cycles.[74] A recent study from Takahira and coworkers, however, finally achieved catalytic cross-metathesis between fluoroalkenes and enol ethers (TON = 13.4).[64] The key reactivity which allows productive cross-metathesis, however, does not involve [Ru]=CF_2. Rather, the ruthenium difluorocarbene complex undergoes metathesis with the enol ether to furnish the ether-containing carbene complex (Scheme 1.11), which can then undergo productive cross-metathesis with fluorinated alkenes.

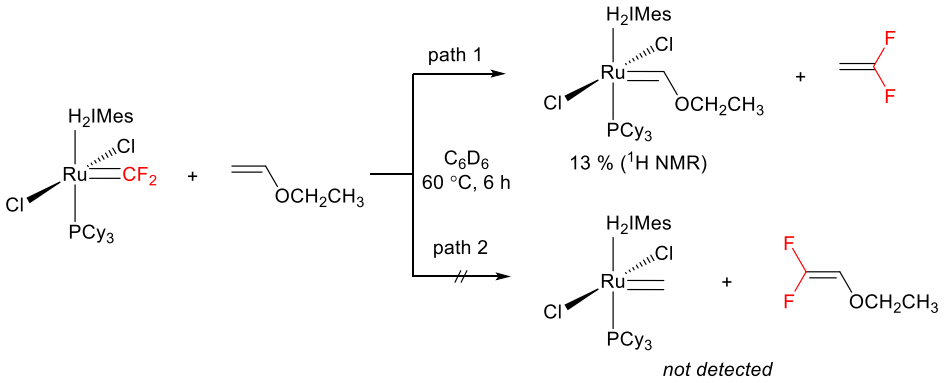

Scheme 1.11. Metathesis with Grubbs-type Ru=CF_2 complex.

1.4.4.4 Reactivity of Transient Metal Fluorocarbene Complexes

Burton and coworkers described the insertion of CF_2 into Cu-R^F (R^F = CF_3, C_6F_5) bonds (Scheme 1.12).[75,76] First, $CuCF_3$, prepared *in situ* from the metathesis reaction of $Cd(CF_3)_2$ with CuX (X = Cl, Br, I, CN), was converted to $CuCF_2CF_3$. Secondly, when $CuCF_3$ was warmed to room temperature from -30 °C in the presence of CuC_6F_5, double CF_2 insertion occurred, resulting in $CuCF_2CF_2C_6F_5$. While the detailed reaction pathway was not fully elucidated, it was proposed that an equilibrium between $CuCF_3$ and copper difluorocarbene complex F_2C=CuF was involved.

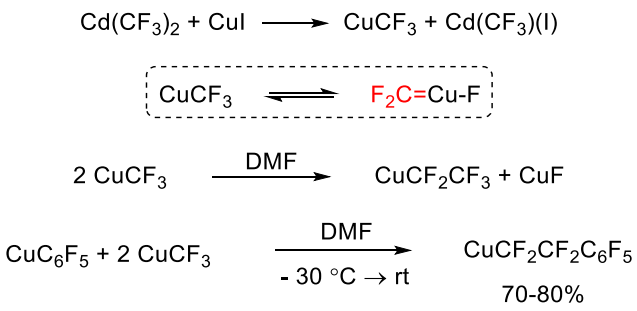

Scheme 1.12. Difluorocarbene insertion into Cu-R^F bonds.

Several reports of metal-catalyzed reactions involving M=CF_2 have surfaced recently. Xiao and coworkers described a palladium catalyzed transfer of difluorocarbene for the synthesis of (difluoromethyl)arenes and –olefins (Scheme 1.13).[77] Mechanistic investigations revealed that a Pd=CF_2 complex is a key intermediate in the transformation, but this species is prone to trimerization in the absence of the starting materials.

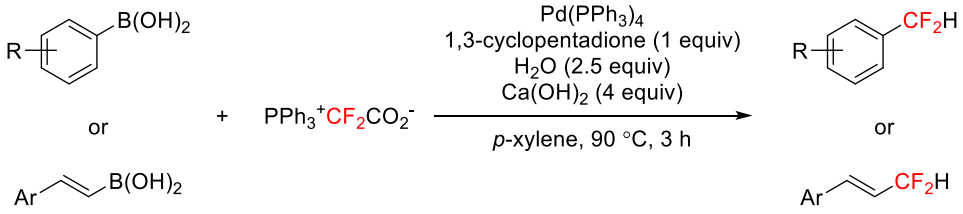

Scheme 1.13. Palladium catalyzed synthesis of (difluoromethyl)arenes and –olefins.

Ichikawa and coworkers reported the copper-catalyzed [4+1] cycloaddition of silyl dienol ethers with sodium bromodifluroacetate.[78] On the basis of high-resolution mass spectrometric analysis, the annulation was proposed to proceed via Cu(I) difluorocarbene complex, which represents the first example of a [4+1] cycloaddition promoted by a metal difluorocarbene complex. Finally, transfer of CF_2 (derived from Me_3SiCF_3/NaI) to *n*-butyl acrylate using a cobalt(II) porphyrin catalyst (5 mol%), produces the corresponding *gem*-difluorocyclopropane (TON = 8).[79] DFT studies reveal that one-electron reduction of a trifluoromethyl cobalt(III)tetraphenylporphyrinato complex [Co(TPP)CF_3] results in formation of

difluorocarbene cobalt(II)porphyrin complex [Co(TPP)CF_2], which is responsible for difluorocarbene transfer to the alkene.

1.4.4.5 Reactivity of Nucleophilic Fluorocarbenes

Metal alkylidenes are involved in a variety of catalytic transformations, most prominently alkene metathesis.[80] Catalysis involving metal fluorocarbenes and metal fluoroalkenes, however, has been shown to be inherently challenging, but overcoming these challenges can possibly lead to development of very important transformations, such as metathesis and polymerization of perfluoroalkenes as outlined in Scheme 1.14.

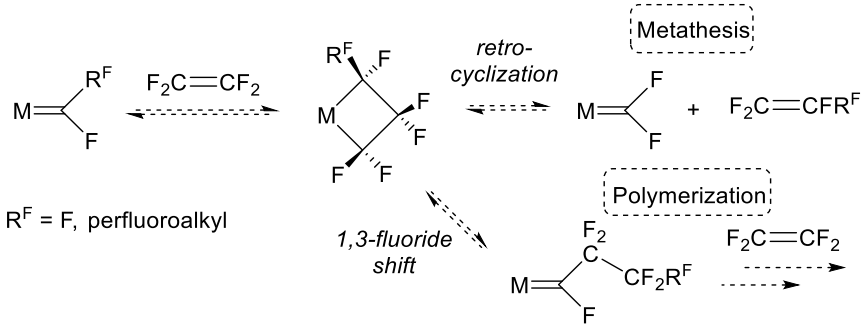

Scheme 1.14. Potential M=CF_2 initiated metathesis or polymerization with perfluoroalkenes.

The metathesis pathway is identical to the established Chauvin mechanism. The polymerization pathway is a modified "fluoro"-Green-Rooney mechanism,[81] which avoids migratory alkene insertion into unreactive M-R^F bonds, in contrast to the typical Cossee-Arlman pathway.[82–84] In order to favor reactivity with electron deficient fluoroalkenes, we became interested in the synthesis and reactivity of metal fluorocarbene complexes with nucleophilic-type reactivity.

We prepared a series of cobalt(I) fluorocarbene complexes, CpCo(=CFR^F)(PR_3) (R^F = F, C_3; PR_3 = PPh_3, $P(OMe)_3$, PPh_2Me), as described in the previous section (Scheme 1.10). The nucleophilic character of these complexes was established through reactions with simple electrophiles (H^+ and Me^+), when protonation with lutidinium bromide and methylation with MeOTf occurred at the carbene carbon.[50] We

then moved on to reactivity with fluoroalkenes, and treatment of $CpCo(=CFR^F)(PPh_2Me)$ with excess TFE resulted in a [2+2] cycloaddition, furnishing perfluorometallacyclobutane complexes after 4 days at room temperature (Scheme 1.15).[51] Notably, we found that using the electron-rich phosphine PPh_2Me was necessary for a reasonable rate of reaction, as $P(OMe)_3$ and PPh_3 resulted in drastically decreasing rates (in order).

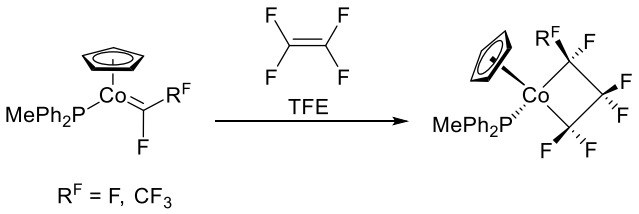

Scheme 1.15. Cycloaddition reaction between cobalt(I) fluorocarbenes and TFE.

Preliminary kinetic data revealed that the rate of reaction was only marginally slower in the presence of 20 equiv of free PPh_2Me, suggesting TFE addition proceeds without phosphine dissociation. These results stand in contrast to observations by Hughes and coworkers that an iridium(I) fluoroalkylidene-ethylene complex, $Cp^*Ir(=CF(CF_3))(C_2H_4)$, remained conformationally locked, with a large calculated barrier to metallacyclobutane formation.[85] The detailed pathway of the [2+2] cycloaddition reaction between $CpCo(=CF_2)(PPh_2Me)$ and TFE was studied computationally, and it was revealed to proceed via a 1,4-singlet diradical intermediate.[52] The stability of the singlet-diradical intermediate results from the formation of a strong CF_2-CF_2 bond coupled with the radical stabilizing effect of a difluoromethylene group.

The perfluorometallacyclobutane products were found to be thermally stable. Reactivity, however, was achieved when these complexes were treated with strong Lewis or Brønsted acids (Scheme 1.16).

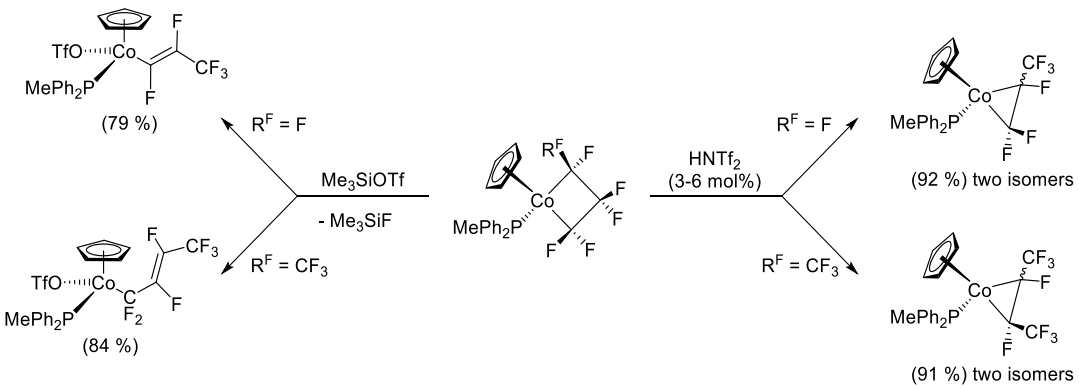

Scheme 1.16. Reactivity of cobalt perfluorocyclobutanes.

When cobalt perfluorocyclobutane complexes were treated with Me_3SiOTf, fluoride abstraction yields perfluoro-*trans*-vinyl or perfluoro-*trans*-allyl products. Catalytic quantities of $HNTf_2$ induce clean isomerization/ring-contraction reactions, producing cobalt hexafluoropropene or perfluoro-2-butene complexes. Experiments with stoichiometric $[HPPh_2Me][NTf_2]$ suggest that both ring-opening and catalytic ring-contraction reactions likely proceed via β-C-F activation and a π-perfluoroallyl intermediate, rather than α-C-F activation observed for perfluorometallacyclopentanes.[86] The nickel(0) difluorocarbene complexes prepared by our group also reacted with TFE to form perfluorometallacyclobutanes, but the reaction is significantly faster than for cobalt.[54] The nickel perfluorocyclobutane products undergo analogous ring-opening and catalytic ring-contraction reactions with Me_3SiOTf and $HNTf_2$, respectively.

1.5 Organometallic Fluoride Complexes

Organometallic fluoride complexes contain a fluorine-metal and carbon-metal bond with the same metal atom, and there are a large number of compounds which fit this description.[87] Incredibly, examples of organometallic fluorides are reported for transition metals from group 3 (Sc[88]), group 4 (Ti,[19] Zr,[89] Hf[90]), group 5 (V,[91] Nb,[92] Ta[93]), group 6 (Cr,[94] Mo,[95] W[96]), group 7 (Mn,[97] Re), group 8 (Ru,[98] Os[98]), group 9 (Co,[99] Rh,[100] Ir[101]), group 10 (Ni,[102] Pd,[103] Pt[104]), and group 11 (Cu,[105] Au[106]). While early-metal organometallic fluoride complexes have been utilized for reactions such as the catalytic reduction of

perfluorocarbons,[107] there has recently been a greater focus on late-metal organometallic fluorides for their application as hydrogen bond acceptors[108] but particularly as mediators of C-F bond forming reactions.[109]

1.5.1 Synthesis and Characterization

The primary synthetic route to organometallic fluorides is metathesis of M-X complexes (X = halide, triflate) with nucleophilic fluoride salts, with examples shown in Scheme 1.19. Richmond and coworkers used $KF \cdot 2H_2O$ to prepare a tungsten(II) fluoride complex,[110] while Caulton and coworkers used CsF to prepare $RuHF(CO)(P^tBu_2Me)_2$ from the Ru-Cl precursor.[111] Bergman and coworkers reported the metathesis of an iridium triflate complex with tris(dimethylamino)sulfonium difluorotrimethylsilicate (TASF) to form an Ir(III) fluoride complex.[101] The most common reagent used to prepare organometallic fluorides is AgF. Notable examples of this are Ir(III) fluoride complexes prepared by Hughes and coworkers, and POCOP-pincer type Ni(II) fluorides prepared by Zargarian and coworkers[102,112] Furthermore, an important palladium(II) fluoride complex, [(BrettPhos)PdAr(F)] (Ar = 2-methyl-4-trifluoromethylphenyl), was prepared by Buchwald and coworkers from [(BrettPhos)PdAr(Br)] and AgF.[103] Other methods to prepare organometallic fluorides include oxidative fluorination using XeF_2, as was employed by Mankad and coworkers to prepare alkylgold(III) fluoride complexes.[106] While single crystal X-ray diffraction is indispensable for the unambiguous structural characterization of organometallic fluoride complexes, ^{19}F NMR spectroscopy is also a critical tool. Organometallic fluorides are typically accompanied by ^{19}F NMR spectra with resonances for M-F which are shifted dramatically upfield, indicative of a high degree of shielding on the fluorine atom.

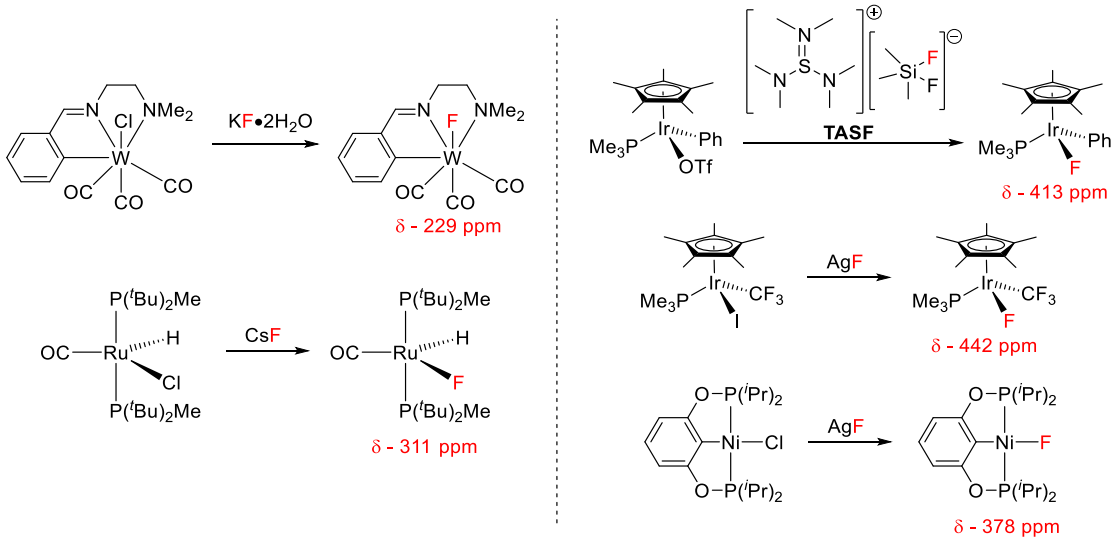

Scheme 1.17. Synthesis of organometallic fluoride complexes and their ^{19}F chemical shifts.

Scheme 1.17 also shows the ^{19}F NMR chemical shift associated with the M-F group of several examples of organometallic fluoride complexes (referenced to $CFCl_3$ at 0.00 ppm). The range of these chemical shifts spans from δ -229 ppm to -442 ppm. Similarly, the ^{19}F spectrum for the palladium(II) fluoride complex [(BrettPhos)PdAr(F)] has a resonance for Pd-F at -208 ppm.

1.5.2 Metal Catalyzed Nucleophilic Fluorination

Organometallic fluoride complexes are of special interest due to M-F bonds playing a key role in C-F bond formation. Metal-mediated or metal-catalyzed fluorination reactions are typically categorized according to the fluorinating reagents used. Reactions utilizing F_2 or F_2-derived reagents, such as Selectfluor® and *N*-fluorobenzenesulfonamide (NFBS), as a source of "F^+" are referred to as electrophilic fluorinations, and have been studied extensively.[113–116] Nucleophilic fluorinations which deliver "F^-", in contrast, can be derived from inexpensive and highly-abundant nucleophilic fluoride salts such as KF, CsF, and AgF. These reagents typically suffer from low solubility, high hygroscopicity, and strong Brønsted basicity, making their employment in chemical synthesis challenging. However, significant progress in the area of metal-mediated/-catalyzed nucleophilic fluorination has been made.[117] Examples of this type of reactivity in the literature are largely based on palladium, although reports utilizing copper have appeared recently, as shown

in Scheme 1.18. The palladium catalyzed fluorination of aryl bromides/triflates reported by Buchwald and coworkers, enabled by pioneering work from Grushin and coworkers,[118] invokes reductive elimination of Ar-F as the key step in a Pd(0)/Pd(II) cycle.[103,119] In a series of publications, Doyle and coworkers describe the palladium catalyzed enantioselective fluorination of allylic chlorides using AgF.[120–122] An important study from Liu and coworkers describes the copper catalyzed fluorination of 2-pyridyl aryl bromides, and preliminary mechanistic studies suggest reductive elimination from ArCu(III)-F species is the key step.[123] A mild, copper catalyzed fluorination of alkyl triflates was described by Lalic and coworkers which employs *N*-heterocyclic carbene complex [IPrCuOTf] and KF as a fluorine source.[124] While the tendency of second and third row transition metals to form weaker bonds to fluorine than 1st row metals has made them useful for catalytic fluorination reactions, there is still a need to develop catalytic reactions based on inexpensive, non-toxic and earth-abundant first row metals.

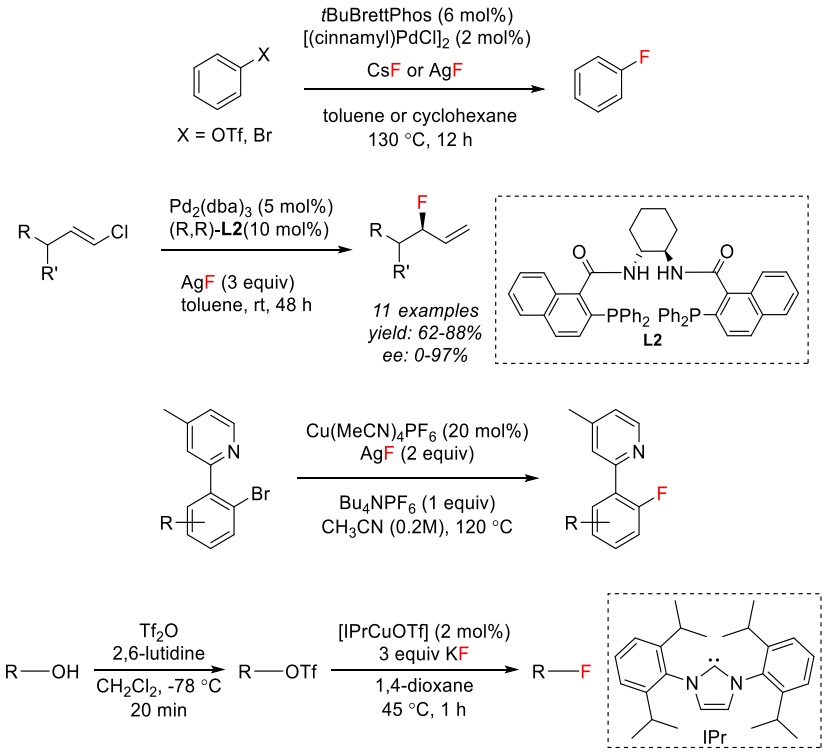

Scheme 1.18. Metal-catalyzed nucleophilic fluorination reactions.

1.6 Summary and Thesis Outline

The importance of fluoro-organometallic chemistry as it relates to C-F and C-R^F bond formation has been introduced. Some of the challenges associated with developing metal-mediated and metal-catalyzed processes for manipulating C-F and C-R^F bonds have also been presented, highlighting the need for a better understanding of the synthesis and reactivity of fluoro-organometallic complexes. An effort has been made to familiarize the reader with many of the details and latest reports regarding the synthesis, characterization, and reactivity of 1) metal fluoroalkyl, 2) metal fluorocarbene, and 3) metal fluoride complexes. In particular, work within our group into the synthesis and reactivity of first-row metal fluorocarbene complexes has been presented. Chapter 2 will explore the reactivity of cobalt(I) fluorocarbenes with aryl-alkynes to form partially fluorinated cobaltacyclobutene complexes. This will include the synthesis and full characterization of several new cobaltacyclobutene complexes, exploration into the scope of the reaction, as well as kinetic and DFT studies into the mechanism of formation of cobaltacyclobutenes. Chapter 3 will introduce a stepwise addition of difluorocarbene to a transition metal center. This involves transfer of CF_2 to a cobalt(I) center to form a cobalt fluorocarbene complex, followed by a second difluorocarbene addition to form cobalt(III) fluoroalkene complexes. Experimental evidence for the stepwise nature of this reaction is discussed. Chapter 4 will focus on the fluoro-organometallic chemistry of cobalt(III) fluoride and bis(perfluoroalkyl) complexes. The cobalt fluoride complexes exhibit interesting properties, such as the most upfield ^{19}F NMR chemical shifts reported to date. The reactivity of these complexes is also explored, and a catalytic nucleophilic fluorination reaction is developed. The bis(perfluoroalkyl) complexes undergo selective fluoride abstraction to form electrophilic cobalt(III) fluorocarbene complexes, which undergo insertion into the remaining metal fluoroalkyl ligand. Chapter 5 further expands the synthesis and reactivity of electrophilic metal fluorocarbenes, with the first examples of nickel(II) and palladium(II) difluorocarbenes, derived from POCOP pincer-type trifluoromethyl complexes. Chapter 6 explores in greater detail the catalytic fluorination reaction first disclosed in chapter 4. Utilizing a high-throughput experimentation platform, 96 cobalt(III) catalysts are screened for their activity in the fluorination of benzoyl fluoride. The scope of the reaction is also expanded to the synthesis of a series of acyl fluoride

products. Chapter 7 will summarize the previous chapters, and provide an outlook for the future directions, and identify the areas of most significance and urgency as related to the projects described in this thesis.

1.7 References

(1) Chen, B.; Vicic, D. A. In *Organometallic Fluorine Chemistry*; Braun, T., Hughes, R. P., Eds.; Topics in Organometallic Chemistry; Springer International Publishing, 2014; pp 113–141.
(2) Campbell, M. G.; Hoover, A. J.; Ritter, T. In *Organometallic Fluorine Chemistry*; Braun, T., Hughes, R. P., Eds.; Topics in Organometallic Chemistry; Springer International Publishing, 2014; pp 1–53.
(3) LaBerge, N. A.; Love, J. A. In *Organometallic Fluorine Chemistry*; Braun, T., Hughes, R. P., Eds.; Topics in Organometallic Chemistry; Springer International Publishing, 2015; pp 55–111.
(4) Ohashi, M.; Ogoshi, S. In *Organometallic Fluorine Chemistry*; Braun, T., Hughes, R. P., Eds.; Topics in Organometallic Chemistry; Springer International Publishing, 2014; pp 197–215.
(5) Wang, J.; Sánchez-Roselló, M.; Aceña, J. L.; del Pozo, C.; Sorochinsky, A. E.; Fustero, S.; Soloshonok, V. A.; Liu, H. *Chem. Rev.* **2014**, *114* (4), 2432–2506.
(6) Jeschke, P. *ChemBioChem* **2004**, *5* (5), 570–589.
(7) Berger, R.; Resnati, G.; Metrangolo, P.; Weber, E.; Hulliger, J. *Chem. Soc. Rev.* **2011**, *40* (7), 3496–3508.
(8) Crutzen, P. J. In *Advances in Fluorine Science*; Tressaud, A., Ed.; Fluorine and the EnvironmentAtmospheric Chemistry, Emissions, & Lithosphere; Elsevier, 2006; Vol. 1, pp xv–xvii.
(9) Hu, J.-Y.; Zhang, J.-L. In *Organometallic Fluorine Chemistry*; Braun, T., Hughes, R. P., Eds.; Topics in Organometallic Chemistry; Springer International Publishing, 2015; pp 143–196.
(10) Blanksby, S. J.; Ellison, G. B. *Acc. Chem. Res.* **2003**, *36* (4), 255–263.
(11) Huang, D.; Koren, P. R.; Folting, K.; Davidson, E. R.; Caulton, K. G. *J. Am. Chem. Soc.* **2000**, *122* (37), 8916–8931.
(12) Goodman, J.; Grushin, V. V.; Larichev, R. B.; Macgregor, S. A.; Marshall, W. J.; Roe, D. C. *J. Am. Chem. Soc.* **2009**, *131* (12), 4236–4238.
(13) Pell, C. J.; Zhu, Y.; Huacuja, R.; Herbert, D. E.; Hughes, R. P.; Ozerov, O. V. *Chem. Sci.* **2017**, *8* (4), 3178–3186.
(14) King, R. B.; King, A. D.; Iqbal, M. Z.; Frazier, C. C. *J. Am. Chem. Soc.* **1978**, *100* (6), 1687–1694.
(15) Connor, J. A.; Zafarani-Moattar, M. T.; Bickerton, J.; El Saied, N. I.; Suradi, S.; Carson, R.; Al Takhin, G.; Skinner, H. A. *Organometallics* **1982**, *1* (9), 1166–1174.
(16) Folga, E.; Ziegler, T. *J. Am. Chem. Soc.* **1993**, *115* (12), 5169–5176.
(17) Yamaguchi, Y.; Ichioka, H.; Klein, A.; Brennessel, W. W.; Vicic, D. A. *Organometallics* **2012**, *31* (4), 1477–1483.
(18) Algarra, A. G.; Grushin, V. V.; Macgregor, S. A. *Organometallics* **2012**, *31* (4), 1467–1476.
(19) Taw, F. L.; Clark, A. E.; Mueller, A. H.; Janicke, M. T.; Cantat, T.; Scott, B. L.; Hay, P. J.; Hughes, R. P.; Kiplinger, J. L. *Organometallics* **2012**, *31* (4), 1484–1499.
(20) McClellan, W. R. *J. Am. Chem. Soc.* **1961**, *83* (7), 1598–1600.
(21) Maleckis, A.; Sanford, M. S. *Organometallics* **2014**, *33* (14), 3831–3839.
(22) Karel, K. J.; Tulip, T. H.; Ittel, S. D. *Organometallics* **1990**, *9* (4), 1276–1282.
(23) King, R. B.; Stafford, S. L.; Treichel, P. M.; Stone, F. G. A. *J. Am. Chem. Soc.* **1961**, *83* (17), 3604–3608.
(24) Burns, R. J.; Bulkowski, P. B.; Stevens, S. C. V.; Baird, M. C. *J. Chem. Soc. Dalton Trans.* **1974**, No. 4, 415–420.
(25) Collman, J. P.; Sears, C. T. *Inorg. Chem.* **1968**, *7* (1), 27–32.
(26) King, R. B.; Efraty, A. *J. Organomet. Chem.* **1971**, *27* (3), 409–420.

(27) Hughes, R. P.; Smith, J. M.; Liable-Sands, L. M.; Concolino, T. E.; Lam, K.-C.; Incarvito, C.; Rheingold, A. L. *J. Chem. Soc. Dalton Trans.* **2000**, No. 6, 873–880.
(28) McCleverty, J. A.; Wilkinson, G. *J. Chem. Soc. Resumed* **1964**, No. 0, 4200–4203.
(29) Winston, M. S.; Wolf, W. J.; Toste, F. D. *J. Am. Chem. Soc.* **2014**, *136* (21), 7777–7782.
(30) Ontiveros, C. D.; Morrison, J. A. *Organometallics* **1986**, *5* (7), 1446–1448.
(31) Nair, H. K.; Morrison, J. A. *J. Organomet. Chem.* **1989**, *376* (1), 149–164.
(32) Loizou, D. C.; Castillo, J.; Oki, A. R.; Hosmane, N. S.; Morrison, J. A. *Organometallics* **1992**, *11* (12), 4189–4193.
(33) Brothers, P. J.; Burrell, A. K.; Clark, G. R.; Rickard, C. E. F.; Roper, W. R. *J. Organomet. Chem.* **1990**, *394* (1–3), 615–642.
(34) Liu, X.; Xu, C.; Wang, M.; Liu, Q. *Chem. Rev.* **2014**.
(35) Kolomeitsev, A.; Movchun, V.; Rusanov, E.; Bissky, G.; Lork, E.; Roschenthaler, G.-V.; Kirsch, P. *Chem. Commun.* **1999**, No. 11, 1017–1018.
(36) Maggiarosa, N.; Tyrra, W.; Naumann, D.; Kirij, N. V.; Yagupolskii, Y. L. *Angew. Chem. Int. Ed.* **1999**, *38* (15), 2252–2253.
(37) Prakash, G. K. S.; Wang, F.; Zhang, Z.; Haiges, R.; Rahm, M.; Christe, K. O.; Mathew, T.; Olah, G. A. *Angew. Chem. Int. Ed.* **2014**, *53* (43), 11575–11578.
(38) Urata, H.; Fuchikami, T. *Tetrahedron Lett.* **1991**, *32* (1), 91–94.
(39) Grushin, V. V.; Marshall, W. J. *J. Am. Chem. Soc.* **2006**, *128* (39), 12644–12645.
(40) Dubinina, G. G.; Furutachi, H.; Vicic, D. A. *J. Am. Chem. Soc.* **2008**, *130* (27), 8600–8601.
(41) Kieltsch, I.; Dubinina, G. G.; Hamacher, C.; Kaiser, A.; Torres-Nieto, J.; Hutchison, J. M.; Klein, A.; Budnikova, Y.; Vicic, D. A. *Organometallics* **2010**, *29* (6), 1451–1456.
(42) Dubinina, G. G.; Brennessel, W. W.; Miller, J. L.; Vicic, D. A. *Organometallics* **2008**, *27* (15), 3933–3938.
(43) Landelle, G.; Panossian, A.; Pazenok, S.; Vors, J.-P.; Leroux, F. R. *Beilstein J. Org. Chem.* **2013**, *9* (1), 2476–2536.
(44) Chen, P.; Liu, G. *Synthesis* **2013**, *45* (21), 2919–2939.
(45) Furuya, T.; Kamlet, A. S.; Ritter, T. *Nature* **2011**, *473* (7348), 470–477.
(46) Bakhmutov, V. I.; Bozoglian, F.; Gómez, K.; González, G.; Grushin, V. V.; Macgregor, S. A.; Martin, E.; Miloserdov, F. M.; Novikov, M. A.; Panetier, J. A.; Romashov, L. V. *Organometallics* **2012**, *31* (4), 1315–1328.
(47) Zhou, Z.; Jablonski, C.; Bridson, J. *Organometallics* **1994**, *13* (3), 781–794.
(48) Richmond, T. G.; Crespi, A. M.; Shriver, D. F. *Organometallics* **1984**, *3* (2), 314–319.
(49) Crespi, A. M.; Shriver, D. F. *Organometallics* **1985**, *4* (10), 1830–1835.
(50) Harrison, D. J.; Gorelsky, S. I.; Lee, G. M.; Korobkov, I.; Baker, R. T. *Organometallics* **2013**, *32* (1), 12–15.
(51) Harrison, D. J.; Lee, G. M.; Leclerc, M. C.; Korobkov, I.; Baker, R. T. *J. Am. Chem. Soc.* **2013**, *135* (49), 18296–18299.
(52) Fuller, J. T.; Harrison, D. J.; Leclerc, M. C.; Baker, R. T.; Ess, D. H.; Hughes, R. P. *Organometallics* **2015**, *34* (21), 5210–5213.
(53) Harrison, D. J.; Daniels, A. L.; Korobkov, I.; Baker, R. T. *Organometallics* **2015**, *34* (18), 4598–4604.
(54) Harrison, D. J.; Daniels, A. L.; Korobkov, I.; Baker, R. T. *Organometallics* **2015**, *34* (24), 5683–5686.
(55) Frenking, G.; Solà, M.; Vyboishchikov, S. F. *J. Organomet. Chem.* **2005**, *690* (24–25), 6178–6204.
(56) Brothers, P. J.; Roper, W. R. *Chem. Rev.* **1988**, *88* (7), 1293–1326.
(57) Dixon, D. A. *J. Phys. Chem.* **1986**, *90* (1), 54–56.
(58) Dalma´zio, I.; Anderson Duarte, H. *J. Chem. Phys.* **2001**, *115* (4).
(59) Reger, D. L.; Dukes, M. D. *J. Organomet. Chem.* **1978**, *153* (1), 67–72.
(60) Koola, J. D.; Roddick, D. M. *Organometallics* **1991**, *10* (3), 591–597.
(61) Huang, D.; Caulton, K. G. *J. Am. Chem. Soc.* **1997**, *119* (13), 3185–3186.

(62) Fustero, S.; Simón-Fuentes, A.; Barrio, P.; Haufe, G. *Chem. Rev.* **2015**, *115* (2), 871–930.
(63) Chatterjee, A. K.; Choi, T.-L.; Sanders, D. P.; Grubbs, R. H. *J. Am. Chem. Soc.* **2003**, *125* (37), 11360–11370.
(64) Takahira, Y.; Morizawa, Y. *J. Am. Chem. Soc.* **2015**, *137* (22), 7031–7034.
(65) Krause, L. J.; Morrison, J. A. *J. Am. Chem. Soc.* **1981**, *103* (11), 2995–3001.
(66) Clark, G. R.; Hoskins, S. V.; Jones, T. C.; Roper, W. R. *J. Chem. Soc. Chem. Commun.* **1983**, No. 13, 719–721.
(67) Roper, W. R. *J. Organomet. Chem.* **1986**, *300* (1), 167–190.
(68) Hughes, R. P.; Laritchev, R. B.; Yuan, J.; Golen, J. A.; Rucker, A. N.; Rheingold, A. L. *J. Am. Chem. Soc.* **2005**, *127* (43), 15020–15021.
(69) Yuan, J.; Hughes, R. P.; Rheingold, A. L. *Eur. J. Inorg. Chem.* **2007**, *2007* (30), 4723–4725.
(70) Wang, F.; Luo, T.; Hu, J.; Wang, Y.; Krishnan, H. S.; Jog, P. V.; Ganesh, S. K.; Prakash, G. K. S.; Olah, G. A. *Angew. Chem. Int. Ed.* **2011**, *50* (31), 7153–7157.
(71) Clark, G. R.; Hoskins, S. V.; Roper, W. R. *J. Organomet. Chem.* **1982**, *234* (1), C9–C12.
(72) Huang, H.; Hughes, R. P.; Rheingold, A. L. *Dalton Trans.* **2011**, *40* (1), 47–55.
(73) Huang, H.; Hughes, R. P.; Landis, C. R.; Rheingold, A. L. *J. Am. Chem. Soc.* **2006**, *128* (23), 7454–7455.
(74) Trnka, T. M.; Day, M. W.; Grubbs, R. H. *Angew. Chem. Int. Ed.* **2001**, *40* (18), 3441–3444.
(75) Wiemers, D. M.; Burton, D. J. *J. Am. Chem. Soc.* **1986**, *108* (4), 832–834.
(76) Yang, Z. Y.; Wiemers, D. M.; Burton, D. J. *J. Am. Chem. Soc.* **1992**, *114* (11), 4402–4403.
(77) Deng, X.-Y.; Lin, J.-H.; Xiao, J.-C. *Org. Lett.* **2016**, *18* (17), 4384–4387.
(78) Fuchibe, K.; Aono, T.; Hu, J.; Ichikawa, J. *Org. Lett.* **2016**, *18* (18), 4502–4505.
(79) Goswami, M.; Bruin, B. de; Dzik, W. I. *Chem. Commun.* **2017**, *53* (31), 4382–4385.
(80) Hoveyda, A. H.; Zhugralin, A. R. *Nature* **2007**, *450* (7167), 243–251.
(81) Ivin, K. J.; Rooney, J. J.; Stewart, C. D.; Green, M. L. H.; Mahtab, R. *J. Chem. Soc. Chem. Commun.* **1978**, No. 14, 604–606.
(82) Cossee, P. *J. Catal.* **1964**, *3* (1), 80–88.
(83) Arlman, E. J.; Cossee, P. *J. Catal.* **1964**, *3* (1), 99–104.
(84) Clawson, L.; Soto, J.; Buchwald, S. L.; Steigerwald, M. L.; Grubbs, R. H. *J. Am. Chem. Soc.* **1985**, *107* (11), 3377–3378.
(85) Yuan, J.; Hughes, R. P.; Golen, J. A.; Rheingold, A. L. *Organometallics* **2010**, *29* (8), 1942–1947.
(86) Burch, R. R.; Calabrese, J. C.; Ittel, S. D. *Organometallics* **1988**, *7* (7), 1642–1648.
(87) Murphy, E. F.; Murugavel, R.; Roesky, H. W. *Chem. Rev.* **1997**, *97* (8), 3425–3468.
(88) Bottomley, F.; Paez, D. E.; White, P. S. *J. Organomet. Chem.* **1985**, *291* (1), 35–41.
(89) Murphy, E. F.; Yu, P.; Dietrich, S.; Roesky, H. W.; Parisini, E.; Noltemeyer, M. *J. Chem. Soc. Dalton Trans.* **1996**, No. 9, 1983–1987.
(90) Antiñolo, A.; Lappert, M. F.; Singh, A.; Winterborn, D. J. W.; Engelhardt, L. M.; Raston, C. L.; White, A. H.; Carty, A. J.; Taylor, N. J. *J. Chem. Soc. Dalton Trans.* **1987**, No. 6, 1463–1472.
(91) Gowik, P.; Klapötke, T.; Thewalt, U. *J. Organomet. Chem.* **1990**, *385* (3), 345–350.
(92) Roesky, H. W.; Sotoodeh, M.; Xu, Y. M.; Schrumpf, F.; Noltemeyer, M. *Z. Anorg. Allg. Chem.* **1990**, *580* (1), 131–138.
(93) Roesky, H. W.; Schrumpf, F.; Noltemeyer, M. *J. Chem. Soc. Dalton Trans.* **1990**, No. 2, 713–714.
(94) Thomas, B. J.; Mitchell, J. F.; Theopold, K. H.; Leafy, J. A. *J. Organomet. Chem.* **1988**, *348* (3), 333–342.
(95) Ellis, R.; Henderson, R. A.; Hills, A.; Hughes, D. L. *J. Organomet. Chem.* **1987**, *333* (1), C6–C10.
(96) Green, M. L. H.; Hughes, A. K.; Lincoln, P.; Martin-Polo, J. J.; Mountford, P.; Sella, A.; Wong, L.-L.; Bandy, J. A.; Banks, T. W.; Prout, K.; Watkin, D. J. *J. Chem. Soc., Dalton Trans.* **1992**, No. 13, 2063–2069.
(97) Abel, E. W.; Towle, I. D. H.; Cameron, T. S.; Cordes, R. E. *J. Chem. Soc., Dalton Trans.* **1979**, No. 12, 1943–1949.

(98) Brewer, S. A.; Coleman, K. S.; Fawcett, J.; Holloway, J. H.; Hope, E. G.; Russell, D. R.; Watson, P. G. *J. Chem. Soc. Dalton Trans.* **1995**, No. 7, 1073–1076.
(99) Bennett, B. K.; Harrison, R. G.; Richmond, T. G. *J. Am. Chem. Soc.* **1994**, *116* (24), 11165–11166.
(100) Burch, R. R.; Harlow, R. L.; Ittel, S. D. *Organometallics* **1987**, *6* (5), 982–987.
(101) Veltheer, J. E.; Burger, P.; Bergman, R. G. *J. Am. Chem. Soc.* **1995**, *117* (50), 12478–12488.
(102) Vabre, B.; Petiot, P.; Declercq, R.; Zargarian, D. *Organometallics* **2014**, *33* (19), 5173–5184.
(103) Watson, D. A.; Su, M.; Teverovskiy, G.; Zhang, Y.; García-Fortanet, J.; Kinzel, T.; Buchwald, S. L. *Science* **2009**, *325* (5948), 1661–1664.
(104) Anderson, C. M.; Crespo, M.; Ferguson, G.; Lough, A. J.; Puddephatt, R. J. *Organometallics* **1992**, *11* (3), 1177–1181.
(105) Vergote, T.; Nahra, F.; Welle, A.; Luhmer, M.; Wouters, J.; Mager, N.; Riant, O.; Leyssens, T. *Chem. – Eur. J.* **2012**, *18* (3), 793–798.
(106) Mankad, N. P.; Toste, F. D. *J. Am. Chem. Soc.* **2010**, *132* (37), 12859–12861.
(107) Kiplinger, J. L.; Richmond, T. G. *J. Am. Chem. Soc.* **1996**, *118* (7), 1805–1806.
(108) Smith, D. A.; Beweries, T.; Blasius, C.; Jasim, N.; Nazir, R.; Nazir, S.; Robertson, C. C.; Whitwood, A. C.; Hunter, C. A.; Brammer, L.; Perutz, R. N. *J. Am. Chem. Soc.* **2015**, *137* (36), 11820–11831.
(109) Campbell, M. G.; Ritter, T. *Chem. Rev.* **2015**, *115* (2), 612–633.
(110) Osterberg, C. E.; King, M. A.; Arif, A. M.; Richmond, T. G. *Angew. Chem. Int. Ed. Engl.* **1990**, *29* (8), 888–890.
(111) Poulton, J. T.; Sigalas, M. P.; Folting, K.; Streib, W. E.; Eisenstein, O.; Caulton, K. G. *Inorg. Chem.* **1994**, *33* (7), 1476–1485.
(112) Bourgeois, C. J.; Garratt, S. A.; Hughes, R. P.; Larichev, R. B.; Smith, J. M.; Ward, A. J.; Willemsen, S.; Zhang, D.; DiPasquale, A. G.; Zakharov, L. N.; Rheingold, A. L. *Organometallics* **2006**, *25* (14), 3474–3480.
(113) Liang, T.; Neumann, C. N.; Ritter, T. *Angew. Chem. Int. Ed.* **2013**, *52* (32), 8214–8264.
(114) Furuya, T.; Benitez, D.; Tkatchouk, E.; Strom, A. E.; Tang, P.; Goddard, W. A.; Ritter, T. *J. Am. Chem. Soc.* **2010**, *132* (11), 3793–3807.
(115) Pérez-Temprano, M. H.; Racowski, J. M.; Kampf, J. W.; Sanford, M. S. *J. Am. Chem. Soc.* **2014**, *136* (11), 4097–4100.
(116) Zhao, S.-B.; Becker, J. J.; Gagné, M. R. *Organometallics* **2011**, *30* (15), 3926–3929.
(117) Hollingworth, C.; Gouverneur, V. *Chem. Commun.* **2012**, *48* (24), 2929–2942.
(118) Grushin, V. V.; Marshall, W. J. *Organometallics* **2007**, *26* (20), 4997–5002.
(119) Lee, H. G.; Milner, P. J.; Buchwald, S. L. *J. Am. Chem. Soc.* **2014**, *136* (10), 3792–3795.
(120) Katcher, M. H.; Doyle, A. G. *J. Am. Chem. Soc.* **2010**, *132* (49), 17402–17404.
(121) Katcher, M. H.; Sha, A.; Doyle, A. G. *J. Am. Chem. Soc.* **2011**, *133* (40), 15902–15905.
(122) Katcher, M. H.; Norrby, P.-O.; Doyle, A. G. *Organometallics* **2014**, *33* (9), 2121–2133.
(123) Mu, X.; Zhang, H.; Chen, P.; Liu, G. *Chem. Sci.* **2013**, *5* (1), 275–280.
(124) Dang, H.; Mailig, M.; Lalic, G. *Angew. Chem. Int. Ed.* **2014**, *53* (25), 6473–6476.

Chapter 2

Reactions of Cobalt Fluorocarbenes with Terminal Aryl-alkynes to give Metallacyclobutenes

2.1 Context and Objectives

Metallacyclobutene complexes are important intermediates in organometallic catalysis, particularly for processes such as enyne metathesis and alkyne polymerization.[1–4] However, *isolable* metallacyclobutenes are relatively uncommon owing to their inherent ring strain, which promotes reactivity. Tebbe and coworkers pioneered work on isolated early-metal metallacyclobutenes,[5] while O'Connor and coworkers isolated cobaltacyclobutene complexes and systematically studied their reactivity.[6,7] The latter work represents the only systematic study of late-metal metallacyclobutene reactivity to date.

In our previous work we prepared the first examples of isolable cobalt fluorocarbene complexes, with formal d^8 electron configurations, and demonstrated their relatively nucleophilic Co=C bonds through reactions with H^+ and Me^+ and stability toward water.[8] We followed these findings with the preparation of new cobalt fluorocarbenes bearing the electron donating ligand PPh_2Me, and their reactivity with tetrafluoroethylene (TFE) to form perfluorometallacyclobutane complexes.[9] This represented the first examples of cycloaddition reactions between a perfluoroalkene and metal perfluorocarbene complexes, and computational investigations into metallacyclobutane formation revealed a stepwise mechanism via a singlet diradical intermediate.[10]

The work in Chapter 2 aims to expand the reactivity of nucleophilic cobalt fluorocarbene complexes to electron deficient alkynes. The reactions furnish isolable, partially-fluorinated cobaltacyclobutene complexes, which are characterized structurally and spectroscopically. Finally, the mechanism of

metallacycle formation is investigated using detailed kinetic studies and DFT calculations, providing further evidence for a 1,4-diradical intermediate.

2.1.1 Published Contributions

Experimental and Computational Evidence for 1,4-Diradical Intermediates in Reactions of Cobalt Fluorocarbene Complexes with Terminal Aryl-alkynes to give Metallacyclobutenes

Lee, G. M.; Leung, A. S. C.; Harrison, D. J.; Korobkov, I.; Hughes, R. P.; Baker, R. T. *Organometallics*, **2017**, *36* (15), 2853-2860.

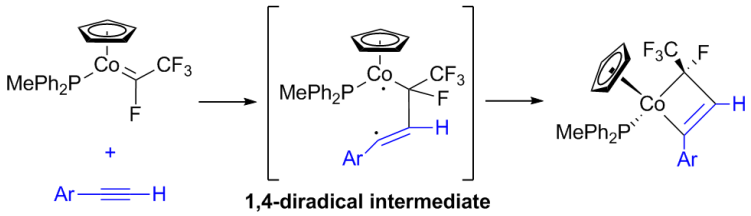

Abstract: Cobalt fluorocarbene complex CpCo(=CF(CF_3))(PPh_2Me) (Cp = η^5-cyclopentadienyl) reacts with *para* substituted phenyl-acetylenes to furnish partially fluorinated cobaltacyclobutene complexes [Cp(PPh_2Me)Co{κ^2-C(Ar)=CHCF(CF_3)}], which were isolated and characterized by elemental analysis, multinuclear NMR and UV-vis spectroscopy and X-ray crystallography. The scope of reactivity between CpCo(=CFR^F)(L) and various alkynes was explored. The detailed pathway for the [2+2] cycloaddition reaction was investigated using a combination of kinetic studies and DFT computational chemistry (M06/def2-TZVP), with a 1,4 diradical species identified as the key intermediate.

Author Contributions: The manuscript was written by GML, RPH, and RTB. GML performed all experiments presented in the paper, except for preparation of complexes **2b-d** and their associated rate studies, which were performed by ASCL under the supervision of GML. Computational studies by RPH. X-ray crystallography by IK.

2.2 Experimental and Computational Evidence for 1,4-Diradical Intermediates in Reactions of Cobalt Fluorocarbene Complexes with Terminal Aryl-alkynes to give Metallacyclobutenes

2.2.1 Introduction

Metallacyclobutene complexes are proposed to be important intermediates or transition states in metal-catalyzed C-C bond forming reactions, such as enyne/"ynene" metathesis,[1,2,11] alkyne polymerization,[3,4,12] and cyclopropenation.[13] Cationic β-diketiminate titanium complexes which catalyze the carboamination and hydrophosphination of diphenylacetylene are proposed to form metallacyclobutenes as part of the catalytic cycle.[14] Furthermore, metallacyclobutenes are intermediates in stoichiometric reactions between zero-valent iron[15] and tungsten[16] complexes and alkynes.

In contrast to those highly reactive species which elude full characterization, metallacyclobutenes can also be sufficiently stable for isolation and structural analysis when the appropriate combination of metal, ancillary ligand(s), and ring substituents are employed, offering opportunities for systematic study of the formation and reactivity of unsaturated metallacycles. Reported examples of isolated metallacyclobutenes are highly varied in terms of structure and synthetic pathway employed for their formation, and several examples are shown in Scheme 2.1. Titanacyclobutene complexes $Cp_2Ti[\kappa^2\text{-}C(R)=CRCH_2]$ (Cp = η^5-cyclopentadienyl, R = Ph or $SiMe_3$) were prepared by Tebbe and co-workers via reaction of alkynes (RC≡CR) with $Cp_2TiCH_2AlClMe_2$.[5,17] Perfluorinated metallacyclobutenes were synthesized by Hughes and co-workers via oxidative addition of perfluorocyclopropene to platinum(0) and iridium(I) complexes.[18,19] An important advance was made by O'Connor and co-workers with the preparation of cobaltacyclobutene $Cp(PPh_3)Co[\kappa^2\text{-}C(SO_2Ph)=C(SiMe_3)CH(CO_2Et)]$ by treating the cobalt-alkyne complex $CpCo(PPh_3)(\eta^2\text{-}Me_3SiC{\equiv}CSO_2Ph)$ with the carbene source ethyl diazoacetate.[6] This discovery led to the first systematic reactivity studies of late-metal metallacyclobutenes, and remains the most thoroughly studied metallacyclobutene system to date.[20–28] Yet another synthetic route to late-metal metallacyclobutenes is the addition of nucleophiles to allenyl or propargyl complexes, used to make complexes of rhenium, as well as

platinum and iridium.[29–31] Finally, ruthenium metallaphosphacyclobutenes have been prepared by Rosenberg and co-workers via addition of alkynes to terminal phosphido complexes.[32]

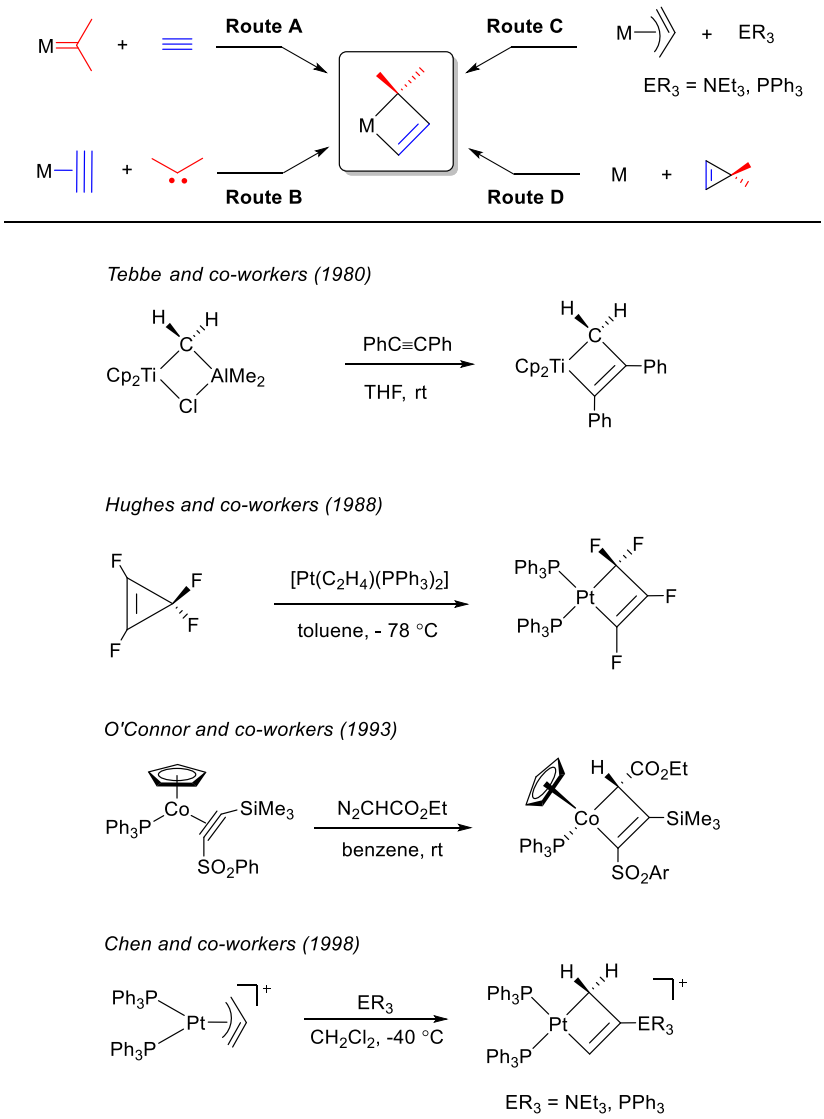

Scheme 2.1. Examples of synthetic routes to metallacyclobutene complexes.

In recent reports, we described the synthesis of several nucleophilic (d^8) cobalt fluorocarbene complexes, including $CpCo(=CF_2)(PPh_2Me)$ (**1a**), $CpCo(=CF(CF_3))(PPh_2Me)$ (**1b**), and $CpCo(=CF(CF_3))(PPh_3)$ (**1c**).[8,9] These fluorocarbene complexes undergo cycloaddition reactions with electrophiles, including [2+1] addition with difluorocarbene ($:CF_2$) to form metallacyclopropanes,[33] and [2+2] addition with C_2F_4 (TFE)

to form metallacyclobutanes.[9] The mechanism of the reaction between **1a** and C_2F_4 was investigated using DFT, and found to proceed via a unique stepwise pathway involving a 1,4-diradical intermediate (Scheme 2.2).[10]

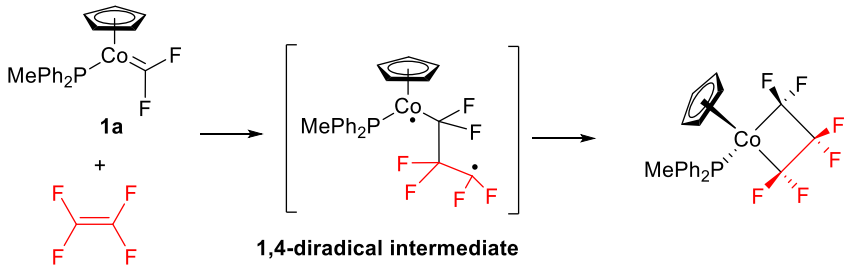

Scheme 2.2. Previously reported pathway for [2+2] cycloaddition reaction of $CpCo(=CF_2)(PPh_2Me)$ and C_2F_4 (TFE).

The perfluorinated nature of the carbene/alkene brings stability to the 1,4-diradical intermediate by forming a strong new CF_2-CF_2 bond, breaking weak Co=C and C=C □-bonds, coupled with the unusual stability of the terminal difluoromethylene radical.

As part of our group's efforts to develop the chemistry of cobalt fluorocarbenes and fluoro-metallacycles, we sought to expand upon the cycloaddition reactions previously reported for $[Co]=CFR^F$, and envisioned the formation of partially-fluorinated cobaltacyclobutenes resulting from analogous reactivity between $CpCo(=CFR^F)(L)$ complexes and alkynes.

2.2.2 Results and Discussion

2.2.2.1 Synthesis of Metallacyclobutenes

It was shown previously that **1b** exhibits enhanced reactivity towards cycloaddition reactions relative to **1a** and **1c**, so we first studied the reaction of **1b** with phenylacetylene (PhC≡CH). When PhC≡CH was added to a stirring navy blue solution of **1b** in toluene, the mixture gradually turned deep red, and the partially fluorinated cobaltacyclobutene complex **2a** was produced, which could be isolated as a red solid in 77% yield (Scheme 2.3). Similarly, *para* substituted phenylacetylene derivatives reacted with **1b** to form **2b, 2c**,

and **2d**, which were also isolated as reddish/brown solids in good yield (66-70%). It was necessary to use 2-4 equivalents of acetylene to ensure complete conversion of **1b** to **2**.

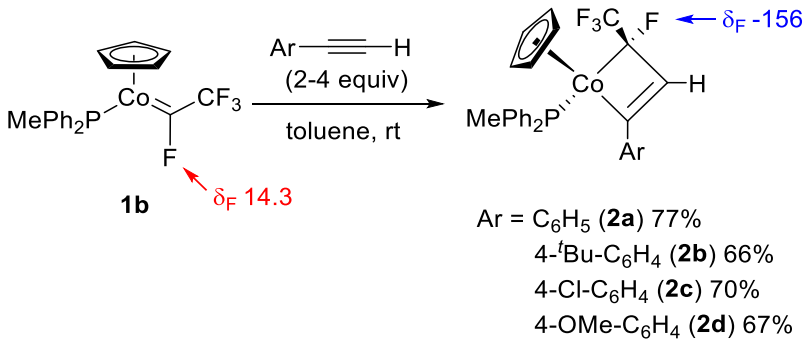

Scheme 2.3. Preparation of cobaltacyclobutene complexes.

Cobaltacyclobutenes **2a-d** were fully characterized using elemental analysis, NMR, UV-Vis spectroscopy and single crystal X-ray diffraction, and exhibit the same general spectroscopic and structural features. In particular, the ^{19}F NMR signals for C_α-F are highly characteristic. Upon formation of **2**, the carbene carbon of **1** undergoes a re-hybridization from sp^2 to sp^3 geometry, resulting in a large upfield shift in the ^{19}F NMR signal that corresponds to Cα-F, from 14.3 ppm in **1** to approximately -156 ppm in **2**. The C_α-F signal appears as an apparent sextet, due to coupling to the CF_3 group ($^3J_{FF}$ = 14 Hz) as well as the phosphorus ligand ($^3J_{FP}$ = 28 Hz). There is only a small coupling between C_α-F and C_β-H of the cyclobutene ring ($^3J_{FH}$ < 3 Hz). This is illustrated by the slight sharpening of the ^{19}F spectrum relative to that of the proton decoupled ^{19}F{^{1}H} spectrum of **2a** (Fig S23). The ^{31}P{^{1}H} NMR signal for the PPh_2Me ligand appears as a broad resonance at 47.8 ppm, due to proximity with the quadrupolar ^{59}Co nucleus (I = 7/2).

The molecular structure of **2a** (Figure 2.1) confirms the regio- and stereoselectivity of the formal [2+2] addition of PhC≡CH to **1**, with the CF_3 group anti to the phosphine ligand. The sum of the angles within the metallacyclobutene ring is 359.8°, indicating planarity. The torsion angle between C_β-H and C_α-F is 55.94°, which, in accordance with a Karplus-type equation relating vicinal proton-fluorine coupling to H-C-C-F torsion angles, is consistent with the observed $^3J_{HF}$ of less than 3 Hz.[34]

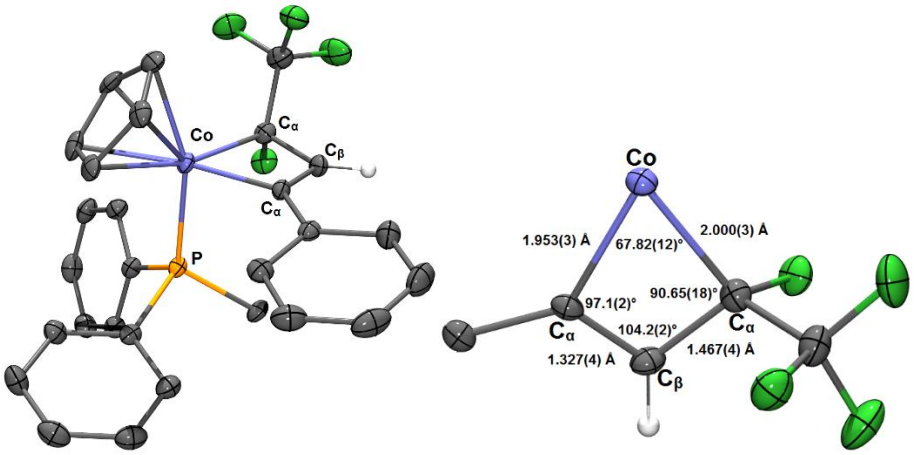

Figure 2.1. ORTEP representation of the molecular structure of 2a with 30% probability ellipsoids. Hydrogen atoms (except C_β-H) omitted for clarity.

Metallacyclobutene complexes **2a-d** are stable in the solid-state for several weeks at ambient temperature under N_2, but were generally stored at -35 °C. Additionally, complex **2a** was found to be stable in the solid-state under ambient air for 3 days. In toluene or benzene solutions, however, the metallacyclobutenes begin to slowly decompose after 24 hours, evidenced by solutions turning from red to brown in color, and broadening of the NMR spectra, indicative of formation of paramagnetic (likely Co^{II}) complexes. When dissolved in more polar solvents (Et_2O, THF, CH_3CN, CH_2Cl_2, $CHCl_3$ or DMF) the solutions change from red to deep purple in color, and NMR analysis again indicates the formation of paramagnetic species. Attempts to study this purple residue crystallographically were unsuccessful.

2.2.2.2 Scope of Alkyne Cycloaddition with Cobalt Fluorocarbene Complexes

Metallacyclobutene formation and stability is understood to be highly sensitive to the ring substituents as well as ancillary ligands on the metal. We have found this to be particularly true with regard to the reaction between cobalt fluorocarbenes and alkynes. We explored the reactivity of **1b** with various alkynes beyond phenylacetylene derivatives. When a C_6D_6 solution of **1b** was stirred with 5 equivalents of either diphenylacetylene (PhC≡CPh) or 3-hexyne (EtC≡CEt) for 24 hours, no reaction took place. Similarly, C_6D_6 solutions of **1b** did not react with 5 equivalents of terminal alkynes ^{t}BuC≡CH or Me_3SiC≡CH.

Changing the ancillary ligand of the cobaltacyclobutene from PPh_2Me to the less basic PPh_3 had a dramatic effect on the stability of the metallacyclic product. When PhC≡CH was added to a stirring solution of **1c** in C_6D_6, the only compounds visible using $^{31}P\{^1H\}$ NMR were **1c** and free PPh_3, with full conversion of **1c** taking place overnight. At this point, analysis of the reaction mixture via ^{19}F NMR revealed the formation of at least 5 reaction products which could not be identified, none of which were present in >20% yield. Three resonances with ^{19}F NMR shifts at δ -190.8 ppm, -190.2 ppm, and -153.2 ppm, consistent with sp^3 hybridized C_α-F groups resulting from metallacycle formation were observed. The general picture we propose based on these data is that metallacyclobutene **4** is likely formed, followed by rapid PPh_3 dissociation to generate a highly reactive 16 e^- species, which leads to formation of the multiple decomposition products observed (Scheme 2.4). Attempts to trap the intermediate using PMe_3, PPh_2Me, or $P(OMe)_3$ were unsuccessful.

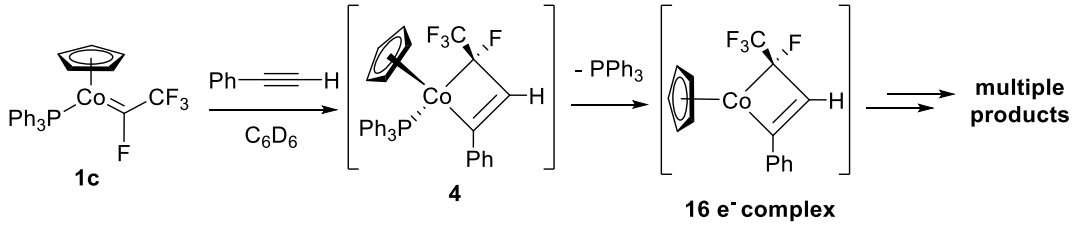

Scheme 2.4. Reactivity of **1c** with PhC≡CH.

Finally, changing the cobalt fluorocarbene from [Co]=CF(CF_3) complex **1b** to [Co]=CF_2 **1a** significantly inhibited the rate of the cycloaddition reaction. PhC≡CH (4 equiv) was added to a stirring solution of **1a** (1 equiv) in toluene-d^8 which was then heated to 50 °C for 18 hours. Analysis of the crude reaction mixture using NMR revealed very broad features in the ^1H spectrum, and the ^{19}F spectrum showed only starting material **1a** and metallacyclobutene product **5** in an 80:20 ratio (Scheme 2.5). The splitting pattern for **5** in the ^{19}F NMR was fully resolved after filtration through Celite, and consisted of two unique signals at δ -62.8 (dd, $^2J_{FF}$ = 174 Hz, $^3J_{FP}$ = 8 Hz) and -69.7 (dd, $^2J_{FF}$ = 174 Hz, $^3J_{FP}$ = 19 Hz), characteristic of geminal fluorines in a 4-membered metallacycle. The significant broadening of the NMR features, poor signal

lock/shim, and precipitation of a brown solid in the NMR tube are consistent with a reduced stability of cobaltacyclobutene **5** compared with **2a**.

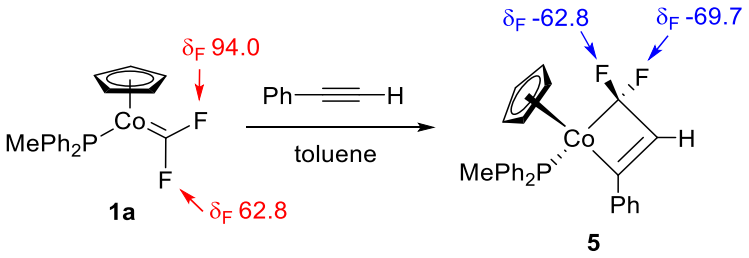

Scheme 2.5. Formation of metallacyclobutene **5**.

Under identical conditions it seems clear that the reaction of **1a** with phenylacetylene is significantly slower than that of **1b**. We attempted to increase the rate of formation of **5** by increasing the concentration of PhC≡CH in the reaction. By adding 25 equivalents of PhC≡CH to a stirring toluene solution of **1a**, and subsequently adding 7.5 equivalents of acetylene every 24 hours, **5** was formed as 77% of the reaction mixture after 4 days, as determined by ^{19}F NMR analysis (14% of **1a** remained, and 9% is associated with unidentified products). Attempts to isolate **5** resulted in partial decomposition and were unsuccessful.

2.2.2.3 Kinetic Studies of Metallacyclobutene Formation

The kinetics of the reaction between **1b** and PhC≡CH were investigated. Monitoring the reaction between **1b** and 10 equiv. PhC≡CH in toluene:C_6D_6 (9:1) at room temperature using ^{19}F NMR revealed near linear growth of [**2a**] during the first 10% of the reaction (Figure 2.2). As such, the initial rate was measured under a range of conditions, by monitoring the concentration of **1b** and **2a** over time using ^{19}F NMR integration versus an internal standard (1,3-bis(trifluoromethyl)benzene).

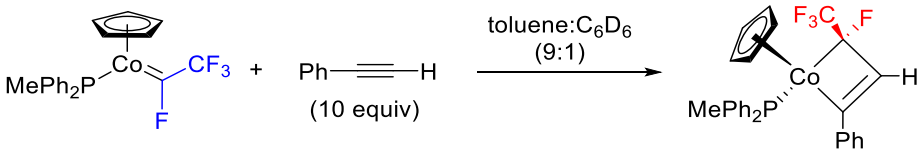

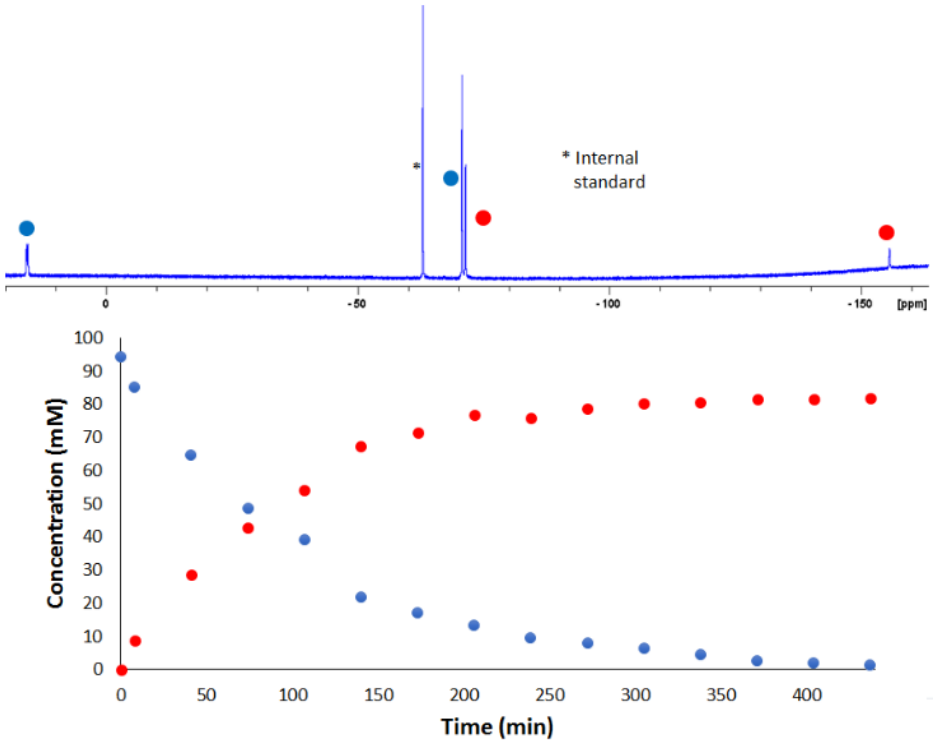

Figure 2.2. Reaction scheme (top), selected ^{19}F NMR spectrum (middle), and kinetic profile (bottom) of the reaction between **1b** and PhC≡CH.

The initial rate showed a linear dependence (R^2 = 0.994) on both $[\mathbf{1b}]_0$ and $[PhC{\equiv}CH]_0$ (Fig. S12-S13). The kinetic profile showed an excellent linear correlation (R^2 = 0.998) when fitted to the second order rate law in eq 1.

$$\ln\frac{[PhC{\equiv}CH][\mathbf{1}]_0}{[\mathbf{1}][PhC{\equiv}CH]_0} = k([PhC{\equiv}CH]_0 - [\mathbf{1}]_0)t \quad \text{(eq 1)}$$

From this, the second-order rate constant k = 1.07 x 10^{-5} $(mM\cdot s)^{-1}$ was extracted (Fig S14). As noted earlier, the reaction between **1b** and PhC≡CH is significantly faster than that of **1a** and PhC≡CH, with the half-life of the former being approximately 80 minutes compared to approximately 40 hours for the latter. As an additional comparison, the previously reported reaction between **1a** and C_2F_4 had a half-life of approximately 20 hours, and also required a large excess of C_2F_4.

The activation parameters for the formation of metallacyclobutene **2a** were obtained from an Eyring plot (Figure 2.3), which was produced by measuring the initial rate of reaction at various temperatures between 30 and 50 °C. The experimentally determined value for $\Delta G^{\ddagger}_{298}$ of 21.1 ± 0.2 kcal/mol was in excellent agreement with the calculated value (see below).

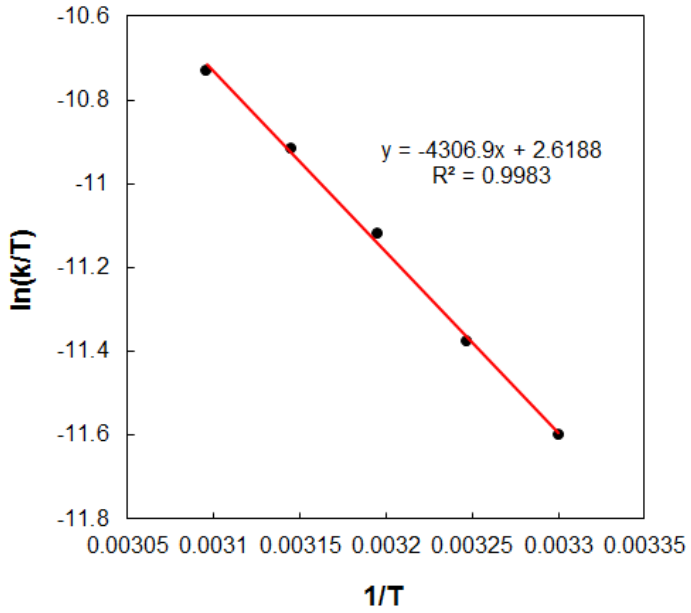

Figure 2.3. Eyring plot for the formation of **2a** (30-50 °C). Experimentally determined activation parameters: $\Delta H^{\ddagger}$ = 8.6 (± 0.2) kcal/mol, $\Delta S^{\ddagger}$ = -40 (± 7) e.u., $\Delta G^{\ddagger}_{298}$ = 21.1 (± 0.2) kcal/mol.

To determine if phosphine dissociation from **1** was necessary for the reaction with PhC≡CH to proceed, the initial rate of formation of **2a** was measured at 40°C with and without the presence of 3.8 equiv PPh_2Me (Figure S15). The control rate was measured at 0.34 mM/min compared to 0.38 mM/min with added phosphine, a slight increase. These observations are consistent with PhC≡CH addition proceeding without phosphine dissociation from the metal, similar to the reaction between **1a,b** and C_2F_4.

The rate effects of *para* substituents on phenylacetylene were also examined experimentally. A Hammett study was conducted by measuring the initial rate of reaction between **1b** and a series of commercially available *p*-substituted phenylacetylene derivatives (*p*-substituent = H, Me, Cl, OMe, OPh, ^{t}Bu). From these

data, the k_X/k_H ratio was calculated and graphs of $\log(k_X/k_H)$ versus a series of substituent constants (σ, σ^+, σ^-, $\sigma^{\cdot}_{\alpha}$ and $c\sigma_p$)[35–37] were plotted.

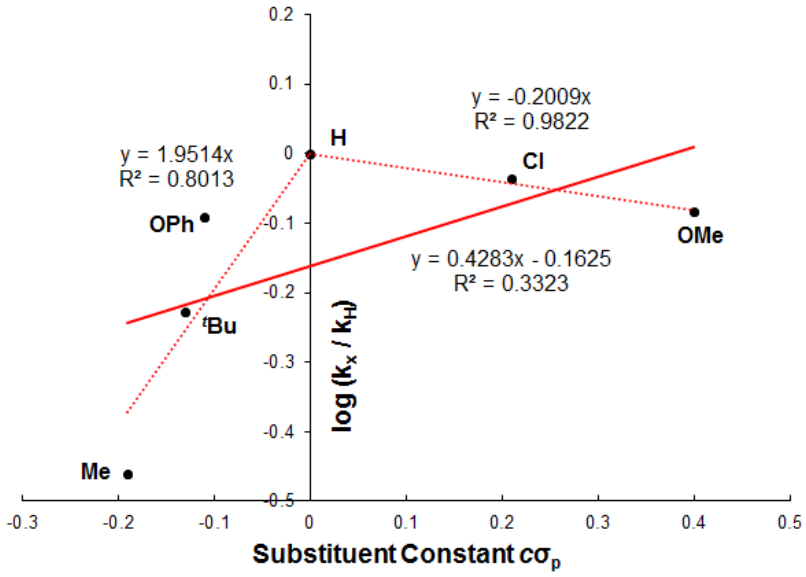

Figure 2.4. Hammett plot for *p*-substituted phenylacetylenes (25 °C). The solid red line indicates the linear fit for all substituents, while the dotted red lines are the linear fits for substituents bearing either negative or positive $c\sigma_p$ values.

When the data were analyzed using the substituent constants σ, σ^+, and σ^-, linear correlation coefficients were very poor and ρ values were between 0 and 0.503, indicating the reaction is insensitive to electronic perturbation at the *p*-position (Fig. S16-S18). Similarly, when the benzyl radical derived substituent constants $\sigma^{\cdot}_{\alpha}$ were analyzed, the ρ value was -2.4 with a very poor linear correlation coefficient ($R^2 = 0.035$) (Figure S19). When the $c\sigma_p$ constants were applied (which are appropriately derived from a ^{19}F NMR shift method), the data warranted consideration of two possible interpretations of the data (dashed and solid red lines, Figure 2.4). One interpretation (dashed red lines) features a concave down shape, with a maximum centered at the origin (H), and correlation coefficients 0.80 and 0.98. A concave down Hammett curve is typically indicative of a change in the rate-determining step,[38] and while it is intriguing to contemplate this scenario in light of our proposed stepwise reaction pathway, the computational data discussed below strongly suggest there is no change in the rate determining step. Therefore, we believe the second

interpretation is correct: a very poor linear correlation coefficient of 0.33 (ρ = 0.43) (solid red line) indicates that *para* substitution on the phenylacetylene has essentially no effect on the reaction pathway.

2.2.2.4 DFT Studies of Metallacyclobutene Formation

The reactions between **1a,b** with a variety of para-substituted phenylacetylenes to furnish cobaltacylobutenes were investigated using DFT, using the full molecules at the M06/def2-TZVP//M06/LACVP** level, with an implicit THF Poisson-Boltzmann solvent model. This combination of functional and basis set gave very good agreement with crystallographically determined parameters of the carbene precursors and metallacyclobutene products. Full details are available as Supporting Information.

Table 2.1. Calculated relative free energies (M06/def2-TZVP/THF) for metallacyclobutene formation with *p*-substituted phenyl-acetylenes; Values for diradical TS1 and INT are Spin-Projected.

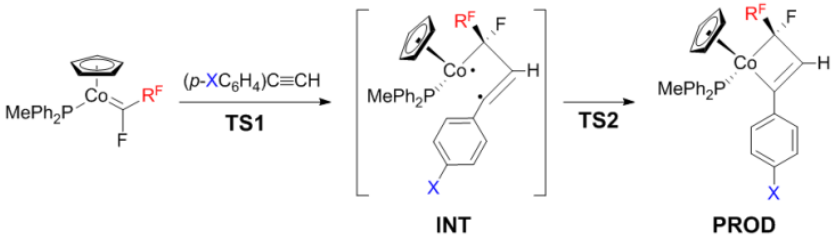

entry	R^F	X	ΔG^{TS1}	ΔG^{INT}	ΔG^{PROD}
1	F	H	27.7	5.8	-16.6
2	F	Cl	27.3	6.7	-17.5
3	F	Me	27.8	5.3	-16.7
4	F	NO_2	23.2	3.8	-17.3
5	F	NMe_2	29.5	8.3	-14.9
6	CF_3	H	21.3	1.3	-24.3
7	CF_3	Cl	20.5	1.0	-25.1
8	CF_3	Me	20.9	1.0	-23.3
9	CF_3	NO_2	17.7	-0.3	-25.9
10	CF_3	NMe_2	20.5	0.8	-22.5

Relative free energies are presented in Table 1, and graphically for phenylacetylene reactions in Figure 2.5. Reactions of **1a,b** with the parent phenylacetylene to give metallacyclobutene products **2a** and **5** are

calculated to be strongly downhill, with the formation of **2a** being almost 8 kcal/mol more exoergic than that of **5**. As with previous calculations on the reaction between **1a** and C_2F_4,[14] the lowest energy pathway for the reactions of **1a,b** with PhC≡CH was found to proceed via an open shell singlet diradical intermediate **INT** formed in the rate limiting step via **TS1** (Figure 2.5). Subsequent closure of **INT** by radical coupling to give the product metallacyclobutene occurs via a very low energy **TS2**, which was located in the case of **1b**, but could not be found for the reaction of **1a** Clearly the first step of the reaction is rate limiting. The calculated spin-projected value for $\Delta G^{\ddagger}_{298}$ = 21.3 kcal/mol for the reaction of **1b** with PhC≡CH via **TS1** is in remarkably close agreement with the experimental value of $\Delta G^{\ddagger}_{298}$ = 21.1 (± 0.2) kcal/mol. In addition the reaction of **1a** with PhC≡CH via an analogous **TS1** has a calculated spin-projected barrier of $\Delta G^{\ddagger}_{298}$ = 27.7 kcal/mol, consistent with the experimentally observed difference in reactivity between **1a** and **1b**. The previously reported energy barrier for the reaction between **1a** and C_2F_4 was 27.8 kcal/mol, and unsurprisingly the reactions of **1a** with C_2F_4 and PhC≡CH have similar rates (see above). Given the significantly more exoergic formation of **2b** compared to **5**, it is perhaps not surprising that the spin-projected energies of the corresponding **INT** and **TS1** are also lower (Figure 2.5), and that the reaction of **1b** is faster than that of **1a**, with an expected earlier transition state. As found for C_2F_4 reactions,[14] the closed-shell zwitterionic singlet analogues of **INT** and **TS1** (Figure 2.5) lie >21 and >5 kcal/mol higher in free energy than their open-shell singlet diradical relatives.

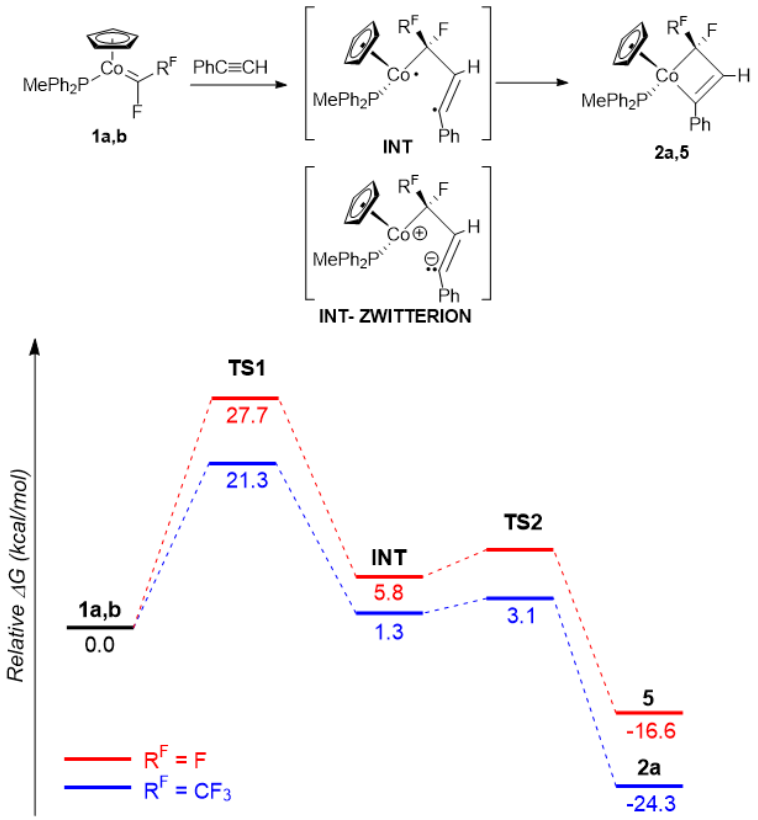

Figure 2.5. Calculated free energy profile (M06/def2-TZVP/THF) for reactions of **1a** (red) and **1b** (blue) with PhC≡CH to form cobaltacyclobutenes **5** and **2a**. All energies are relative to starting materials.

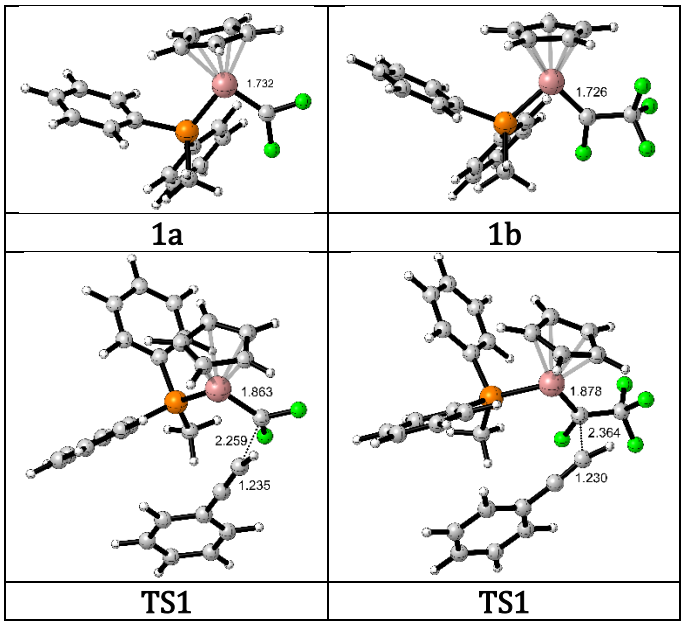

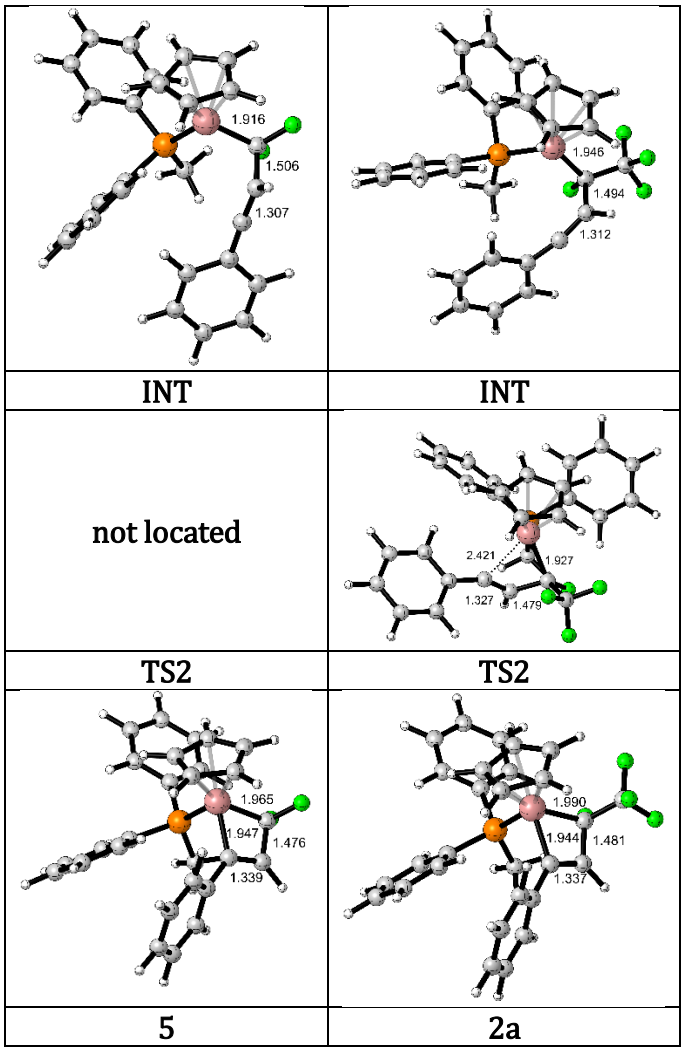

Figure 2.6. Calculated structures for **1a** and **1b**, the open shell singlet diradicals **TS1**,**INT**, **TS2**, and the metallacyclobutene products **2a**, **5** for reactions with PhC≡CH, including relevant bond lengths (Å).

The calculated structures of starting materials **1a,b**, the singlet diradical geometries of transition states **TS1**, **TS2** (for reaction of **1b**), and intermediate **INT**, and final metallacyclic products of their reactions with parent phenylacetylene are shown in Figure 2.6. The transition states **TS1** and **INT** geometries are conformationally different from those previously reported for the C_2F_4 reactions. The alkyne group is almost perpendicular to the [Co]=CFR^F bond, in contrast to the antiperiplanar conformations for the C_2F_4 reactions shown in Scheme 2.2. Consequently, for the alkyne system, less reorganization is required to access **TS2** and subsequently form the cobaltacyclobutene product.

In agreement with the idea of an earlier transition state (*vide supra*) for the reaction of **1b** the new C-C bond is less well developed in the transition state for **1b** (2.364Å) than for **1a** (2.259Å), even though the corresponding C-C bond in the intermediate is shorter for **1b** (1.494Å) than for **1a** (1.506Å).

The singlet diradical nature of the intermediates and their preceding transition states are illustrated by the calculated excess spin densities, as shown in Figure 2.7. In the transition states there is negligible spin delocalization into the aryl ring, in contrast to the corresponding intermediates.

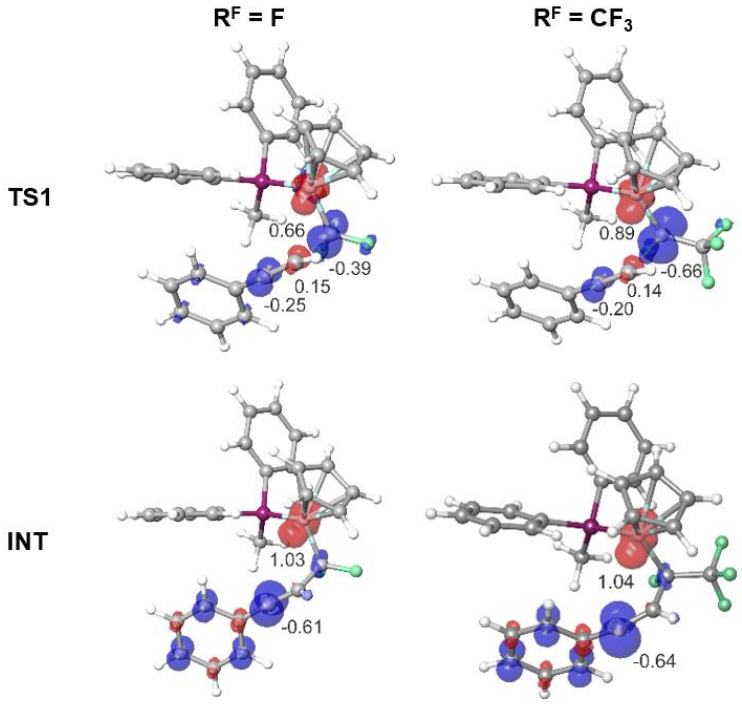

Figure 2.7. Calculated spin densities (α-β) for the singlet diradical **TS1** and **INT** species derived from the reactions between **1a,b** and PhC≡CH.

The analogous energetics for the reactions between **1a,b** and *para*-substituted phenylacetylenes are also presented in Table 1. The *para*-X substituents (X = H, Cl, Me, NO_2, NMe_2) were chosen to give a wide range of π-donor/acceptor effects, and include some substituents for which experimental data were also obtained. Entries 1 and 6 in Table 1 contain the values previously shown in Figure 2.5. It is clear from these data that the previously described trends hold: all reactions with **1b** are more exoergic than for **1a** and all reactions with **1b** are calculated to have significantly lower energy transition states. Notably, within each

series there is a relatively small span of values of ΔG^{TS1} for a range of substituents, with the lowest values calculated for NO_2; all other values cluster around that for the parent phenylacetylene. The relative insensitivity to para-substitution, but with *p*-NO_2 being slightly more stabilizing is characteristic of radical reactions. Unfortunately p-nitrophenylacetylene was unavailable as a substrate for experimental work. The insensitivity of reaction rate to para-subsitution is also consistent with negligible spin delocalization into the aromatic ring in the transition states (Figure 2.7).

2.2.3 Conclusions

We have isolated and characterized a series of partially fluorinated metallacyclobutene complexes from the reaction between cobalt fluorocarbenes and phenyacetylenes. Terminal acetylenes with electron withdrawing groups are required for metallacylobutene formation, and nucleophilic phosphines are required for product stability. DFT and kinetic studies determined that the reaction proceeds is a stepwise fashion, via rate limiting formation of a 1,4-diradical intermediate, with subsequent fast closure to give the product of overall [2+2] addition. A marked difference in the reactivity of $Co{=}CF_2$ and $Co{=}CFCF_3$ carbene precursors was noted, interpreted in terms of an earlier transition state in the $Co{=}CFCF_3$ system. However, substitution of phenylacetylenes at the *para* position was found to have no effect on the overall reaction mechanism, and a negligible effect on the rate, consistent with formation of a diradical intermediate and its preceding transition state.

2.3 Experimental Details for Section 2.2

2.3.1 General Information

Experiments were conducted under nitrogen, using Schlenk techniques or an MBraun glove box. All solvents were deoxygenated by purging with nitrogen. Toluene, hexanes, diethyl ether, dimethylformamide (DMF) and tetrahydrofuran (THF) were dried on columns of activated alumina using a J. C. Meyer (formerly Glass Contour®) solvent purification system. Dichloromethane (DCM), chloroform-*d* ($CDCl_3$), and acetonitrile-d_3(CD_3CN) were dried by refluxing over calcium hydride under a nitrogen flow, followed by distillation and filtration through a column of activated alumina (ca. 10 wt %). Benzene-d_6 (C_6D_6) was

dried by stirring over activated alumina (ca. 10 wt. %) overnight, followed by filtration. All solvents were stored over activated (heated at ca. 250 °C for >10 h under vacuum) 4 Å molecular sieves. The following chemicals were obtained commercially, as indicated: [$CpCo(CO)_2$] (Cp = cyclopentadienyl) (Strem, 95%), sodium (Alfa Aesar, 99%), mercury (Strem, 99.998%), CF_3I (SynQuest, 99%), CF_3CF_2I (SynQuest, 99%), PPh_2Me (Strem, 99%), phenylacetylene (Alfa Aesar, 98%), 4-*t*-butylphenylacetlyne (Strem, 96%), 4-Cl-phenylacetylene (Strem, 98%), 4-OMe-phenylacetylene (Strem, 97%), 4-Me-phenylacetylene (Strem, 97%), 4-OPh-phenyacetylene (Strem, 97%), diphenylacetylene (Strem, 98%), 3-hexyne (Strem, 99%), trimethylsilylacetylene (Strem, 98%), *t*-butylacetylene (Strem, 98%). ^{1}H, ^{19}F and $^{31}P\{^{1}H\}$NMR spectra were recorded on either a 300 MHz Bruker Avance or 300 MHz Bruker Avance II instrument at room-temperature (21-23 ^{o}C). ^{1}H NMR spectra were referenced to the residual proton peaks associated with the deuterated solvents (C_6D_6: 7.16 ppm). ^{19}F NMR spectra were referenced to internal 1,3-bis(trifluoromethyl)benzene (BTB) (Aldrich, 99%) set to –63.5 ppm. $^{31}P\{^{1}H\}$NMR data were referenced to external H_3PO_4 (85% aqueous solution), set to 0.0 ppm. UV-vis spectra were recorded on a Cary 100 instrument, using sealable quartz cuvettes (1.0 cm pathlength). Elemental analyses were performed by the Elemental Analysis Service, Université de Montréal (Montréal, Québec).

2.3.2 General Procedure for the Synthesis of 2

Terminal alkyne, 4-X-PhC≡CH (**2a**, X = H, 363 mg, 3.55 mmol; **2b**, X = *t*Bu, 163 mg, 1.03 mmol; **2c**, X = Cl, 156 mg, 1.18 mmol; **2d**, X = OMe, 161 mg, 1.18 mmol) was added to a navy blue solution of $CpCo(=CF(CF_3)(PPh_2Me)$ (**1b**) (**2a**, 377 mg, 0.89 mmol; **2b**, 257 mg, 0.61 mmol; **2c,d**, 250 mg, 0.59 mmol) in toluene (15 mL). The reaction vessel was sealed and stirred overnight (ca. 18 hours) at ambient temperature. ^{19}F NMR analysis of the crude mixture confirmed that the reaction had reached completion. After the solvent was removed under vacuum, the resulting dark red residue was dissolved in minimal toluene (2 mL) and hexanes (5 mL). An orange-red solid precipitated out of solution after overnight storage (ca. 20 hours) at -35°C. The solid was collected by filtration, washed with cold (-35°C) hexanes (10 mL), and dried under vacuum. All complexes had limited solubility in C_6D_6 and slowly decomposed in C_6D_6

under N_2, leading to peak broadening in NMR spectra. Single crystals suitable for X-ray diffraction were grown at -35°C from toluene:hexanes (1:9) (**2a,b,d**) or THF:Et_2O (1:9) (**2c**).

*Cp(PPh$_2$Me)Co[κ^2-C(Ph)=CHCF(CF$_3$)] (**2a**)* Yield: 360 mg (77%). Anal. Calc. for $C_{28}H_{24}F_4PCo$: C, 63.89, H, 4.60. Found: C, 63.78, H, 4.61. ^{1}H NMR (300 MHz, C_6D_6) δ 1.35 (d, ^{2}JHP ≈ 10 Hz, 3H, Me), 4.56 (s, 5H, Cp), 6.98 (m, 5H, Ar-H), 7.10 (m, 3H, Ar-H), 7.19 (m, 3H, Ar-H), 7.43 (m, 2H, Ar-H), 7.69 (m, 2H, Ar-H) ^{19}F NMR (282 Hz, C_6D_6) δ –157.0(dq, F, ^{3}JFP = 28 Hz, ^{3}JFF = 14 Hz), -72.1 (d, CF_3), -63.5 (s, BTB). ^{31}P{^{1}H} (121 MHz, C_6D_6) δ 47.8 (s, br). UV-vis (1 mM in hexanes): λmax(ε) = 405 (865).

*Cp(PPh$_2$Me)Co[κ^2-C(4-^{t}Bu-Ph)=CHCF(CF$_3$)] (**2b**).* Yield: 231 mg (66%). Anal. Calc. for $C_{32}H_{32}CoF_4P$: C, 65.98, H, 5.54. Found: C, 66.19, H, 5.62. ^{1}H NMR (300 MHz, C_6D_6) δ 1.28 (s, 9H, ^{t}Bu), 1.32 (d, $^2J_{HP}$ ≈ 10 Hz, 3H, CH_3), 4.55 (s, 5H, Cp), 6.95 (m, 5H, Ar-H), 7.06 (m, 2H, Ar-H), 7.09 (m, 2H, Ar-H), 7.24 (m, 2H, Ar-H), 7.40 (m, 2H, Ar-H), 7.65 (m, 2H, Ar-H). 19F NMR (282 Hz, C_6D_6) δ -156.47 (dq, F, $^3J_{FP}$ = 28 Hz, $^3J_{FF}$ = 14 Hz), -71.9 (d, CF3), -63.5 (s, BTB). ^{31}P{^{1}H} (121 MHz, C_6D_6) δ 51.3 (s, br). UV-Vis (0.25 mM in hexanes): λmax(ε) = 406 (1079), λmax(ε) = 500 (931).

*Cp(PPh$_2$Me)Co[κ^2-C(4-Cl-Ph)=CHCF(CF$_3$)] (**2c**).* Yield: 228 mg (70%). Anal. Calc. for $C_{28}H_{23}ClCoF_4P$: C, 59.96, H, 4.13. Found: C, 58.63, H, 4.01. ^{1}H NMR (300 MHz, C_6D_6) δ 1.29 (d, $^2J_{HP}$ ≈ 10 Hz, 3H, CH_3), 4.49 (s, 5H, Cp), 6.89 (m, 5H, Ar-H), 7.03 (m, 2H, Ar-H), 7.09 (m, 3H, Ar-H), 7.66 (m, 2H, Ar-H). ^{19}F NMR (282 Hz, C_6D_6) δ -157.2 (dq, F, $^3J_{FP}$ = 28 Hz, $^3J_{FF}$ = 14 Hz), -72.0 (d, CF_3), -63.5 (s, BTB). ^{31}P{^{1}H} (121 MHz, C_6D_6) δ 47.5 (s, br). UV-Vis (0.25 mM in DCM): λmax(ε) = 498 (1675).

*Cp(PPh$_2$Me)Co[κ^2-C(4-OMe-Ph)=CHCF(CF$_3$)] (**2d**).* Yield: 220 mg (67%). Anal. Calc. for $C_{29}H_{26}CoF_4OP$: C, 62.60, H, 4.71. Found: C, 59.09, H, 4.37. ^{1}H NMR (300 MHz, C_6D_6) δ 1.40 (d, $^2J_{HP}$ ≈ 10 Hz, 3H, CH_3), 3.40 (s, 3H, CH_3), 4.60 (s, 5H, Cp), 6.59 (m, 1H, Ar-H), 6.80 (m, 3H, Ar-H), 6.95 (m, 5H, Ar-H), 7.38 (m, 3H, Ar-H), 7.72 (m, 3H, Ar-H). ^{19}F NMR (282 Hz, C_6D_6) δ -155.37 (dq, F, $^3J_{FP}$ = 29 Hz, $^3J_{FF}$ = 14 Hz), -72.0 (d, CF_3), -63.5 (s, BTB). ^{31}P{^{1}H} (121 MHz, C_6D_6) δ 48.3 (s, br). UV-Vis (0.25 mM in DCM): λmax(ε) = 412 (3163), λmax(ε) = 500 (4754).

2.3.3 General Procedure for Initial-Rate Kinetic Experiments

Stock solutions of PhC≡CH and BTB were prepared in a 9:1 toluene/C_6D_6 solution, and 0.5 mL of this solution (containing between 2-10 equiv PhC≡CH as needed, and 0.15 equiv BTB) was transferred to a vial containing **1b** (typically 10 mg, 0.024 mmol). The mixture was then transferred to an NMR tube, and within 5 minutes of mixing, the tube was placed in the NMR probe (preheated to desired temperature). The reaction was monitored by ^{19}F NMR for 1 h (1 spectrum/3.5 min). The growth in product **2a** was evaluated by comparing the integration of the ^{19}F signal for the CF_3 group with that of BTB (-63.5 ppm). All data point values are averages of two runs.

2.3.4 General Procedure for Hammett Study

A stock solution of *p*-substituted phenylacetylene and BTB was prepared in a 9:1 toluene/C_6D_6 solution, and 0.5 mL of this solution (containing 4.0 equiv acetylene and 0.15 equiv BTB) was transferred to a vial containing **1b** (10 mg, 0.024 mmol). The mixture was then transferred to an NMR tube, and within 5 minutes of mixing, the tube was placed in the NMR probe (25.0°C). The reaction was monitored by ^{19}F NMR for 1 h at 25.0°C (1 spectrum/3.5 min). The growth in product **2** was evaluated by comparing the integration of the ^{19}F signal for the CF_3 group with that of BTB (-63.5 ppm). All data point values are averages of two runs.

2.3.5 Computational Studies

All calculations were carried out using the Jaguar quantum mechanical program from Schrodinger.(*Jaguar, versions 7.0-8.9*, Schrödinger, LLC, New York, NY: 2007-2015.) Structures were optimized with the M06 functional combined with the LACVP** basis set. Stationary point structures were confirmed to be minima or first-order saddle points by calculating the vibrational frequencies using analytical second derivatives. Full details are provided as Supporting Information.

2.4 References

(1) Galan, B. R.; Giessert, A. J.; Keister, J. B.; Diver, S. T. *J. Am. Chem. Soc.* **2005**, *127* (16), 5762–5763.
(2) Solans-Monfort, X. *Dalton Trans.* **2014**, *43* (11), 4573–4586.
(3) Grubbs, R. H.; Tumas, W. *Science* **1989**, *243* (4893), 907–915.

(4) Naumov, S.; Buchmeiser, M. R. *Organometallics* **2012**, *31* (3), 847–856.
(5) Tebbe, F. N.; Harlow, R. L. *J. Am. Chem. Soc.* **1980**, *102* (19), 6149–6151.
(6) O'Connor, J. M.; Ji, H.; Iranpour, M.; Rheingold, A. L. *J. Am. Chem. Soc.* **1993**, *115* (4), 1586–1588.
(7) O'Connor, J. M.; Baldridge, K. K.; Vélez, C. L.; Rheingold, A. L.; Moore, C. E. *J. Am. Chem. Soc.* **2013**.
(8) Harrison, D. J.; Gorelsky, S. I.; Lee, G. M.; Korobkov, I.; Baker, R. T. *Organometallics* **2013**, *32* (1), 12–15.
(9) Harrison, D. J.; Lee, G. M.; Leclerc, M. C.; Korobkov, I.; Baker, R. T. *J. Am. Chem. Soc.* **2013**, *135* (49), 18296–18299.
(10) Fuller, J. T.; Harrison, D. J.; Leclerc, M. C.; Baker, R. T.; Ess, D. H.; Hughes, R. P. *Organometallics* **2015**, *34* (21), 5210–5213.
(11) Nadif, S. S.; Kubo, T.; Gonsales, S. A.; VenkatRamani, S.; Ghiviriga, I.; Sumerlin, B. S.; Veige, A. S. *J. Am. Chem. Soc.* **2016**, *138* (20), 6408–6411.
(12) Sheng, Y.; Wu, Y.-D.; Leszczynski, J. *Organometallics* **2004**, *23* (13), 3189–3196.
(13) Liu, C.-B.; Meng, W.; Li, F.; Wang, S.; Nie, J.; Ma, J.-A. *Angew. Chem. Int. Ed.* **2012**, *51* (25), 6227–6230.
(14) Zhao, G.; Basuli, F.; Kilgore, U. J.; Fan, H.; Aneetha, H.; Huffman, J. C.; Wu, G.; Mindiola, D. J. *J. Am. Chem. Soc.* **2006**, *128* (41), 13575–13585.
(15) Semmelhack, M. F.; Tamura, R.; Schnatter, W.; Springer, J. *J. Am. Chem. Soc.* **1984**, *106* (18), 5363–5364.
(16) Foley, H. C.; Strubinger, L. M.; Targos, T. S.; Geoffroy, G. L. *J. Am. Chem. Soc.* **1983**, *105* (10), 3064–3073.
(17) McKinney, R. J.; Tulip, T. H.; Thorn, D. L.; Coolbaugh, T. S.; Tebbe, F. N. *J. Am. Chem. Soc.* **1981**, *103* (18), 5584–5586.
(18) Hemond, R. C.; Hughes, R. P.; Robinson, D. J.; Rheingold, A. L. *Organometallics* **1988**, *7* (10), 2239–2241.
(19) Hughes, R. P.; King, M. E.; Robinson, D. J.; Spotts, J. M. *J. Am. Chem. Soc.* **1989**, *111* (24), 8919–8920.
(20) O'Connor, J. M.; Ji, H. L.; Rheingold, A. L. *J. Am. Chem. Soc.* **1993**, *115* (21), 9846–9847.
(21) O'Connor, J. M.; Fong, B. S.; Ji, H.-L.; Hiibner, K.; Rheingold, A. L. *J. Am. Chem. Soc.* **1995**, *117* (30), 8029–8030.
(22) Donovan-Merkert, B. T.; Malik, J.; Gray, L. V.; O'Connor, J. M.; Fong, B. S.; Chen, M.-C. *Organometallics* **1998**, *17* (6), 1007–1009.
(23) O'Connor, J. M.; Chen, M.-C.; Fong, B. S.; Wenzel, A.; Gantzel, P.; Rheingold, A. L.; Guzei, I. A. *J. Am. Chem. Soc.* **1998**, *120* (5), 1100–1101.
(24) Holland, R. L.; Bunker, K. D.; Chen, C. H.; DiPasquale, A. G.; Rheingold, A. L.; Baldridge, K. K.; O'Connor, J. M. *J. Am. Chem. Soc.* **2008**, *130* (31), 10093–10095.
(25) Holland, R. L.; O'Connor, J. M. *Organometallics* **2009**, *28* (2), 394–396.
(26) Holland, R. L.; O'Connor, J. M.; Rheingold, A. L. *J. Clust. Sci.* **2009**, *20* (2), 261–265.
(27) O'Connor, J. M.; Chen, M.-C.; Holland, R. L.; Rheingold, A. L. *Organometallics* **2011**, *30* (3), 369–371.
(28) O'Connor, J. M.; Baldridge, K. K.; Vélez, C. L.; Rheingold, A. L.; Moore, C. E. *J. Am. Chem. Soc.* **2013**, *135* (24), 8826–8829.
(29) Casey, C. P.; Yi, C. S. *J. Am. Chem. Soc.* **1992**, *114* (16), 6597–6598.
(30) Casey, C. P.; Nash, J. R.; Yi, C. S.; Selmeczy, A. D.; Chung, S.; Powell, D. R.; Hayashi, R. K. *J. Am. Chem. Soc.* **1998**, *120* (4), 722–733.
(31) Cheng, Y.-C.; Chen, Y.-K.; Huang, T.-M.; Yu, C.-I.; Lee, G.-H.; Wang, Y.; Chen, J.-T. *Organometallics* **1998**, *17* (14), 2953–2957.
(32) Derrah, E. J.; McDonald, R.; Rosenberg, L. *Chem. Commun.* **2010**, *46* (25), 4592–4594.
(33) Lee, G. M.; Harrison, D. J.; Korobkov, I.; Baker, R. T. *Chem. Commun.* **2014**, *50* (9), 1128–1130.

(34) Thibaudeau, C.; Plavec, J.; Chattopadhyaya, J. *J. Org. Chem.* **1998**, *63* (15), 4967–4984.
(35) Hansch, C.; Leo, A.; Taft, R. W. *Chem. Rev.* **1991**, *91* (2), 165–195.
(36) Dust, J. M.; Arnold, D. R. *J. Am. Chem. Soc.* **1983**, *105* (5), 1221–1227.
(37) Singh, N. K.; Popelier, P. L. A.; O'Malley, P. J. *Chem. Phys. Lett.* **2006**, *426* (1–3), 219–221.
(38) Hoz, S.; Ben-Zion, M. *J. Chem. Soc. Chem. Commun.* **1980**, No. 10, 453–454.

Chapter 3

Direct Transfer of Difluorocarbene to a Transition Metal Center

3.1 Context and Objectives

The scarcity of metal fluorocarbene complexes can be attributed in part to challenges associated with their synthesis, as outlined in Chapter 1. As an example, the iridium[1] and cobalt[2,3] fluorocarbene complexes prepared by the group of Hughes and our own group, respectively, rely on the successful oxidative addition reaction of perfluoroalkyl iodides, followed by a two-electron reduction step. While the synthetic protocols provide clean product formation and good yields, the overall procedure is not practical for generating fluorocarbene complexes in the context of a potential catalytic process.

The work presented in Chapter 3 investigates the feasibility of transferring difluorocarbene directly to a cobalt(I) complex, with CF_2 being generated in situ from readily available Me_3SiCF_3.[4] This method of metal fluorocarbene synthesis avoids the two-electron oxidation/reduction cycle previously employed, and represents an attractive approach for developing practical catalytic processes. This chapter also demonstrates that the Co(I) fluorocarbenes generated from this process react readily with electrophilic CF_2 to form Co(III) perfluoroalkene complexes, and that these alkene complexes are likely not formed by reaction of Co(I) with TFE, formed in situ from dimerization of CF_2.

Since the work in Chapter 3 was published in 2013, the direct transfer of difluorocarbene to a metal has been employed in several studies, including catalytic processes, as discussed in Chapter 1. Ozerov and coworkers prepared (PNP)Rh=CF_2 complexes using a very similar protocol to that discussed here.[5] Xiao and coworkers described the synthesis of (difluoromethyl)arenes using a palladium catalyzed transfer of difluorocarbene, which involves a Pd=CF_2 complex generated in situ using $Ph_3P^+CF_2CO_2^-$ as the difluorocarbene source.[6] Ichikawa and coworkers reported the synthesis of *β,β*-difluorocyclopentanones

using a copper catalyzed [4+1] addition of silyl dienol ethers with sodium bromodifluoroacetate, where a $Cu{=}CF_2$ complex generated in situ is proposed to be a key intermediate.[7] In total, these studies emphasize the important role that direct synthetic methods play in developing metal difluorocarbene reactivity for catalytic applications.

3.1.1 Published Contributions

Stepwise Addition of Difluorocarbene to a Transition Metal Centre

Graham M. Lee, Daniel J. Harrison, Ilia Korobkov and R. Tom Baker. *Chem. Commun.* **2013**, *50*, 1128-1130.

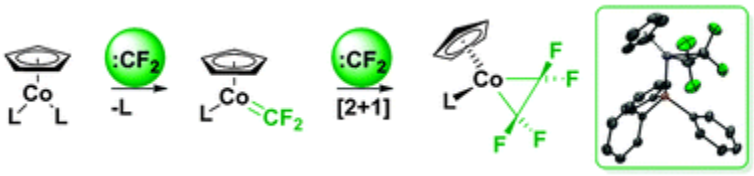

The Ruppert–Prakash reagent (Me_3SiCF_3) is used to introduce difluorocarbene (CF_2) and tetrafluoroethylene (TFE) ligands to cobalt(I) metal centres, whereby the TFE ligand is generated *via* [2+1] cycloaddition between $[Co]{=}CF_2$ and CF_2.

Author Contributions: The manuscript was written by GML. GML performed all experiments presented in the paper. X-ray crystallography by IK.

3.2 Stepwise Addition of Difluorocarbene to a Transition Metal Center

3.2.1 Introduction

Among the most versatile tools for the synthesis of metal-fluoroalkyl complexes is the Ruppert–Prakash reagent (Me_3SiCF_3).[8] It has been used to prepare a variety of transition metal complexes with trifluoromethyl (CF_3) ligands, including examples of first-row (Ti,[9] Ni,[10] Cu[11]), second-row (Ru,[12,13] Rh,[14–

[16] Pd[17]) and third-row (Pt[18,19], Au[20]) metals. Recently, conditions were reported that render Me_3SiCF_3 an excellent source of difluorocarbene (CF_2) (eqn 1), as applied to the synthesis of difluorocyclopropanes and difluorocyclopropenes,[21] as well as unusual fluorinated carbacycle motifs.[22] Iodide activates Me_3SiCF_3 to liberate the trifluoromethyl anion, which decomposes into CF_2 and F^-. The fluoride ion also reacts with Me_3SiCF_3 to release CF_3^-.[23,24]

$$Me_3SiCF_3 \xrightarrow[THF]{NaI(initiator)} Me_3SiF + :CF_2 \quad \text{(eqn 1)}$$

Here, we present a novel application of Me_3SiCF_3 for directly introducing the CF_2 group to transition metal compounds, providing new routes to metal difluorocarbene ([Co]=CF_2) and metal tetrafluoroethylene (TFE) complexes {[Co](η^2-C_2F_4)}. Such compounds are under investigation as intermediates in potential catalytic cycles utilizing perfluoroalkenes (*e.g.*, metathesis and polymerization).[3]

Examples of metal fluorocarbenes ([M]=CFR^F, R^F = F or CF_3) are rare and, relative to metal alkylidenes or other types of Fischer carbenes, have been the subject of few reactivity studies.[25,26] Almost without exception, [M]=CF_2 complexes are prepared *via* fluoride abstraction/elimination from metal fluoroalkyl precursors.[1] Notably, Caulton and co-workers showed that Me_3SiCF_3reacts with a ruthenium fluoride complex to give [Ru(CF_3)(H)(CO)(L_2)]; α fluoride migration from the CF_3 group to the metal centre yields [Ru(=CF_2)(F)(H)(CO)(L_2)].[13] This difluorocarbene complex is electrophilic at the carbenoid carbon atom, demonstrated by hydride migration in the presence of coordinating solvent.[12,13] Recently, we reported the synthesis of nucleophilic cobalt fluorocarbenes (Scheme 3.1a),[2] using a procedure adapted from Hughes and co-workers.[1] The [Co]=CFR^Fcomplexes undergo [2+2] cycloaddition reactions with tetrafluoroethylene (TFE) to give perfluorometallacyclobutanes.[3] The metallacyclobutane compounds exhibit rich reactivity upon activation of C_β–F bonds, including the catalytic isomerization to alkene complexes under acid catalysis (Scheme 3.1b).

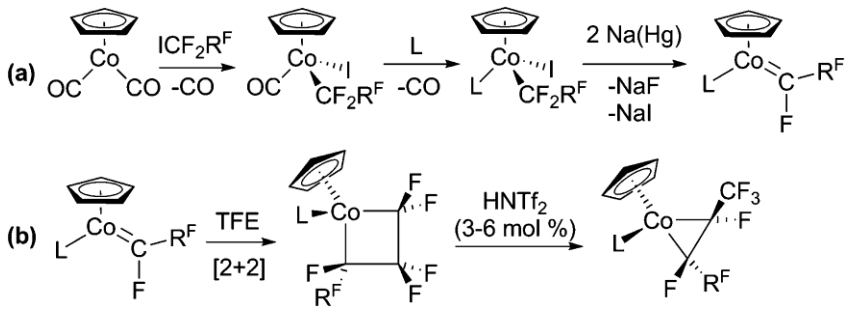

Scheme 3.1. Previously reported synthesis (a), and reactivity (b) of cobalt fluorocarbenes. L = phosphine or phosphite, R^F = F or CF_3.

For the present work, we investigated $CpCoL_2$ complexes [Cp = η^5-C_5H_5; **1a**, L = CO; **1b**, L = PPh_3; **1c**, L = $P(O^iPr)_3$] as potential CF_2 acceptors in reactions with the Ruppert–Prakash reagent. Compounds of type **1** were selected based on our previous work that demonstrated the [CpCoL] substructure can support the CF_2 fragment, making it an attractive platform for CF_2-transfer screening reactions.

3.2.2 Results and Discussion

Treatment of **1** with Me_3SiCF_3 (2 equivalents) and catalytic quantities of NaI in THF at 65 °C gave a mixture of the corresponding cobalt fluorocarbenes **2a–c**, and novel cobalt tetrafluoroethylene complexes **3a–c** (Scheme 3.2). The products were readily identified in solution by their distinct ^{19}F NMR signals.

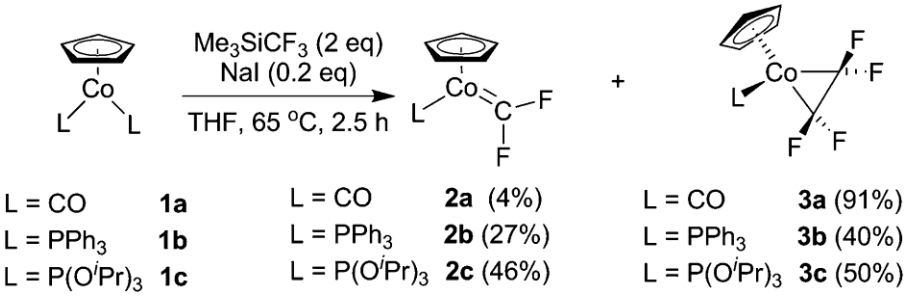

Scheme 3.2. Structures of cobalt fluorocarbenes **2**, and TFE complexes **3** (NMR determined yields) from Co(I) complexes **1**. Yields based on **1**. For the reaction of **1b**, low yields are attributed to incomplete conversion of Me_3SiCF_3 as well as formation of Ph_3PF_2 as a by-product, identified using ^{19}F and ^{31}P NMR.[27]

Selectivity for products **2***vs.***3** depends on the nature of the ancillary ligands. When L = CO (*i.e.*, **1a**), the TFE complex **3a** is the major product, and only minor quantities of **2a** are observed. The ^{19}F NMR spectrum of **2a** displays two characteristically downfield resonances at δ = 112.5 ppm and 83.4 ppm ($^{2}J_{FF}$ = 152 Hz), consistent with data previously reported for [CpCo(=CF$_2$)(L)] complexes.[2,3] Complex **3a** was isolated as a brown-yellow oil in 69% yield, whereas the carbene complex **2a** could only be observed spectroscopically. We previously reported that attempts to prepare **2a** *via* reduction of [CpCo(CO)I(CF$_3$)] were unsuccessful.[2] Complexes **1b** or **1c** (with PPh$_3$ or P(O^{i}Pr)$_3$ ligands) react under the same conditions to yield cobalt fluorocarbenes **2b** (reported previously)[2] or **2c**, respectively, as the minor products (although in much higher yields than **2a**), along with major products **3b** and **3c**. Using four equivalents of Me$_3$SiCF$_3$ increases the yield of alkene complexes **3b** and **3c** significantly, while carbenes **2b** and **2c** are no longer observed in solution. The crystal structures of **3b** and **3c** are presented in Fig. 3.1.

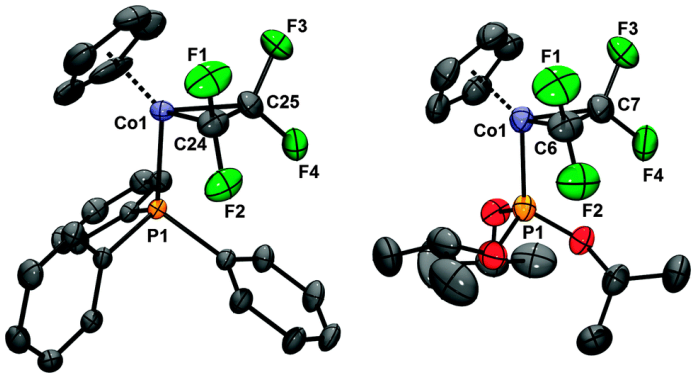

Figure 3.1. Molecular structures of **3b** (left) and **3c** (right). The ellipsoids are set to 50% probability, and hydrogen atoms are omitted for clarity. Selected bond distances (Å) and angles (°): 3b: Co1–C24 1.884(3), Co1–C25 1.897(3), Co1–P1 2.1930(7), Co1–Cp(centroid) 1.735(6), C24–F1 1.357(5), C24–F2 1.361(4), C25–F3 1.362(4), C25–F4 1.347(5), C24–Co1–C25 44.49, Co1–C25–C24 67.27, C25–C24–Co1 68.24. 3c: Co1–C6 1.880(2), Co1–C7 1.896(2), Co1–P1 2.1478(6), Co1–Cp(centroid) 1.711(2), C6–F1 1.372(3), C6–F2 1.376(3), C7–F3 1.370(2), C7–F4 1.356(3), C6–Co1–C7 43.92, Co1–C7–C6 67.45, C7–C6–Co1 68.62.

The ^{19}F NMR spectra of η^2-TFE complexes **3a–c** are highly characteristic. In THF or C$_6$D$_6$ at room temperature, the signals for the TFE ligand exhibit second order coupling indicative of either an AA′BB′ spin system for **3a**, or an AA′BB′X spin system for **3b** and **3c** (X = ^{31}P), and C_s symmetry for all three

complexes. The observation of two resonances with well-resolved splitting patterns suggests the C_2F_4 fragment does not rotate with respect to the metal on the NMR timescale in solution, in contrast to related η^2-C_2F_4 complexes of Ni and Pd described by Ogoshi and co-workers,[28,29] or Ru and Ir complexes described by Hughes and co-workers.[30,31]

Under the reaction conditions outlined in Scheme 3.2, we envision two likely pathways for formation of TFE complexes **3a–c**, as illustrated in Scheme 3.3. In pathway A, tetrafluoroethylene, formed *in situ* from two equivalents of CF_2, reacts directly with complexes **1a–c**. ^{19}F NMR analysis of a mixture of only Me_3SiCF_3 and NaI in THF confirms that TFE is formed cleanly as the major product upon heating, with concomitant formation of Me_3SiF (Fig. S1, ESI). In order to probe the feasibility of path A, complexes **1a–c** were treated with TFE (1.7 atm) in THF at 65 °C. Complexes **1a** and **1c** did not react under these conditions, and the addition of NaI also had no effect. Small amounts of **3a** were observed in a complex mixture when a THF solution of **1a** was photolyzed (medium-pressure Hg lamp) in the presence of TFE (1.7 atm), presumably through photolytically-generated [CpCo(CO)].[32] Interestingly, Stone and co-workers reported in 1961 that **1a** reacts with excess TFE in cyclohexane at high temperatures (160 °C) to produce the perfluorocyclopentane complex $[CpCo(CF_2)_4(CO)]$ in 11% yield.[33] While **3a** is likely an intermediate in this process, we did not observe the 5-membered ring product under the conditions we explored.

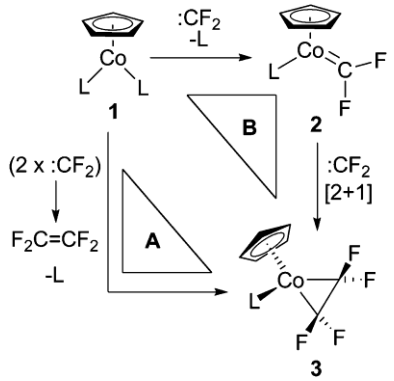

Scheme 3.3. Proposed pathways for generation of 3. Path A involves direct addition of TFE to 1, while path B is comprised of the stepwise addition of CF_2, with 2 formed as a stable intermediate.

In contrast to **1a** and **1c**, complex **1b** reacts with TFE to produce **3b** in 89% yield by ^{19}F NMR. These results indicate that under the conditions explored, path A does not likely contribute to the formation of **3a** and **3c**, but *can* contribute to the formation of **3b**, if TFE is formed in appreciable quantities. The increased reactivity toward TFE of **1b***vs.***1a,c** is apparently due to the increased lability of PPh_3 relative to π-accepting CO and $P(O^iPr)_3$, allowing generation of $16e^-$ complex $[CpCo(PPh_3)]$ in solution. These results suggest a dissociative mechanism for pathway A.

Pathway B represents a new synthetic route to metal fluoroalkene complexes. In this scheme, a metal fluorocarbene intermediate **2** is formed initially, which undergoes [2+1] cycloaddition reaction with a second equivalent of CF_2 to yield perfluoroalkene complexes **3**. Indeed, independently-synthesized **2b** and **2c** react with Me_3SiCF_3/NaI, producing **3b** and **3c**, respectively, in high yield (>90% by ^{19}F NMR). Similarly, the fluoro(trifluoromethyl) carbene complex **4** (reported previously)[2] is converted to the corresponding fluoroalkene complex **5** in high yield under the same conditions. These reactions are summarized in Scheme 3.4, and the crystal structure of **5** is presented in Fig. 3.2.

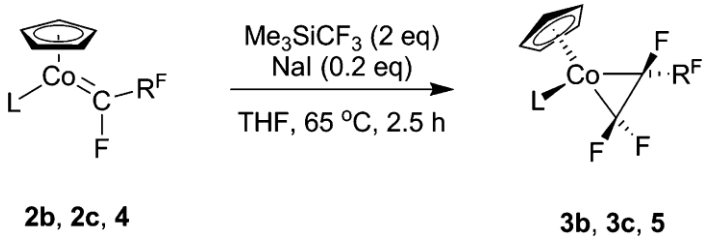

Scheme 3.4. Synthesis of fluoroalkene complexes *via* [2+1] cycloaddition between CF_2 and pre-isolated cobalt fluorocarbenes. For complexes **4** and **5**, L = PPh_3, R^F = CF_3.

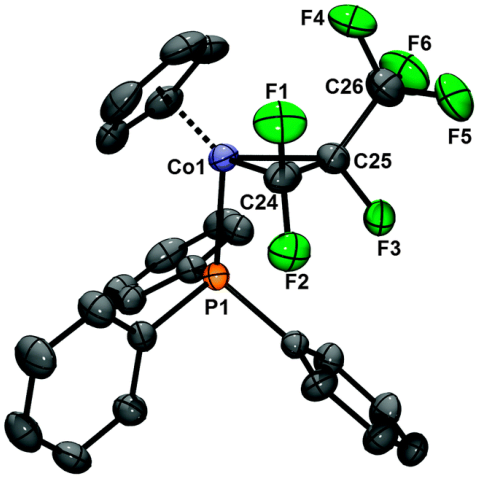

Figure 3.2. Molecular structure of 5. The ellipsoids are set to 50% probability, and hydrogen atoms are omitted for clarity. Selected bond distances (Å) and angles (°): Co1–C24 1.902(3), Co1–C25 1.943(2), Co1–P1 2.2267(6), Co1–Cp(centroid) 1.718(3), C24–F1 1.373(3), C24–F2 1.351(3), C25–F3 1.388(3), C24–Co1–C25 44.08, Co1–C25–C24 66.47, C25–C24–Co1 69.45.

From these results, it can be reasoned that path B likely contributes, along with path A, to the formation of **3b**. In the case of **3a** and **3c**, B appears to be the dominant pathway. The detailed mechanism of pathway B, (difluorocarbene addition to complexes **1** and **2**) is under further investigation using DFT calculations. The unique [2+1] reactions described here, involving highly electrophilic difluorocarbene,[34] are consistent with the nucleophilic character of the Co=C bond of the Co(I) fluorocarbene complexes.[2,3] Upon addition of CF_2, the Co(I) metal centre of carbenes **2** are formally oxidized to Co(III). The Co–C (TFE) bonds in **3b** (Co1–C24 1.884 Å; Co1–C25 1.897 Å) are significantly longer than the Co=C bond of **2b** (1.7395 Å), and the same is true for the analogous Co–C (TFE) bonds of **5** (Co1–C24 1.902 Å; Co1–C25 1.943 Å) relative to the Co=C bond of **4** (1.751 Å).

3.2.3 Conclusions

In conclusion, we have demonstrated that cobalt difluorocarbenes and η^2-TFE complexes are generated *via* sequential addition of CF_2, generated from Me_3SiCF_3 and catalytic NaI, to $CpCoL_2$ complexes. We also note that Me_3SiCF_3/NaI can be used as a safe and convenient precursor for

generating tetrafluoroethylene. Future work will extend the methods described here to synthesize new difluorocarbene and perfluoroalkene transition metal complexes with potential relevance to catalytic processes involving fluorocarbon substrates.

3.3 Experimental Details for Section 3.2

3.3.1 General Information

Experiments were conducted under nitrogen, using Schlenk techniques or an MBraun glove box. All solvents were deoxygenated by purging with nitrogen. Toluene, hexanes, diethyl ether (DEE) and tetrahydrofuran (THF) were dried on columns of activated alumina using a J. C. Meyer (formerly Glass Contour®) solvent purification system. Benzene-d_6 (C_6D_6) was dried by stirring over activated alumina (*ca.* 10 wt. %) overnight, followed by filtration. All solvents were stored over activated (heated at *ca.* 250°C for >10 h under vacuum) 4 Å molecular sieves. Glassware was oven-dried at 150°C for >2 h. The following chemicals were obtained commercially, as indicated: [$CpCo(CO)_2$] (Cp = cyclopentadienyl) (Strem, 95%), sodium (Alfa Aesar, 99%), mercury (Strem, 99.998%), Me_3SiCF_3 (Synquest, 98%). Compounds **2b** and **4** were prepared as previously reported.[2] Compounds **1b** and **1c** were prepared according to slightly modified literature procedures.[3] Tetrafluoroethylene (TFE) was made by pyrolysis of polytetrafluoroethylene (Scientific Polymer Products, powdered) under vacuum, using a slightly modified literature procedure (10-20 mTorr, 650°C, 30 g scale, product stabilized with R(+)-limonene (Aldrich, 97%), giving TFE of *ca.* 97% purity).[1] ^{1}H, ^{19}F and ^{31}P{^{1}H}NMR spectra were recorded on either a 300 MHz Bruker Avance or 300 MHz Bruker Avance II instrument at room-temperature (21-23°C). ^{1}H NMR spectra were referenced to the residual proton peaks associated with the deuterated solvents (C_6D_6: 7.16 ppm). ^{19}F NMR spectra were referenced to internal 1,3-bis(trifluoromethyl)benzene (BTB) (Aldrich, 99%, deoxygenated by purging with nitrogen, stored over activated 4 Å molecular sieves), set to –63.5 ppm. Note: for NMR solutions containing both BTB and hexafluorobenzene (C_6F_6) (Aldrich, 99%), the chemical shift of C_6F_6 appears at –163.6 in C_6D_6 (with BTB at –63.5 ppm). ^{1}H NMR data for BTB: (300 MHz, C_6D_6) δ 6.60 (m, 1H, Ar-5-H), 7.12 (m, 2H, Ar-4,6-H), 7.76 (m, 1H, Ar-2-H); (300 MHz, CD_3CN) δ 7.76-7.84 (m, 1H, Ar–H), 7.95-8.04 (m,

3H, Ar–H). $^{31}P\{^{1}H\}$NMR data were referenced to external H_3PO_4 (85% aqueous solution), set to 0.0 ppm. IR data were collected on a Varian 640 FT-IR spectrometer. Elemental analyses were performed by the Elemental Analysis Service, Université de Montréal (Montréal, Québec).

[1] Hunadi, R. J.; Baum, K. *Synthesis* **1982**, *39*, 454.

[2] D. J. Harrison, S. I. Gorelsky, G. M. Lee, I. Korobkov and R. T. Baker, *Organometallics*, **2012**, *32*, 12-15.

[3] *Inorganic Synthesis, vol. 26*, H. D. Kaesz, ed., John Wiley & Sons, Inc., **1989**, p.191.

3.3.2 General Procedure for Reactions of 1 with Me_3SiCF_3

Complex **1** (0.1 mmol), NaI (0.02 mmol) and THF (3 mL) were charged into a 50 mL ampoule. Me_3SiCF_3 (0.2 mmol) was added, and the ampoule was sealed and stirred at 65 °C in an oil bath. After 2.5 h, the ampoule was allowed to cool to room temperature. Internal standard (BTB, 15 mol%) was added and the mixture was analyzed using ^{19}F NMR.

3.3.3 Synthesis and Characterization for $CpCo(=CF_2)(P(O^iPr_3)$ (2c)

A solution of $CpCoI(CO)CF_3$ (500 mg, 1.44 mmol in toluene (5 mL) was stirred in a schlenk tube, and a solution of $P(O^iPr)_3$ (330 mg, 1.58 mmol) in toluene (5 mL) was then added via cannula transfer over 5 min. The resulting solution was stirred under dynamic N_2 (to accommodate the release of CO) for 3 h. The solution was then degassed using 3 freeze-pump-thaw cycles. The dark brown solution was transferred to a 100 mL round bottom flask containing an amalgam of Na (69 mg, 3 mmol) and Hg (0.064 mL) (0.8 wt% Na/Hg) in toluene (10 mL), which had been stirred vigorously for 10 minutes. This solution was stirred for 20 hours, and the color changed from dark brown to dark red/orange. The volatiles were removed under vacuum, and the resulting red/orange residue was extracted with hexanes/DEE (1:1) (20 mL) and filtered through a plug of celite. The solvent was removed from the filtrate under vacuum, giving 422 mg of **2c** as red/orange oil (76% yield). ^1H NMR (300 MHz, C_6D_6) δ 1.16 (d, 18H, Me, ^{i}Pr), 4.72 (m, 3H, ^{i}Pr), 4.82 (s, 5H, Cp). ^{19}F NMR (282 MHz, C_6D_6) δ 63.95 (dd, 1F, $^2J_{FF}$ = 101 Hz, $^3J_{FP}$ = 45 Hz), 94.97 (dd, 1F, $^3J_{FP}$ = 18 Hz). $^{31}P\{^1H\}$ NMR (121 MHz, C_6D_6) δ 164.7.

3.3.4 Synthesis and Characterization for $CpCo(\eta^2\text{-}C_2F_2)(CO)$ (3a)

$CpCo(CO)_2$ (200 mg, 1.11 mmol), NaI (33 mg, 0.22 mmol), and THF (10 mL) were charged into a 100 mL ampoule, resulting in a dark red solution. Me_3SiCF_3 (400 mg, 2.81 mmol) was added, and the ampoule was sealed and stirred at 65 °C in an oil bath. After approximately 30 minutes, the red solution turned yellow in color, and the solution was heated for an additional 1.5 hours. The volatiles were removed under vacuum, leaving a brown oily residue. The residue was extracted with hexane (8 mL) and filtered through a plug of celite. The hexane solution was dried under vacuum, giving 193 mg of **3a** as golden-brown oil (69% yield). IR (cm^{-1}) : 2050 (s br, ν_{CO}). ^1H NMR (300 MHz, C_6D_6) δ 4.39 (s, 5H, Cp). ^{19}F NMR (282 MHz, C_6D_6) δ –113.2 (m, 2F, CF_2=CF_2), -107.1 (m, 2F, CF_2=CF_2). $^{13}C\{^1H\}$ NMR (75 MHz, C_6D_6) δ 88.86 (s, Cp), 121.8 (m, CF_2=CF_2), 199.04 (br s, CO). Anal. Calc. for $C_8H_5F_4Co_1O_1$: C, 38.12, H, 2.00. Found: C, 38.25, H, 2.08.

3.3.5 Synthesis and Characterization for $CpCo(\eta^2\text{-}C_2F_4)(PPh_3)$ (3b)

Complex **2b** (200mg, 0.458 mmol), NaI (13 mg, 0.086 mmol), and THF (10 mL) were charged into a 100 mL ampoule. To the red solution, Me_3SiCF_3 (163 mg, 1.15 mmol) was added, and the ampoule was sealed and stirred at 65 °C in an oil bath. After 2.5 h, volatiles were removed under vacuum, leaving a brown oily residue. The residue was extracted with toluene (6 mL), and filtered through a plug of celite. Volatiles were again removed under vacuum, and the residue was recrystallized from a concentrated solution in toluene/hexanes at -35 °C, giving **3b** as brown/orange crystalline solid (150 mg, 67% yield). Crystals of **3b** suitable for X-ray analysis were grown from concentrated toluene/hexanes at -35 °C. ^1H NMR (300 MHz, C_6D_6) δ 4.53 (s, 5H, Cp), 6.97 (ov m, 9H), 7.63 (m, 6H). ^{19}F NMR (282 MHz, C_6D_6) δ –114.1 (m, 2F, CF_2=CF_2), -110.2 (m, 2F, CF_2=CF_2). $^{31}P\{^1H\}$ NMR (121 MHz, C_6D_6) δ 58.1. Anal. Calc. for $C_{25}H_{20}F_4Co_1P_1$: C, 61.74, H, 4.15. Found: C, 64.28, H, 4.58.

3.3.6 Synthesis and Characterization for $CpCo(\eta^2\text{-}C_2F_4)(P(O^iPr)_3$ (3c)

$CpCo(P(O^iPr)_3)_2$ (150 mg, 0.28 mmol), NaI (9 mg, 0.06 mmol), and THF (6 ml) were charged into a 100 mL ampoule. Me_3SiCF_3 (118 mg, 0.83 mmol) was added, and the ampoule was sealed and stirred at 65 °C

in an oil bath. After 2.5 h, the volatiles were removed under vacuum, leaving an orange residue. The residue was extracted with hexane (6 mL) and filtered through celite. The filtrate was concentrated to ca. 1 mL and cooled to -35 °C. A yellow solid precipitated from the solution, and was collected and washed with cold hexanes. The solid was died under vacuum, giving **3c** as yellow crystals (75 mg, 62 % yield). ^{1}H NMR (300 MHz, C_6D_6) δ 1.08 (d, 18H, Me, ^{i}Pr), 4.55 (m, 3H, ^{i}Pr), 4.79 (s, 5H, Cp). ^{19}F NMR (282 MHz, C_6D_6) δ –115.7 (m, 2F, CF_2=CF_2), -111.2 (m, 2F, CF_2=CF_2). ^{31}P{^{1}H} NMR (121 MHz, C_6D_6) δ 151.6. Anal. Calc. for $C_{16}H_{26}F_4Co_1P_1O_3$: C, 44.46, H, 6.06. Found: C, 44.49, H, 6.06.

3.3.7 Synthesis and Characterization for CpCo(η^2-$CF_2CF(CF_3)$)(PPh_3) (5)

Complex **4** (200 mg, 0.413 mmol), NaI (13 mg, 0.086 mmol), and THF (10 mL) were charge into a 100 mL ampoule. To the blue solution, Me_3SiCF_3 (146 mg, 1.028 mmol) was added, and the ampoule was sealed and stirred at 65 °C in an oil bath. After 2.5 h, volatiles were removed under vacuum, leaving a yellow/brown residue. The residue was extracted with toluene and hexanes (4 mL: 4 mL), and filtered through a plug of celite. Volatiles were again removed under vacuum, and the residue was recrystallized from a concentrated solution of toluene/hexanes at -35 °C, giving **5** as orange crystals (120 mg, 54% yield). Crystals of **5** suitable for x-ray analysis were grown from concentrated toluene/hexanes at -35 °C. ^{1}H NMR (300 MHz, C_6D_6) δ 4.49 (s, 5H, Cp), 6.98 (ov m, 9H), 7.64 (m, 6H). ^{19}F NMR (282 MHz, C_6D_6) δ –195.4 (m, 1F), -96.3 (dtm, 1F, $^{2}J_{FF(gem)}$ = 125 Hz), -94.6 (ddm, 1F, $^{2}J_{FF(gem)}$ = 125 Hz), -66.2 (t, 3F, CF_3). ^{31}P{^{1}H} NMR (121 MHz, C_6D_6) δ 52.3. Anal. Calc. for $C_{26}H_{20}F_6Co_1P_1$: C, 58.23, H, 3.76. Found: C, 58.23, H, 3.83.

3.4 References

(1) Hughes, R. P.; Laritchev, R. B.; Yuan, J.; Golen, J. A.; Rucker, A. N.; Rheingold, A. L. *J. Am. Chem. Soc.* **2005**, *127* (43), 15020–15021.
(2) Harrison, D. J.; Gorelsky, S. I.; Lee, G. M.; Korobkov, I.; Baker, R. T. *Organometallics* **2013**, *32* (1), 12–15.
(3) Harrison, D. J.; Lee, G. M.; Leclerc, M. C.; Korobkov, I.; Baker, R. T. *J. Am. Chem. Soc.* **2013**, *135* (49), 18296–18299.
(4) Liu, X.; Xu, C.; Wang, M.; Liu, Q. *Chem. Rev.* **2015**, *115* (2), 683–730.
(5) Pell, C. J.; Zhu, Y.; Huacuja, R.; Herbert, D. E.; Hughes, R. P.; Ozerov, O. V. *Chem. Sci.* **2017**, *8* (4), 3178–3186.

(6) Deng, X.-Y.; Lin, J.-H.; Xiao, J.-C. *Org. Lett.* **2016**, *18* (17), 4384–4387.
(7) Fuchibe, K.; Aono, T.; Hu, J.; Ichikawa, J. *Org. Lett.* **2016**, *18* (18), 4502–4505.
(8) Taw, F. L.; Clark, A. E.; Mueller, A. H.; Janicke, M. T.; Cantat, T.; Scott, B. L.; Hay, P. J.; Hughes, R. P.; Kiplinger, J. L. *Organometallics* **2012**, *31* (4), 1484–1499.
(9) Taw, F. L.; Scott, B. L.; Kiplinger, J. L. *J. Am. Chem. Soc.* **2003**, *125* (48), 14712–14713.
(10) Dubinina, G. G.; Brennessel, W. W.; Miller, J. L.; Vicic, D. A. *Organometallics* **2008**, *27* (15), 3933–3938.
(11) Dubinina, G. G.; Furutachi, H.; Vicic, D. A. *J. Am. Chem. Soc.* **2008**, *130* (27), 8600–8601.
(12) Huang, D.; Caulton, K. G. *J. Am. Chem. Soc.* **1997**, *119* (13), 3185–3186.
(13) Huang, D.; Koren, P. R.; Folting, K.; Davidson, E. R.; Caulton, K. G. *J. Am. Chem. Soc.* **2000**, *122* (37), 8916–8931.
(14) Vicente, J.; Gil-Rubio, J.; Guerrero-Leal, J.; Bautista, D. *Organometallics* **2004**, *23* (21), 4871–4881.
(15) Vicente, J.; Gil-Rubio, J.; Guerrero-Leal, J.; Bautista, D. *Organometallics* **2005**, *24* (23), 5634–5643.
(16) Goodman, J.; Grushin, V. V.; Larichev, R. B.; Macgregor, S. A.; Marshall, W. J.; Roe, D. C. *J. Am. Chem. Soc.* **2009**, *131* (12), 4236–4238.
(17) Grushin, V. V.; Marshall, W. J. *J. Am. Chem. Soc.* **2006**, *128* (39), 12644–12645.
(18) Naumann, D.; Kirij, N. V.; Maggiarosa, N.; Tyrra, W.; Yagupolskii, Y. L.; Wickleder, M. S. *Z. Für Anorg. Allg. Chem.* **2004**, *630* (5), 746–751.
(19) Menjón, B.; Martínez-Salvador, S.; Gómez-Saso, M. A.; Forniés, J.; Falvello, L. R.; Martín, A.; Tsipis, A. *Chem. – Eur. J.* **2009**, *15* (26), 6371–6382.
(20) Zopes, D.; Kremer, S.; Scherer, H.; Belkoura, L.; Pantenburg, I.; Tyrra, W.; Mathur, S. *Eur. J. Inorg. Chem.* **2011**, *2011* (2), 273–280.
(21) Wang, F.; Luo, T.; Hu, J.; Wang, Y.; Krishnan, H. S.; Jog, P. V.; Ganesh, S. K.; Prakash, G. K. S.; Olah, G. A. *Angew. Chem. Int. Ed.* **2011**, *50* (31), 7153–7157.
(22) Chia, P. W.; Bello, D.; Slawin, A. M. Z.; O'Hagan, D. *Chem. Commun.* **2013**, *49* (22), 2189–2191.
(23) Maggiarosa, N.; Tyrra, W.; Naumann, D.; Kirij, N. V.; Yagupolskii, Y. L. *Angew. Chem. Int. Ed.* **1999**, *38* (15), 2252–2253.
(24) Kolomeitsev, A.; Movchun, V.; Rusanov, E.; Bissky, G.; Lork, E.; Roschenthaler, G.-V.; Kirsch, P. *Chem. Commun.* **1999**, No. 11, 1017–1018.
(25) Clark, G. R.; Hoskins, S. V.; Jones, T. C.; Roper, W. R. *J. Chem. Soc. Chem. Commun.* **1983**, No. 13, 719–721.
(26) Brothers, P. J.; Burrell, A. K.; Clark, G. R.; Rickard, C. E. F.; Roper, W. R. *J. Organomet. Chem.* **1990**, *394* (1–3), 615–642.
(27) Doxsee, K. M.; Hanawalt, E. M.; Weakley, T. J. R. *Inorg. Chem.* **1992**, *31* (21), 4420–4421.
(28) Ohashi, M.; Kambara, T.; Hatanaka, T.; Saijo, H.; Doi, R.; Ogoshi, S. *J. Am. Chem. Soc.* **2011**, *133* (10), 3256–3259.
(29) Ohashi, M.; Shibata, M.; Saijo, H.; Kambara, T.; Ogoshi, S. *Organometallics* **2013**, *32* (13), 3631–3639.
(30) Curnow, O. J.; Hughes, R. P.; Mairs, E. N.; Rheingold, A. L. *Organometallics* **1993**, *12* (8), 3102–3108.
(31) Hughes, R. P.; Tucker, D. S. *Organometallics* **1993**, *12* (12), 4736–4738.
(32) Snee, P. T.; Payne, C. K.; Kotz, K. T.; Yang, H.; Harris, C. B. *J. Am. Chem. Soc.* **2001**, *123* (10), 2255–2264.
(33) Coyle, T. D.; Kings, R. B.; Pitcher, E.; Stafford, S. L.; Teichel, P.; Stone, F. G. A. *J. Inorg. Nucl. Chem.* **1961**, *20* (1), 172–173.
(34) Yang, Z.-Y. *J. Am. Chem. Soc.* **1996**, *118* (34), 8140–8141.

Chapter 4

Cobalt(III) Fluoroalkyl, Fluorocarbene, and Fluoride Complexes

4.1 Context and Objectives

Chapters 2 and 3 focused largely on the synthesis and reactivity of cobalt(I) fluorocarbene complexes. In Chapter 4 we explore in greater detail the fluoro-organometallic chemistry of cobalt(III) complexes, in particular cobalt(III) fluorides and fluorocarbenes.

In Chapter 1 we introduced the importance of nucleophilic fluorination reactions, and the synthesis of organometallic fluoride complexes. In this chapter we describe the synthesis of cobalt(III) fluoride complexes, which exhibit very interesting spectroscopic properties. These complexes were shown to react stoichiometrically with an acyl chloride compound to furnish the corresponding acyl fluoride. From this, we developed a rare example of a cobalt catalyzed nucleophilic fluorination reaction.

Also in Chapter 1, we introduced the idea of switching the reactivity of metal fluorocarbenes from nucleophilic to electrophilic by changing the oxidation state of the metal.[1] In Chapter 4, we prepare the first examples of Co(III) fluorocarbenes. These electrophilic cobalt fluorocarbenes undergo important insertion reactions with adjacent perfluoroalkyl ligands, possibly providing a blueprint for metal catalyzed perfluoro-olefin polymerization.

4.1.1 Published Contributions

Perfluoroalkyl Cobalt(III) Fluoride and Bis(perfluoroalkyl) Complexes: Catalytic Fluorination and Selective Difluorocarbene Formation

Leclerc, M. C.[†]; Bayne, J. M.; Lee, G. M.[†]; Gorelsky, S. I.; Vasiliu, M.; Korobkov, I.; Harrison, D. J.; Dixon, D. A.; Baker, R. T. *J. Am. Chem. Soc.*, **2015**, *137*, 16064-16073.

[†]Equal contributions

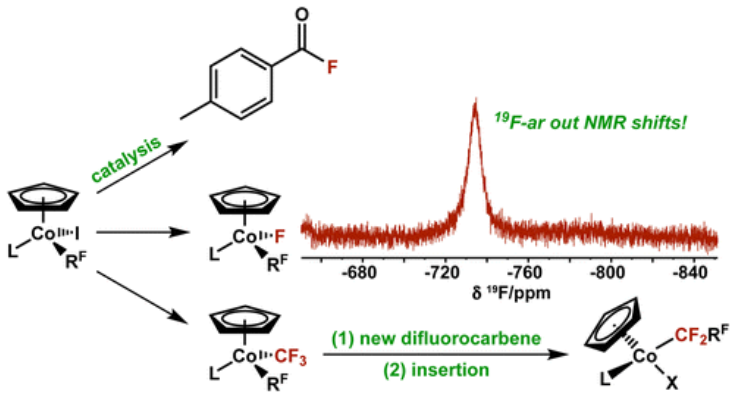

Abstract: Four perfluoroalkyl cobalt(III) fluoride complexes have been synthesized and characterized by elemental analysis, multinuclear NMR spectroscopy, X-ray crystallography, and powder X-ray diffraction. The remarkable cobalt fluoride ^{19}F NMR chemical shifts (−716 to −759 ppm) were studied computationally, and the contributing paramagnetic and diamagnetic factors were extracted. Additionally, the complexes were shown to be active in the catalytic fluorination of *p*-toluoyl chloride. Furthermore, two examples of cobalt(III) bis(perfluoroalkyl)complexes were synthesized and their reactivity studied. Interestingly, abstraction of a fluoride ion from these complexes led to selective formation of cobalt difluorocarbene complexes derived from the trifluoromethyl ligand. These electrophilic difluorocarbenes were shown to undergo insertion into the remaining perfluoroalkyl fragment, demonstrating the elongation of a perfluoroalkyl chain arising from a difluorocarbene insertion on a cobalt metal center. The reactions of both the fluoride and bis(perfluoroalkyl) complexes provide insight into the potential catalytic applications of these model systems to form small fluorinated molecules as well as fluoropolymers.

Author Contributions: The manuscript was written in equal parts by MCL and GML. MCL was responsible for the synthesis and characterization of complexes **5**, **7** and **9**. GML was responsible for the synthesis and characterization of complexes **6**, **8** and **10**. Preliminary experiments involving complexes **5-8** were performed by JMB, under the supervision of GML and MCL. The catalytic fluorination chemistry was developed by MCL. The formation of **Int 1-4** was established by GML, and finalizing characterization work was performed by MCL. DFT studies done by MV and DAD. X-ray crystallography by IK.

4.2 Perfluoroalkyl Cobalt(III) Fluoride and Bis(perfluoroalkyl) Complexes: Catalytic Fluorination and Selective Difluorocarbene Formation

4.2.1 Introduction

Transition metal complexes bearing fluoride or fluorocarbon ligands have attracted considerable interest because they are used to mediate/catalyze C–F or C–R^F bond-forming reactions, which are highly important in the pharmaceutical, agrochemical, and advanced materials industries.[2,3] Despite this widespread interest, the fundamental chemistry of these species is considerably less developed than that of analogous hydrocarbon compounds. In particular, reports of complexes bearing two fluorinated ligands (i.e., one perfluoroalkyl and one fluoride, or two perfluoroalkyls) are very rare, with most examples belonging to second or third row metals.[4–7] Recently, examples of Ni complexes bearing two perfluoroalkyl ligands have been reported.[8–10] There are synthetic challenges associated with preparing such complexes: The most direct approach would be via oxidative addition of the C–F or C–C bond of a perfluoroalkane (CF_4, C_2F_6, C_3F_8, etc.) to a low-valent metal, but the inert nature of perfluoroalkanes makes this route inaccessible.[2] Here, we use alternative synthetic routes to access the products of the hypothetical oxidative addition reaction between perfluoroalkanes and first row metals. Our general strategy is to utilize the oxidative addition of iodoperfluoroalkanes (R^F–I) to install the first perfluoroalkyl group on the metal, followed by exchange of the iodide ligand for either a fluoride or a trifluoromethyl group (Scheme 4.1).

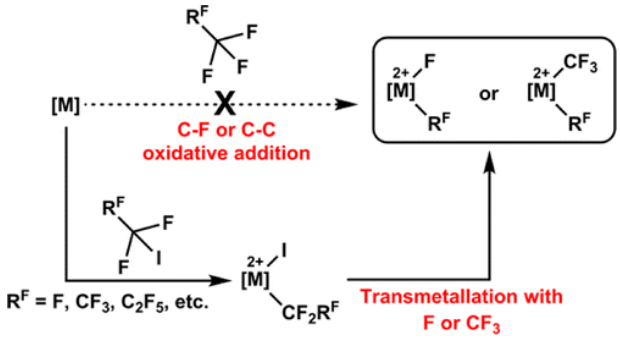

Scheme 4.1. Alternative Synthetic Route to Transition Metal Fluorides and Perfluoroalkyls

Oxidative addition of R^F–I to metal complexes has been shown to proceed for group 9 metals,[11,12] and methods for converting [M]–X (X = halide) to [M]–F[13,14] or to[M]–CF_3[3,15–19] are known. Reactions between the inexpensive and commercially available cobalt(I) complex $CpCo(CO)_2$ (Cp = η^5-cyclopentadienyl) and R^F–I (R^F = CF_3 and CF_2CF_3) furnish cobalt(III) complexes $CpCo(R^F)(I)(CO)$.[20] Substitution of the carbonyl ligand with a phosphine is facile and leads to the series of isolable starting materials $CpCo(R^F)(I)(L)$ (**1**–**4**), as shown in Scheme 4.2.[21]

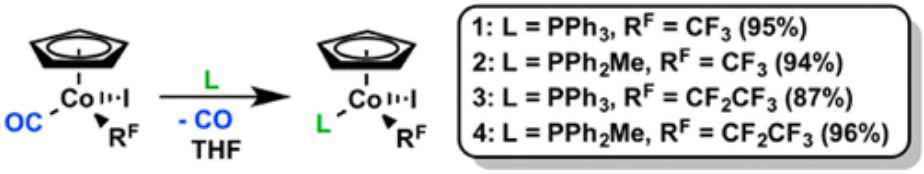

Scheme 4.2. Synthetic Scheme for Phosphine Substitutions

In recent reports, we described the two-electron reduction of complexes **1**–**4** with sodium to furnish a series of nucleophilic Co^I perfluorocarbene complexes, and demonstrated [2 + 2] cycloaddition reactions with tetrafluoroethylene.[22,23] The resulting cobalt(III) perfluorometallacyclobutane complexes reacted with both Lewis and Brønsted acids to give ring-opening/isomerization products. However, the chemistry of cobalt(III) systems with multiple perfluorinated ligands remains largely unexplored, and herein we expand that area.

4.2.2 Results and Discussion

4.2.2.1 Synthesis and Characterization of Perfluoroalkyl Cobalt Fluorides

Seeking to isolate the hypothetical products that would arise from the oxidative addition of perfluoroalkanes to a cobalt center, we opted for a pathway involving the substitution of iodide for fluoride, using a method previously reported by Hughes et al. to afford analogous perfluoroalkyl Ir^{III} fluorides.[14] Reactions of complexes **1**–**4** with 3 equiv of AgF in dichloromethane at room temperature over 20 h in the absence of light afforded perfluoroalkyl Co^{III} fluoride complexes of the general formula $CpCo(R^F)(F)(L)$ (Cp = η^5-cyclopentadienyl, R^F = CF_3 and CF_2CF_3, L = PPh_3 and PPh_2Me) (**5**–**8**) in 68–91% isolated yield as dark-

green solids (Scheme 4.3). Complexes **5**–**8** were characterized spectroscopically and structurally, and the results were further analyzed by density functional theory (DFT) calculations with the B3LYP[24] and PW91[25,26] exchange-correlation functionals and polarized double- and triple-ζ basis sets. Structurally, complexes **5** and **6** represent the expected products arising from the oxidative addition of perfluoromethane to cobalt, whereas complexes **7** and **8** are those that would arise from the same type of reaction with perfluoroethane. As previously mentioned, these oxidative addition reactions are not feasible; thus, it is necessary to utilize other synthetic methods to obtain such complexes.

Scheme 4.3. Synthetic Scheme for Cobalt(III) Fluorides

Cobalt fluorides are uncommon in the literature, and the few that have been presented mostly feature cobalt in either the +1 or the +2 oxidation state.[27,28] There are only three examples featuring cobalt in the +3 oxidation state: cobaltocenium fluoride, CoF_3, and an example from Klein et al. with a cyclometalated complex featuring azine as an anchoring group.[29] Cobaltocenium fluoride was synthesized by Richmond et al. in 1994, and has been applied to several stoichiometric fluorination reactions.[30] This extremely hygroscopic reagent is formed from the reaction of the one-electron reductant cobaltocene with an excess of perfluorodecalin in toluene at low temperature. CoF_3 is commercially available, although it is often too reactive to promote transformations in a selective manner. Of these three systems, only cobaltocenium fluoride and the cyclometalated cobalt fluoride are truly organometallic complexes, but they do not offer any opportunity for varying the ligand environment on cobalt because their scaffolds are limited as a result of the conditions of forming the fluorides, contrary to complexes **5**–**8**, which offer the ability to modify both the nature of the phosphine ligands and the perfluoroalkyl ligands on cobalt.

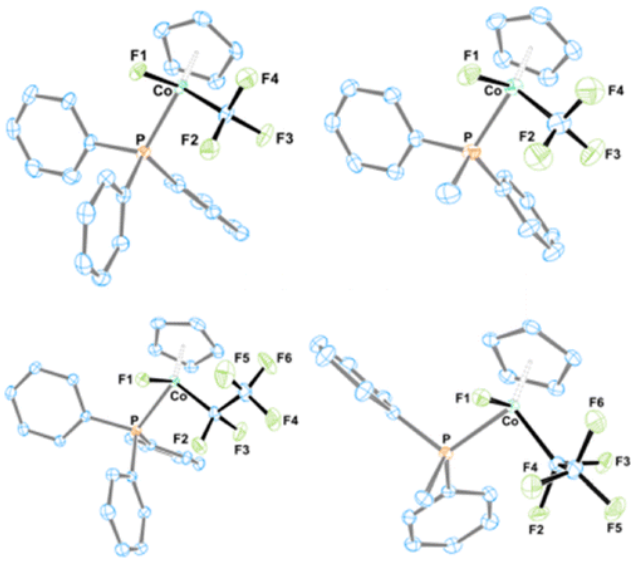

Figure 4.1. Crystallographic representations of 5 (top left), 6 (top right), 7 (bottom left), and 8 (bottom right) with 30% probability thermal ellipsoids. Hydrogen atoms are omitted for clarity. One molecule of acetonitrile has been removed from 5. Sample of 6 crystallized with two molecules in the unit cell.

X-ray structural studies confirm that complexes **5**–**8** are well-defined monomeric Co^{III} fluorides featuring cyclopentadienyl, phosphine, and perfluoroalkyl ligands (Figure 4.1). The Co–F bond distances in complexes **5**–**8** range from 1.86 to 1.88 Å (Table S1), similar to the value of 1.89 Å found in CoF_3.[31] For perfluoroethyl complexes **7** and **8**, the C_α–F bond distances (avg. 1.378(2) and 1.393(2) Å) are significantly longer than C_β–F (avg. 1.326(2) and 1.333(2) Å) as observed previously for an Ir analog.[14] The Co–P distances are approximately 0.04 Å shorter with PPh_2Me as compared to PPh_3 because the former is known to be a slightly more basic donor ligand. Moreover, the Co–C bond distances are shorter for the trifluoromethyl ligand versus the perfluoroethyl fragment by 0.2 Å for the PPh_3 derivatives and 0.4 Å for the PPh_2Me examples. Seminal work by Stone et al. has established that [M]–C bonds are shorter with perfluoroalkyls than with analogous hydrocarbons, an effect observed in this system as well.[32] Recently, another example of a transition metal simultaneously bearing a fluoride and a perfluoroalkyl was reported that features a bis(trifluoromethyl) nickel dimer with bridging fluoride ligands.[33]

DFT calculations were used to gain insight into the electronic structure of **5** as a representative example. TD-DFT calculations at the B3LYP/TZVP level with the SMD solvent model[34] reproduced the electronic absorption spectrum in CH_2Cl_2 well, with two principal experimental bands at 16 300 cm^{-1} (263 M^{-1} cm^{-1}, calcd = 15 600 cm^{-1}) and 21 800 cm^{-1} (1190 M^{-1} cm^{-1}, calcd = 21 700 cm^{-1}). (See Figure S1 and the band assignments in the Supporting Information.) Relative to typical Co^{III} octahedral inorganic complexes, the high intensities of these two absorption bands indicate significant charge-transfer character in the corresponding electron excitations. Calculated Mayer bond orders[35] for **5** provide values for Co–Cp (2.37), Co–PPh_3(0.98), and Co–CF_3 bonds (0.91) that are unsurprising. However, the value for the Co–F bond (0.61) indicates significant ionic character in this metal–ligand interaction and that the Co–F is the least covalent among the metal–ligand bonds.

The ^{19}F NMR spectra of **5**–**8** exhibit extreme upfield resonances for the fluoride ligands ranging from δ −716 to −759 ppm. These shifts are significantly upfield from the analogous Ir complexes previously reported by both Hughes et al.[14] (δ(^{19}F) = −437 to −446 ppm) and Bergman et al.[36] (δ(^{19}F) = −413 to −415 ppm). To the best of our knowledge, these represent the most upfield resonances reported for a ^{19}F NMR signal. The resonances at half-height are very broad (900–1900 Hz) and featureless, presumably because of the fluorides being bound to ^{59}Co, a nuclide with a spin of $^{7}/_{2}$, a natural abundance of 100%, and a large quadrupolar coupling constant of 42.0 × 10^{-30} m^2, all of which contribute to a significant broadening of the fluoride signal. The addition of molecular sieves to an NMR sample of **5**–**8** did not affect the broadness of the fluoride signals, indicating that the signal is not broadened artificially by the presence of moisture.

From the results of DFT computational studies, we are now able to understand the unique nature of these chemical shifts. The results for all of the calculated Co–F chemical shifts and their diamagnetic and paramagnetic tensor components are shown in the Supporting Information. There are minor quantitative differences between the three sets of chemical calculations but not qualitative differences. There is reasonable agreement with experiment for the CF_3 and CF_2 chemical shifts with differences of up to 30 ppm, which is typical of such fluorine NMR calculations. The differences between the experimental and the calculated shifts for the F bonded to the Co are larger by 30–100 ppm depending on the method, with

the BLYP/TZVP2 results being the closest to experiment for this shift. The magnitudes of the calculated shifts for the Co–F were found to be very sensitive to the bond distance, suggesting why the difference between the calculated and experimental values for this shift can be large. For L = PPh_3 and R = CF_3, the calculations predict a small value for the ^{19}F shift of the CF_3group (ca. −20 ppm as compared to the experimental value of −2 ppm), so the difference in the diamagnetic and paramagnetic components are comparable to those of the standard $CFCl_3$(BLYP/TZ2P σ(standard) = 118.8 ppm) with the diamagnetic component larger than the paramagnetic component. The ^{19}F chemical shift for the F bonded to the Co is large and negative, resulting from the fact that the diamagnetic and paramagnetic components have the same sign, both shielding. The paramagnetic component is larger than the diamagnetic component. We note that the diamagnetic shielding component for the F bonded to C and of the F bonded to Co are very similar, within ∼10 ppm, so the large changes are due to the differences in the paramagnetic components between the "normal" value for the F in the CF_3group and the value predicted for the F bonded to Co.

The fact that the paramagnetic component tensor has the same sign as the diamagnetic component tensor has been noted previously for ClF because of mixing of the appropriate π orbitals with the σ* orbital in the presence of a magnetic field.[37–39] Although F_2 has the same mixing interactions, the presence of symmetry prevents the paramagnetic component from being shielding. The high-lying occupied and low-lying unoccupied molecular orbitals (HOMO and LUMO, respectively) for $CpCo(CF_3)(F)(PH_3)$ and $CpCo(CF_3)(F)(PPh_3)$ are shown in the Supporting Information. The orbitals are essentially the same for both compounds. The HOMO, HOMO-1, and HOMO-2 are lone pairs on the F bonded to Co interacting with different d orbitals on the Co. For the Co contribution, the HOMO is the $d_{x^2y^2}$, the HOMO-1 is the d_{z^2}, and the HOMO-2 is the d_{xy}. The LUMO is the Co–F σ* orbital with the d_{xz} on the Co, and the LUMO+1 is predominantly the Co–C σ*. Thus, the HOMO, HOMO-1, and HOMO-2 serve as the equivalent to the π-type orbitals in ClF, and the LUMO is the equivalent of the ClF σ*. It is the interaction of these orbitals in the presence of a magnetic field that leads to the paramagnetic component being shielding, similar to what is found for ClF.

4.2.2.2 Reactivity of Fluoride Complexes

The importance of fluorinated organic substrates has been amply demonstrated.[40] Efficient, reliable techniques for the introduction of fluorine into such products have been the subject of widespread research for many years.[41] Consequently, and encouraged by the ionic character of the Co–F bonds in our system, we sought to determine the ability of these cobalt systems to fluorinate simple organic compounds. Reactions with *p*-toluoyl chloride were explored as a potential route toward fluorination to form *p*-toluoyl fluoride. Gray et al. have recently demonstrated this reaction in stoichiometric fashion, proceeding through halide metathesis with cyclometalated iridium fluoride complexes.[42] Stoichiometric reactions with complex **6** in C_6D_6showed clean and essentially complete conversion of the starting substrate within 2 h and formation of the *p*-toluoyl fluoride product, proceeding through overall halide metathesis with the cobalt fluoride complex. Prompted by the initial results of these stoichiometric reactions, we aimed to develop a catalytic process whereby, starting with the iodide complex **2**, the fluoride complex **6** could be generated in situ by the presence of an excess of AgF.

Control experiments convincingly demonstrated that stoichiometric reactions between *p*-toluoyl chloride and the fluoride sources AgF, CsF, KF, and CoF_3 gave minimal conversion of the starting reagent to the target compound overnight in dichloromethane (<5% in all cases). Optimized reaction conditions led to essentially quantitative conversion of the starting chloride to the fluoride within 4 h, using 5 mol % of **2** and 3 equiv of AgF. (See Table 1 for selected control experiments and Table S16 for a full list.) This catalytic fluorination occurs cleanly, affording an approximately 1:1 mixture of the Co–F and Co–Cl complexes upon completion. Relatively few methods of producing *p*-toluoyl fluoride exist in the literature, and they feature either exotic or potentially harmful reagents such as cyanuric fluoride,[43] cesium fluoroxysulfate,[44] potassium bifluoride,[45] and hydrogen fluoride.[46] Furthermore, this substrate is not commercially available, but Pd-based systems are used to produce it catalytically.[47] Two stoichiometric reactions were run in parallel, one of them containing excess PPh_2Me (5 equiv), and analyzed at the same time. Both reactions provided the same amount of conversion to the target product. It thus appears unlikely

that the reaction proceeds through a dissociative mechanism, wherein the phosphine could dissociate from the metal and vacate a coordination site for the acyl chloride to bind.

Table 4.1. Catalytic Fluorination Reactions

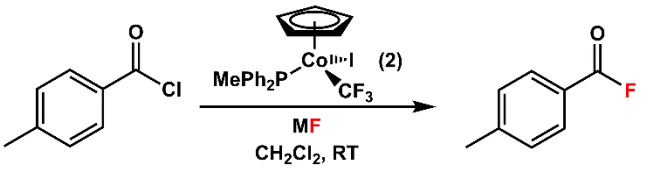

Entry	MF (eq)	Catalyst Loading (mol%)	t (h)	Yield (%)
1	AgF (1.0)	-	16	2
2	CsF (1.0)	-	16	5
3	KF (1.0)	-	16	< 1
4	CoF_3 (1.0)	-	16	2
10	AgF (3.0)	10	4	99
14	AgF (3.0)	5	4	99
15	AgF (3.0)	1	4	47
16	AgF (3.0)	0.1	4	26

With this information in hand, a proposed catalytic cycle is shown in Scheme 4.4. Starting from iodide complex **2**, fluoride analogue **6** is first formed using AgF as the fluoride source. The ionic nature of the Co–F bond provides a latent source of fluoride, which can react readily with the electrophilic carbon center of the acyl chloride. Expulsion of the chloride from the organic substrate gives the target compound, generating a cobalt chloride complex, which can react with AgF to regenerate the catalytically active complex **6** and form the inactive AgCl. Many examples of electrophilic fluorination of organic substrates have been explored over recent years,[48] and efficient catalytic nucleophilic fluorination has more recently made major strides as well.[49] Importantly, transition metals have been used to perform the nucleophilic fluorination of a variety of alkyl fluorides,[50–52] alkenyl fluorides,[53–55] and aryl fluorides.[56–60] Alkyl fluorides have been synthesized by Toste et al. from gold(III)[50] systems and by Sanford et al. from palladium(IV)[52,56] systems. Electrophilic gold(I)[53,54] complexes have been used almost exclusively for the synthesis of alkenyl fluorides, affording good yields and regioselectivity. Aryl fluorides have been

synthesized by the groups of Sanford et al. and Gagné et al. through the use of palladium(IV)[56] and platinum(IV),[57] respectively, as well as certain silver salts[58,58–60] and some copper complexes.[61–63] Additionally, Grushin et al. have reported various fluorination examples with palladium(II) and rhodium(I) systems.[64–66] Of these examples, only copper stands out as a nonprecious, first row transition metal. Catalytic systems incorporating these types of abundant and nontoxic metals are very important and are active areas of research as the search for renewable and efficient methods of producing target fluorinated reagents continues. Moreover, the catalytic formation of C(sp^2)–F bonds has mostly been limited to examples with palladium[62,67,68] as well as a few with copper[61] and gold.[53,54]

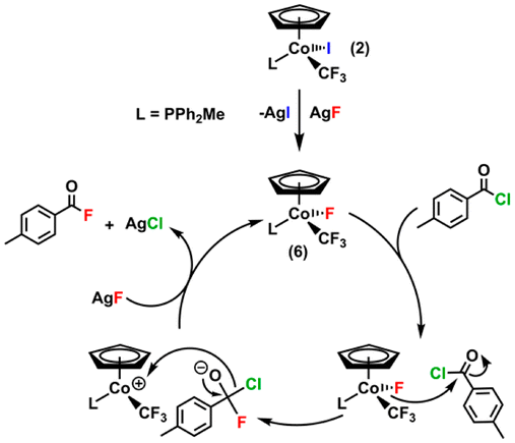

Scheme 4.4. Proposed Catalytic Cycle for the Fluorination of *p*-Toluoyl Chloride

The tendency of third row transition metals to form weaker bonds to fluorine than most first row transition metals has made them useful for catalytic reactions,[2,69] but it is essential to develop methods that utilize inexpensive, nontoxic, and abundant metals such as cobalt. Interestingly, it appears that the significant ionic character of the Co–F bond in this system, as demonstrated by the calculated Mayer bond orders, might be a major contributing factor to its catalytic potential. Furthermore, this reaction does not require the use of extravagant reagents and represents a step toward the potential uses of cobalt in additional catalytic fluorination reactions.

4.2.2.3. Synthesis and Characterization of Cobalt Bis(perfluoroalkyls)

The isolation of perfluoroalkyl cobalt(III) halide complexes **1**–**8** motivated efforts to generate bis(perfluoroalkyl) complexes via transmetalation of the halide group with CF_3. Converting [M]–X complexes to [M]–CF_3 is an established process, first presented by Fuchikami et al.[70] using a copper system and Me_3SiCF_3 and subsequently by other groups.[17,18] We initiated our investigation by studying the reactivity of the Co^{III} perfluoroalkyl halide complexes with Me_3SiCF_3, using CsF as the initiator and DMF as solvent. Reactions with PPh_3 derivatives mostly resulted in decomposition and very low yields of the desired products. However, reactions with PPh_2Me derivatives (**2**, **4**, **6**, and **8**) led to the desired bis(perfluoroalkyl) products (**9** and **10**) in good yields (**9** = 71% and **10** = 75% from [Co]–F, **9** = 57% and **10** = 52% from [Co]–I) after only 2 h as stable yellow-orange powders (Scheme 4.5). Although the relative yields are lower when starting from [Co]–I complexes, it is an overall more direct approach to complexes **9** and **10**.

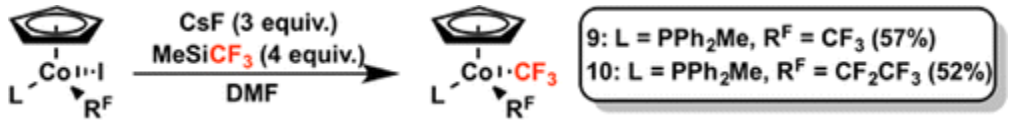

Scheme 4.5. Synthesis Scheme for Cobalt(III) Bis(perfluoroalkyls)

It has been demonstrated previously that Me_3SiCF_3 undergoes activation by fluoride to liberate CF_3. Important studies by Yagupolskii et al.[71] and Röschenthaler et al.[72] independently demonstrated that this activation involves the in situ formation of pentacoordinate silicate anions, either $[Me_3SiF(CF_3)]^-$ or $[Me_3Si(CF_3)_2]^-$, which extrude $[CF_3]^-$ to form Me_3SiF or Me_3SiCF_3, respectively. We propose that in our system, CsF reacts with Me_3SiCF_3 to produce the cesium salts of the aforementioned pentacoordinate silicates, which then effect the transmetalation with [Co]–X. This is in contrast to a report by Wang et al.,[73] where the reaction between AgF and Me_3SiCF_3 forms a proposed [$AgCF_3$] species that can effect transmetalation. It is important to note that for [Co]–I complexes **2** and **4**, CsI is formed during the course of the reaction. In addition, experiments in our lab show the following: (1) When CsI is used in the place

of CsF, no transmetalation takes place. (2) [Co]–I complexes **2** and **4** do not react with CsF in DMF to produce [Co]–F complexes **6** and **8**. These observations are consistent with the lower yield of products **9**/**10** when starting from [Co]–I (**2**/**4**) rather than [Co]–F (**6**/**8**).

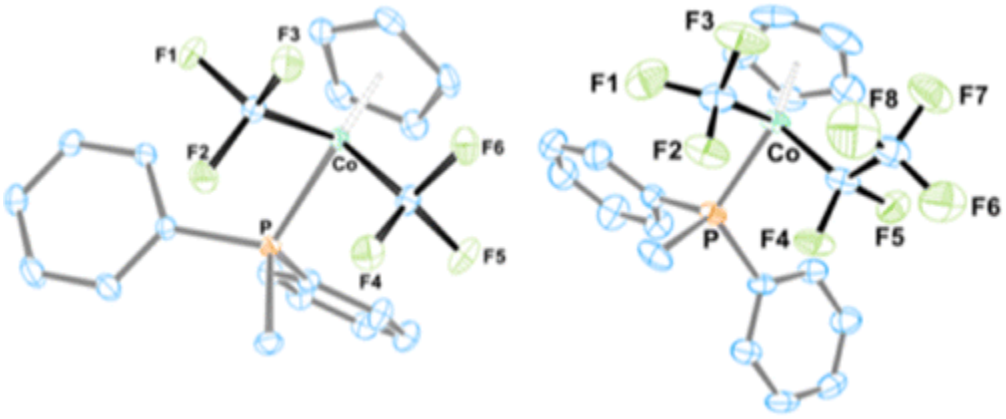

Figure 4.2. Crystallographic representations of 9 (left) and 10 (right) with 30% probability thermal ellipsoids. Hydrogen atoms are omitted for clarity. One molecule of toluene has been removed from both 9 and 10.

Complexes **9** and **10** were studied through X-ray crystallography (Figure 4.2). The Co–C bond distance of 1.940 Å in **9** is significantly longer than the Ni–C bond distances in analogous nickel bis(trifluoromethyl) complexes: The (bipy)Ni(CF_3)$_2$ complex from Vicic et al.[8] has a distance of 1.88 Å, and an example from Mirica et al.[9] has a distance of 1.91 Å with the Ni^{II} complex. However, the latter's bond lengths increase to 1.97 Å when the metal is oxidized to Ni^{III}. A recent report by Sanford et al. features an octahedral Ni^{IV} complex, TpNi(Ph)(CF_3)$_2$ (Tp = trispyrazolylborate), with Ni–C bond distances of 1.99 Å.[10] It is interesting to compare this complex with **9** because they are both d^6 systems, and the Ni^{IV} complex was proven capable of promoting Aryl–CF_3 coupling through reductive elimination.

DFT calculations were used to obtain insight into the electronic structure of **9**. TD-DFT calculations at the B3LYP/TZVP level reproduce the electronic absorption spectrum well (Figure S1). The absorption bands in **9** are blue-shifted relative to the spectrum of **5**. The assignment of two bands at 23 000 cm^{-1} (shoulder)

and 25 800 cm^{-1} (730 M^{-1} cm^{-1}) is shown in the Supporting Information. Calculated Mayer bond orders for **9** are 2.31 for the Co–Cp bond, 1.01 for Co–PPh_2Me, and 0.93 and 0.95 for the two Co–CF_3 bonds. These bond orders are almost identical to those in **5**. Thus, replacement of the fluoride ligand in **5** with the more strongly covalently bound CF_3 ligand does not affect the covalency of other Co–ligand interactions.

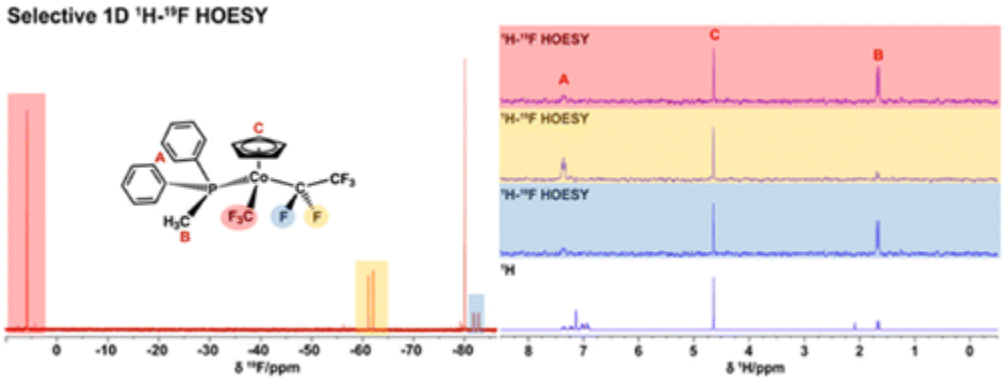

Figure 4.3. Selective 1D ^1H–^{19}F HOESY experiment in C_6D_6 to help in the assignment of the two [Co]–C$F_2$$CF_3$ fluorine signals is shown. The Cp signals were set to equal intensity for the purposes of clarity. Colored boxes above the ^1H spectrum demonstrate the effect of selective saturation of the appropriate fluorine signal and showing which signals are correlated by a through-space interaction.

Full NMR characterization of these complexes was obtained, and assignment of the nonequivalent methylene fluorine resonances in the various ^{19}F spectra was achieved. A 1D ^1H–^{19}F HOESY experiment allowed the selective pulsing of each of the three different fluorine resonances to determine the relative spatial proximity to the three closest protons in the structure (Figure 4.3). Additionally, a ^{19}F–^{19}F NOESY was collected to observe how the trifluoromethyl ligand correlated through space to the different methylene fluorines of the perfluoroethyl ligand (Figure S34). These experiments indicate that the relative orientation of the ligands is essentially the same in solution as in the solid state.

The 1D ^1H–^{19}F HOESY experiment has been utilized recently by Claridge et al.[74] in the analysis of fluorinated pyrrolidines. This experiment offers the advantage of being much faster than the more prevalent 2D ^{19}F–^{19}F NOESY experiments found in the literature. In our case, by taking advantage of two nuclides in ^1H and ^{19}F that each have essentially 100% natural abundance, the 1D method offers the possibility to

obtain similar conformational information in a matter of minutes, as opposed to several hours for the traditional 2D method.

4.2.2.4 Reactivity of Bis(Perfluoroalkyl) Complexes

Transition metal perfluoroalkyl complexes can be precursors to metal fluorocarbenes. We previously reported the two-electron reduction of perfluoroalkyl Co^{III} iodide complexes **1**–**4** to afford Co^{I} fluorocarbene complexes, which exhibit nucleophilic type reactivity at the carbene carbon.[22,23] We are interested in preparing analogous Co^{III} fluorocarbenes in order to probe the effect that changing the oxidation state of cobalt will have on carbene reactivity, with the expectation that Co^{III} fluorocarbenes might react as electrophiles. This concept was previously demonstrated in an elegant study by Roper et al., where they showed that Ru^{0} and Ru^{II}fluorocarbenes differed by having nucleophilic and electrophilic reactivity at the carbene carbon, respectively.[1]

Our strategy to prepare Co^{III} fluorocarbenes consisted of abstracting a fluoride from a perfluoroalkyl ligand using a Lewis acid, similar to the preparation of other fluorocarbene complexes in the literature. Our initial attempts to abstract a fluoride from perfluoroalkyl Co^{III}iodides **1**–**4** were unsuccessful because reactions with the Lewis acids Me_3SiOTf and $B(C_6F_5)_3$did not result in the formation of fluorocarbenes, presumably as a result of a preference by the Lewis acid to abstract the iodide ligand. However, bis(perfluoroalkyl) complexes **9**–**10** were attractive precursors for fluorocarbene formation because they both eliminate the possibility of an undesirable metal halide abstraction. Indeed, reactions of **9** and **10** with Lewis acids (Me_3SiOTf and $B(C_6F_5)_3$) in DCM led to fluoride abstraction and formation of cobalt difluorocarbene complexes (**Int 1**–**4**, Scheme 4.6). Addition of the Lewis acid to a solution of the bis(perfluoroalkyl) precursors led to a color change from yellow-orange to deep red over the course of 1 h at room temperature, and NMR analysis demonstrated that quantitative conversion was achieved. The ^{19}F NMR resonances for the difluorocarbene ligand in complexes **Int 1**–**4** are highly characteristic, with downfield chemical shifts

ranging between δ 178 and 180 ppm.[75,76] This is in contrast to the difluorocarbene ligand of previously reported Co^{I} complexes, with resonances for the two unique fluorine environments at δ 63 and 94 ppm.[22,23]

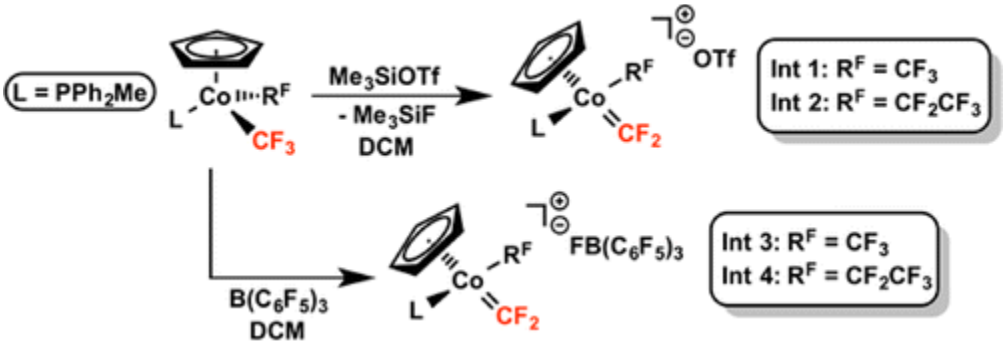

Scheme 4.6. Formation of Cobalt(III) Difluorocarbenes

Both Lewis acids provided selective fluoride abstraction from complex **10** because only abstraction from the trifluoromethyl ligand was observed, leaving the perfluoroethyl fragment untouched (Scheme 4.7). This is supported by ^{19}F NMR, where the only fluorocarbene signal that is observed is the one associated with the difluorocarbene fragment and not that of the fluoro(trifluoromethyl) carbene. The selectivity of fluoride abstraction from CF_3 and not CF_2CF_3can be rationalized by comparing the π-donating ability of F and CF_3 fragments. Metal carbene bonds are typically stabilized by contributions of d orbital electrons from the metal. However, because the Co^{III} carbene complexes here have two fewer d electrons compared to the Co^{I}carbenes we reported previously (d^6 vs d^8), the M═C bond is likely more reliant on donation from the other carbene substituents for stabilization. Therefore, because F is a better π-donating substituent than CF_3, fluoride abstraction from CF_3 rather than CF_2CF_3 is preferred. Efforts to increase electron density around the metal by utilizing PMe_3 in the hopes of promoting some amount of fluoride abstraction from the perfluoroethyl ligand were unsuccessful.

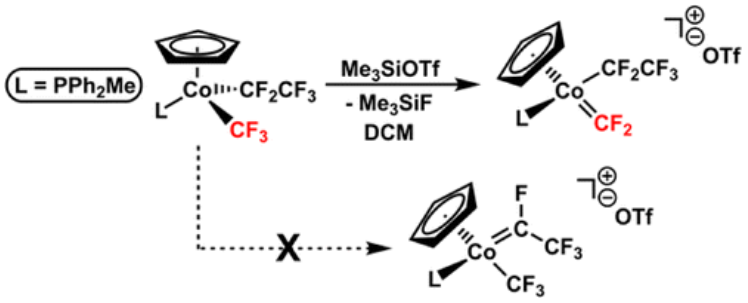

Scheme 4.7. Selectivity of Fluoride Abstraction

The newly formed difluorocarbene complexes underwent two primary reactions in solution, which prevented their isolation in pure form. One involves the insertion of difluorocarbene into the remaining perfluoroalkyl fragment, effectively increasing the length of the perfluoroalkyl chain on the transition metal center by one CF_2 unit (Scheme 4.8, top). These products are clearly identified using ^{19}F NMR because the resulting perfluoroethyl and perfluoropropyl ligands have highly characteristic chemical shifts and splitting patterns, which are identical to those of previously isolated Co^{III} complexes.[77] Previous work by Burton et al.[78,79] on copper demonstrated a rare example of this type of perfluoroalkyl chain growth from CF_2 insertion on a transition metal. This reaction demonstrates a step toward potential perfluoroalkene polymerization using a transition metal catalyst, a sought-after process that has been stunted at least in part by the difficulties involved in promoting such insertion reactions,[80] in large part due to the strength of various [M]–R^F bonds. Attaining better control of this reaction is an area of ongoing study within our group.

The second reaction is the well-known hydrolysis of the difluorocarbene ligand by trace H_2O to furnish a carbonyl ligand and 2 equiv of HF (Scheme 4.8, bottom).[81] This reaction occurs almost instantaneously and is a common reaction with metal difluorocarbenes that have formal d^6 metal centers.[1,82] Although the hydrolysis of difluorocarbene ligands is undesirable, the observation of electrophilic reactivity by our Co^{III} fluorocarbenes further highlights a key difference from our previously reported Co^{I} fluorocarbenes, which did not react with 20 equiv of H_2O in acetonitrile solutions.

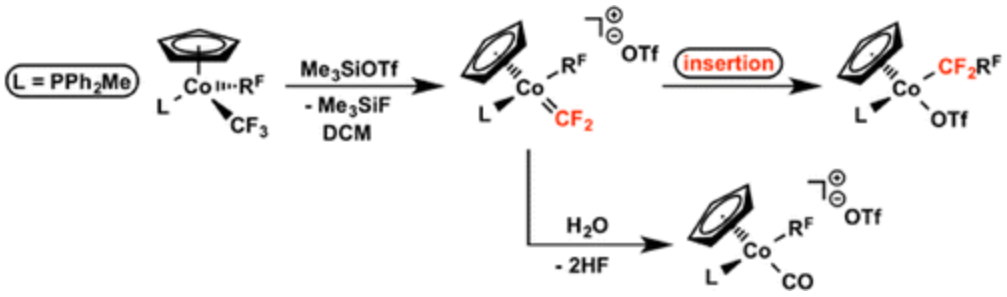

Scheme 4.8. Reactivity of Cobalt(III) Difluorocarbenes

4.2.3 Conclusions

We have isolated and characterized four perfluoroalkyl Co^{III} fluoride complexes. These complexes exhibit remarkable ^{19}F NMR shifts, largely due to an unusual paramagnetic component that is shielding. Additionally, these complexes were shown to be active in the catalytic fluorination of *p*-toluoyl chloride. Furthermore, both the fluoride and iodide complexes could be used in the synthesis of Co^{III} bis(perfluoroalkyl) complexes, potential precursors in the development of catalytically relevant systems. These complexes were shown to react with different Lewis acids to form electrophilic Co^{III} difluorocarbenes. The insertion of these difluorocarbenes into the remaining perfluoroalkyl fragment on the metal demonstrated the elongation of a perfluoroalkyl chain on a transition metal by one carbon. Further studies on the catalytic activity of these complexes are currently underway in our laboratory.

4.3 Experimental Details for Section 4.2

4.3.1 General Considerations

All manipulations were carried out using standard Schlenk techniques or in an MBraun glovebox. All glassware was oven-dried at >150 °C for a minimum of 2 h prior to use or flame-dried using a torch. Toluene, hexanes, tetrahydrofuran (THF), diethyl ether (DEE), and dimethylformamide (DMF) were dried on columns of activated alumina using a J. C. Meyer (formerly Glass Contour) solvent purification system. Dichloromethane (DCM), chloroform-*d* ($CDCl_3$), and acetonitrile-d_3(CD_3CN) were dried by refluxing over calcium hydride under a nitrogen flow, followed by distillation and filtration through a column of activated

alumina (ca. 10 wt %). Benzene-d_6 (C_6D_6) was dried by standing over activated alumina (ca. 10 wt %) overnight followed by filtration. The following chemicals were used as purchased, without further purification: $CpCo(CO)_2$ (Cp = η^5-cyclopentadienyl) (Strem, 95%), CF_3I (SynQuest, 99%), CF_3CF_2I (SynQuest, 98%), PPh_3(Strem, 99%), PPh_2Me (Strem, 99%), Me_3SiOTf (OTf = SO_3CF_3) (Aldrich, 98%), AgF (Strem, 98%), CsF (Strem, 99+%), KF (Aldrich 99+%), CoF_3 (Aldrich, 98%), and *p*-toluoyl chloride (Aldrich, 98%). Starting complexes $CpCo(R^F)(I)(CO)$ (Cp = η^5-cyclopentadienyl; R^F = CF_3 and CF_2CF_3) were synthesized according to slightly modified literature procedures from $CpCo(CO)_2$. From these complexes, facile substitution of the CO ligands provided the phosphine analogues according to a slightly modified literature procedure. (See the Supporting Information for complete details on isolation of these complexes.) ^1H, ^{19}F, $^{19}F\{^1H\}$, and $^{31}P\{^1H\}$ NMR spectra were recorded on either a 300 MHz Bruker Avance or 300 MHz Bruker Avance II spectrometer at room temperature. ^1H NMR spectra were referenced to the residual proton peaks associated with the deuterated solvents (C_6D_6 = 7.16 ppm, $CDCl_3$ = 7.26 ppm, CD_3CN = 1.94 ppm). ^{19}F and $^{19}F\{^1H\}$ NMR spectra were referenced to internal 1,3-bis(trifluoromethyl)benzene (BTB) (Aldrich, 99%, deoxygenated by purging with nitrogen and stored over 4 Å molecular sieves), set to −63.5 ppm. $^{31}P\{^1H\}$ NMR spectra were referenced to external H_3PO_4 (85% aqueous solution), set to 0.0 ppm. The ^{19}F NMR signals corresponding to the different [Co]–CF_2CF_3 complexes are labeled as A and A′. For labeling information, see Figure S24. Assignments were derived from 2D experiments with $CpCo(CF_2CF_3)(CF_3)(PPh_2Me)$ and applied to the other complexes because instrumental constraints did not permit the same experiments to be undertaken with the various fluoride complexes. Throughout this manuscript, F^A refers to the more upfield resonance and $F^{A'}$ refers to the more downfield resonance. UV–vis spectra were recorded on a Cary 100 instrument, using sealable quartz cuvettes (1.0 cm path length). Elemental analyses were performed by the Laboratoire d'Analyse Élémentaire de l'Université de Montréal (Montréal, Québec, Canada) and the G. G. Hatch Stable Isotope Laboratory at the University of Ottawa (Ottawa, Ontario, Canada). A Micromass Q-ToF 1 (positive mode) was used for electrospray ionization (ESI), with samples diluted to ca. 5 μg/mL in methanol. Infrared spectroscopy was carried out on a Thermo Nicolet NEXUS 670 FTIR instrument. Powder X-ray diffraction

(PXRD) experiments were performed using a RIGAKU Ultima IV, equipped with a Cu Kα radiation source (λ = 1.541836 Å), and a graphite monochromator. Scanning of the 2θ range was performed from 5 to 40°. PXRD pattern was consistent in 2θ values with the generated pattern from XRD, with slight discrepancies in some intensities of peaks attributed to preferred crystallite orientation.

4.3.2 General Procedure for the Synthesis of $CpCo(R^F)(F)(L)$ ($R^R = CF_3$ or CF_2CF_3; L = PPh_3 or PPh_2Me

A 100 mL round-bottomed Schlenk flask was charged with $CpCo(R^F)(I)(L)$ (0.58 mmol) dissolved in CH_2Cl_2 (ca. 15 mL). AgF (1.74 mmol) was added, and the resulting solution/suspension was stirred at room temperature for approximately 20 h in the absence of light. After this time, a color change to dark green was observed. The resulting mixture was filtered through a plug of Celite, and the volatiles were removed in vacuo. The crude product was recrystallized from a concentrated solution of CH_2Cl_2 and hexanes at −35 °C. Pure product was collected via filtration, washed with cold (−35 °C) hexanes, and dried in vacuo. The products were obtained as dark-green powders. Crystals suitable for X-ray crystallography were obtained by diffusion of hexanes into a concentrated solution of the appropriate complex in toluene. Complexes **5** and **7** were not viable for elemental analysis (approximately 1–2% off) because we suspect a small amount of unidentified paramagnetic impurity. The latter also potentially contributes to the broadness of the ^{1}H NMR spectra for these complexes. The use of various solvents and variable temperature NMR were unsuccessful in diminishing the broadening. Sublimation, additional recrystallizations, and column chromatography were attempted to try and purify these complexes. Column chromatography with a solvent mixture of THF/MeOH (8:2), followed by recrystallization from a concentrated solution of toluene proved most effective, but a small amount of impurity was retained. Additionally, THF inserts within the crystal lattice and cannot be removed under high vacuum (ca. 10^{-3} mtorr), even with heating. As such, PXRD patterns were compared with the calculated pattern from XRD in order to confirm the bulk-phase purity of complex **7** (Figure S37). The patterns were in excellent agreement with one another, thus confirming the

crystalline-phase purity of the sample. The same comparison with complex **5** was unsuccessful because of the presence of solvent within the unit cell of the crystallographic data.

CpCo(CF$_3$)(F)(PPh$_3$) (5)

Yield: 245 mg, 89% based on CpCo(CF$_3$)(I)(PPh$_3$). UV–vis (1.0 mM in CH_2Cl_2) $\lambda_{max}(\varepsilon)$ = 459 (1190), 615 (263). ^{1}H NMR (300 MHz, C_6D_6) δ 4.60 (s, 5H, Cp), 6.98 (m, 6H, *m*- and *p*-C*H*(PPh)), 7.89 (m, 4H, *o*-CH(PPh)). ^{19}F NMR (282 MHz, C_6D_6) δ −2.0 (d, $^3J_{FF} \approx 8$ Hz, 3F, CF_3), −734 (br, $\omega_{1/2} \approx 1900$ Hz, 1F, Co–*F*). ^{31}P{^{1}H} NMR (121 MHz, C_6D_6) δ 29.8 (br, $\omega_{1/2} \approx 65$ Hz). Elemental analysis for $C_{24}H_{20}F_4PCo$ Calcd: C, 60.77; H, 4.25. Found: C, 58.73; H, 4.36.

CpCo(CF$_3$)(F)(PPh$_2$Me) (6)

Yield: 198 mg, 83% based on CpCo(CF$_3$)(I)(PPh$_2$Me). UV–vis (0.5 mM in CH_2Cl_2) $\lambda_{max}(\varepsilon)$ = 450 (1640), 604 (347). ^{1}H NMR (300 MHz, C_6D_6) δ 1.57 (d, $^2J_{HP} \approx 13$ Hz, 3H, CH_3), 4.60 (s, 5H, Cp), 7.05 (m, 6H, *m*- and *p*-C*H*(PPh)), 7.52 (dt, $^3J_{HH} \approx 8$ Hz, $^3J_{HP} \approx 78$ Hz, 4H, *o*-C*H*(PPh)). ^{19}F NMR (282 MHz, C_6D_6) δ −3.3 (d, $^3J_{FF} \approx 9$ Hz, 3F, CF_3), −716 (br, $\omega_{1/2} \approx 1300$ Hz, 1F, Co–*F*). ^{31}P{^{1}H} NMR (121 MHz, C_6D_6) δ 33.7 (br, $\omega_{1/2} \approx 130$ Hz). Elemental analysis for $C_{19}H_{18}F_4PCo$ Calcd: C, 55.36; H, 4.40. Found: C, 54.98; H, 4.69.

CpCo(CF$_2$CF$_3$)(F)(PPh$_3$) (7)

Yield: 277 mg, 91% based on CpCo(CF$_2$CF$_3$)(I)(PPh$_3$). UV–vis (0.5 mM in CH_2Cl_2) $\lambda_{max}(\varepsilon)$ = 473 (1420), 621 (340). ^{1}H NMR (300 MHz, $CDCl_3$) δ 4.61 (s, 5H, Cp), 7.40 (m, 6H, *m*- and *p*-C*H*(PPh)), 7.79 (m, 4H, *o*-C*H*(PPh)). ^{19}F NMR (282 MHz, $CDCl_3$) δ −68.6 (d, $^2J_{FF} \approx 240$ Hz, 1F, $CF^AF^{A'}$; $F^{A'}$), −79.8 (d, $^4J_{FF} \approx 10$ Hz, 3F, CF_3), −81.0 (ddd, $^3J_{FF} \approx 8$ Hz, $^3J_{FP} \approx 46$ Hz, 1F, $CF^AF^{A'}$; F^A), −759 (br, $\omega_{1/2} \approx 1000$ Hz, 1F, Co–*F*). ^{31}P{^{1}H} NMR (121 MHz, $CDCl_3$) δ 26.3 (br, $\omega_{1/2} \approx 95$ Hz). Elemental analysis for $C_{25}H_{20}F_6PCo$ Calcd: C, 57.27; H, 3.84. Found: C, 55.93; H, 3.97.

CpCo(CF$_2$CF$_3$)(F)(PPh$_2$Me) (8)

Yield: 268 mg, 68% based on $CpCo(CF_2CF_3)(I)(PPh_2Me)$. UV–vis (0.25 mM in CH_2Cl_2) $\lambda_{max}(\varepsilon)$ = 461 (3140), 605 (680). ^{1}H NMR (300 MHz, C_6D_6) δ 1.51 (d, $^2J_{HP} \approx 13$ Hz, 3H, CH_3), 4.60 (s, 5H, Cp), 7.07 (m, 6H, *m*- and *p*-C*H*(PPh)), 7.45 (dt, $^3J_{HH} \approx 7$ Hz, $^3J_{HP} \approx 55$ Hz, 4H, *o*-C*H*(PPh)). ^{19}F NMR (282 MHz, C_6D_6) δ −70.8 (d, $^2J_{FF} \approx 248$ Hz, 1F, $CF^AF^{A'}$; $F^{A'}$), −79.7 (d, $^4J_{FF} \approx 12$ Hz, 3F, CF_3), −80.7 (dd, $^3J_{FP} \approx 43$ Hz, 1F, $CF^AF^{A'}$; F^A), −734 (br, $\omega_{1/2} \approx 900$ Hz, 1F, Co–*F*). ^{31}P{^{1}H} NMR (121 MHz, C_6D_6) δ 31.9 (br, $\omega_{1/2} \approx 130$ Hz). Elemental analysis for $C_{20}H_{18}F_6PCo$ Calcd: C, 51.97; H, 3.93. Found: C, 51.45; H, 4.06.

4.3.3 General Procedure for the Synthesis of $CpCo(R^F)(CF_3)(PPh_2Me)$ (R^F = CF_3 or CF_2CF_3)

$CpCo(R^F)(I)(PPh_2Me)$ (0.877 mmol) was dissolved in DMF (15 mL), and CsF (2.63 mmol) was added as a solid. The resulting solution was stirred at room temperature for 5 min. To this solution was added dropwise Me_3SiCF_3 (4.22 mmol) in toluene (5 mL) over 3 min, and the reaction was stirred at room temperature for approximately 3 h. During this time, the color of the reaction mixture changed from dark green to bright orange. The mixture was then filtered through a pad of Celite, washed with ∼10 mL of toluene, and the filtrate was evaporated under vacuum to dryness. The resulting residue was triturated with DEE (4 × 10 mL). The orange solid was dissolved in minimal toluene and mounted on a silica-gel column. DEE was used as the eluent and pushed through the column until the washings were clear. The solvent was again removed under vacuum to afford pure product as a yellow-orange powder. Crystals suitable for X-ray crystallography were obtained from a concentrated solution of the appropriate complex in toluene cooled to −35 °C.

$CpCo(CF_3)_2(PPh_2Me)$ (9)

Yield: 231 mg, 57% based on $CpCo(CF_3)(I)(PPh_2Me)$. UV–vis (0.5 mM in CH_2Cl_2) $\lambda_{max}(\varepsilon)$ = 388 (1335), 430 (shoulder of the principal band). ^{1}H NMR (300 MHz, C_6D_6) δ 1.70 (d, $^2J_{HP} \approx 11$ Hz, 3H, CH_3), 4.63 (s, 5H, Cp), 7.01 (m, 6H, *m*- and *p*-C*H*(PPh)), 7.34 (m, 4H, *o*-C*H*(PPh)). ^{19}F NMR (282 MHz, C_6D_6) δ 3.6 (d, $^3J_{FP} \approx 3$ Hz, 6F, CF_3). ^{31}P{^{1}H} NMR (121 MHz, C_6D_6) δ 40.3 (br, $\omega_{1/2} \approx 150$ Hz). Elemental analysis for $C_{20}H_{18}F_6PCo$ Calcd: C, 51.97; H, 3.93. Found: C, 51.83; H, 3.99.

CpCo(CF_2CF_3)(CF_3)(PPh_2Me) (10)

Yield: 235 mg, 52% based on CpCo(CF_2CF_3)(I)(PPh_2Me). UV–vis (0.75 mM in CH_2Cl_2) $\lambda_{max}(\varepsilon)$ = 375 (730), 450 (shoulder of the principal band). ^{1}H NMR (300 MHz, CD_3CN) δ 1.69 (d, $^2J_{HP} \approx 11$ Hz, 3H, CH_3), 4.67 (s, 5H, Cp), 6.99 (m, 6H, *m*- and *p*-C*H*(PPh)), 7.31 (dt, $^3J_{HH} \approx 9$ Hz, $^3J_{HP} \approx 40$ Hz, 4H, *o*-C*H*(PPh)). ^{19}F NMR (282 MHz, CD_3CN) δ 5.2 (m, 3F, Co–CF_3), −62.3 (dd, $^2J_{FF} \approx 258$ Hz, $^3J_{FP} \approx 16$ Hz, 1F, $CF^AF^{A'}$; $F^{A'}$), −80.7 (m, 3F, Co–CF_2CF_3), −82.9 (dm, $^2J_{FF} \approx 258$ Hz, 1F, $CF^AF^{A'}$; F^A). ^{31}P{^{1}H} NMR (121 MHz, CD_3CN) δ 37.2 (br, $\omega_{1/2} \approx 140$ Hz). Elemental analysis for $C_{21}H_{18}F_8PCo$ Calcd: C, 49.24; H, 3.54. Found: C, 49.16; H, 3.70.

4.3.4 General Procedure for the Determination of NMR Yields in the Formation of [CpCo(R^F)(=CF_2)(PPh_2Me)](X) (R^F = CF_3 or CF_2CF_3; X = OTf^- or $[FB(C_6F_5)_3]^-$) and the Products Derived from These Intermediates

Note that as the difluorocarbene complexes form they react either with any trace quantities of water present (immediately) or in an insertion reaction (over a period of several hours). Furthermore, the reactions involving the difluorocarbene intermediates occur more quickly when using Me_3SiOTf as compared to $B(C_6F_5)_3$. Because of the enhanced stability of the difluorocarbenes formed by using $B(C_6F_5)_3$, yields for these complexes are reported for a certain reaction time. Because of the nature of these reactions, yields for the products deriving from the reactions with water and the insertion reactions will be presented for an elapsed reaction time with Me_3SiOTf and when possible with $B(C_6F_5)_3$.

Method A

CpCo(R^F)(CF_3)(PPh_2Me) (0.043 mmol) was dissolved in DCM (0.8 mL), and BTB (0.043 mmol) was added. The solution was transferred to an NMR tube, and Me_3SiOTf (0.043 mmol) was added with a microliter syringe. The NMR tube was sealed and shaken vigorously. The ^{19}F NMR yields were determined by integration of signals with respect to BTB. Complete conversion of starting material was observed within 60 min.

Method B

$CpCo(R^F)(CF_3)(PPh_2Me)$ (0.043 mmol) was dissolved in DCM (0.4 mL), and BTB (0.043 mmol) was added. The solution was transferred to an NMR tube, and a solution of $B(C_6F_5)_3$ (0.043 mmol) in DCM (0.4 mL) was added. The NMR tube was sealed and shaken vigorously. The ^{19}F NMR yields were determined by integration of signals with respect to BTB. Complete conversion of starting material was observed within 30 min.

[CpCo(CF₃)(═CF₂)(PPh₂Me)][OTf] (Int 1)

^{19}F NMR (282 MHz, CH_2Cl_2 with C_6D_6 capillary) δ 180.0 (br, 2F, Co═CF_2), 9.0 (br, Co–CF_3), −78.9 (br, 3F, C$F_3SO_3^-$). $^{31}P\{^1H\}$ NMR (121 MHz, CH_2Cl_2 with C_6D_6 capillary) δ 40.1 (br, $\omega_{1/2} \approx 136$ Hz).

[CpCo(CF₂CF₃)(═CF₂)(PPh₂Me)][OTf] (Int 2)

Yield: 68% based on Co = CF_2 after 30 min (20% after 4 h). ^{19}F NMR (282 MHz, CH_2Cl_2 with C_6D_6 capillary) δ 179.5 (br, 2F, Co═CF_2), −58.4 (d, $^2J_{FF} \approx 228$ Hz, 1F, $CF^AF^{A'}$; $F^{A'}$), −75.3 (dd, $^2J_{FF} \approx 228$ Hz, $^3J_{FP} \approx$ 36 Hz 1F, $CF^AF^{A'}$; F^A), −80.9 (br, 3F, Co–CF_2CF_3). $^{31}P\{^1H\}$ NMR (121 MHz, CH_2Cl_2 with C_6D_6 capillary) δ 35.6 (br, $\omega_{1/2} \approx 142$ Hz).

[CpCo(CF₃)(═CF₂)(PPh₂Me)][FB(C₆F₅)₃] (Int 3)

^{19}F NMR (282 MHz, CH_2Cl_2 with C_6D_6 capillary) δ 178.8 (br, 2F, Co═CF_2), 9.4 (br, Co–CF_3), −134.4 (d, br, $^3J_{FF} \approx 18$ Hz, 6F, FB(*o*-C_6F_5)$_3$), −159.1 (s, br, 3F, FB(*o*-C_6F_5)$_3$), −165.8 (m, br, 6F, FB(*m*-C_6F_5)$_3$), −188.8 (s, br, 1F, *F*B(C_6F_5)$_3$). $^{31}P\{^1H\}$ NMR (121 MHz, CH_2Cl_2 with C_6D_6capillary) δ 37.6 (br, $\omega_{1/2} \approx 136$ Hz).

[CpCo(CF₂CF₃)(═CF₂)(PPh₂Me)][FB(C₆F₅)₃] (Int 4)

Yield: 75% based on Co═CF_2 after 30 min (60% after 4 h). ^{19}F NMR (282 MHz, CH_2Cl_2 with C_6D_6 capillary) δ 178.2 (t, br, $^4J_{FF} \approx 7$ Hz, 2F, Co═CF_2), −57.2 (dm, $^2J_{FF} \approx 225$ Hz, 1F, $CF^AF^{A'}$; $F^{A'}$), −74.6

(dd, $^{2}J_{FF} \approx$ 225 Hz, $^{3}J_{FP} \approx$ 35 Hz 1F, $CF^{A}F^{A'}$; F^{A}), −80.8 (br, 3F, Co–CF_2CF_3), −189.0 (s, br, 1F, *F*B(C_6F_5)$_3$). $^{31}P\{^{1}H\}$ NMR (121 MHz, CH_2Cl_2 with C_6D_6 capillary) δ 37.5 (br, $\omega_{1/2} \approx$ 148 Hz).

Analysis of the Proposed Products Derived from Int 1–4 by ^{19}F NMR and Mass Spectrometry

[CpCo(CF$_3$)(CO)(PPh$_2$Me)][OTf] (from Int 1)

Yield: 14% based on Co–C*F*$_3$ after 60 min. ^{19}F NMR (282 MHz, CH_2Cl_2 with C_6D_6 capillary) δ 2.79 (br, 3F, Co–C*F*$_3$), −78.3 (br, 3F, C*F*$_3SO_3^-$). $^{31}P\{^{1}H\}$ NMR (121 MHz, CH_2Cl_2 with C_6D_6capillary) δ 35.8 (br, $\omega_{1/2} \approx$ 75 Hz). IR: 2241 cm^{-1} (s, br, Co–*CO*).

CpCo(CF$_2$CF$_3$)(OTf)(PPh$_2$Me) (from Int 1)

Yield: 18% based on Co–CF_2C*F*$_3$ after 60 min. ^{19}F NMR (282 MHz, CH_2Cl_2 with C_6D_6 capillary) δ −74.7 (dm, $^{2}J_{FF} \approx$ 247 Hz, 1F, $CF^{A}F^{A'}$; $F^{A'}$), −78.1 (br, 3F, C*F*$_3SO_3^-$), −80.3 (br, 3F, Co–CF_2C*F*$_3$), −83.9(dd, $^{2}J_{FF} \approx$ 247 Hz,$^{3}J_{FP} \approx$ 30 Hz 1F, $CF^{A}F^{A'}$; F^{A}). $^{31}P\{^{1}H\}$ NMR (121 MHz, CH_2Cl_2 with C_6D_6 capillary) δ 30.0 (br, $\omega_{1/2} \approx$ 97 Hz). MS [ESI (positive mode), solvent: MeOH] Calcd *m*/*z* (% intensity) for [CpCo(CF_2CF_3)(PPh_2Me^+)] 443.04 (100), 444.04 (22), 445.05 (2). Found: 443.04 (100), 444.04 (23).

[CpCo(CF$_2$CF$_3$)(CO)(PPh$_2$Me)][OTf] (from Int 2)

Yield and NMR assignments could not be obtained because of peak overlap. IR: 2243 cm^{-1} (s, br, Co–*CO*).

CpCo(CF$_2$CF$_2$CF$_3$)(OTf)(PPh$_2$Me) (from Int 2)

Yield: 13% based on Co–CF_2C*F*$_2$$CF_3$ after 4 h. Only the F_β signals of the perfluoropropyl fragment could be assigned with certainty because of peak overlap. ^{19}F NMR (282 MHz, $CH_2Cl_2$with C_6D_6 capillary) δ −115.1 (d, $^{2}J_{FF}$ = 282 Hz, 1F, Co–CF_2C*F*$_2$$CF_3$), −116.8 (d, $^{2}J_{FF}$ = 282 Hz, 1F, Co–CF_2C*F*$_2$$CF_3$). MS [ESI (positive mode), solvent: MeOH] Calcd *m*/*z* (% intensity) for [CpCo($CF_2CF_2CF_3$)(PPh_2Me^+)]: 493.04 (100), 494.04 (23), 495.05 (3). Found: 493.04 (100), 494.04 (24). Calcd *m*/*z* (% intensity) for [$CF_3CF_2CF_2^+$]: 168.99 (100), 169.99 (3). Found: 168.99 (100), 169.99 (3).

[CpCo(CF_3)(CO)(PPh_2Me)][$FB(C_6F_5)_3$] (from Int 3)

Yield: 60% based on CpCo(CF_3)$_2$(PPh_2Me) after 4 h. ^{19}F NMR (282 MHz, CH_2Cl_2 with C_6D_6capillary) δ 12.1 (d, $^3J_{FP}$ = 4 Hz, 3F, Co–CF_3). ^{31}P{^{1}H} NMR (121 MHz, CH_2Cl_2 with C_6D_6capillary) δ 33.0 (br, $\omega_{1/2} \approx$ 60 Hz).

CpCo(CF_2CF_3)($FB(C_6F_5)_3$)(PPh_2Me) (from Int 3)

Yield: 35% based on CpCo(CF_3)$_2$(PPh_2Me) after 4 h. ^{19}F NMR (282 MHz, CH_2Cl_2 with C_6D_6capillary) δ −76.7 (dd, $^2J_{FF} \approx$ 251 Hz, $^3J_{FP} \approx$ 14 Hz, 1F, $CF^AF^{A'}$; $F^{A'}$), −80.5 (br, 3F, Co–CF_2CF_3), −86.6 (dd, $^2J_{FF} \approx$ 251 Hz, $^3J_{FP} \approx$ 35 Hz 1F, $CF^AF^{A'}$; F^A). ^{31}P{^{1}H} NMR (121 MHz, CH_2Cl_2 with C_6D_6 capillary) δ 25.2 (br, $\omega_{1/2} \approx$ 96 Hz).

[CpCo(CF_2CF_3)(CO)(PPh_2Me)][$FB(C_6F_5)_3$] (from Int 4)

Yield and NMR assignments could not be obtained because of peak overlap.

CpCo($CF_2CF_2CF_3$)($FB(C_6F_5)_3$)(PPh_2Me) (from Int 4)

Yield: 10% based on Co–$CF_2CF_2CF_3$ after 24 h. Only the F_β signals of the perfluoropropyl fragment could be assigned with certainty because of peak overlap. ^{19}F NMR (282 MHz, $CH_2Cl_2$with C_6D_6 capillary) δ −112.6 (d, $^2J_{FF}$ = 284 Hz, 1F, Co–$CF_2CF_2CF_3$), −114.3 (d, $^2J_{FF}$ = 284 Hz, 1F, Co–$CF_2CF_2CF_3$).

4.3.5 General Procedure for the Catalytic Formation of *p*-Toluoyl Fluoride

The formation of *p*-toluoyl fluoride could be easily established by the growth of a sharp singlet at δ(^{19}F) = 16.5 ppm. The only other signals observed via ^{19}F NMR were a mixture of CpCo(CF_3)(Cl)(PPh_2Me) and CpCo(CF_3)(F)(PPh_2Me) (**6**). Yields for the formation of the target compound were established by integration to BTB. See Table 4.1 for yields and selected control experiments and Table S16 for a full list.

Control Reactions with Various Fluoride Sources

To 0.8 mL of DCM in a vial was added AgF (92 mg, 0.72 mmol), CsF (110 mg, 0.72 mmol), KF (42 mg, 0.72 mmol), or CoF_3 (84 mg, 0.72 mmol). To this suspension were added *p*-toluoyl chloride (32 μL, 0.24 mmol) and BTB (18.6 μL, 0.12 mmol). The reaction was stirred vigorously (in the absence of light in the case of AgF) for 16 h and then transferred to an NMR tube with a C_6D_6 capillary.

Catalytic Reactions with Varying Catalyst Loadings

A stock solution (0.0152 M) was prepared for the reactions involving 5, 1, and 0.1 mol % $CpCo(CF_3)(I)(PPh_2Me)$ (**2**). The complex (40 mg, 0.076 mmol) was dissolved in DCM (5 mL), affording a dark-yellow-brown solution.

10 mol % Loading

$CpCo(CF_3)(I)(PPh_2Me)$ (**2**) (13 mg, 0.024 mmol) was added to a vial, along with AgF (92 mg, 0.72 mmol) and DCM (0.8 mL). To this dark-yellow-brown solution were added *p*-toluoyl chloride (32 μL, 0.24 mmol) and BTB (18.6 μL, 0.12 mmol). The reaction was stirred vigorously (in the absence of light) for 4 h and then transferred to an NMR with a C_6D_6 capillary.

5 mol % Loading

$CpCo(CF_3)(I)(PPh_2Me)$ (**2**) (0.79 mL, 0.012 mmol) was added to a vial, along with AgF (92 mg, 0.72 mmol). To this dark-yellow-brown solution were added *p*-toluoyl chloride (32 μL, 0.24 mmol) and BTB (18.6 μL, 0.12 mmol). The reaction was stirred vigorously (in the absence of light) for 4 h and then transferred to an NMR with a C_6D_6 capillary.

1 mol % Loading

$CpCo(CF_3)(I)(PPh_2Me)$ (**2**) (0.16 mL, 0.0024 mmol) was added to a vial, along with AgF (92 mg, 0.72 mmol) and DCM (0.64 mL). To this pale-yellow-brown solution were added *p*-toluoyl chloride (32 μL,

0.24 mmol) and BTB (18.6 μL, 0.12 mmol). The reaction was stirred vigorously (in the absence of light) for 4 h and then transferred to an NMR with a C_6D_6 capillary.

0.1 mol % Loading

To 0.8 mL of DCM in a vial was added $CpCo(CF_3)(I)(PPh_2Me)$ (**2**) (79 μL, 0.0012 mmol) and AgF (92 mg, 0.72 mmol). To this pale-yellow-brown solution were added *p*-toluoyl chloride (32 μL, 0.24 mmol) and BTB (18.6 μL, 0.12 mmol). The reaction was stirred vigorously (in the absence of light) for 4 h and then transferred to an NMR with a C_6D_6 capillary.

4.4 References

(1) Clark, G. R.; Hoskins, S. V.; Jones, T. C.; Roper, W. R. *J. Chem. Soc. Chem. Commun.* **1983**, No. 13, 719–721.
(2) Murphy, E. F.; Murugavel, R.; Roesky, H. W. *Chem. Rev.* **1997**, *97* (8), 3425–3468.
(3) Taw, F. L.; Clark, A. E.; Mueller, A. H.; Janicke, M. T.; Cantat, T.; Scott, B. L.; Hay, P. J.; Hughes, R. P.; Kiplinger, J. L. *Organometallics* **2012**, *31* (4), 1484–1499.
(4) Emeléus, H. J.; Haszeldine, R. N. *J. Chem. Soc. Resumed* **1949**, No. 0, 2953–2956.
(5) Martínez-Salvador, S.; Falvello, L. R.; Martín, A.; Menjón, B. *Chem. – Eur. J.* **2013**, *19* (43), 14540–14552.
(6) Blaya, M.; Bautista, D.; Gil-Rubio, J.; Vicente, J. *Organometallics* **2014**, *33* (22), 6358–6368.
(7) Burton, D. J.; Wiemers, D. M. *J. Am. Chem. Soc.* **1985**, *107* (17), 5014–5015.
(8) Yamaguchi, Y.; Ichioka, H.; Klein, A.; Brennessel, W. W.; Vicic, D. A. *Organometallics* **2012**, *31* (4), 1477–1483.
(9) Tang, F.; P. Rath, N.; M. Mirica, L. *Chem. Commun.* **2015**, *51* (15), 3113–3116.
(10) Bour, J. R.; Camasso, N. M.; Sanford, M. S. *J. Am. Chem. Soc.* **2015**, *137* (25), 8034–8037.
(11) Bourgeois, C. J.; Hughes, R. P.; Husebo, T. L.; Smith, J. M.; Guzei, I. M.; Liable-Sands, L. M.; Zakharov, L. N.; Rheingold, A. L. *Organometallics* **2005**, *24* (26), 6431–6439.
(12) Hughes, R. P.; Lindner, D. C.; Smith, J. M.; Zhang, D.; Incarvito, C. D.; Lam, K.-C.; Liable-Sands, L. M.; Sommer, R. D.; Rheingold, A. L. *J. Chem. Soc., Dalton Trans.* **2001**, No. 15, 2270–2278.
(13) Tomashenko, O. A.; Grushin, V. V. *Chem. Rev.* **2011**, *111* (8), 4475–4521.
(14) Bourgeois, C. J.; Garratt, S. A.; Hughes, R. P.; Larichev, R. B.; Smith, J. M.; Ward, A. J.; Willemsen, S.; Zhang, D.; DiPasquale, A. G.; Zakharov, L. N.; Rheingold, A. L. *Organometallics* **2006**, *25* (14), 3474–3480.
(15) Taw, F. L.; Scott, B. L.; Kiplinger, J. L. *J. Am. Chem. Soc.* **2003**, *125* (48), 14712–14713.
(16) Vabre, B.; Petiot, P.; Declercq, R.; Zargarian, D. *Organometallics* **2014**, *33* (19), 5173–5184.
(17) Liu, X.; Xu, C.; Wang, M.; Liu, Q. *Chem. Rev.* **2015**, *115* (2), 683–730.
(18) Huang, D.; Caulton, K. G. *J. Am. Chem. Soc.* **1997**, *119* (13), 3185–3186.
(19) Vicente, J.; Gil-Rubio, J.; Guerrero-Leal, J.; Bautista, D. *Organometallics* **2004**, *23* (21), 4871–4881.
(20) King, R. B.; Treichel, P. M.; Stone, F. G. A. *J. Am. Chem. Soc.* **1961**, *83* (17), 3593–3597.
(21) Burns, R. J.; Bulkowski, P. B.; Stevens, S. C. V.; Baird, M. C. *J. Chem. Soc. Dalton Trans.* **1974**, No. 4, 415–420.

(22) Harrison, D. J.; Gorelsky, S. I.; Lee, G. M.; Korobkov, I.; Baker, R. T. *Organometallics* **2013**, *32* (1), 12–15.
(23) Harrison, D. J.; Lee, G. M.; Leclerc, M. C.; Korobkov, I.; Baker, R. T. *J. Am. Chem. Soc.* **2013**, *135* (49), 18296–18299.
(24) Lee, C.; Yang, W.; Parr, R. G. *Phys. Rev. B* **1988**, *37* (2), 785–789.
(25) Perdew, J. P.; Wang, Y. *Phys. Rev. B* **1992**, *45* (23), 13244–13249.
(26) Burke, K.; Perdew, J. P.; Wang, Y. In *Electronic Density Functional Theory*; Dobson, A. J. F., Vignale, P. G., Das, D. M. P., Eds.; Springer US, 1998; pp 81–111.
(27) Dugan, T. R.; Sun, X.; Rybak-Akimova, E. V.; Olatunji-Ojo, O.; Cundari, T. R.; Holland, P. L. *J. Am. Chem. Soc.* **2011**, *133* (32), 12418–12421.
(28) Dugan, T. R.; Goldberg, J. M.; Brennessel, W. W.; Holland, P. L. *Organometallics* **2012**, *31* (4), 1349–1360.
(29) Li, X.; Sun, H.; Yu, F.; Flörke, U.; Klein, H.-F. *Organometallics* **2006**, *25* (19), 4695–4697.
(30) Bennett, B. K.; Harrison, R. G.; Richmond, T. G. *J. Am. Chem. Soc.* **1994**, *116* (24), 11165–11166.
(31) Hepworth, M. A.; Jack, K. H.; Peacock, R. D.; Westland, G. J. *Acta Crystallogr.* **1957**, *10* (1), 63–69.
(32) Treichel, P. M.; Stone, F. G. A. *Adv. Organomet. Chem.* **1964**, *1*, 143–220.
(33) Zhang, C.-P.; Wang, H.; Klein, A.; Biewer, C.; Stirnat, K.; Yamaguchi, Y.; Xu, L.; Gomez-Benitez, V.; Vicic, D. A. *J. Am. Chem. Soc.* **2013**, *135* (22), 8141–8144.
(34) Marenich, A. V.; Cramer, C. J.; Truhlar, D. G. *J. Phys. Chem. B* **2009**, *113* (18), 6378–6396.
(35) Mayer, I. *Theor. Chim. Acta* **1985**, *67* (4), 315–322.
(36) Veltheer, J. E.; Burger, P.; Bergman, R. G. *J. Am. Chem. Soc.* **1995**, *117* (50), 12478–12488.
(37) Wiberg, K. B.; Hammer, J. D.; Zilm, K. W.; Cheeseman, J. R.; Keith, T. A. *J. Phys. Chem. A* **1998**, *102* (45), 8766–8773.
(38) *J. Chem. Phys.* **1964**, *41* (7), 2098–2107.
(39) *J. Chem. Phys.* **1966**, *44* (3), 874–880.
(40) Ahrens, T.; Kohlmann, J.; Ahrens, M.; Braun, T. *Chem. Rev.* **2015**, *115* (2), 931–972.
(41) Champagne, P. A.; Desroches, J.; Hamel, J.-D.; Vandamme, M.; Paquin, J.-F. *Chem. Rev.* **2015**, *115* (17), 9073–9174.
(42) Maity, A.; Stanek, R. J.; Anderson, B. L.; Zeller, M.; Hunter, A. D.; Moore, C. E.; Rheingold, A. L.; Gray, T. G. *Organometallics* **2015**, *34* (1), 109–120.
(43) Birrell, J. A.; Desrosiers, J.-N.; Jacobsen, E. N. *J. Am. Chem. Soc.* **2011**, *133* (35), 13872–13875.
(44) Stavber, S.; Košir, I.; Zupan, M. *J. Org. Chem.* **1997**, *62* (15), 4916–4920.
(45) Motie, R. E.; Satchell, D. P. N.; Wassef, W. N. *J. Chem. Soc. Perkin Trans. 2* **1993**, No. 6, 1087–1090.
(46) Lee, I.; Shim, C. S.; Chung, S. Y.; Kim, H. Y.; Lee, H. W. *J. Chem. Soc. Perkin Trans. 2* **1988**, No. 11, 1919–1923.
(47) Okano, T.; Harada, N.; Kiji, J. *Bull. Chem. Soc. Jpn.* **1992**, *65* (6), 1741–1743.
(48) Campbell, M. G.; Ritter, T. *Chem. Rev.* **2015**, *115* (2), 612–633.
(49) Hollingworth, C.; Gouverneur, V. *Chem. Commun.* **2012**, *48* (24), 2929–2942.
(50) Mankad, N. P.; Toste, F. D. *Chem. Sci.* **2011**, *3* (1), 72–76.
(51) Hull, K. L.; Anani, W. Q.; Sanford, M. S. *J. Am. Chem. Soc.* **2006**, *128* (22), 7134–7135.
(52) Racowski, J. M.; Gary, J. B.; Sanford, M. S. *Angew. Chem. Int. Ed.* **2012**, *51* (14), 3414–3417.
(53) Akana, J. A.; Bhattacharyya, K. X.; Müller, P.; Sadighi, J. P. *J. Am. Chem. Soc.* **2007**, *129* (25), 7736–7737.
(54) Gorske, B. C.; Mbofana, C. T.; Miller, S. J. *Org. Lett.* **2009**, *11* (19), 4318–4321.
(55) Schuler, M.; Silva, F.; Bobbio, C.; Tessier, A.; Gouverneur, V. *Angew. Chem. Int. Ed.* **2008**, *47* (41), 7927–7930.
(56) Ball, N. D.; Sanford, M. S. *J. Am. Chem. Soc.* **2009**, *131* (11), 3796–3797.
(57) Zhao, S.-B.; Wang, R.-Y.; Nguyen, H.; Becker, J. J.; Gagné, M. R. *Chem. Commun.* **2011**, *48* (3), 443–445.

(58) Furuya, T.; Strom, A. E.; Ritter, T. *J. Am. Chem. Soc.* **2009**, *131* (5), 1662–1663.
(59) Furuya, T.; Ritter, T. *Org. Lett.* **2009**, *11* (13), 2860–2863.
(60) Tang, P.; Ritter, T. *Tetrahedron* **2011**, *67* (24), 4449–4454.
(61) Fier, P. S.; Hartwig, J. F. *J. Am. Chem. Soc.* **2012**, *134* (26), 10795–10798.
(62) Mu, X.; Liu, G. *Org. Chem. Front.* **2014**, *1* (4), 430–433.
(63) Casitas, A.; Canta, M.; Solà, M.; Costas, M.; Ribas, X. *J. Am. Chem. Soc.* **2011**, *133* (48), 19386–19392.
(64) Grushin, V. V. *Acc. Chem. Res.* **2010**, *43* (1), 160–171.
(65) Grushin, V. V. *Chem. – Eur. J.* **2002**, *8* (5), 1006–1014.
(66) Macgregor, S. A.; Roe, D. C.; Marshall, W. J.; Bloch, K. M.; Bakhmutov, V. I.; Grushin, V. V. *J. Am. Chem. Soc.* **2005**, *127* (43), 15304–15321.
(67) Wang, X.; Mei, T.-S.; Yu, J.-Q. *J. Am. Chem. Soc.* **2009**, *131* (22), 7520–7521.
(68) Chan, K. S. L.; Wasa, M.; Wang, X.; Yu, J.-Q. *Angew. Chem. Int. Ed.* **2011**, *50* (39), 9081–9084.
(69) Doherty, N. M.; Hoffmann, N. W. *Chem. Rev.* **1991**, *91* (4), 553–573.
(70) Urata, H.; Fuchikami, T. *Tetrahedron Lett.* **1991**, *32* (1), 91–94.
(71) Maggiarosa, N.; Tyrra, W.; Naumann, D.; Kirij, N. V.; Yagupolskii, Y. L. *Angew. Chem. Int. Ed.* **1999**, *38* (15), 2252–2253.
(72) Kolomeitsev, A.; Movchun, V.; Rusanov, E.; Bissky, G.; Lork, E.; Roschenthaler, G.-V.; Kirsch, P. *Chem. Commun.* **1999**, No. 11, 1017–1018.
(73) Wang, X.; Xu, Y.; Mo, F.; Ji, G.; Qiu, D.; Feng, J.; Ye, Y.; Zhang, S.; Zhang, Y.; Wang, J. *J. Am. Chem. Soc.* **2013**, *135* (28), 10330–10333.
(74) Combettes, L. E.; Clausen-Thue, P.; King, M. A.; Odell, B.; Thompson, A. L.; Gouverneur, V.; Claridge, T. D. W. *Chem. – Eur. J.* **2012**, *18* (41), 13133–13141.
(75) Richmond, T. G.; Crespi, A. M.; Shriver, D. F. *Organometallics* **1984**, *3* (2), 314–319.
(76) Trnka, T. M.; Day, M. W.; Grubbs, R. H. *Angew. Chem. Int. Ed.* **2001**, *40* (18), 3441–3444.
(77) Jablonski, C. R.; Zhou, Z. *Can. J. Chem.* **1992**, *70* (10), 2544–2551.
(78) Wiemers, D. M.; Burton, D. J. *J. Am. Chem. Soc.* **1986**, *108* (4), 832–834.
(79) Yang, Z. Y.; Wiemers, D. M.; Burton, D. J. *J. Am. Chem. Soc.* **1992**, *114* (11), 4402–4403.
(80) Wilford, J. B.; Stone, F. G. A. *Inorg. Chem.* **1965**, *4* (1), 93–97.
(81) Williams, D. B. G.; Lawton, M. *J. Org. Chem.* **2010**, *75* (24), 8351–8354.
(82) Brothers, P. J.; Roper, W. R. *Chem. Rev.* **1988**, *88* (7), 1293–1326.

Chapter 5

Fluoroalkyl and Difluorocarbene Complexes of Group 10 Metals

5.1 Context and Objectives

Our group was interested in expanding the chemistry of first-row metal fluorocarbenes beyond cobalt. As such, the first examples of nickel fluorocarbene complexes were prepared by our group via the two-electron reduction method, and have formal d^{10} electronic structures.[1] These nickel fluorocarbenes exhibited nucleophilic reactivity, as demonstrated by their cyclization reactions with TFE to form nickel perfluorocyclobutane complexes. These complexes were described in Chapter 1, along with the idea of metal fluorocarbene reactivity being controlled by the metal oxidation state.[2]

Chapter 5 explores the synthesis and reactivity of nickel and palladium difluorocarbene complexes with formal d^8 electronic configurations, which are expected to exhibit electrophilic type reactivity in contrast to the previously reported nickel fluorocarbenes. The Ni and Pd difluorocarbenes in this chapter are prepared by α-fluoride abstraction from trifluoromethyl POCOP-type pincer complexes using Lewis acids. The work in this chapter represents the first d^8 fluorocarbene complexes with group 10 metals, and the first characterization of a well-defined terminal difluorocarbene complex of palladium. A $Pd{=}CF_2$ complex has been put forth as a key intermediate in a catalytic synthesis of (difluoromethyl)arenes, but attempts to isolate this intermediate were unsuccessful, as only a [Pd-CF_2]-trimer could be isolated.[3]

5.1.1 Published Contributions

d8 Nickel and Palladium Difluorocarbenes Derived from Trifluoromethyl POCOP-type Pincer Complexes

Lee, G. M.; Korobkov, I.; Baker, R. T. *J. Organomet. Chem.* **2017**

Accepted as part of the Special Issue for John Gladysz's 65th Birthday

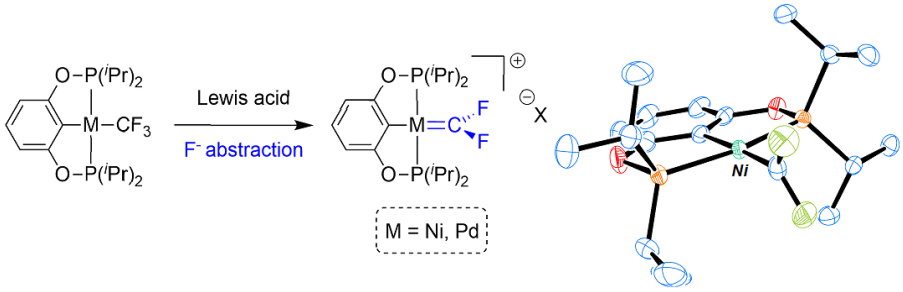

Abstract: In this study, trifluoromethyl POCOP-type pincer complexes (^{iPr}POCOP)Ni(CF_3) (**1-CF3**) and (^{iPr}POCOP)Pd(CF_3) (**2-CF3**) are prepared. These complexes undergo Lewis acid-mediated fluoride abstraction to furnish cationic d^8 difluorocarbene complexes of the type [(^{iPr}POCOP)M(=CF_2)]$^+$[X]$^-$, which are characterized in solution and for M = Ni using single-crystal X-ray diffraction analysis. The electrophilic nature of these difluorocarbene complexes is discussed, including their reactivity with pyridines.

Author Contributions: The manuscript was written by GML. All experiments in this paper performed by GML. X-ray crystallography done by IK.

5.2 d^8 Nickel and Palladium Difluorocarbenes Derived from Trifluoromethyl POCOP-type Pincer Complexes

5.2.1 Introduction

Metal complexes with fluorinated ligands are of significant interest due to their applications in the synthesis of fluorinated organic products.[4–7] The successful synthesis, characterization, and controlled reactivity of M=CF_2 complexes, however, remains a challenging and ongoing area of research. Reported strategies for M=CF_2 synthesis include 2-electron reduction of metal perfluoroalkyl complexes,[8] direct transfer of CF_2 to a metal center,[9,10] and α-fluoride abstraction from metal perfluoroalkyl ligands.[11] One method of controlling the reactivity of M=CF_2 complexes is by changing the oxidation state of the metal, as first demonstrated by Roper et al. whereby a Ru^0=CF_2 (d^8) complex reacts as a nucleophile at the carbene carbon, and Ru^{II}=CF_2

(d^6) reacts as an electrophile.[2] Our group has shown that a similar dynamic exists between nucleophilic Co^I (d^8) fluorocarbenes (Figure 5.1A)[12–14] and electrophilic Co^{III} (d^6) fluorocarbenes (Figure 5.1B).[15] While examples of fluorocarbene complexes have also been documented based on metals from group 6 (Mo[16,17]), and group 7 (Mn[11]), only recently have any examples from group 10 been reported.

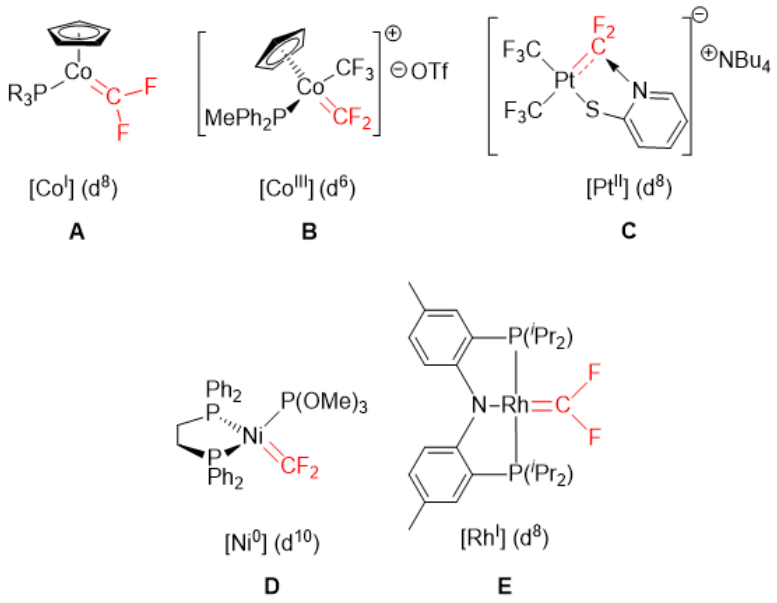

Figure 5.1. Selected examples of metal difluorocarbene complexes.

The first example of a group 10 fluorocarbene complex was the base-stabilized Pt complex $[NBu_4][Pt(CF_3)_2(\kappa^C,\kappa^S\text{-}CF_2NC_5H_4S)]$ (formally d^8) (Figure 5.1C), although the reactivity of this complex was not discussed.[18] Our group recently published the first isolated examples of nickel difluorocarbene complexes (Figure 5.1D), which are also the first examples of $M{=}CF_2$ complexes with formal d^{10} electronic configuration; these were shown to exhibit nucleophilic reactivity through [2 + 2] cycloaddition reactions with tetrafluoroethylene (TFE).[1] Previous to this, nickel difluorocarbenes had only been studied in the gas phase[19] or proposed as intermediates in the catalytic reaction of highly fluorinated epoxides with halogens.[20] To date, there are no reported examples of experimentally observed palladium fluorocarbene complexes, although they have been proposed as key species in the catalytic synthesis of (difluoromethyl)arenes.[3] Finally, an important study by Ozerov et al. described the formation of a PNP-type pincer complex of

rhodium bearing a difluorocarbene ligand (Figure 5.1E), which can serve as a precursor to a rhodium fluorocarbyne.[10]

Nickel and palladium complexes bearing diphosphinito pincer-type POCOP [POCOP = $\kappa^P,\kappa^C,\kappa^P$–(2,6-$(R_2PO)_2$-$C_6H_3$)] ligands have been used for catalytic transformations such as hydroamination of acrylonitrile and olefination of aryl chlorides.[21–25] These complexes feature strong terdentate metal-ligand bonding and one free coordination site at the metal, which can be occupied by either an anionic or neutral ligand, affording neutral (POCOP)$M^{II}X$ or cationic $[(POCOP)M^{II}L]^+$ species, respectively. Therefore, we hypothesized that POCOP complexes of group 10 metals would be a stable platform for interconversion between anionic CF_3 and neutral CF_2 ligands, via potentially reversible fluoride abstraction using a Lewis acid. The goal of the present study is to prepare and characterize the first examples of M=CF_2 complexes of nickel and palladium with formal d^8 electronic configurations, and explore what we expect to be electrophilic-type reactivity.

5.2.2 Results and Discussion

5.2.2.1 Preparation of (POCOP)M(CF_3) (M = Ni, Pd)

We began by preparing nickel and palladium ^{iPr}POCOP [^{iPr}POCOP = $\kappa^P,\kappa^C,\kappa^P$–(2,6-(^{i}Pr$_2$PO)$_2$-$C_6H_3$)] complexes (^{iPr}POCOP)MCl (M = Ni (**1-Cl**), Pd (**2-Cl**)), **1-Cl** according to a direct, one-pot method,[26] and **2-Cl** using standard stepwise procedures (Scheme 5.1).[27]

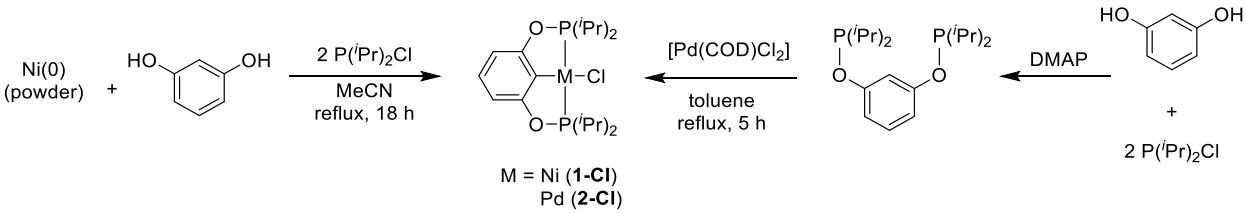

Scheme 5.1. Previously reported syntheses of **1-Cl** and **2-Cl**.

Zargarian and co-workers recently reported the synthesis of fluoro and trifluoromethyl derivatives of POCOP nickel complexes, including trifluoromethyl complex (^{iPr}POCOP)Ni(CF_3) (**1-CF3**) by treating **1-Cl** with Me_3SiCF_3/AgF overnight at 45 °C in THF.[17] Here, we report an alternative synthetic protocol

for the preparation of nickel and palladium trifluoromethyl POCOP complexes. Treatment of both **1-Cl** and **2-Cl** with Me_3SiCF_3/CsF for 2 h at room temperature in DMF results in formation of the trifluoromethyl pincer complexes **1-CF3** (yellow solid, 80% isolated yield) and (^{iPr}POCOP)Pd(CF_3) (**2-CF3**) (white solid, 74% isolated yield), respectively (Scheme 5.2).

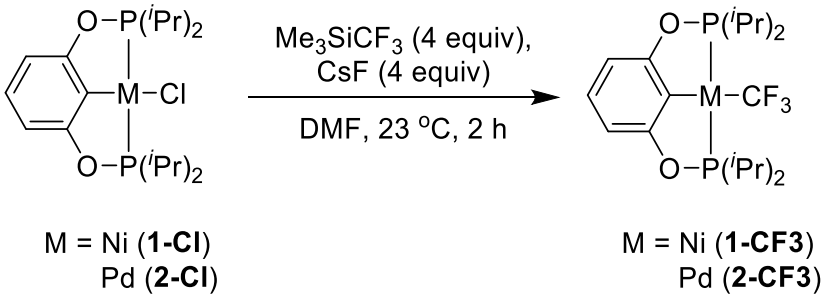

Scheme 5.2. Synthesis of trifluoromethyl Ni and Pd (^{iPr}POCOP) complexes **1-CF3** and **2-CF3**.

Complex **2-CF3** was characterized using elemental analysis, multinuclear NMR spectroscopy, and single crystal X-ray diffraction. The ^{19}F and ^{31}P NMR spectra of **2-CF3** are highly characteristic. The ^{19}F spectrum displays a single resonance appearing as a triplet at -8.24 ppm (J_{FP} = 14 Hz), and the ^{31}P{^{1}H} spectrum shows a single resonance for equivalent phosphinite groups coupled to the CF_3 ligand, appearing as a quartet at 191.6 ppm. The ^{1}H spectrum displays the typical resonances associated with the ^{iPr}POCOP ligand. The X-ray structure of **2-CF3** confirms the Pd center has square planar geometry (Figure 1), with typical angular distortions about the Pd center consistent with the small bite angle of the POCOP ligand (P-Pd-P < C_{POCOP}-Pd-C_F; C_{POCOP}-Pd-P < P-Pd-C_F) (Table 5.1). The Pd-CF_3 bond distance in **2-CF3** is 2.1139(17) Å, in comparison with the corresponding distance in (POCOP-*i*Pr)Pd-CH_3 of 2.125(3) Å.[25]

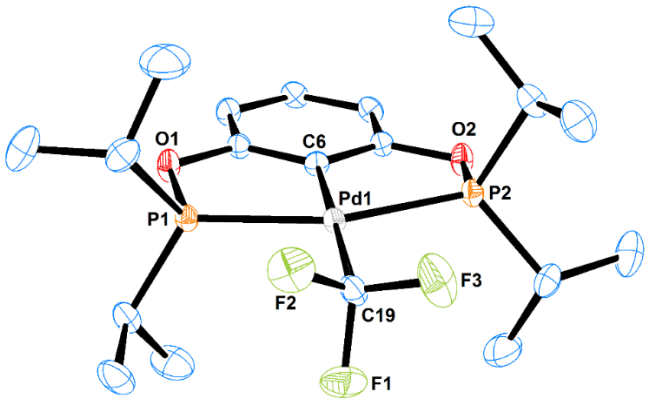

Figure 5.2. ORTEP drawing of complex 2-CF3. Hydrogen atoms are omitted for clarity. Thermal ellipsoids are set to the 50% probability level.

5.2.2.2 Preparation of [(POCOP)M(=CF_2)]$^+$ (M = Ni, Pd)

Our strategy to prepare d^8 Ni and Pd difluorocarbene complexes consisted of abstracting a fluoride from a trifluoromethyl ligand using a Lewis acid. The reactivity of cationic d^8 nickel and palladium difluorocarbene complexes is expected to be electrophilic, different than the nucleophilic type reactivity observed for d^{10} nickel difluorocarbene complexes previously studied.[1] We began our investigation by treating complex **3** with 1 equiv of Me_3SiOTf (OTf = SO_3CF_3) in CH_2Cl_2 (Figure 5.3).

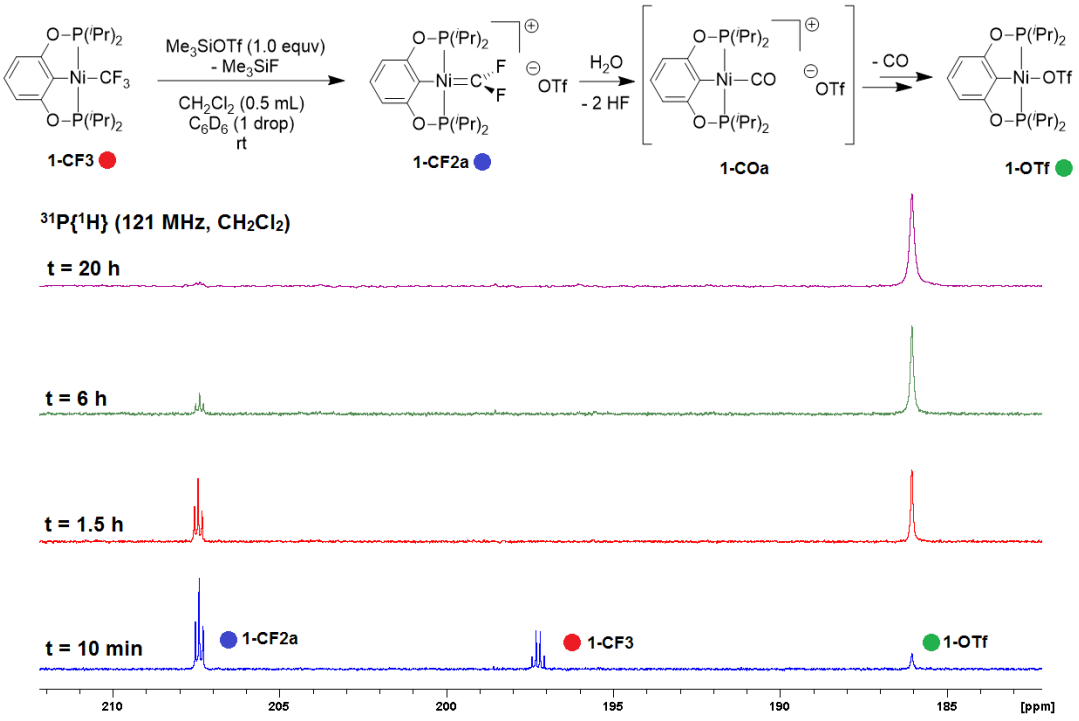

Figure 5.3. Reaction of 1-CF3 with Me_3SiOTf, analyzed using $^{31}P\{^1H\}$ NMR.

After 10 minutes of stirring, analysis of the reaction mixture using ^{31}P and ^{31}F NMR spectroscopy indicated the formation of the cationic nickel difluorocarbene complex [(^{iPr}POCOP)Ni(=CF_2)][OTf] (**1-CF2a**) with concomitant formation of Me_3SiF, along with (^{iPr}POCOP)Ni(OTf) (**1-OTf**) and unreacted starting material **1-CF3**. Within 1.5 h trifluoromethyl complex **1-CF3** was completely consumed, and over the course of 20 h difluorocarbene complex **1-CF2a** was all converted to **1-OTf**. The difluorocarbene complex reacts with trace moisture (despite rigorous attempts to remove water from solvents) to furnish 2 equiv of HF and a carbonyl complex (**1-COa**), which is not detected using NMR spectroscopy as the CO ligand is immediately displaced by the triflate group. The ^{19}F and $^{13}P\{^1H\}$ NMR signals for **1-CF2a** are highly characteristic. The ^{19}F NMR signal for the difluorocarbene ligand appears as a highly de-shielded broad singlet at 169.1 ppm, typical for metal difluorocarbene complexes with electrophilic reactivity patterns, along with the signal for outer-sphere triflate at -78.3 ppm. The $^{13}P\{^1H\}$ signal appears at 206.4 ppm as a triplet, due to coupling with the CF_2 ligand ($^3J_{PF}$ = 14 Hz). The distinct changes in chemical shift and splitting pattern of the $^{31}P\{^1H\}$

NMR signals between (POCOP)M(CF_3) and [(POCOP)M(=CF_2)] complexes makes this a particularly useful tool for evaluating reactivity. Repeated attempts at growing single crystals of **1-CF2a** suitable for X-ray diffraction were unsuccessful.

The observed sensitivity of complex **1-CF2a** to hydrolysis is a clear indication that choice of solvent, drying method, and reaction concentration are crucial factors in determining the reaction yield. A quantitative study of common organic solvents subjected to a variety of desiccants showed the combination of CH_2Cl_2 and activated 3 Å molecular sieves (10% m/v) for 24 h produced extremely dry solvent, with residual water content of 0.1 ± 0.1 ppm as determined by Karl Fischer titration.[28] Indeed, when complex **1-CF3** was reacted with Me_3SiOTf in solvents other than dry CH_2Cl_2 (toluene, C_6D_6, hexane, or MeCN) yields of **1-CF2a** suffered dramatically, or the reaction was quenched entirely. Therefore, CH_2Cl_2 (and occasionally CD_2Cl_2 and CD_3Cl) is the solvent of choice for investigations of d^8 nickel and palladium difluorocarbene complexes.

In an effort to establish a reliable, high yielding route for the formation of difluorocarbene complexes, we explored the reactivity of complex **1-CF3** with a variety of Lewis acids. When 1 equiv of $BF_3 \cdot Et_2O$ was added to a solution of **1-CF3** in CH_2Cl_2 and analyzed using NMR spectroscopy after 2 h, $^{31}P\{^1H\}$ NMR revealed the formation of [($^{i\text{Pr}}$POCOP)Ni(=CF_2)][BF_4] (**1-CF2b**) in approximately 67% yield. After 16 h, however, **1-CF2b** was no longer detected, having undergone hydrolysis to form [($^{i\text{Pr}}$POCOP)Ni(CO)][BF_4] (**1-COb**). When complex **1-CF3** was treated with the weaker Lewis acid BPh_3, no reaction took place. Similarly, complex **1-CF3** did not react with $NaBPh_4$.

Tris(pentafluorophenyl)borane $B(C_6F_5)_3$ is a strong Lewis acid which has been reported to facilitate C-F activation.[15,29] When complex **1-CF3** was treated with 1 equiv of $B(C_6F_5)_3$ (added as a solid), an immediate color change from yellow to orange was observed, and [($^{i\text{Pr}}$POCOP)Ni(=CF_2)][$FB(C_6F_5)_3$] (**1-CF2c**) was formed cleanly in 98% yield as determined by NMR analysis (Scheme 5.3).

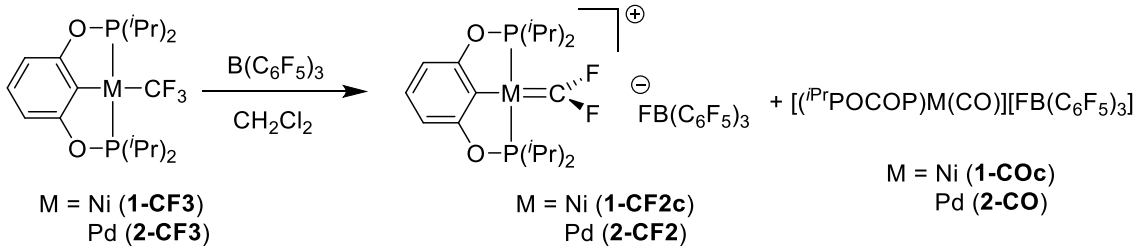

Scheme 5.3. Formation of cationic difluorocarbene complexes **1-CF2c** and **2-CF2.**

Furthermore, **1-CF2c** was still present in 85% yield after 11 h. After 26 h, however, **1-CF2c** had been completely hydrolysed to [($^{i\text{Pr}}$POCOP)Ni(CO)][FB(C_6F_5)$_3$] (**1-COc**). It is noteworthy that **5c-COc** is significantly more stable in solution than **1-COa**, apparently due to the reduced ability of the bulky [FB(C_6F_5)$_3$] anion to coordinate to Ni relative to [OTf]. The NMR spectra of **1-CF2c** are highly characteristic, and similar to those of OTf and BF_4 derivatives **1-CF2a** and **1-CF2b**. The ^{19}F spectrum features the Ni=CF_2 signal at 167.3 ppm, which appears as a well resolved triplet due to coupling with the phosphinite groups ($^3J_{FP}$ = 14 Hz). The ^{19}F signals associated with the [FB(C_6F_5)$_3$] anion are characteristic of the tetrahedral geometry at boron, including a broad B-F resonance at ca. -190 ppm for the abstracted fluoride, and consistent with those previously reported. The ^{31}P{^{1}H} spectrum features a triplet resonance at 206.4 ppm with the corresponding coupling to the CF_2 group. **1-COc** is identified by a characteristic sharp singlet in the ^{31}P{^{1}H} spectrum at 209.1 ppm, and a carbonyl stretching frequency at 2095 cm^{-1} in the IR spectrum.

The reactivity of palladium trifluoromethyl complex **2-CF3** with B(C_6F_5)$_3$ was also investigated. A concentrated CH_2Cl_2 solution of **2-CF3** was treated with 1 equiv B(C_6F_5)$_3$, resulting in an immediate colour change from a colourless solution to yellow. After 10 minutes, NMR analysis revealed the cationic difluorocarbene [($^{i\text{Pr}}$POCOP)Pd(=CF_2)][FB(C_6F_5)$_3$] (**2-CF2**) was formed in 76% yield, along with [($^{i\text{Pr}}$POCOP)Pd(CO)][FB(C_6F_5)$_3$] (**2-CO**) in 26% yield. After 17 h, the distribution was 63% of **2-CF2** and 37% of the hydrolysis product. The ^{31}P{^{1}H} NMR spectrum for **2-CF2** consists of a broad singlet at 199.2 ppm at room temperature (23 °C). The ^{19}F NMR spectrum features the characteristic downfield Pd=CF_2

peak at ca. 185 ppm, which also appears as a broad singlet at 23 °C. The coupling between the phosphinite groups and Pd=CF_2 could be resolved by cooling the NMR sample to -30 °C (Figure 5.4), revealing a coupling constant of 13 Hz. This observation indicates a reduced barrier for rotation of the CF_2 ligand in **2-CF2** compared to **1-CF2**.

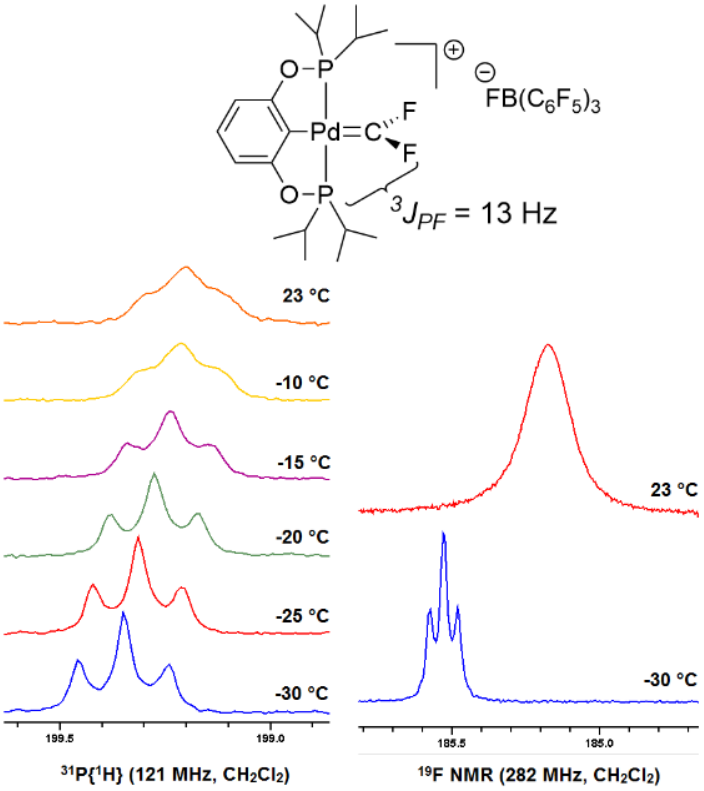

Figure 5.4. Variable-temperature $^{31}P\{^{1}H\}$ and ^{19}F NMR spectra of 2-CF2.

Yellow crystals of **1-CF2c** were grown from a concentrated CH_2Cl_2 solution at -35 °C, and analyzed using single crystal X-ray crystallography (Figure 5.5). The structure of **1-CF2c** reveals square planar geometry at the Ni center, and overall C_{2v} symmetry of the complex. The Ni=CF_2 bond is 1.780(3) Å, compared to 1.9296(15) Å for the Ni-CF_3 bond of **1-CF3**. As a further comparison, the Ni=CF_2 bond of tetrahedral d^{10} nickel fluorocarbene complex Ni(DPPE)[$P(OMe)_3$](=CF_2) (DPPE = $Ph_2P(CH_2)_2PPh_2$) is 1.771(4).[10] The carbene carbon of **1-CF2c** is sp^2 hybridized, with the fluorine atoms oriented above and below the plane of the POCOP ligand. The C-F bonds are 1.277(4) Å and 1.304(4) Å, significantly shorter than those of the

CF_3 group in complex **1-CF3** (average of 1.3668 Å). Repeated attempts at growing crystals of palladium difluorocarbene complex **2-CF2** suitable for X-ray diffraction were unsuccessful.

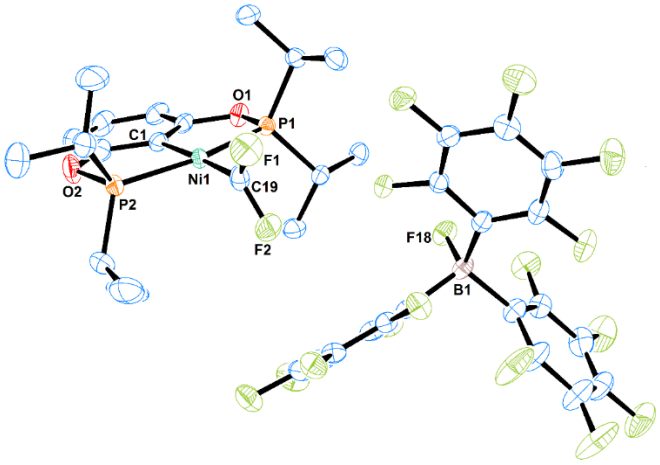

Figure 5.5. ORTEP drawing of complex **1-CF2c**. Hydrogen atoms are omitted for clarity. Thermal ellipsoids are set to the 50% probability level.

Table 5.1. Selected bond distances (Å) and angles (°) of 1-CF3[a], 2-CF3, and 1-CF2c.

	[(POCOP)Ni(CF_3)] **1-CF3**	[(POCOP)Pd(CF_3)] **2-CF3**	[(POCOP)Ni(=CF_2)]$^+$ **1-CF2c**
M-$C_{(POCOP)}$	1.9076(13)	2.0143(14)	1.902(3)
M-$P_{(POCOP)}$	2.1518(4), 2.1591(4)	2.2758(4), 2.2774(4)	2.1629(8), 2.1684(8)
M-C_F	1.9296(15)	2.1139(17)	1.780(3)
C-F	1.3653(18), 1.3721(19), 1.363(2)	1.362(2), 1.349(2), 1.340(2)	1.277(4), 1.304(4)
P-O	1.6579(11), 1.6577(11)	1.6474(11), 1.6553(11)	1.633(2), 1.622(2)
O-C	1.3893(18), 1.3883(17)	1.3943(17), 1.3902(19)	1.391(4), 1.389(4)
C_{POCOP}-M-C_F	177.53(6)	178.09(6)	177.46(14)
P-M-P	163.660(16)	159.136(15)	162.72(3)
C_{POCOP}-M-P	81.72(4), 82.02(4)	79.69(4), 79.61(4)	81.39(9), 81.34(9)

C_F-M-P	98.00(5), 98.31(5)	99.79(4), 100.98(4)	97.45(10), 99.83(10)
F-C_F-F	101.83(13), 102.01(15), 101.47(13)	104.68(15), 104.94(15), 103.87(13)	104.9(3)

[a] The x-ray structure of **1-CF3** was determined independently from the structure reported by Zargarian et al., with virtually identical unit cell and structural parameters.[30]

5.2.2.3 Reactivity of [(POCOP)M(=CF_2)] (M = Ni, Pd) with pyridines

The facile hydrolysis of the difluorocarbene ligands in **1-CF2c** and **2-CF2** to furnish CO ligands is unavoidable, even when using rigorously dried solvents. Therefore, reactivity studies are conducted on a freshly prepared mixture of difluorocarbene complexes **1-CF2c** or **2-CF2** and **1-COc** or **2-CO** in CH_2Cl_2, and analyzed using $^{31}P\{^1H\}$ and ^{19}F NMR spectroscopy before and after the reaction (Scheme 5.4). When **1-CF2c** is treated with 1 equiv of pyridine, there is near quantitative conversion to the adduct [($^{i\text{Pr}}$POCOP)Ni(CF_2(NC_5H_5))][FB(C_6F_5)$_3$] (**1-CF2-py**). The identity of complex **1-CF2-py** is suggested especially by a characteristic ^{19}F NMR signal for the Ni-CF_2N fragment, which appears as a triplet at ca. -31 ppm ($^3J_{FP}$ = 23 Hz). This resonance in **1-CF2-py** is shifted up-field dramatically relative to the Ni=CF_2 peak in **1-CF2c**, due to the change at the carbon atom to sp^3 from sp^2 hybridization upon formation of the C-N bond. In addition, the $^{31}P\{^1H\}$ NMR spectrum for **1-CF2-py** appears as a triplet at ca. 191 ppm with coupling to the CF_2 moiety. The other products present in the reaction mixture include [($^{i\text{Pr}}$POCOP)Ni(NC_5H_5)][FB(C_6F_5)$_3$] , formed via displacement of the CO ligand on the hydrolyzed complex by pyridine, and a small amount of **1-CF3**. The formation of **1-CF3** is proposed to result from the reaction of **1-CF2c** with F^-, generated via displacement of the B-F bond in the [FB(C_6F_5)$_3$] anion by pyridine, resulting in concomitant formation of the pyridine-B(C_6F_5)$_3$ adduct. Treatment of **1-CF2c** with 1 equiv of 2-phenylpyridine gives **1-CF3** as the major product, along with formation of the 2-phenylpyridine-B(C_6F_5)$_3$ adduct. The added steric hindrance at the 2 position of pyridine prevents formation of the C(F_2)-N bond, as well as the displacement of the CO ligand on **1-COc**.

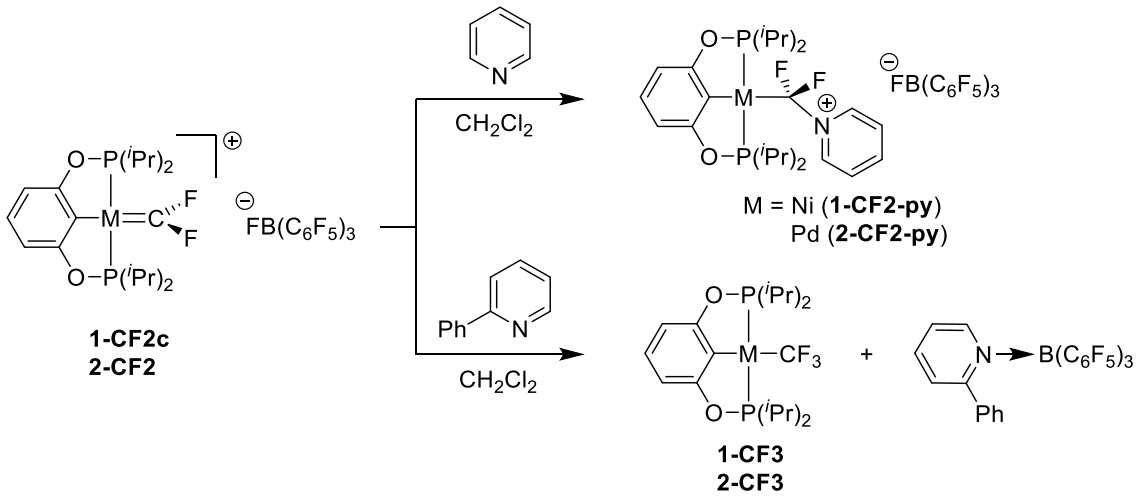

Scheme 5.4. Reactivity of 5c and 6 with pyridine and 2-phenylpyridine.

The reactivity patterns of palladium difluorocarbene complex **2-CF2** with pyridine and 2-phenylpyridine are similar to that of **1-CF2c**. Treatment of **2-CF2** with pyridine yields [($^{i\text{Pr}}$POCOP)Pd($CF_2(NC_5H_5)$)][$FB(C_6F_5)_3$] (**2-CF2-py**) as the major product. The Pd-CF_2N fragment in **2-CF2-py** appears in the ^{19}F NMR spectrum as a triplet at ca. -34 ppm ($^3J_{FP}$ = 18 Hz), and the phosphinite groups appear in the $^{31}P\{^1H\}$ NMR spectrum as a triplet at ca. 189 ppm. When 2-phenylpyridine is allowed to react with **2-CF2**, trifluoromethyl complex **2-CF3** is the major product along with 2-phenylpyridine-$B(C_6F_5)_3$. In contrast to the analogous nickel complex, 2-phenylpyridine readily displaces the CO ligand of **2-CO** to form the Pd-N complex.

5.2.3 Conclusions

Here, we demonstrated that ($^{i\text{Pr}}$POCOP)Ni(CF_3) (**1-CF3**) and ($^{i\text{Pr}}$POCOP)Pd(CF_3) (**2-CF3**) react cleanly with $B(C_6F_5)_3$ to furnish cationic d^8 difluorocarbene complexes [($^{i\text{Pr}}$POCOP)Ni(=CF_2)][$FB(C_6F_5)_3$] (**1-CF2c**) and [($^{i\text{Pr}}$POCOP)Pd (=CF_2)][$FB(C_6F_5)_3$] (**2-CF2**). The identity of these complexes was confirmed unambiguously using ^{19}F and $^{31}P\{^1H\}$ NMR spectroscopy, as well as single crystal X-ray diffraction for **1-CF2c**. The use of $B(C_6F_5)_3$ as the Lewis acid was significant, as the resulting $[FB(CF_6F_5)_3]^-$ anion contained sufficient steric bulk so as to prolong **1-CF2c** in solution. The expected electrophilic reactivity of these

difluorocarbene complexes was confirmed by their observed high-sensitivity to hydrolysis by adventitious moisture, as well as their reactivity with the N-donor pyridine. Overall, we have shown that trifluoromethyl pincer-type complexes are a robust platform for the formation of difluorocarbene complexes via α-fluoride abstraction by a sterically bulky Lewis acid, and can serve as the basis for future structural and reactivity studies.

5.2.4 Experimental Details for Section 2

5.2.4.1 General Procedures

Experiments were conducted under nitrogen, using Schlenk techniques or an MBraun glove box. All solvents were deoxygenated by purging with nitrogen. Toluene, hexanes, diethyl ether (Et_2O) and tetrahydrofuran (THF) were dried on columns of activated alumina using a J. C. Meyer (formerly Glass Contour®) solvent purification system. Benzene-d_6 (C_6D_6) and were dried by standing over activated alumina (ca. 10 wt. %) overnight, followed by filtration. Dichloromethane (DCM) was dried by storing over activated (heated at ca. 250 °C for >10 h under vacuum) 4 Å molecular sieves for 24 h. Acetonitrile (MeCN), acetonitrile-d^3 (CD_3CN) and CD_2Cl_2 were dried by refluxing over calcium hydride under nitrogen. After distillation, they were dried further by filtration through activated alumina (ca. 5-10 wt. %). Dichloromethane-d_2 (CD_2Cl_2) was vacuum-transferred before use. All solvents were stored over activated (heated at ca. 250 °C for >10 h under vacuum) 4 Å molecular sieves. Glassware was oven-dried at 150 °C for >2 h or flame-dried using a torch. The following chemicals were obtained commercially, as indicated: Me_3SiCF_3 (Oakwood Chemical, 98%), Me_3SiOTf (Tf = SO_2CF_3, Aldrich, 98%), $B(C_6F_5)_3$ (Strem, 97%), chlorodiphenylphosphine ($ClPPh_2$, Aldrich, 99%), resorcinol (Aldrich, 98%), pyridine (Aldrich, anhydrous, 99.8%), 2-phenylpyridine (Aldrich, 98%), Ni powder (Strem, 99.5%), Pd[COD]Cl_2 (Aldrich, 99%), CsF (Aldrich, 99%) (CsF was dried under vacuum at 250 °C for several h). ^1H, ^{19}F and $^{31}P\{^1H\}$NMR spectra were recorded on either a 300 MHz Bruker Avance or 300 MHz Bruker Avance II instrument at room temperature (21-23 °C). ^1H NMR spectra were referenced to the residual proton peaks associated with the deuterated solvents (C_6D_6: 7.16 ppm, $CDCl_3$: 7.26 ppm, CD_3CN: 1.94 ppm, CD_2Cl_2: 5.32 ppm). ^{19}F NMR

spectra were referenced to internal 1,3- bis(trifluoromethyl)benzene (BTB) (Aldrich, 99%, deoxygenated by purging with nitrogen, stored over activated 4 Å molecular sieves), set to –63.5 ppm. ^{1}H NMR data for BTB: (300 MHz, C6D6) δ 6.60 (m, 1H, Ar-5-H), 7.12 (m, 2H, Ar-4,6-H), 7.76 (m, 1H, Ar-2-H); (300 MHz, CD3CN) δ 7.76-7.84 (m, 1H, Ar–H), 7.95-8.04 (m, 3H, Ar–H). ^{31}P{^{1}H}NMR data were referenced to external H_3PO_4 (85% aqueous solution), set to 0.0 ppm. Elemental analyses were performed by the CENTC Elemental Analysis Facility at the University of Rochester.

5.2.4.2 Synthesis of [(^{iPr}POCOP)Ni(CF_3)] ***1-CF3***

A solution of [(^{iPr}POCOP)Ni(Cl)] (610 mg, 1.40 mmol) was stirred in DMF (6 mL) and CsF (850 mg, 5.60 mmol) was added as a solid. After 5 minutes of additional stirring, Me_3SiCF_3 (800 mg, 5.60 mmol) was added drop-wise to the suspension, over a span of 5 minutes. After stirring for 1.5 h, hexane (10 mL) was added to the solution and the mixture was filtered over a pad of Celite, washing with hexane (5 mL). The resulting yellow solution was dried under vacuum, and the remaining residue was extracted with toluene and hexane (10 mL, 1:1) and filtered through a plug of Celite. The filtrate was concentrated to 1 mL and placed at -35 ^{o}C for 24 h. Yellow crystals formed, and were collected by filtration and washed with cold hexane (5 mL), giving [(^{iPr}POCOP)Ni(CF_3)] (530 mg, 80% isolated yield). Slow evaporation of a concentrated THF/Et_2O solution gave crystals suitable for X-ray diffraction. X-ray and spectroscopic data are in agreement with those previously published. ^{1}H NMR ($CDCl_3$, 300 MHz) δ 1.24-1.37 (m, 24H, CH_3), 2.42 (m, J_{HH} = 7.1 Hz, 4H, C*H*(CH_3)$_2$), 6.46 (d, *J* = 7.9 Hz, 2H, *m*-H), 6.98 (t, *J* = 7.9 Hz, 1H, *p*-H). ^{19}F NMR ($CDCl_3$, 282 MHz) δ -6.7 (t, $^{3}J_{FP}$ = 14.9 Hz). ^{31}P{^{1}H} NMR ($CDCl_3$, 121 MHz) δ 196.3 (q, $^{3}J_{PF}$ = 14.9 Hz).

5.2.4.3 Synthesis of [(^{iPr}POCOP)Pd(CF_3)] ***2-CF3***

A solution of [(^{iPr}POCOP)Pd(Cl)] (450 mg, 0.93 mmol) was stirred in DMF (6 mL) and CsF (550 mg, 3.62 mmol) was added as a solid. After 5 minutes of additional stirring, Me_3SiCF_3 (610 mg, 4.28 mmol) was added drop-wise to the suspension, over a span of 5 minutes. After stirring for 1.5 h, hexane (10 mL) was

added to the solution and the mixture was filtered over a pad of celite, washing with hexane (5 mL). The resulting yellow solution was dried under vacuum, and the remaining residue was extracted with toluene and hexane (10 mL, 1:1) and filtered through a plug of Celite. The filtrate was concentrated to 1 mL and placed at -35 ºC for 24 h. White crystals formed, and were collected by filtration and washed with cold hexane (5 mL), giving [($^{i\text{Pr}}$POCOP)Pd(CF_3)] (356 mg, 74% isolated yield). ^{1}H NMR ($CDCl_3$, 300 MHz) δ 1.20-1.33 (m, 24H, CH_3), 2.39 (m, J_{HH} = 7.2 Hz, 4H, C*H*(CH_3)$_2$), 6.56 (d, J_{HH} = 7.8, 2H, *m*-H), 6.98 (tm, J_{HH} = 7.8 Hz, 1H, *p*-H). ^{19}F NMR ($CDCl_3$, 282 MHz) δ -8.2 (t, $^3J_{FP}$ = 13.8 Hz). ^{31}P{^{1}H} NMR ($CDCl_3$, 121 MHz) δ 191.6 (q, $^3J_{PF}$ = 13.8 Hz). Anal. Calcd for $C_{19}H_{31}F_3O_2P_2Pd$: C, 44.16; H, 6.05%. Found: C, 44.45; H, 5.63.

*5.2.4.4 Synthesis and characterization of [($^{i\text{Pr}}$POCOP)Ni(=CF_2)][OTf]**1-CF2a** in situ*

To a solution of (POCOP-^{i}Pr)Ni(CF_3) (20 mg, 0.0426 mmol) in CH_2Cl_2 (0.5 mL) and C_6D_6 (60 μL) was added neat Me_3SiOTf (1 equiv, 8 μL). After 15 minutes, the reaction mixture was analyzed using ^{19}F and ^{31}P{^{1}H} NMR spectroscopy, which revealed the formation of [($^{i\text{Pr}}$POCOP)Ni(=CF_2)][OTf](**1-CF2a**) in 82% yield.^{19}F NMR (282 MHz, CH_2Cl_2) δ 169.1 (br. s, 2F, CF_2), -78.3 (br. s, 3F, OTf). ^{31}P{^{1}H} (121 MHz, CH_2Cl_2) δ 206.4 (t, 2P, $^3J_{PF}$ = 14 Hz).

*5.2.4.5 Synthesis and characterization of [($^{i\text{Pr}}$POCOP)Ni(=CF_2)][BF_4]**1-CF2b** in situ*

To a solution of (POCOP-^{i}Pr)Ni(CF_3) (20 mg, 0.0426 mmol) in CH_2Cl_2 (0.5 mL) and C_6D_6 (60 μL) was added $BF_3\cdot Et_2O$ (1 equiv, 6 μL, 0.0486 mmol). After 2 h, the mixture was analyzed using ^{19}F and ^{31}P{^{1}H} NMR spectroscopy, which revealed the formation of [($^{i\text{Pr}}$POCOP)Ni(=CF_2)][BF_4] (**1-CF2b**) in 67% yield. ^{19}F NMR (282 MHz, CH_2Cl_2) δ 172.3 (br. s, 2F, CF_2), -149.6 (br. s, 4F, BF_4). ^{31}P{^{1}H} (121 MHz, CH_2Cl_2) δ 207.1 (br, s).

*5.2.4.6 Synthesis of [($^{i\text{Pr}}$POCOP)Ni(=CF_2)][$BF(C_6F_5)_3$] **1-CF2c***

To a solution of [($^{i\text{Pr}}$POCOP)Ni(CF_3)] (20 mg, 0.043 mmol) in CH_2Cl_2 (0.5 mL) was added $B(C_6F_5)_3$ (22 mg, 0.043 mmol) as a solid, resulting in an immediate colour change from yellow to orange. After 15 minutes, analysis of the crude mixture using NMR spectroscopy revealed the formation of [($^{i\text{Pr}}$POCOP)Ni(=CF_2)][$BF(C_6F_5)_3$] in 98% yield, along with [($^{i\text{Pr}}$POCOP)Ni(CO)][$BF(C_6F_5)_3$] (**1-COc**) (2% yield). ^{19}F NMR (282 MHz, CH_2Cl_2) δ 167.3 (t, $^3J_{FP}$ = 14 Hz, 2F, CF_2), -135.2 (m, J_{FF} = 12.6 Hz, *o*-F, 6F), -162.5 (t, J_{FF} = 19.8 Hz, *p*-F, 3F), -166 (m, J_{FF} = 19.8 Hz, *m*-F, 6F), -190.3 (br. s, B-F). ^{31}P{^{1}H} (121 MHz, CH_2Cl_2) δ 206.4 (t, 2P, $^3J_{PF}$ = 14 Hz). Addition of H_2O results in nearly quantitative conversion to [($^{i\text{Pr}}$POCOP)Ni(CO)][$BF(C_6F_5)_3$] (**1-COc**): IR (neat): 2095 cm^{-1}. ^{31}P{^{1}H} (121 MHz, CH_2Cl_2) δ 209.1 (s).

*5.2.4.7 Synthesis of [($^{i\text{Pr}}$POCOP)Pd(=CF_2)][$BF(C_6F_5)_3$] **2-CF2***

To a solution of [($^{i\text{Pr}}$POCOP)Pd(CF_3)] (20 mg, 0.039) in CH_2Cl_2 (0.5 mL) was added $B(C_6F_5)_3$ (20 mg, 0.039 mmol) as a solid, resulting in an immediate colour change from colourless to dark yellow-orange. After 15 minutes, analysis of the crude mixture using NMR spectroscopy revealed the formation of [($^{i\text{Pr}}$POCOP)Pd(=CF_2)][$BF(C_6F_5)_3$] in 98% yield, along with [($^{i\text{Pr}}$POCOP)Pd(CO)][$BF(C_6F_5)_3$] (**2-CO**) (2% yield). ^{19}F NMR (282 MHz, CH_2Cl_2) δ 185.2 (t, $^3J_{FP}$ = 14 Hz, 2F, CF_2), -135.2 (m, J_{FF} = 12.6 Hz, *o*-F, 6F), -162.5 (t, J_{FF} = 19.8 Hz, *p*-F, 3F), -166 (m, J_{FF} = 19.8 Hz, *m*-F, 6F), -190.3 (br. s, B-F). ^{31}P{^{1}H} (121 MHz, CH_2Cl_2) δ 199.2 (23 °C: br. s, 2P; -30 °C: t, 2P, $^3J_{PF}$ = 13 Hz). Addition of H_2O results in nearly quantitative conversion to [($^{i\text{Pr}}$POCOP)Pd(CO)][$BF(C_6F_5)_3$] (**2-CO**): IR (CH_2Cl_2): 2110 cm^{-1}. ^{31}P{^{1}H} (121 MHz, CH_2Cl_2) δ 201.1 (s).

*5.2.4.8 Reaction of **1-CF2c** with pyridine*

To a solution of [($^{i\text{Pr}}$POCOP)Ni(CF_3)] (15 mg, 0.032 mmol) in CH_2Cl_2 (0.5 mL) was added $B(C_6F_5)_3$ (17 mg, 0.032 mmol) as a solid. After 5 minutes, the orange solution was transferred to an NMR tube and analyzed using ^{19}F and ^{31}P{^{1}H} NMR spectroscopy to establish the formation of **1-CF2c**. Pyridine (3 μL, 1.1 equiv) was then added to the solution, resulting in an immediate colour change to yellow-orange, and analyzed again using ^{19}F and ^{31}P{^{1}H} NMR, revealing the formation of

[(^{iPr}POCOP)Ni(CF_2(NC_5H_5))][$FB(C_6F_5)_3$] (**1-CF2-py**). See supporting information for spectra. [(^{iPr}POCOP)Ni(CF_2(NC_5H_5))][$FB(C_6F_5)_3$]: $^{31}P\{^1H\}$ (121 MHz, CH_2Cl_2) δ 191.2 (t, $^3J_{PF}$ = 23 Hz). ^{19}F NMR (282 MHz, CH_2Cl_2) δ -30.6 (t, 2F, $^3J_{FP}$ = 23 Hz) -135.2 (m, J_{FF} = 12.6 Hz, o-F, 6F), -162.5 (t, J_{FF} = 19.8 Hz, p-F, 3F), -166 (m, J_{FF} = 19.8 Hz, m-F, 6F), -190.3 (br. s, B-F).

*5.2.4.9 4.9 Reaction of **2-CF2** with pyridine*

To a solution of [(^{iPr}POCOP)Pd(CF_3)] (11 mg, 0.021 mmol) in CH_2Cl_2 (0.5 mL) was added $B(C_6F_5)_3$ (11 mg, 0.021 mmol) as a solid. After 5 minutes, the orange solution was transferred to an NMR tube and analyzed using ^{19}F and $^{31}P\{^1H\}$ NMR spectroscopy to establish the formation of **2-CF2**. Pyridine (2 μL, 1.1 equiv) was then added to the solution, resulting in an immediate colour change to yellow-orange, and analyzed again using ^{19}F and $^{31}P\{^1H\}$ NMR, revealing the formation of [(^{iPr}POCOP)Pd(CF_2(NC_5H_5))][$FB(C_6F_5)_3$] (**2-CF2-py**). See supporting information for spectra. [(^{iPr}POCOP)Pd(CF_2(NC_5H_5))][$FB(C_6F_5)_3$]: $^{31}P\{^1H\}$ (121 MHz, CH_2Cl_2) δ 189.3 (t, $^3J_{PF}$ = 18 Hz). ^{19}F NMR (282 MHz, CH_2Cl_2) δ -33.9 (t, 2F, $^3J_{FP}$ = 18 Hz) -135.2 (m, J_{FF} = 12.6 Hz, *o*-F, 6F), -162.5 (t, J_{FF} = 19.8 Hz, *p*-F, 3F), -166 (m, J_{FF} = 19.8 Hz, *m*-F, 6F), -190.3 (br. s, B-F).

*5.2.4.10 Reaction of **1-CF2c** with 2-phenylpyridine*

To a solution of [(^{iPr}POCOP)Ni(CF_3)] (15 mg, 0.032 mmol) in CH_2Cl_2 (0.5 mL) was added $B(C_6F_5)_3$ (17 mg, 0.032 mmol) as a solid. After 5 minutes, the orange solution was transferred to an NMR tube and analyzed using ^{19}F and $^{31}P\{^1H\}$ NMR spectroscopy to establish the formation of **1-CF2c**. 2-phenylpyridine (4 μL, 1.1 equiv) was then added to the solution, resulting in an immediate colour change to yellow-orange, and analyzed again using ^{19}F and $^{31}P\{^1H\}$ NMR, revealing the formation of **1-CF3** as the major product. See supporting information for spectra.

*5.2.4.11 Reaction of **2-CF2** with 2-phenylpyridine*

To a solution of [($^{i\text{Pr}}$POCOP)Pd(CF_3)] (11 mg, 0.021 mmol) in CH_2Cl_2 (0.5 mL) was added $B(C_6F_5)_3$ (11 mg, 0.021 mmol) as a solid. After 5 minutes, the orange solution was transferred to an NMR tube and analyzed using ^{19}F and $^{31}P\{^1H\}$ NMR spectroscopy to establish the formation of **2-CF2**. 2-phenylpyridine 3 μL, 1.1 equiv) was then added to the solution, resulting in an immediate colour change to yellow-orange, and analyzed again using ^{19}F and $^{31}P\{^1H\}$ NMR, revealing the formation of **2-CF3** as the major product. See supporting information for spectra.

5.2.4.12 X-ray crystallographic studies

Colourless single crystals of **2-CF3** suitable for X-ray diffraction were grown by slow evaporation from a concentrated THF/Et_2O solution. Yellow single crystals of **1-CF2c** suitable for X-ray diffraction were grown at -35 °C from a concentrated CH_2Cl_2 solution. The crystals were mounted on thin glass fibers using paraffin oil and were cooled to 200°K prior to data collection. Data were collected on a Bruker AXS KAPPA single crystal diffractometer equipped with a sealed Mo tube source (wavelength 0.71073 Å) APEX II CCD detector. Raw data collection and processing were performed with APEX II software package from BRUKER AXS.7 Diffraction data were collected with a sequence of 0.5° ω scans at 0, 90, 180, and 270° in ϕ. Initial unit cell parameters were determined from 60 data frames collected at the different sections of the Ewald sphere. Semi-empirical absorption corrections based on equivalent reflections were applied. Systematic absences in the diffraction data set and unit-cell parameters were consistent with triclinic systems. Solutions in centrosymmetric space group yielded chemically reasonable and computationally stable results of refinement. The structures were solved by direct methods, completed with difference Fourier synthesis, and refined with full-matrix least-squares procedures based on F^2. In the structure, compound molecules are situated in the general position. All non-hydrogen atoms were refined anisotropically with satisfactory thermal parameters values. To achieve satisfactory thermal parameters, it was not necessary to use constraints. Additional crystallographic data and selected data collection parameters are reported in Table 5.2. The cif files for the following structures are available as Supporting Information.

Table 5.2. Crystal refinement data for **2-CF3** and **1-CF2c**.

Identification code	**2-CF3**	**1-CF2c**
Empirical formula	C19 H31 F3 O2 P2 Pd	C37 H31 B F18 Ni O2 P2
CCDC deposition number	1543097	1543098
Formula weight	516.78	981.08
Temperature	200(2) K	200(2) K
Wavelength	0.71073 Å	0.71073 Å
Crystal system	Triclinic	Triclinic
Space group	P -1	P -1
a, Å	8.1848(2)	11.6548(4)
b, Å	10.3310(3)	12.7644(4)
c, Å	14.6517(4)	13.8891(4)
α, deg	100.5912(12)	92.4984(18)
β, deg	104.3629(11)	95.9449(17)
γ, deg	101.6362(12)	101.9326(18)
Volume	1139.26(5) $Å^3$	2006.22(11) $Å^3$
Z	2	2
Density (calculated)	1.506 Mg/m^3	1.624 Mg/m^3
Absorption coefficient	0.990 mm^{-1}	0.681 mm^{-1}
F(000)	528	988
Crystal size	0.390 x 0.240 x 0.100 mm^3	0.215 x 0.111 x 0.080 mm^3
Theta range for data collection	2.077 to 28.332°	1.634 to 28.383°
Index ranges	-9<=h<=10	-15<=h<=15

	-13<=k<=13	-17<=k<=16
	-19<=l<=19	-18<=l<=14
Reflections collected	17505	27389
Independent reflections	5502 [R(int) = 0.0145]	9743 [R(int) = 0.0408
Completeness to theta = 25.242°	98.6 %	98.0 %
Absorption correction	Semi-empirical from equivalents	Semi-empirical from equivalents
Max. and min. transmission	0.7457 and 0.6537	0.7457 and 0.6750
Refinement method	Full-matrix least-squares on F^2	Full-matrix least-squares on F^2
Data / restraints / parameters	5502 / 0 / 244	9743 / 0 / 550
Goodness-of-fit on F^2	1.034	1.012
Final R indices [I>2sigma(I)]	R1 = 0.0201, wR2 = 0.0522	R1 = 0.0497, wR2 = 0.1221
R indices (all data)	R1 = 0.0224, wR2 = 0.0535	R1 = 0.0870, wR2 = 0.1402
Extinction coefficient	n/a	n/a
Largest diff. peak and hole	0.383 and -0.325 e.Å^{-3}	0.529 and -0.360 e.Å^{-3}

5.3 References

(1) Harrison, D. J.; Daniels, A. L.; Korobkov, I.; Baker, R. T. *Organometallics* **2015**, *34* (24), 5683–5686.
(2) Clark, G. R.; Hoskins, S. V.; Jones, T. C.; Roper, W. R. *J. Chem. Soc. Chem. Commun.* **1983**, No. 13, 719–721.
(3) Deng, X.-Y.; Lin, J.-H.; Xiao, J.-C. *Org. Lett.* **2016**, *18* (17), 4384–4387.
(4) Furuya, T.; Kamlet, A. S.; Ritter, T. *Nature* **2011**, *473* (7348), 470–477.
(5) Landelle, G.; Panossian, A.; Pazenok, S.; Vors, J.-P.; Leroux, F. R. *Beilstein J. Org. Chem.* **2013**, *9*, 2476–2536.
(6) Hollingworth, C.; Gouverneur, V. *Chem. Commun.* **2012**, *48* (24), 2929–2942.
(7) Belhomme, M.-C.; Besset, T.; Poisson, T.; Pannecoucke, X. *Chem. – Eur. J.* **2015**, *21* (37), 12836–12865.
(8) Hughes, R. P.; Laritchev, R. B.; Yuan, J.; Golen, J. A.; Rucker, A. N.; Rheingold, A. L. *J. Am. Chem. Soc.* **2005**, *127* (43), 15020–15021.
(9) Lee, G. M.; Harrison, D. J.; Korobkov, I.; Baker, R. T. *Chem. Commun.* **2014**, *50* (9), 1128–1130.

(10) Pell, C. J.; Zhu, Y.; Huacuja, R.; Herbert, D. E.; Hughes, R. P.; Ozerov, O. V. *Chem. Sci.* **2017**, *8* (4), 3178–3186.
(11) Richmond, T. G.; Crespi, A. M.; Shriver, D. F. *Organometallics* **1984**, *3* (2), 314–319.
(12) Harrison, D. J.; Gorelsky, S. I.; Lee, G. M.; Korobkov, I.; Baker, R. T. *Organometallics* **2013**, *32* (1), 12–15.
(13) Harrison, D. J.; Lee, G. M.; Leclerc, M. C.; Korobkov, I.; Baker, R. T. *J. Am. Chem. Soc.* **2013**, *135* (49), 18296–18299.
(14) Fuller, J. T.; Harrison, D. J.; Leclerc, M. C.; Baker, R. T.; Ess, D. H.; Hughes, R. P. *Organometallics* **2015**, *34* (21), 5210–5213.
(15) Leclerc, M. C.; Bayne, J. M.; Lee, G. M.; Gorelsky, S. I.; Vasiliu, M.; Korobkov, I.; Harrison, D. J.; Dixon, D. A.; Baker, R. T. *J. Am. Chem. Soc.* **2015**, *137* (51), 16064–16073.
(16) Reger, D. L.; Dukes, M. D. *J. Organomet. Chem.* **1978**, *153* (1), 67–72.
(17) Koola, J. D.; Roddick, D. M. *Organometallics* **1991**, *10* (3), 591–597.
(18) Martínez-Salvador, S.; Menjón, B.; Forniés, J.; Martín, A.; Usón, I. *Angew. Chem. Int. Ed.* **2010**, *49* (25), 4286–4289.
(19) Halle, L. F.; Armentrout, P. B.; Beauchamp, J. L. *Organometallics* **1983**, *2* (12), 1829–1833.
(20) Yang, Z.-Y. *J. Am. Chem. Soc.* **1996**, *118* (34), 8140–8141.
(21) Pandarus, V.; Zargarian, D. *Organometallics* **2007**, *26* (17), 4321–4334.
(22) Castonguay, A.; Spasyuk, D. M.; Madern, N.; Beauchamp, A. L.; Zargarian, D. *Organometallics* **2009**, *28* (7), 2134–2141.
(23) Salah, A. B.; Offenstein, C.; Zargarian, D. *Organometallics* **2011**, *30* (20), 5352–5364.
(24) Morales-Morales, D.; Redon, R.; Yung, C.; Jensen, C. M. *Chem. Commun.* **2000**, No. 17, 1619–1620.
(25) Adhikary, A.; Schwartz, J. R.; Meadows, L. M.; Krause, J. A.; Guan, H. *Inorg. Chem. Front.* **2014**, *1* (1), 71–82.
(26) Vabre, B.; Lindeperg, F.; Zargarian, D. *Green Chem.* **2013**, *15* (11), 3188–3194.
(27) Morales-Morales, D.; Grause, C.; Kasaoka, K.; Redón, R.; Cramer, R. E.; Jensen, C. M. *Inorganica Chim. Acta* **4**, *300–302* (0), 958–963.
(28) Williams, D. B. G.; Lawton, M. *J. Org. Chem.* **2010**, *75* (24), 8351–8354.
(29) Caputo, C. B.; Stephan, D. W. *Organometallics* **2012**, *31* (1), 27–30.
(30) Vabre, B.; Petiot, P.; Declercq, R.; Zargarian, D. *Organometallics* **2014**, *33* (19), 5173–5184.

Chapter 6

Cobalt-Catalyzed Nucleophilic Fluorination of Acyl Chlorides

6.1 Context and Objectives

Transition metal-catalyzed nucleophilic fluorinations are an important class of C-F bond forming reaction.[1] However, most of the catalysts for nucleophilic fluorination are based on precious metals,[2] highlighting a space for the development of first-row metal fluorination catalysts. In Chapter 4 we established the synthesis and characterization of cobalt(III) fluoride complexes, as well as the capacity of a cobalt(III) complex to catalyze the nucleophilic fluorination of *p*-toluoyl chloride,[3] we sought to explore this catalytic fluorination in greater detail, by examining the effects of modifying the ancillary ligands of our previously disclosed Co(III) scaffold, and by extending the fluorination reaction to a broad scope of acyl chloride substrates.

High-throughput experimentation (HTE) techniques have been successfully employed in the context of organometallic catalysis, rapidly providing information regarding improved design of metal based catalysts and reaction conditions.[4–7] In addition, HTE has recently been used to optimize the reaction conditions of a photocatalytic C-H fluorination for the preparative synthesis of Odanacatib.[8] An enantioselective organocatalytic α-fluorination of cyclic ketones was also optimized using HTE, by screening a new library of amine catalysts.[9] As such, we took an opportunity to utilize this technology in our investigation into the effect of the ancillary ligands of cobalt(III) fluorination catalysts.

6.1.1 Published Contributions

High-Throughput Evaluation of Cobalt (III) Catalysts Generated In Situ for Acyl Fluoride Synthesis

Lee, G. M.; Clément, R.; Baker, R. T. *Submitted.*

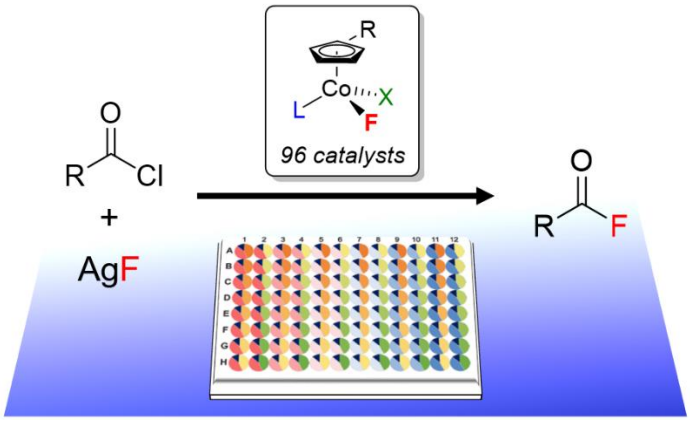

Abstract: Using a high-throughput experimental procedure, a series of cobalt(III) complexes of the general formula $Cp^{R}Co(I)(X)(L)$ were prepared and screened for their activity towards the catalytic nucleophilic fluorination of benzoyl chloride. A highly active catalyst was identified, and successfully employed in a mild and effective protocol for the synthesis of a group of acyl fluoride compounds.

Author Contributions: The manuscript was written by GML. All experiments in this paper performed by GML, except for high-throughput experiments, which were performed by GML and RC.

6.2 High-Throughput Evaluation of Cobalt (III) Catalysts Generated In Situ for Acyl Fluoride Synthesis

6.2.1 Introduction

Fluorination is known to impart unique chemical and biological properties to organic molecules. Therefore, development of synthetic methods for introducing fluorine into various environments is an important area of research. Nucleophilic fluorination methods are attractive as they utilize abundant fluoride salts as the F^- source. In particular, metal-catalyzed nucleophilic fluorination reactions have received much attention.[1,10] The majority of metal catalyzed fluorination reactions utilize palladium complexes.[2,11,12] Cobalt, by

comparison, has seen fewer applications in catalytic C-F bond forming processes. In one example, cobalt salen complexes were used for enantioselective fluorination reactions via epoxide ring opening.[13] In an elegant study, Hiroya et al. reported the cobalt catalyzed hydrofluorination of unactivated olefins, also using a cobalt salen complex.[14]

Acyl fluorides are a synthetically useful group of compounds. Rovis et al. reported that acyl fluorides can be used as substrates in nickel-catalyzed cross-coupling with organozinc reagents.[15] Furthermore, acyl fluorides generated in situ can be used as precursors to carboxylic acid esters, thioesters, and amides.[16,17] Matsuda et al. described a unique three component, one-pot coupling reaction with trimethylsilylmethylphosphonate, aldehyde, and acyl fluoride.[18] The preparation of acyl fluorides can be accomplished via halogen exchange with acyl chlorides using KF,[19] HF,[20] HF-pyridine,[21] or ZnF_2.[22] Alternatively, they can be prepared via deoxofluorination of carboxylic acids using SF_4,[23] DAST (NEt_2-SF_3),[24] and Deoxo-Fluor ($(CH_3OCH_2)_2NSF_3$).[25] The drawbacks to these methods, however, include the use of hazardous reagents, stoichiometric amounts of specialized fluorine sources, or sluggish reactivity requiring high temperature and/or long reaction times.

Recently, we reported a series of perfluoroalkyl Co(III) fluoride complexes $CpCo(CF_2R^F)(F)(PR_3)$ (Cp = η^5-cyclopentadienyl; R^F = F, CF_3; PR_3 = PPh_2Me, PPh_3), prepared by transmetalating $CpCo(CF_2R^F)(I)(PR_3)$ with AgF in CH_2Cl_2 at room temperature.[3] $CpCo(CF_3)(F)(PPh_2Me)$ was shown to react stoichiometrically with *p*-toluoyl chloride to furnish $CpCo(CF_3)(Cl)(PPh_2Me)$ and *p*-toluoyl fluoride. This reaction was extended to a catalytic variant, where *p*-toluoyl chloride was converted quantitatively to *p*-toluoyl fluoride within 4 hours using 5 mol% of $CpCo(CF_3)(I)(PPh_2Me)$ and AgF (3 equiv) as a fluoride source (Figure 6.1).

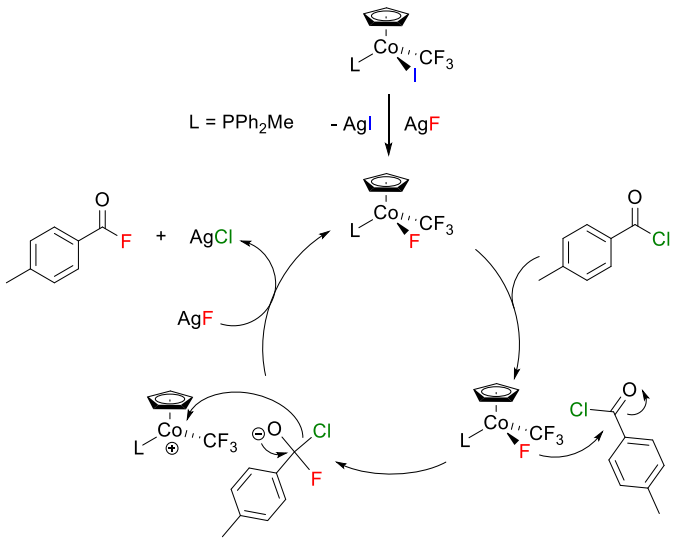

Figure 6.1. Previously reported cobalt(III) catalyzed nucleophilic fluorination of *p*-toluoyl chloride.

It was noted that in the presence of excess PPh_2Me, the rate of reaction did not decrease, suggesting the phosphine ligand can remain coordinated to cobalt during the fluorination step. While the activity of $CpCo(CF_3)(I)(PPh_2Me)$ proved promising, the effect of modifying each ancillary ligand on the key fluorination step remained unexplored.

Herein, we describe the application of high-throughput experimentation technology to prepare 96 unique cobalt(III) catalysts and evaluate their activity towards the nucleophilic fluorination of acyl chlorides. We also seek to expand the scope of this catalytic protocol to include a series of acyl fluoride products.

6.2.2 Results and Discussion

In order to evaluate the effect of each of the ancillary ligands on cobalt(III) catalysts for the fluorination of acyl chlorides, we sought to prepare a large group of complexes with the general formula $Cp^RCo(F)(X)(L)$, and screen their activity towards the fluorination of benzoyl chloride (**1a**). The blueprint for our high-throughput experiment is summarized in Scheme 6.1. First we prepared a series of $Cp^RCo(I)(X)(CO)$ complexes from the oxidative addition of I-X to $Cp^RCo(CO)_2$ (vide infra). Subsequent substitution of the carbonyl ligand on $Cp^RCo(I)(X)(CO)$ complexes with either a phosphine or phosphite is facile, generating

$Cp^RCo(I)(X)(L)$, followed by transmetalation with AgF to form $Cp^RCo(F)(X)(L)$. Importantly, the ligand substitution and transmetalation steps are easily accomplished in situ, which makes catalyst preparation particularly amenable to high-throughput experimentation (HTE) using a robotic platform.

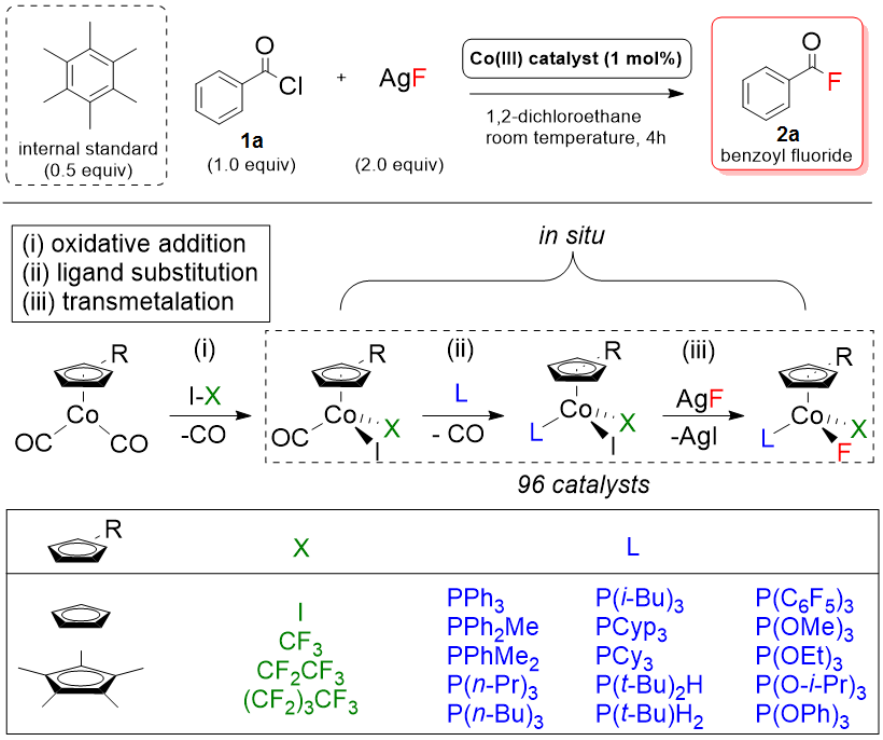

Scheme 6.1. Strategy for the high-throughput screening process; in situ catalyst preparation, and fluorination of benzoyl chloride.

For Cp^R, we examine the difference between Cp (η^5-cyclopentadienyl) and Cp^* (η^5-pentamethylcyclopentadienyl). The anionic ligand X will vary between weakly bound I, and strongly covalent perfluoroalkyl groups CF_3, CF_2CF_3, and $CF_2CF_2CF_2CF_3$. The neutral ligand L will be CO or one of 15 monodentate phosphines/phosphites with a wide range of steric and electronic properties.

The $Cp^RCo(I)(X)(CO)$ complexes used as the foundation of our high-throughput experiment are prepared according to Scheme 6.2. Commercially available $CpCo(CO)_2$ was allowed to react with $I\text{-}R^F$ (R^F = CF_3, CF_2CF_3, $(CF_2)_3CF_3$) and I_2, which underwent oxidative addition and loss of CO to furnish

$CpCo(I)(CF_3)(CO)$ (**M1**), $CpCo(I)(CF_2CF_3)(CO)$ (**M2**), $CpCo(I)((CF_2)_3CF_3)(CO)$ (**M3**), and $CpCo(I)_2(CO)$ (**M4**).

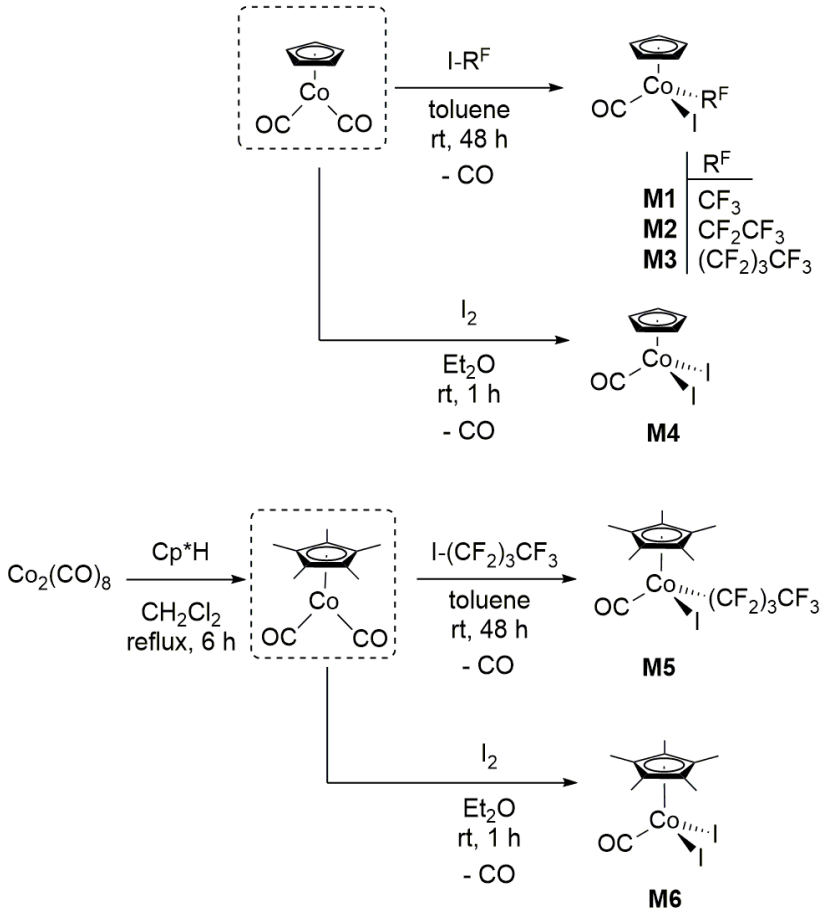

Scheme 6.2. Synthesis of CpCo(I)(X)(CO) complexes **M1**-**M6**.

$Cp^*Co(CO)_2$, prepared according to a previously published procedure,[26] was combined in analagous fashion with $I\text{-}(CF_2)_3CF_3$ and I_2 to furnish $Cp^*Co(I)((CF_2)_3CF_3)(CO)$ (**M5**) and $Cp^*Co(I)_2(CO)$ (**M6**), respectively. Perfluorobutyl complexes **M3** and **M5** are fully characterized using elemental analysis, IR, and multinuclear NMR spectroscopy.

With complexes **M1**-**M6** in hand, we selected a group of 15 phosphine/phosphite ligands (**L1**-**L15**) with a wide variety of steric and electric properties (Scheme 6.1). The full matrix combination of **M1**-**M6** with **L1**-**L15**, along with using complexes **M1**-**M6** without added ligands, furnishes a total of 96 unique

complexes (suitable for a full standard 96-well plate typically used in HTE). We chose to screen these complexes for activity towards the catalytic fluorination of **1a**, in part because the reaction product benzoyl fluoride (**2a**) is one of the few acyl fluoride compounds commercially available, enabling calibration of the GC-FID with authentic samples of **1a**, **2a**, and internal standard hexamethylbenzene (HMB) to ensure accurate quantification of reaction yields and conversions. Silver(I) fluoride is relatively insensitive to decomposition due to light exposure compared to other silver compounds, allowing AgF to be handled without exclusion of light during the course of the experiment. Stock solutions of **M1-M6**, **L1-L15**, **1a**, and HMB are prepared using 1,2-dichloroethane (DCE) as the solvent. DCE has a higher viscosity than dichloromethane (DCM) (0.84 mPa·s vs 0.43 mPa·s at 20 °C), which enables higher accuracy during liquid volumetric transfers. Stock solutions of **M1-M6** and **L1-L15** are each prepared to deliver 1 mol% (relative to **1a**) to the reaction mixture. The low catalyst loading is used to ensure the reactions do not uniformly reach completion prior to stopping the reaction via removal of AgF by filtration through a silica gel plug. The detailed procedure for implementing the high-throughput experiment is shown in Scheme 6.3.

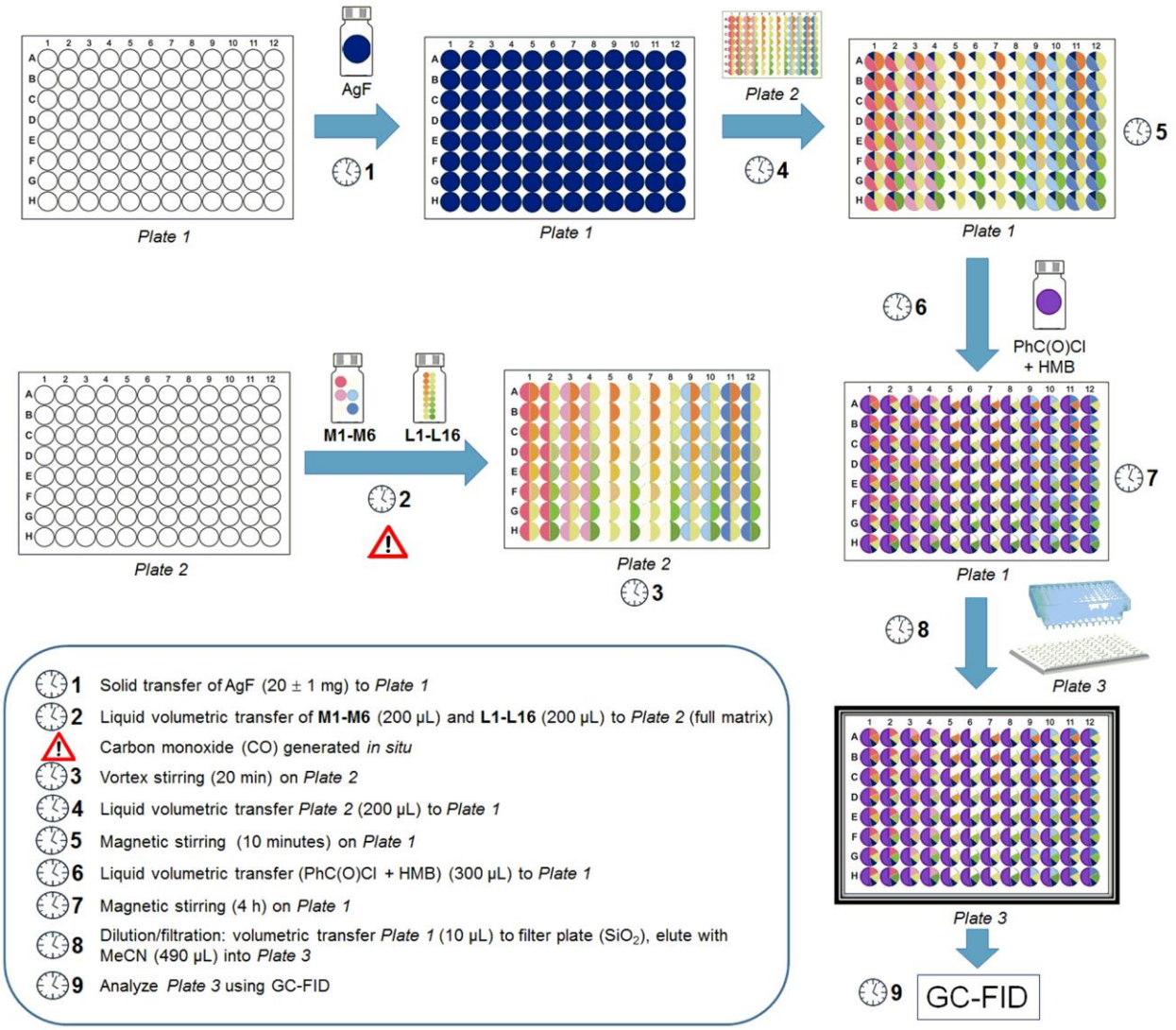

Scheme 6.3. HTE procedure using Freeslate CM3 robotic platform (steps 1-7).

The experiment was conducted using a Freeslate CM3 platform, housed inside a glovebox filled with N_2. First, a full 96-well plate (plate 1) is loaded with solid AgF (20 ± 1 mg) and a small magnetic stir bar in each 1 mL glass reaction vial. Into a separate 96-well plate (plate 2), 200 µL of each stock solution of **M1-M6** are dispensed into 16 vials per metal complex. Subsequently added to each vial in plate 2 are 200 µL of stock solutions of **L1-L15** (also, for **L16**: 200 µL of DCE). The resulting mixtures produce a small amount of CO as it is displaced from the cobalt center by the ligands, which is removed from the glovebox by purging with N_2. Plate 2 is then sealed and mixed using vortex stirring (60 rpm) for 20 min. An aliquot

(200 μL) of the reaction mixtures in plate 2 is transferred volumetrically to plate 1, which is then sealed. The resulting heterogeneous mixture is allowed to react for 10 minutes with magnetic stirring. After stirring is paused, an aliquot (300 μL) of the stock solution containing a mixture of **1a** and HMB is transferred to each vial, plate 1 is resealed, and stirring is resumed for 4 h. Plate 1 is then removed from the glovebox, where an aliquot (10 μL) from each vial is filtered through a small plug of silica gel and eluted with 490 μL MeCN into a final 96-well plate (plate 3). Finally, the reactions are analyzed using GC-FID.

The results of the catalyst screen are shown in Figure 6.1. At a glance, it is clear that $Cp^{R}Co(F)(X)(L)$ complexes represent a robust class of catalysts for the fluorination of benzoyl chloride, with 19 combinations of a Co(III) precursor and phosphine ligand producing **2a** in >80% yield. One way to analyze the data in Figure 1 is to consider the average yield of **2a** for **M1-M6** across all ligands, and for **L1-L16** across all metal complexes. Complexes **M1-M3** had comparable average yields, between 42-46%. A slight increase in average yield was observed for **M5**, with 56%. Finally, complexes **M4** and **M6** gave the best results, with average yields of 64% and 66%, respectively. The average yields for **M1-M6** suggest the following: 1) variation of the length of the perfluoroalkyl auxillary ligand has a negligible impact on the fluorination of **1a**, 2) employment of the more electron-rich Cp* ligand instead of Cp results in a moderate increase in fluorination activity, and 3) replacing the strongly bound perfluoroalkyl ligand with the readily ionizable iodide ligand results in a significant increase in fluorination activity. The steric and electronic differences between CF_3, CF_2CF_3, and $CF_2CF_2CF_2CF_3$ ligands are evidently small enough so as to be insignificant in the context of the nucleophilic fluorination of **1a**.

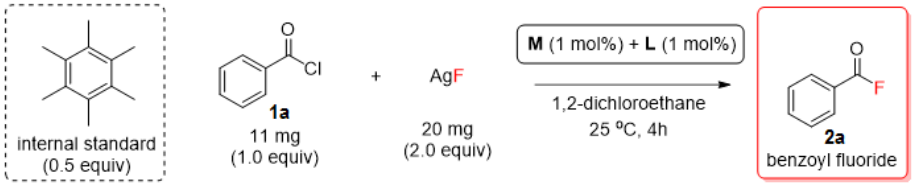

		M1	M2	M3	M4	M5	M6	
PPh_3	L1	26	32	33	70	39	60	43
PPh_2Me	L2	83	84	86	90	87	83	86
$PPhMe_2$	L3	53	35	36	83	93	90	65
$P(n\text{-}Pr)_3$	L4	23	25	30	82	41	90	49
$P(n\text{-}Bu)_3$	L5	49	37	32	95	89	98	67
$P(i\text{-}Bu)_3$	L6	38	62	59	87	41	57	57
$PCyp_3$	L7	67	69	68	78	87	90	77
PCy_3	L8	59	59	34	56	74	80	60
$P(t\text{-}Bu)_2H$	L9	59	64	74	72	50	89	68
$P(t\text{-}Bu)H_2$	L10	37	29	38	46	48	39	40
$P(C_6F_5)_3$	L11	22	20	50	47	19	25	31
$P(OMe)_3$	L12	34	57	46	29	77	75	53
$P(OEt)_3$	L13	35	62	48	32	51	56	47
$P(O\text{-}i\text{-}Pr)_3$	L14	18	18	24	63	33	30	31
$P(OPh)_3$	L15	41	34	32	28	38	45	36
none	L16	26	39	43	65	36	44	42
		42	45	46	64	56	66	*Average*

Yield (%): 0, 10, 20, 30, 40, 50, 60, 70, 80, 90, 100

Figure 6.2. High-throughput evaluation of cobalt catalysts generated in situ for the synthesis of benzoyl fluoride (yields determined using GC-FID analysis).

Improved reactivity when using Cp* instead of Cp is consistent with the idea that increasing the electron donating ability of the cyclopentadienyl ligand results in a more nucleophilic [Co]-F bond, possibly better facilitating the key fluorination step. The increase in fluorination activity observed when diiodide complexes **M4** and **M6** are used can at once be understood on the basis of there now being a second site for transmetalation with AgF to occur, furnishing $Cp^RCo(F)(I)(L)$, but there are other intriguing possibilities to consider. For one, it is known that addition of a phosphine ligand to $Cp^RCo(I)_2(L)$ can readily displace an iodide to afford $[Cp^RCo(I)(L)_2]^+[I]^-$ type complexes.[27] For this reason, care was taken to administer equimolar amounts of **M** and **L**, as the first equivalent of phosphine should selectively displace CO. However, this does not completely discount the possibility of $[Cp^RCo(I)(L)_2]^+[I]^-$ being formed in solution,

and therefore fluorination reactions catalyzed by $[Cp^RCo(F)(L)_2]^+[I]^-$ or $[Cp^RCo(I)(L)_2]^+[F]^-$ complexes should be considered in future studies. A second scenario involves a possible double transmetalation to form $Cp^RCo(F)_2(L)$. In pioneering work by Richard Heck, he reported that $CpCo(Br)_2(CO)$ is decomposed by light, and even in the dark at room temperature, while $CpCo(Cl)_2(CO)$ decomposes rapidly above -20 °C.[28] Therefore, $CpCo(F)_2(CO)$ is likely highly unstable, and the preparation of $Cp^RCo(F)_2(L)$ complexes has not been reported, to our knowledge. In our hands, attempts to isolate complexes of this type resulted in intractable material. However, given the experimental procedure followed, where **M4** and **M6** are exposed to a relative 200 equiv of AgF for 10 minutes prior to the addition of **1a**, it is reasonable to suggest the intractable material might be active for the catalytic fluorination reaction. Further study is needed to fully elucidate the structures of active catalyst species.

The ligand providing the highest average yield of **2a** across **M1-M6** was PPh_2Me (**L2**), with 86%. P(*t*-Bu)$_2$H (**L9**), P(*n*-Bu)$_3$ (**L5**), and $PPhMe_2$ (**L3**) also performed well, with average yields of 68%, 67%, and 65%, respectively. It is also noteworthy that using CO (**L16**) leads to an observed average yield of 42%, higher than for P(*t*-Bu)H_2 (**L10**, 40%), $P(OPh)_3$ (**L15**, 36%), $P(C_6F_5)_3$ (**L11**, 31%), and P(O-*i*-Pr)$_3$ (**L14**, 31%). We observed in our previous study that fluorination of *p*-toluoyl chloride (**1d**) using $CpCo(CF_3)(I)(PPh_2Me)$ is not inhibited by the presence of an excess of PPh_2Me, suggesting that the phosphine can be coordinated to cobalt during the C-F bond forming step. Increasing electron donor ability of PR_3 or $P(OR)_3$ should favor phosphine coordination, while increased steric bulk might mitigate this to some extent. Therefore, we expect a balance between these ligand properties leading to improved catalytic fluorination of **1a**. Parameterization of phosphine-metal complexes has been used to shed light on hypotheses regarding structural influence of various phosphines on reaction mechanism.[29] We utilized the steric and electronic parameters outlined in the seminal work by Tolman to analyze the average reaction yields of the 11 ligands tested for which data was available (Figure 6.2).[30]

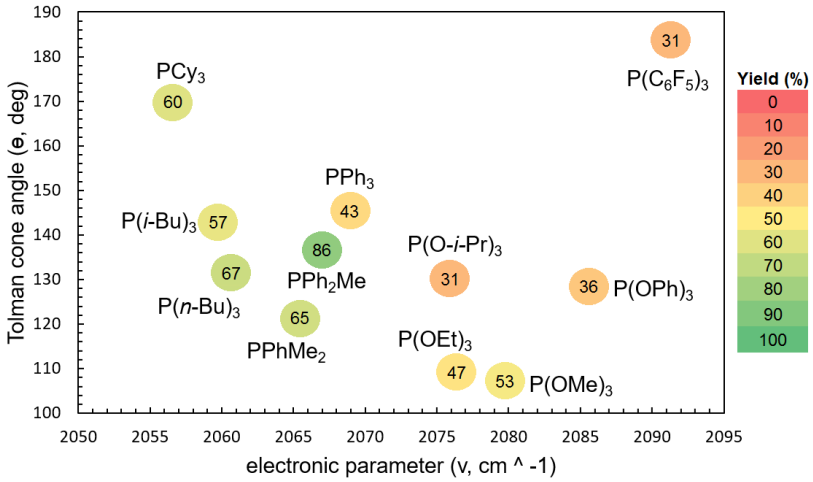

Figure 6.3. Steric and electronic properties of selected ligands used for the fluorination of **1a**. Yields are the average values across reactions with **M1**-**M6**.

Linear regression analysis for the average reaction yield versus the Tolman electronic pararameter (ν, cm^{-1}) reveals a p-value of -1.05 (R^2 = 0.48) indicative of a correlation, albeit a somewhat weak one, between increasing electronic donating ability and increasing reaction yield. Similar treatment for reaction yield versus Tolman cone angle (θ, deg) gives a p-value of -0.13 (R^2 = 0.03), indicating there is virtually no correlation between decreasing steric bulk and increasing reaction yield. Clearly, this simplified approach does not account for additional factors which likely contribute to improved fluorination reactions, and the dataset is incomplete for the ligands tested. In the case of P(*t*-Bu)$_2$H (**L9**), it is noteworthy that the Tolman electronic parameter is 2064 cm^{-1} (similar to that of PPh_2Me, 2067 cm-1), but the cone angle for **L9** has not been reported. Overall, while the data in Figure 1 provides a number of discernable trends which inform a potential pathway for catalytic fluorination and catalyst design, questions remain about possible catalyst structures responsible for activity, and details of certain relevant ligand exchange dynamics.

With new information regarding improved catalyst design, and several possible complexes with strong performance potential, we sought to expand the scope of the catalytic fluorination of acyl chlorides. With consideration given to both high performance, as well as ease of synthesis in terms of practical handling and availability of materials, we decided to prepare the known complex $CpCo(I)_2(PPh_2Me)$.[27] We

tested this catalyst in the fluorination of a series of acyl chlorides (**1a-n**) using 5 mol% catalyst and 2.5 equiv AgF in CH_2Cl_2 for 4-4.5 h, with the exclusion of light (Scheme 6.4). In all cases, excellent yields of acyl fluoride product **2** were obtained, as determined using ^{19}F NMR analysis with an internal standard, with many examples giving nearly quantitative yields. The ^{19}F NMR chemical shift of **2a-n** is shown in Scheme 4, ranging between δ 15.9 – 52.6 ppm. Phenyl based acyl chlorides **1a-k** were tolerant of a variety of electron-donating and electron-withdrawing substituents. Only *m*-Br compound **1g** was slightly hindered, with product **2g** obtained in 80% yield after 4 h. Thiophene compounds are also tolerated, as **1l** could be fluorinated to **2l** in 82% yield. Naphthalene derivative **2m** was prepared in 82% yield, while benzyl derivative **2n** was obtained in quantitatively. Reactions with two substrates, **1b** and **1k**, were scaled up and the products **2b** (75%) and **2k** (58%) were isolated according to a very simple work-up procedure. In total, a simple, mild, and effective catalytic protocol for the synthesis of acyl fluorides from acyl chlorides has been established.

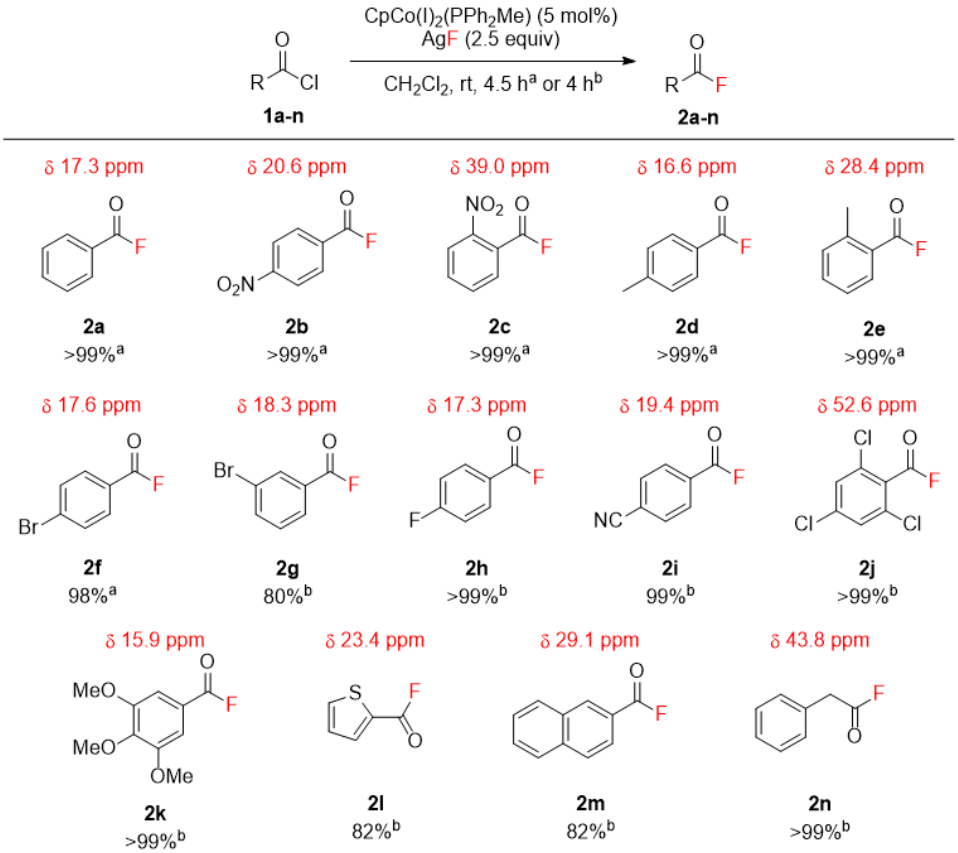

Scheme 6.4. Cobalt-catalyzed fluorination of acyl chlorides. Yields determined using ^{19}F NMR analysis with internal standard (1,3-bis(trifluoromethyl)benzene).

6.2.3 Conclusions

We have utilized high-throughput experimentation to generate and screen 96 unique cobalt (III) complexes of the general formula $Cp^RCo(I)(X)(L)$ for their activity towards the catalytic nucleophilic fluorination of benzoyl chloride using AgF. From these experiments, several determinations were made as to what effect modifying the ancillary ligands (Cp^R, X, or L) has toward fluorination activity. When X = R^F, increasing the length of the perfluoroalkyl group has little impact on catalyst activity. For Cp^R, Cp* shows enhanced activity relative to Cp. When X = I, there is a significant increase in catalyst activity. Increasing the electron-donating ability of L was found to increase catalyst activity, and PPh_2Me was identified as the best ligand studied for the fluorination of benzoyl chloride. With these findings in mind, we employed $CpCo(I)_2PPh_2Me$ as a catalyst in the synthesis of a series of 14 acyl fluoride compounds. The mild and effective protocol demonstrated here provides acyl fluorides in excellent yields, while avoiding the use of high-boiling solvents, hazardous or exotic fluorination agents, high temperature, and long reaction times. Furthermore, this work represents a rare example of cobalt catalyzed nucleophilic fluorination. Future research should be directed toward developing new cobalt based catalysts for the fluorination of a wide range of organic substrates, including alkyl- or allyl- halides and triflates, as well as carboxylic acids.

6.3 Experimental Details for Section 6.2

6.3.1 General Considerations

Experiments were conducted under nitrogen, using Schlenk techniques or an MBraun glove box. All solvents were deoxygenated by purging with nitrogen. Toluene, hexanes, diethyl ether (Et_2O), and 1,2-dichloroethane (DCE) were dried on columns of activated alumina using a J. C. Meyer (formerly Glass Contour®) solvent purification system. Benzene-d_6 (C_6D_6) was dried by standing over activated alumina (ca. 10 wt. %) overnight, followed by filtration. Dichloromethane (DCM) was dried by storing over

activated (heated at ca. 250 °C for >10 h under vacuum) 4 Å molecular sieves for 24 h. Acetonitrile (MeCN), was dried by refluxing over calcium hydride under nitrogen. After distillation, it was dried further by filtration through activated alumina (ca. 5-10 wt. %). All solvents were stored over activated (heated at ca. 250 °C for >10 h under vacuum) 4 Å molecular sieves. Glassware was oven-dried at 150 °C for >2 h or flame-dried using a torch. The following chemicals were obtained commercially, as indicated: $CpCo(CO)_2$ (Strem, 95%), 1,2,3,4,5,-pentamethylcyclopentadiene (Sigma, 95%), iodine (Sigma, >99.8%), $Co_2(CO)_8$ (Strem, stabilized with 1-5% hexanes), CF_3I (SynQuest, 99%), CF_3CF_2I (SynQuest, 99%), $CF_3CF_2CF_2CF_2I$ (Sigma, 98%), benzoyl fluoride (Alfa Aesar, 97%). Phosphine/phosphite ligands were obtained commercially from Sigma Aldrich. Acyl chlorides **1a-n** were obtained commercially from Acros Organics. ^1H, ^{19}F and $^{31}P\{^1H\}$NMR spectra were recorded on either a 300 MHz Bruker Avance or 300 MHz Bruker Avance II instrument at room temperature (21-23 °C). ^1H NMR spectra were referenced to the residual proton peaks associated with the deuterated solvents (C_6D_6: 7.16 ppm, $CDCl_3$: 7.26 ppm). ^{19}F NMR spectra were referenced to internal 1,3- bis(trifluoromethyl)benzene (BTB) (Aldrich, 99%, deoxygenated by purging with nitrogen, stored over activated 4 Å molecular sieves), set to –63.5 ppm. ^1H NMR data for BTB: (300 MHz, C6D6) δ 6.60 (m, 1H, Ar-5-H), 7.12 (m, 2H, Ar-4,6-H), 7.76 (m, 1H, Ar-2-H); (300 MHz, CD3CN) δ 7.76-7.84 (m, 1H, Ar–H), 7.95-8.04 (m, 3H, Ar–H). $^{31}P\{^1H\}$NMR data were referenced to external H_3PO_4 (85% aqueous solution), set to 0.0 ppm. Elemental analyses were performed by the CENTC Elemental Analysis Facility at the University of Rochester. High-throughput reactions were analyzed by gas chromatography (GC) using an Agilent 6850 Series II GC equipped with a flame ionization detector (FID) detector and a Agilent HP-1 methyl siloxane column. Retention times were confirmed by comparison with authentic materials. Peak areas were referenced against HMB (hexamethylbenzene) as internal standard, interpolating from calibration curves spanning the experimental concentration regime. Agreement between replicate runs was within ±5%.

6.3.2 General Procedure for the Synthesis of $Cp^RCo(I)((CF_2)_3CF_3)(CO)$ (Cp^R = η^5-cyclopentadienyl or η^5-pentamethylcyclopentadienyl)

Caution: this experiment produces CO gas. A solution of $ICF_2CF_2CF_2CF_3$ (2.89 g, 11.65 mmol) in toluene (5 mL) was added to a 100 mL bomb containing a solution of $Cp^RCo(CO)_2$ (2.87 mmol) (5 mL) and stirred under N_2 (with allowance for pressure release caused by CO generation), at room temperature for 48 hours. Over the course of the reaction, the color changed from dark red to green-brown. The solvent/volatiles were removed under vacuum, affording a dark green-brown solid, which was purified by washing with hexane (3 x 15 mL), followed by recrystallization from a concentrated CH_2Cl_2 solution and further washing with cold hexane.

*$CpCo(I)((CF_2)_3CF_3)(CO)$ (**M3**).* Yield: 550 mg (40%). ^{1}H NMR (C_6D_6, 300 MHz) δ 4.46 (s, 5H). ^{19}F NMR (C_6D_6, 282 MHz) δ -55.2 (dd, $^2J_{FF}$ = 16 Hz, $^3J_{FF}$ = 13 Hz, 2F, -$CF_2$$CF_2CF_2CF_3$, $F_A/_B$), -81.6 (m, 3F, -$CF_2CF_2CF_2CF_3$), -108.9 (d, $^2J_{FF}$ = 280 Hz, 1F, -$CF_2CF_2$$CF_2CF_3$, $F_A/_B$), -112.5 (d, $^2J_{FF}$ = 280 Hz, 1F, -$CF_2CF_2$$CF_2CF_3$, $F_A/_B$), -124.3 (d, $^2J_{FF}$ = 258 Hz, 1F, -$CF_2CF_2CF_2$$CF_3$, $F_A/_B$), -126.6 (d, $^2J_{FF}$ = 258 Hz, 1F, -$CF_2CF_2CF_2$$CF_3$, $F_A/_B$). ^{13}C{^{1}H} NMR (C_6D_6, 75 MHz) δ 199.6 (s), 120.5 (m), 116.7 (m), 113.0 (m), 110.2 (m), 90.2 (s). IR (nujol) 2059, 2080 cm^{-1}. Anal. Calcd for $C_{10}H_5CoF_9IO$: C, 24.12; H, 1.01%. Found: C, 23.57, H: 0.883%.

*$Cp^*Co(I)((CF_2)_3CF_3)(CO)$ (**M5**).* Yield: 526 mg (50%). ^{1}H NMR (C_6D_6, 300 MHz) δ 1.41 (s, 15H, CH_3). ^{19}F NMR (C_6D_6, 282 MHz) δ -68.2 (d, $^2J_{FF}$ = 261 Hz, 1F, -$CF_2$$CF_2CF_2CF_3$, $F_A/_B$) -70.8 (d, $^2J_{FF}$ = 261 Hz, 1F, -$CF_2$$CF_2CF_2CF_3$, $F_A/_B$), -81.5 (s, 3F, -$CF_2CF_2CF_2CF_3$), -106.9 (d, $^2J_{FF}$ = 288 Hz, 1F, -$CF_2CF_2$$CF_2CF_3$, $F_A/_B$), -110.0 (d, $^2J_{FF}$ = 288 Hz, 1F, -$CF_2CF_2$$CF_2CF_3$, $F_A/_B$), -124.8 (dt, $^2J_{FF}$ = 289 Hz, $^3J_{FF}$ = 15 Hz, 1F, -$CF_2CF_2CF_2$$CF_3$, $F_A/_B$), -126.0 (dt, $^2J_{FF}$ = 289 Hz, $^3J_{FF}$ = 15 Hz, 1F, -$CF_2CF_2CF_2$$CF_3$, $F_A/_B$). ^{13}C{^{1}H} NMR (C_6D_6, 75 MHz) δ 203.3 (s) 120.6 (m), 116.7 (m), 113.2 (m), 110.3 (m), 106.7 (m), 103.4 (s), 10.3 (s). IR (nujol) Frequency: 2006, 2051 cm^{-1}. Anal. Calcd. for $C_{15}H_{15}CoF_9IO$: C, 31.71; H, 2.66%. Found: C, 31.91; H, 2.58%.

6.3.3 Synthesis of $CpCo(I)_2(PPh_2Me)$

Caution: this experiment produces CO gas. A solution of PPh_2Me (197 mg, 1.02 mmol) in toluene (5 mL) was slowly addded via cannula transfer to a 100 mL bomb coantaining a solution of $CpCo(I)_2(CO)$ (400

mg, 0.99 mmol) in toluene (5 mL) and a magnetic stir bar, and bubbling was observed upon mixing. The reaction was allowed to stir under N_2 overnight (ca. 18 h), resulting in a black solution. Volatiles were the removed under vauum, and the resulting black solid was washed with cold hexanes (3 x 15 mL) and then dried, giving $CpCo(I)_2(PPh_2Me)$. Yield: 466 mg (81%). ^{1}H NMR (C_6D_6, 300 MHz) δ 7.71 (m, 4H), 7.05 (m, 6H), 4.51 (s, 5H, Cp), 2.29 (d, 3H, CH_3). $^{31}P\{^1H\}$ NMR δ 23.7 ppm.

6.3.4 General Procedure for Catalytic Fluorination of Acyl Chlorides

A glass vial was charged with a magnetic stir bar, AgF (55 mg, 0.434 mmol), $CpCo(I)_2(PPh_2Me)$ (5 mg, 0.0086 mmol), and CH_2Cl_2 (1.0 mL). The vial was capped and covered with aluminum foil, and stirred for 5 minutes. A solution of acyl chloride **1** (0.173 mmol) in CH_2Cl_2 (1.0 mL) was added, and the resulting mixture was again covered with aluminum foil and stirred for 4 or 4.5 hours. A solution of 1,3-bis(triluoromethyl)benzene (0.026 mmol) in $CDCl_3$ (0.5 mL) was then added to the mixture, and an aliquot was then analyzed using ^{19}F NMR to determine the yield of **2**.

6.3.5 General Procedure for the Synthesis of Acyl Fluorides 2b, 2k

A glass vial was charged with a magnetic stir bar, AgF (205 mg, 1.62 mmol), $CpCo(I)_2(PPh_2Me)$ (16 mg, 0.028 mmol), and CH_2Cl_2 (2.0 mL). The vial was capped and covered with aluminum foil, and stirred for 5 minutes. A solution of acyl chloride **1b/k** (0.54 mmol) in CH_2Cl_2 (2.0 mL) was added, and the resulting mixture was again covered with aluminum foil and stirred for 4 hours. The mixture was then filtered through a small plug of silica gel, and eltued with CH_2Cl_2 (5 mL). The filtrate was then evaporated to dryness, and the resulting residue was triturated with Et_2O (2 mL), and dried under vacuum to give **2b/k**.

*4-nitrobenzoyl fluoride (**2b**)*. Yield: 68 mg (75%). ^{1}H NMR ($CDCl_3$, 300 MHz) δ 8.39 (d, $^3J_{HH}$ = 8.5 Hz, 2H, *o*-Ar-H), 8.25 (d, $^3J_{HH}$ = 8.5 Hz, 2H, *m*-Ar-H). ^{19}F NMR ($CDCl_3$, 282 MHz) δ 20.6 (s).

*3,4,5-tris(methoxy)benzoyl fluoride (**2k**)*. Yield: 67 mg (58%). ^{1}H NMR ($CDCl_3$, 300 MHz) δ 7.27 (s, 2H, *o*-Ar-H), 3.95 (s, 3H, *p*-OMe), 3.91 (s, 6H, *m*-OMe). ^{19}F NMR ($CDCl_3$, 282 MHz) δ 15.9 (s).

6.4 References

(1) Hollingworth, C.; Gouverneur, V. *Chem. Commun.* **2012**, *48* (24), 2929–2942.
(2) Katcher, M. H.; Norrby, P.-O.; Doyle, A. G. *Organometallics* **2014**, *33* (9), 2121–2133.
(3) Leclerc, M. C.; Bayne, J. M.; Lee, G. M.; Gorelsky, S. I.; Vasiliu, M.; Korobkov, I.; Harrison, D. J.; Dixon, D. A.; Baker, R. T. *J. Am. Chem. Soc.* **2015**, *137* (51), 16064–16073.
(4) Rasu, L.; John, J. M.; Stephenson, E.; Endean, R.; Kalapugama, S.; Clément, R.; Bergens, S. H. *J. Am. Chem. Soc.* **2017**, *139* (8), 3065–3071.
(5) Lee, G. M.; Loechtefeld, R.; Menssen, R.; Bierer, D. E.; Riedl, B.; Baker, R. T. *Tetrahedron Lett.* **2016**, *57* (49), 5464–5468.
(6) Blacquiere, J. M.; Jurca, T.; Weiss, J.; Fogg, D. E. *Adv. Synth. Catal.* **2008**, *350* (18), 2849–2855.
(7) Monfette, S.; Blacquiere, J. M.; Fogg, D. E. *Organometallics* **2011**, *30* (1), 36–42.
(8) Halperin, S. D.; Kwon, D.; Holmes, M.; Regalado, E. L.; Campeau, L.-C.; DiRocco, D. A.; Britton, R. *Org. Lett.* **2015**, *17* (21), 5200–5203.
(9) Kwiatkowski, P.; Beeson, T. D.; Conrad, J. C.; MacMillan, D. W. C. *J. Am. Chem. Soc.* **2011**, *133* (6), 1738–1741.
(10) Petrone, D. A.; Ye, J.; Lautens, M. *Chem. Rev.* **2016**, *116* (14), 8003–8104.
(11) Lee, H. G.; Milner, P. J.; Buchwald, S. L. *J. Am. Chem. Soc.* **2014**, *136* (10), 3792–3795.
(12) Hollingworth, C.; Hazari, A.; Hopkinson, M. N.; Tredwell, M.; Benedetto, E.; Huiban, M.; Gee, A. D.; Brown, J. M.; Gouverneur, V. *Angew. Chem. Int. Ed.* **2011**, *50* (11), 2613–2617.
(13) Kalow, J. A.; Doyle, A. G. *J. Am. Chem. Soc.* **2010**, *132* (10), 3268–3269.
(14) Shigehisa, H.; Nishi, E.; Fujisawa, M.; Hiroya, K. *Org. Lett.* **2013**, *15* (20), 5158–5161.
(15) Zhang, Y.; Rovis, T. *J. Am. Chem. Soc.* **2004**, *126* (49), 15964–15965.
(16) Ueda, T.; Konishi, H.; Manabe, K. *Org. Lett.* **2013**, *15* (20), 5370–5373.
(17) Zamiri, M.; Grierson, D. S. *Synthesis* **2017**, *49* (03), 571–578.
(18) Umezawa, T.; Seino, T.; Matsuda, F. *Org. Lett.* **2012**, *14* (16), 4206–4209.
(19) Krespan, C. G.; Dixon, D. A. *J. Org. Chem.* **1991**, *56* (12), 3915–3923.
(20) Lee, I.; Shim, C. S.; Chung, S. Y.; Kim, H. Y.; Lee, H. W. *J. Chem. Soc., Perkin Trans. 2* **1988**, No. 11, 1919–1923.
(21) Chen, C.; Chien, C.-T.; Su, C.-H. *J. Fluor. Chem.* **2002**, *115* (1), 75–77.
(22) Nenajdenko, V. G.; Lebedev, M. V.; Balenkova, E. S. *Tetrahedron Lett.* **1995**, *36* (35), 6317–6320.
(23) Ritter, S. K.; Hill, B. K.; Odian, M. A.; Dai, J.; Noftle, R. E.; Gard, G. L. *J. Fluor. Chem.* **1999**, *93* (1), 73–79.
(24) Lal, G. S.; Pez, G. P.; Pesaresi, R. J.; Prozonic, F. M.; Cheng, H. *J. Org. Chem.* **1999**, *64* (19), 7048–7054.
(25) Beaulieu, F.; Beauregard, L.-P.; Courchesne, G.; Couturier, M.; LaFlamme, F.; L'Heureux, A. *Org. Lett.* **2009**, *11* (21), 5050–5053.
(26) Sun, B.; Yoshino, T.; Matsunaga, S.; Kanai, M. *Adv. Synth. Catal.* **2014**, *356* (7), 1491–1495.
(27) Knizhnikov, V. A.; Shirokii, V. L.; Bazhanov, A. V.; Tychinskaya, L. Y.; Maier, N. A. *Russ. J. Gen. Chem.* **2002**, *72* (5), 701–703.
(28) Heck, R. F. *Inorg. Chem.* **1965**, *4* (6), 855–857.
(29) Niemeyer, Z. L.; Milo, A.; Hickey, D. P.; Sigman, M. S. *Nat. Chem* **2016**, *8* (6), 610–617.
(30) Tolman, C. A. *Chem. Rev.* **1977**, *77* (3), 313–348.

Chapter 7

Conclusions and Future Directions

7.1 Overview

The field of fluoro-organometallic chemistry has seen a resurgence in interest in recent years, with as many research groups investigating this area today as ever before. The work presented in this thesis constitutes a significant contribution to the fluoro-organometallic chemistry of first-row transition metals, particularly cobalt and nickel, and there are many directions future research in this area can take. This chapter will provide a brief summary of the original research presented in the previous 5 chapters, and outline opportunities for future work on these projects.

7.2 Chapter 2

Metallacyclobutene complexes which are stable enough to be isolated are not very common, and examples bearing fluorine substituents are very rare. Chapter 2 presented the synthesis and characterization of partially fluorinated cobaltacyclobutene complexes, prepared via the addition of terminal aryl-alkynes to cobalt fluorocarbene complexes. We found that deviating from terminal-aryl alkynes, or from the electron donating PPh_2Me ligand, greatly hindered the formation of cobaltacyclobutenes, or reduced the stability of the products. We also found that while $CpCo(=CF(CF_3))(PPh_2Me)$ reacted smoothly with PhC≡CH, the same reaction with $CpCo(=CF_2)(PPh_2Me)$ was significantly slower, consistent with a lower calculated energy reaction barrier and later transition state for the former. Based on kinetic experiments and DFT calculations, we have proposed a mechanism that addresses cobaltacyclobutene formation, identifying a singlet 1,4-diradical species as a key intermediate in the stepwise ring closing pathway. Future work in this area should focus on the development of productive reactivity of partially fluorinated cobaltacyclobutenes. An example could involve a net insertion into the terminal C-H bond of the alkyne, forming $ArC{\equiv}CCFR^FH$ (Figure 7.1). Selectivity for the alkyne product over the cyclopropene would complement the selectivity observed for metal-free reactions of alkynes and fluorocarbenes.

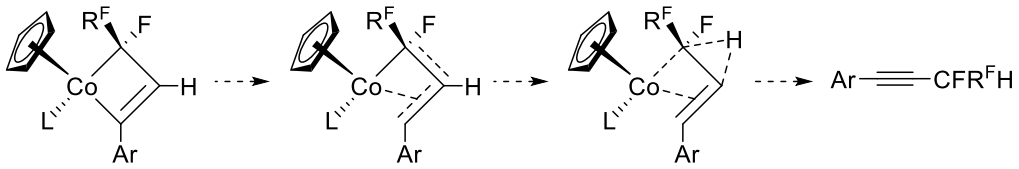

Figure 7.1. Example of productive reactivity of a partially fluorinated metallacyclobutene.

7.3 Chapter 3

Chapter 3 dealt with the addition of difluorocarbene to cobalt(I) complexes, furnishing a mixture of cobalt(I) fluorocarbenes and cobalt(III) fluoroalkene complexes. The product distribution favours formation of the fluoroalkene complexes, as the Co(I) fluorocarbenes react rapidly with highly electrophilic CF_2. The source of difluorocarbene in this chapter was a combination of Me_3SiCF_3 and NaI, which in the absence of metal complexes react to form TFE from the dimerization of CF_2. The stepwise nature of the difluorocarbene addition was established by investigating the reactivity of isolated Co(I) fluorocarbenes with CF_2, as well as reactions of $CpCoL_2$ with TFE under standard reaction conditions. Ongoing research efforts should be focused on extending Me_3SiCF_3 as a difluorocarbene source for the synthesis of a variety of metal fluorocarbene complexes. The goal should not only be to isolate new metal fluorocarbene complexes, but to discover highly reactive metal fluorocarbenes which facilitate catalytic formation of fluorinated organic products. Future research should also explore alternative difluorocarbene sources, particularly $Ph_3P^+CF_2CO_2^-$ and $Na^+CF_2BrCO_2^-$.

7.4 Chapter 4

While the previous chapters focused on nucleophilic cobalt(I) fluorocarbenes, chapter 4 concerns the synthesis and reactivity of cobalt(III) complexes. In particular, we prepared complexes with two fluorinated ligands (one fluoride and one perfluoroalkyl or two perfluoroalkyls) which are very uncommon. Four examples of perfluoroalkyl cobalt(III) fluorides were presented, and their extreme upfield ^{19}F NMR chemical shifts were discussed in detail, along with their role as catalysts for the fluorination of *p*-toluoyl chloride. In addition, two bis(perfluoroalkyl) cobalt(III) complexes were prepared: a bis(trifluoromethyl) complex and a mixed trifluoromethyl-perfluoroethyl complex. It was demonstrated that α-fluoride

abstraction by Lewis acids resulted in the selective formation of electrophilic Co(III) difluorocarbenes. Importantly, we also observed migratory insertion of the difluorocarbene ligand into the remaining perfluoroalkyl group, elongating the perfluoroalkyl fragment by one CF_2 unit. This represented a rare demonstration of perfluoroalkyl chain growth in the inner coordination sphere of a transition metal. Future work on this project should include crystallographic characterization of cobalt(III) fluorocarbene complexes. In addition, the detailed mechanism of fluorocarbene insertion into perfluoroalkyl ligands should be investigated. Furthermore, new bis(perfluoroalkyl) metal complexes should be prepared, with the perfluoroalkyl groups in a mutually *cis* arrangement. Metal complexes based on cobalt, as well as nickel, palladium, iron, and ruthenium should be explored. Subsequent Lewis acid-mediated α-fluoride abstraction and fluorocarbene insertion reactions can then be investigated using this platform.

7.5 Chapter 5

The previous chapters focus on the fluoro-organometallic chemistry of cobalt, but chapter 5 shifts to the chemistry of nickel and palladium. Specifically, POCOP-type pincer ligated nickel and palladium complexes bearing trifluoromethyl and difluorocarbene ligands were prepared. Similar to the Co(III) fluorocarbenes introduced in the previous chapter, nickel and palladium fluorocarbene complexes in chapter 5 are cationic and electrophilic, having been prepared by Lewis acid-mediated α-fluoride abstraction from trifluoromethyl ligands. We noted the importance of using a Lewis acid which results in a sterically bulky counter anion, as this leads to a prolonged lifetime of the difluorocarbene complexes in solution. We described the limitations associated with the highly moisture-sensitive nature of these cationic fluorocarbene complexes, and also explored their reactivity with pyridine and 2-phenylpyridine. The former compound formed a simple CF_2-N adduct, while the latter was precluded from CF_2-N bond formation by the added steric hindrance. Forthcoming investigations could take advantage of the large body of knowledge regarding pincer ligand scaffolds, and prepare *para*-substituted POCOP derivatives of Ni and Pd difluorocarbene complexes, using a variety of electron-donating and electron-withdrawing substituents, to systematically probe their effect on the $M=CF_2$ bond properties and reactivity.

7.6 Chapter 6

Chapter 6 takes a closer look at the cobalt(III)-catalyzed nucleophilic fluorination reaction which was introduced in chapter 4. In this chapter, we utilized high-throughput experimentation (HTE) technology to generate 96 unique cobalt(III) complexes and screen their activity toward the catalytic fluorination of benzoyl fluoride. The results from this experiment indicated which ancillary ligands led to improved catalytic fluorination performance. In particular, PPh_2Me gave the best average yields among the L donor ligands screened, Cp* provided moderately improved yields relative to Cp, while diiodide complexes gave superior yields compared to perfluoroalkyl iodide complexes. Also based on the results of the HTE, we used $CpCo(I)_2(PPh_2Me)$ as a catalyst for the synthesis of a wider scope of acyl fluoride compounds. This catalyst provided excellent yields, with short reaction times and mild reaction conditions compared to previously established methods for acyl fluoride synthesis. There is tremendous potential for expanding the area of cobalt-catalyzed fluorination reactions. Regarding the acyl fluoride synthesis presented in chapter 6, more work is needed to establish a detailed reaction pathway, and identify the active catalyst species. This work is very likely to be important for rationally extending the cobalt-catalyzed nucleophilic fluorination reaction to different organic substrates. In addition to nucleophilic fluorination reactions, cobalt(III) complexes could potentially serve as catalysts for *electrophilic* fluorinations. That is, fluorine sources derived from F_2 such as *N*-fluorobenzenesulfonamide or Selectfluor® might be used to develop a cobalt-catalyzed fluorination of C-H bonds, a potentially high-impact process for pharmaceutical industries.

7.7 Final Remarks

Fluoro-organometallic chemistry of first-row transition metals is a fascinating area of research which has provided many opportunities to discover new complexes and reactivity. Our work has focused primarily on the synthesis and reactivity of metal fluorocarbene complexes, although chapters 4 and 6 also explore the chemistry of cobalt fluoride complexes. Our group has contributed significantly to the field, as we have prepared the first examples of nucleophilic *and* electrophilic cobalt and nickel fluorocarbene complexes. We have collaborated with leading computational experts in the field to provide needed fundamental insight

into the bonding and reactivity of metal fluorocarbene complexes, as well as the properties of cobalt fluoride complexes. The [2+2] cycloaddition reactions reported for nucleophilic cobalt(I) fluorocarbenes, as well as the perfluoroalkyl-insertion reactions for electrophilic cobalt(III) fluorocarbenes, are key steps toward developing potentially powerful metal-catalyzed metathesis/polymerization processes based on perfluorocarbons. Cobalt-catalyzed fluorination reactions are a largely unexplored area which could be an attractive alternative to many of the current processes utilizing precious metals.

Appendix A – Supplementary Information for Chapter 2

Table of Contents

1. NMR Spectra for Various Reactions of 1a, 1c, and PhC≡CH

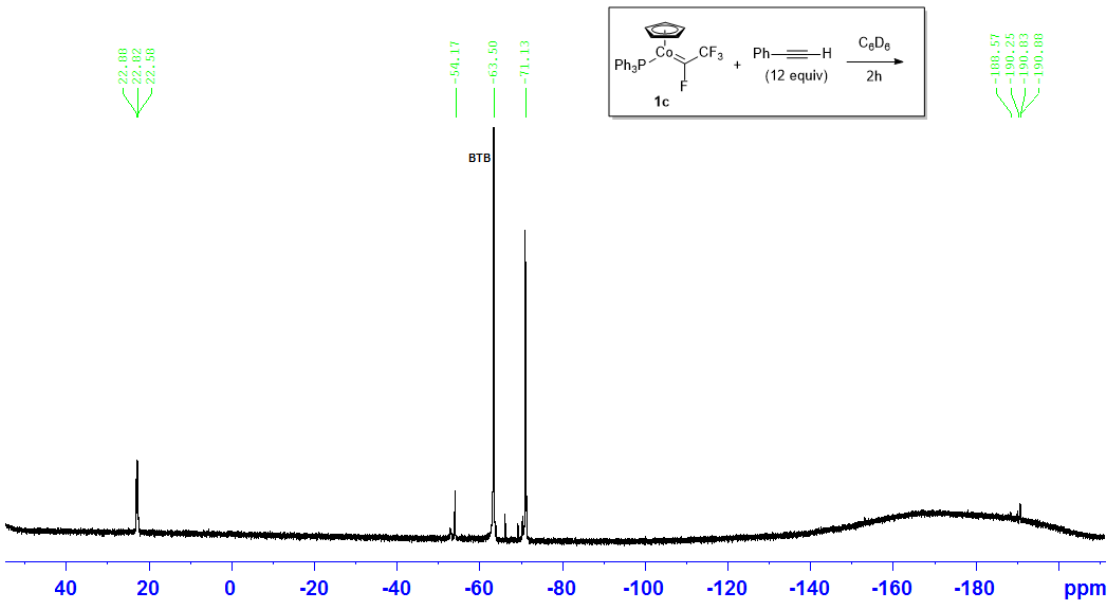

Figure S1. ^{19}F NMR spectra for the reaction between **1c** (21 mg, 0.043 mmol) and PhC≡CH (54 mg, 0.53 mmol, 12 equiv) in C_6D_6 (0.6 mL) at ambient temperature for 2 hours.

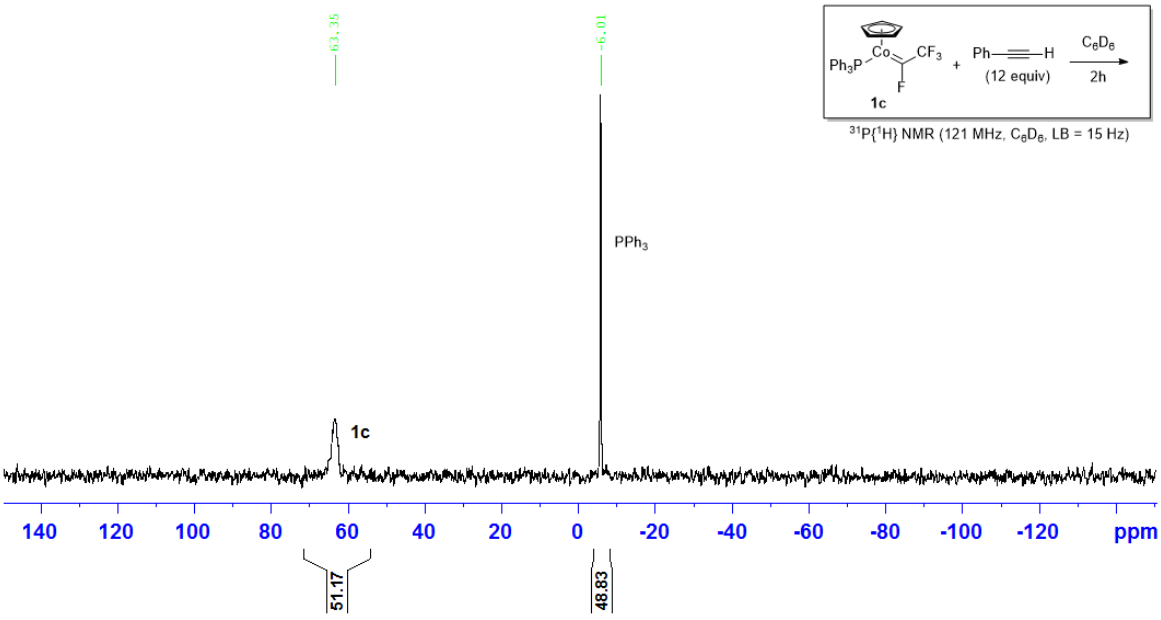

Figure S2. $^{31}P\{^{1}H\}$ NMR spectra for the reaction between **1c** (21 mg, 0.043 mmol) and PhC≡CH (54 mg, 0.53 mmol, 12 equiv) in C_6D_6 (0.6 mL) at ambient temperature for 2 hours.

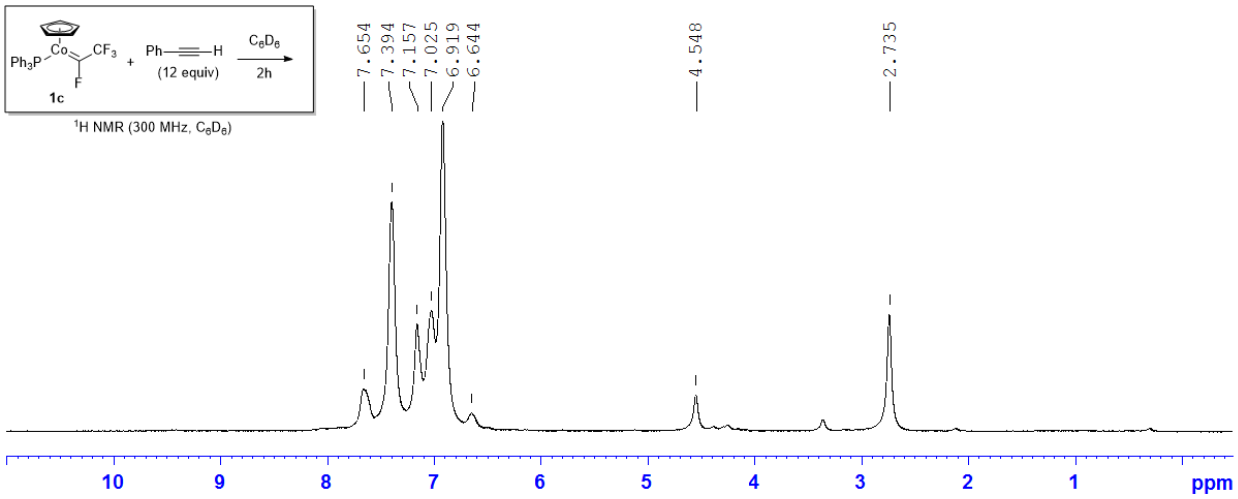

Figure S3. ^{1}H NMR spectra for the reaction between **1c** (21 mg, 0.043 mmol) and PhC≡CH (54 mg, 0.53 mmol, 12 equiv) in C_6D_6 (0.6 mL) at ambient temperature for 2 hours.

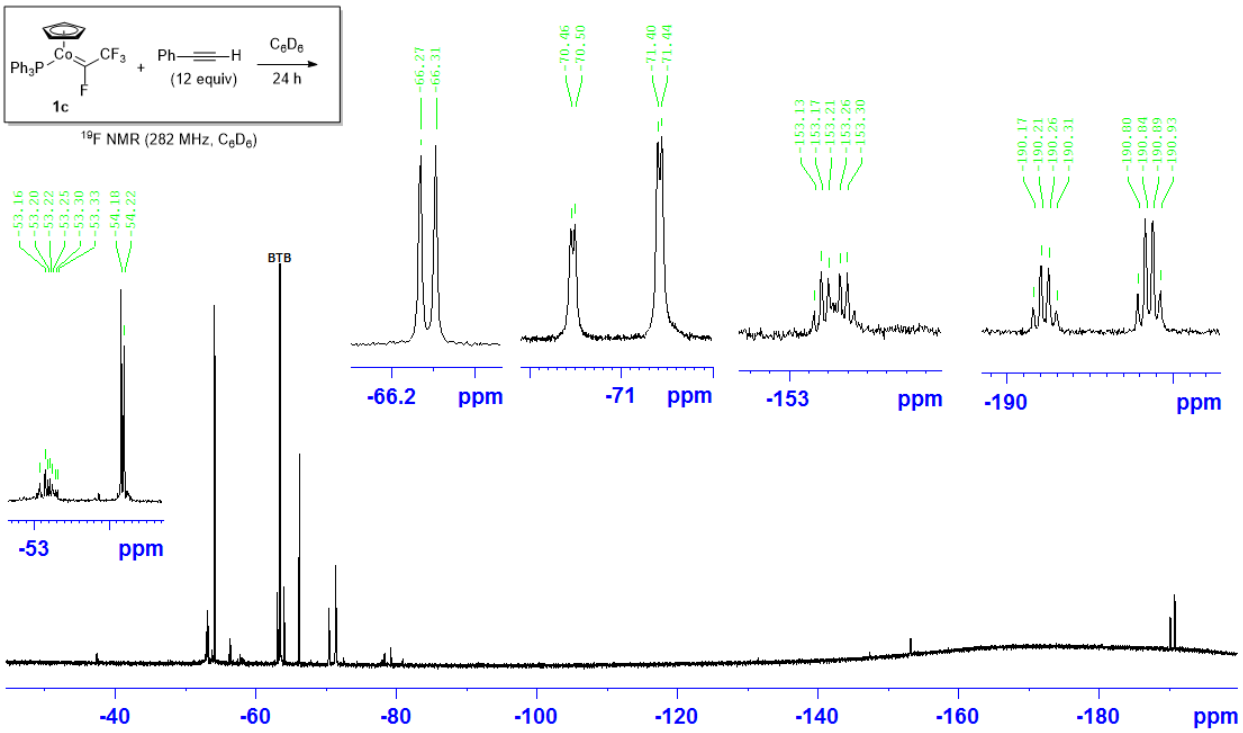

Figure S4. ^{19}F NMR spectra for the reaction between **1c** (21 mg, 0.043 mmol) and PhC≡CH (54 mg, 0.53 mmol, 12 equiv) in C_6D_6 (0.6 mL) at ambient temperature for 24 hours, after filtration through celite.

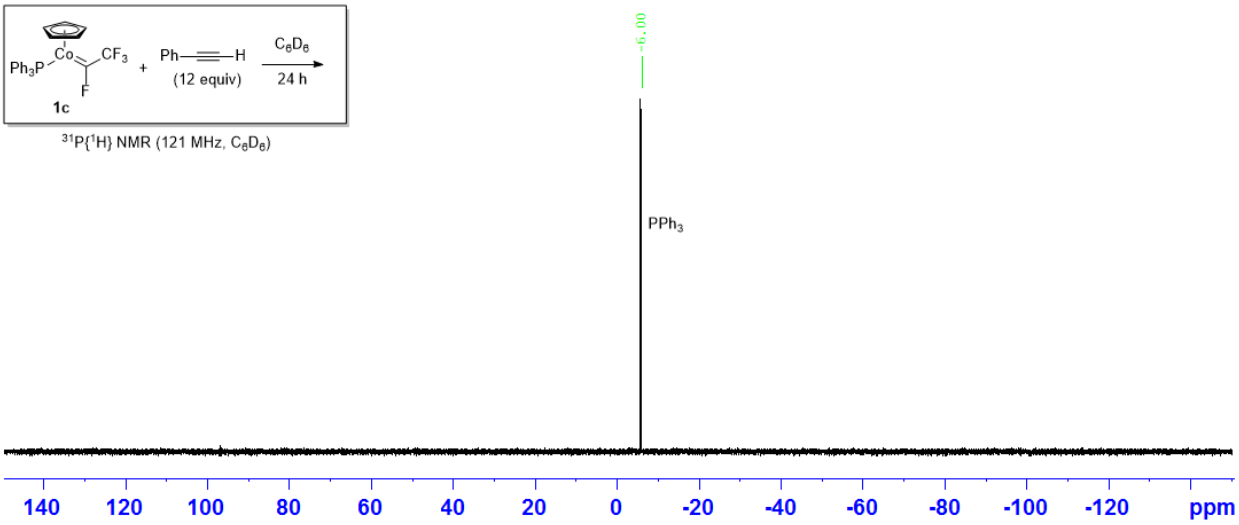

Figure S5. $^{31}P\{^{1}H\}$ NMR spectra for the reaction between **1c** (21 mg, 0.043 mmol) and PhC≡CH (54 mg, 0.53 mmol, 12 equiv) in C_6D_6 (0.6 mL) at ambient temperature for 24 hours, after filtration through celite.

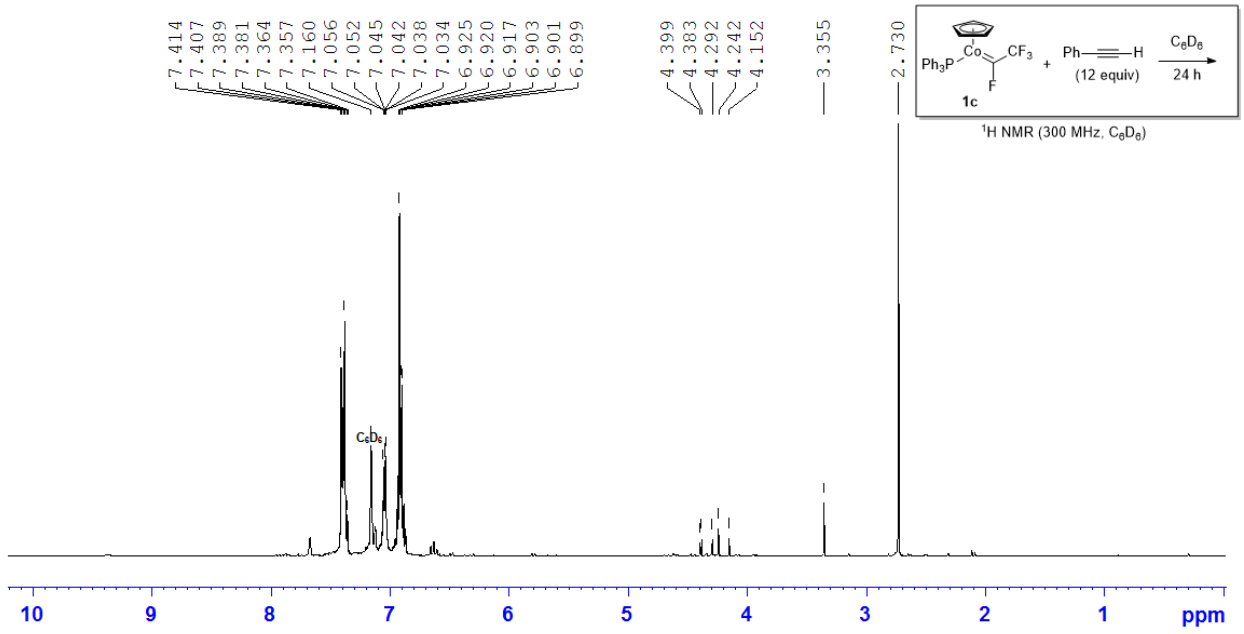

Figure S6. ^{1}H NMR spectra for the reaction between **1c** (21 mg, 0.043 mmol) and PhC≡CH (54 mg, 0.53 mmol, 12 equiv) in C_6D_6 (0.6 mL) at ambient temperature for 24 hours, after filtration through celite.

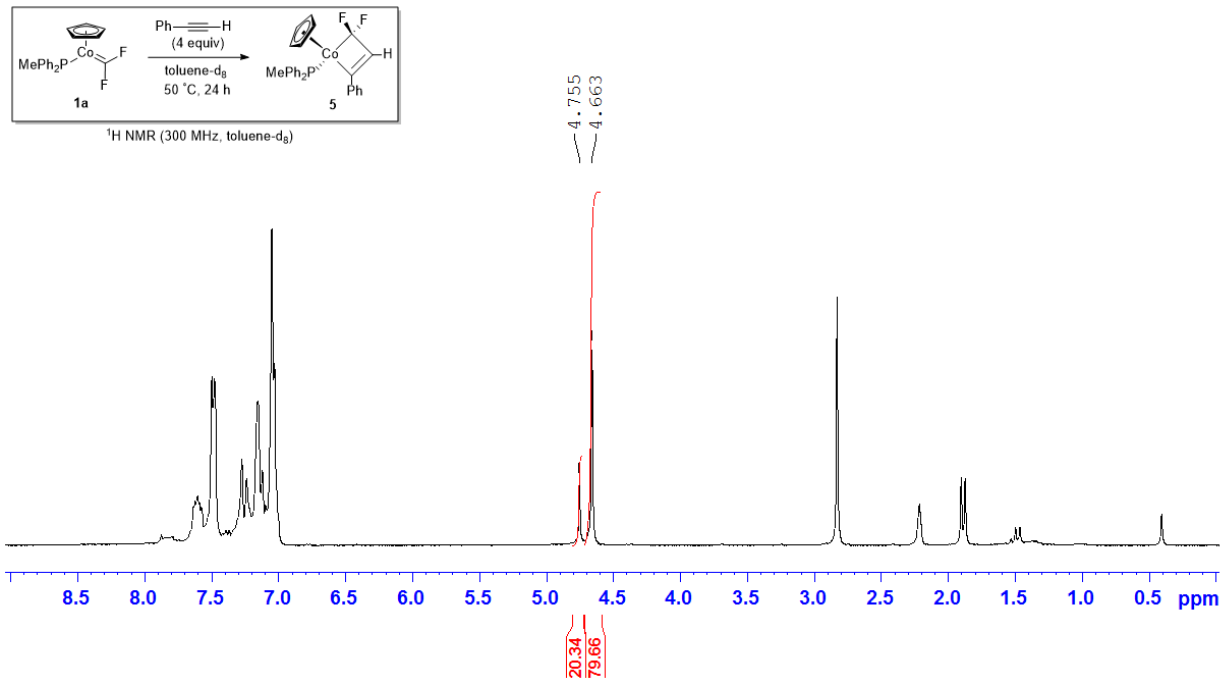

Figure S7. ^{1}H NMR spectra for the reaction between **1a** (20 mg, 0.53 mmol) and PhC≡CH (22 mg, 0.22 mmol, 4 equiv) in toluene-d^{8} (0.6 mL) at 50 °C for 24 hours, after filtration through celite.

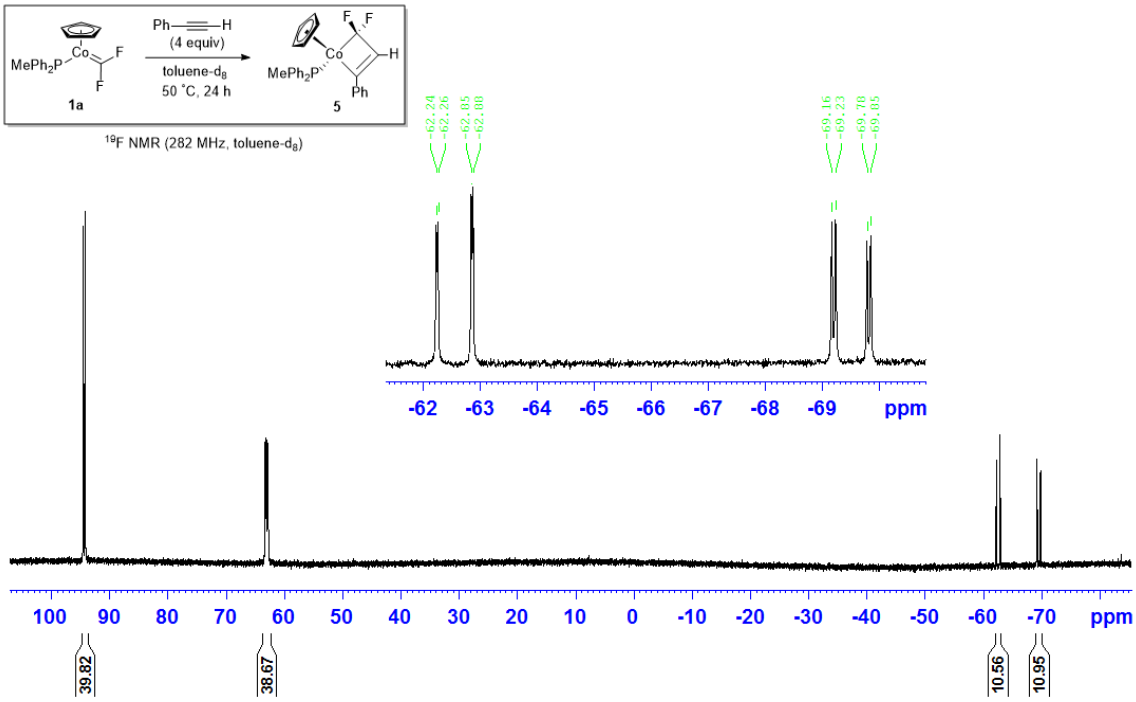

Figure S8. ^{19}F NMR spectra for the reaction between **1a** (20 mg, 0.53 mmol) and PhC≡CH (22 mg, 0.22 mmol, 4 equiv) in toluene-d^8 (0.6 mL) at 50 °C for 24 hours, after filtration through celite.

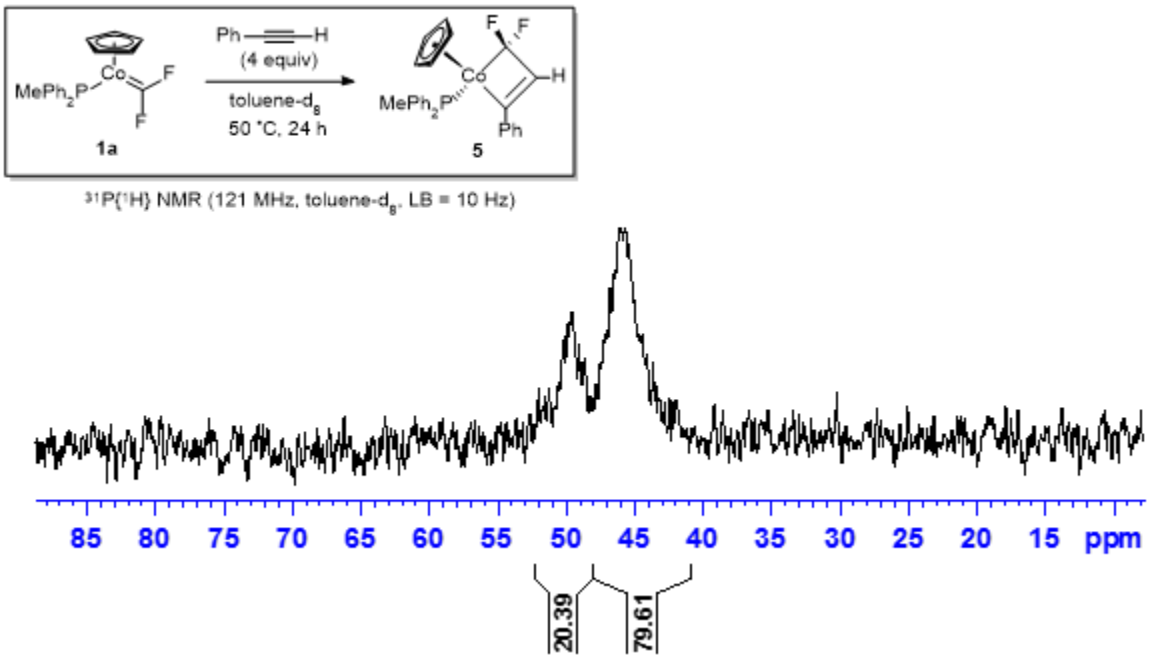

Figure S9. $^{31}P\{^{1}H\}$ NMR spectra for the reaction between **1a** (20 mg, 0.53 mmol) and PhC≡CH (22 mg, 0.22 mmol, 4 equiv) in toluene-d^8 (0.6 mL) at 50 °C for 24 hours, after filtration through celite.

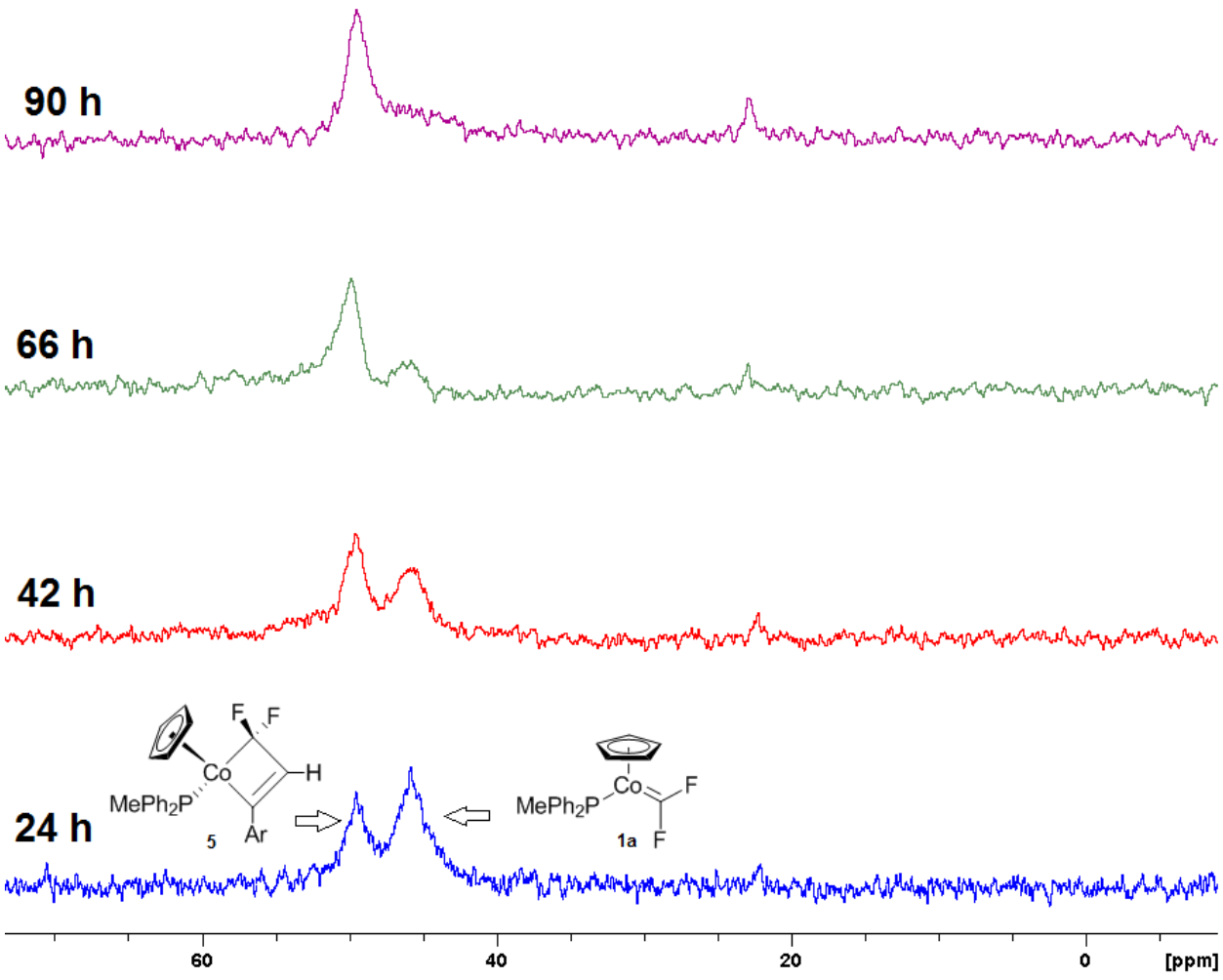

Figure S10. $^{31}P\{^{1}H\}$ NMR spectra for the reaction between **1a** (0.2 mmol) and PhC≡CH (5.0 mmol, 25 equiv) in toluene (2 mL) at 30 °C. Every 24 h, additional PhC≡CH (1.5 mmol) was added. The spectra have been processed with 20 Hz line broadening and intensities were modified to help illustrate the change in product concentration.

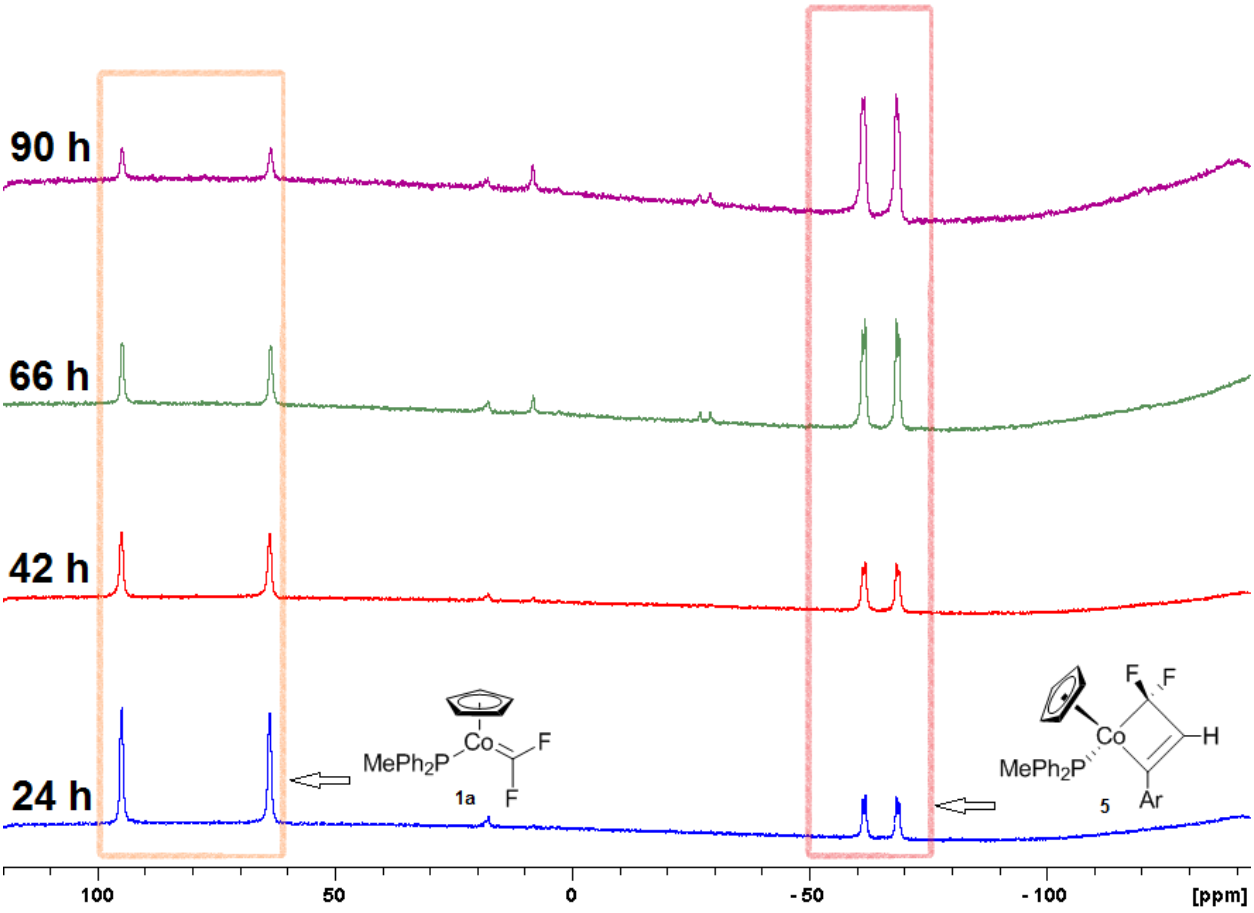

Figure S11. ^{19}F NMR spectra for the reaction between **1a** (0.2 mmol) and PhC≡CH (5.0 mmol, 25 equiv) in toluene (2 mL) at 30 °C. Every 24 h, additional PhC≡CH (1.5 mmol) was added. The spectra have been processed with 15 Hz line broadening and intensities were adjusted to illustrate the change in product concentration.

2. Kinetic Data

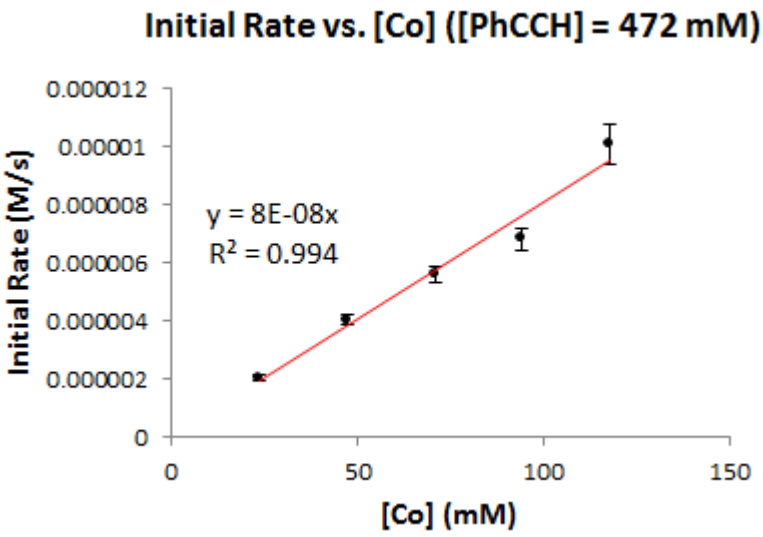

Figure S12. Initial rate of reaction between **1b** and PhC≡CH vs. [**1b**] in toluene:C_6D_6 (9:1) as a function of $[\mathbf{1b}]_0$, determined using ^{19}F NMR. Each data point is an average of two runs, collected at 23 °C.

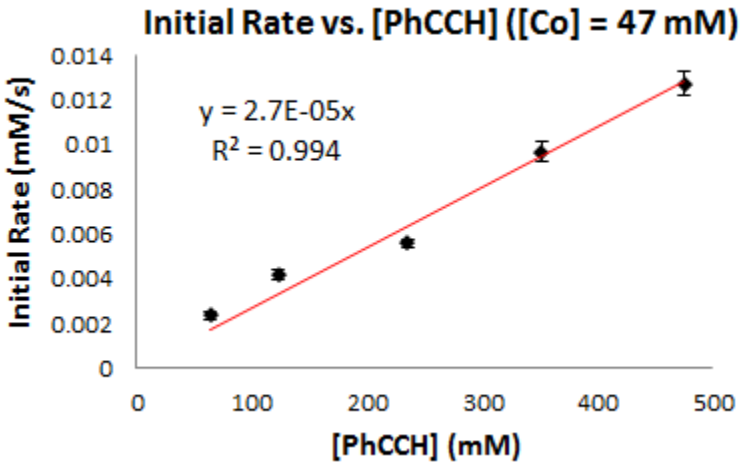

Figure S13. Initial rate of reaction between **1b** and PhC≡CH vs. [PhC≡CH] in toluene:C_6D_6 (9:1) as a function of $[PhC{\equiv}CH]_0$, determined using ^{19}F NMR. Each data point is an average of two runs, collected at 23 ºC.

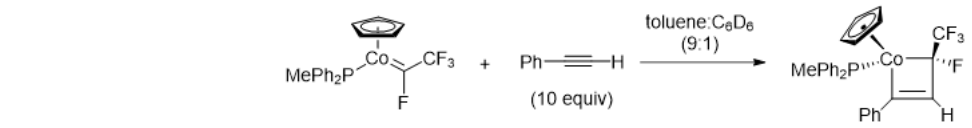

$$\ln\frac{[PhCCH][Co]_0}{[Co][PhCCH]_0} = k([PhCCH]_0 - [Co]_0)t$$

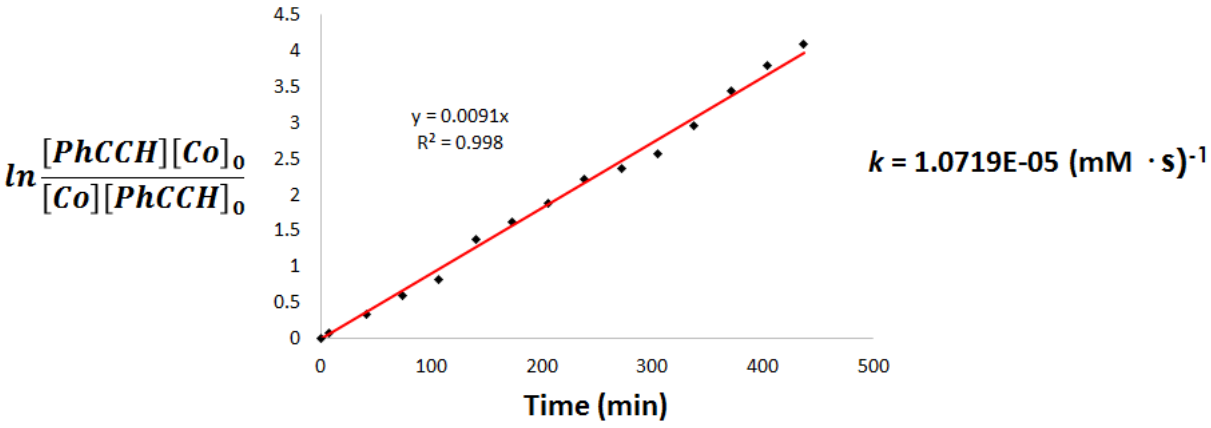

Figure S14. Reaction profile of **1b** and PhC≡CH fitted to the second order rate law.

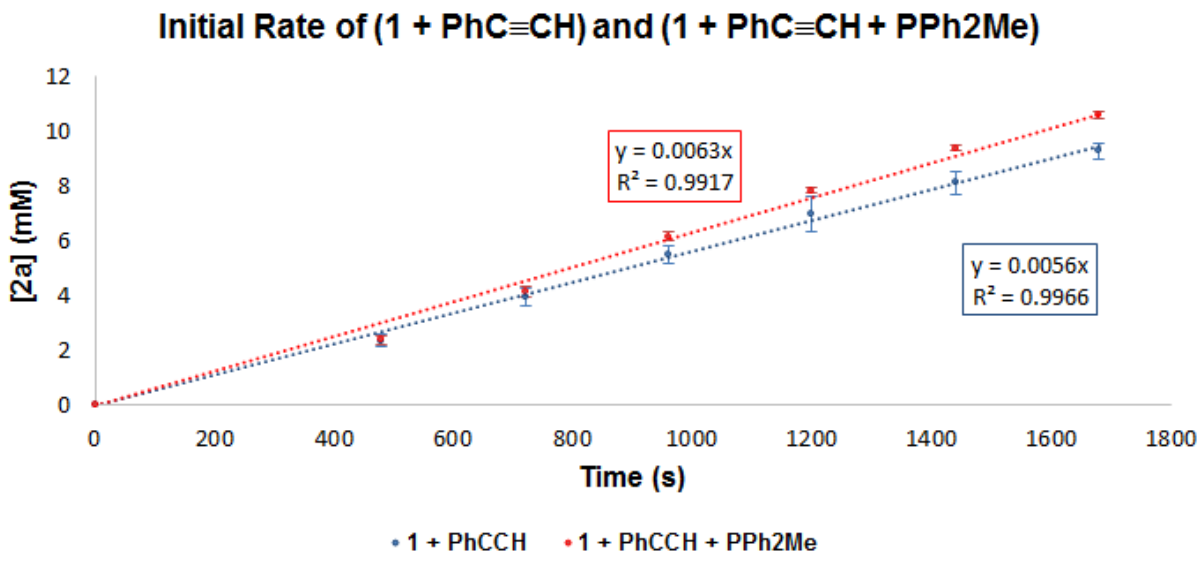

Figure S15. Kinetic profile of reaction for **1b** + PhC≡CH (5 equiv) and **1b** + PhC≡CH (5 equiv) + PPh_2Me (3.8 equiv), at 40 ºC.

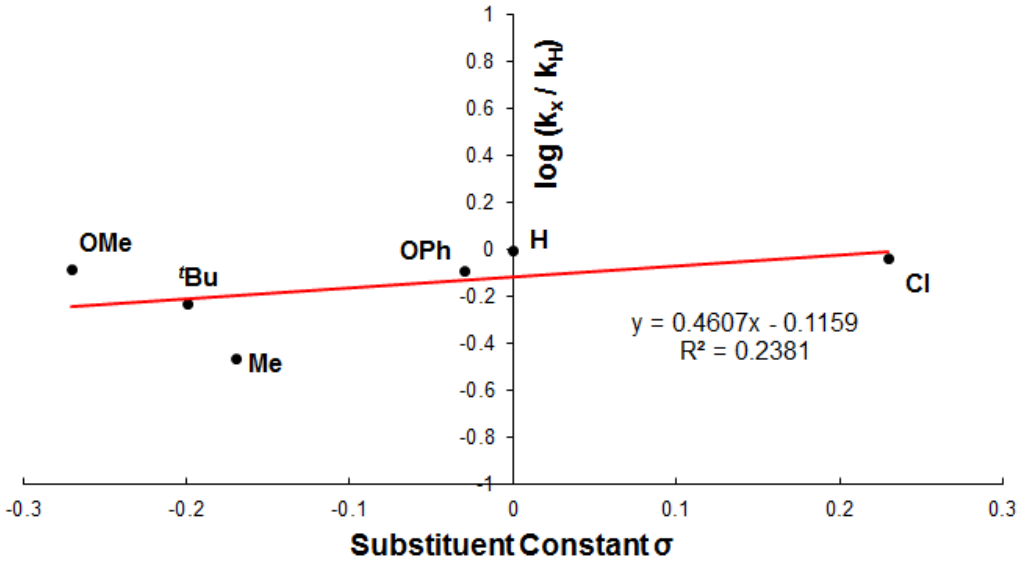

Figure S16. Hammett plot (σ) for reaction between **1b** and 4-X-PhC≡CH at 25 ºC.

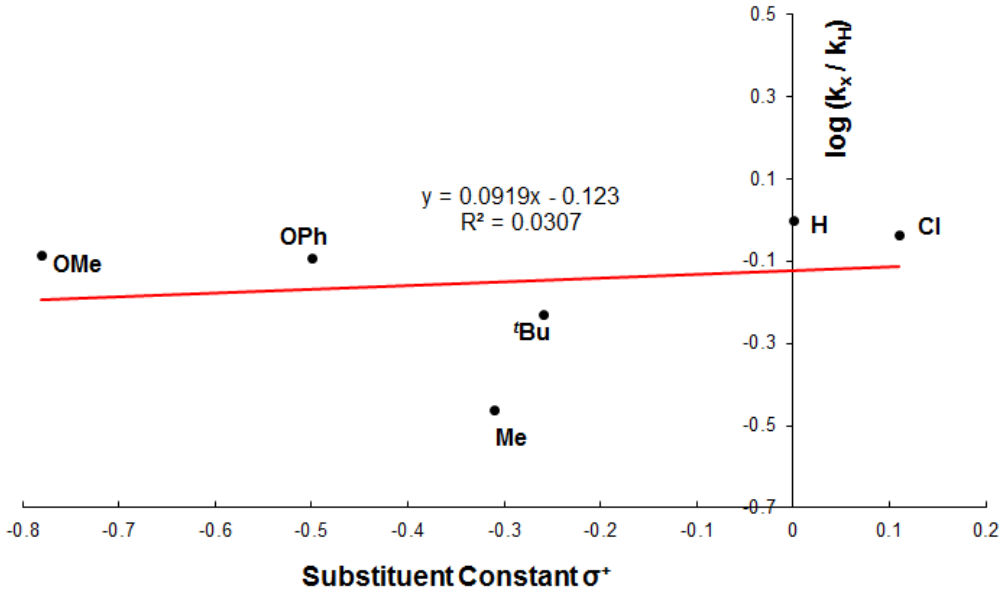

Figure S17. Hammett plot (σ^+) for reaction between **1b** and 4-X-PhC≡CH at 25 ºC.

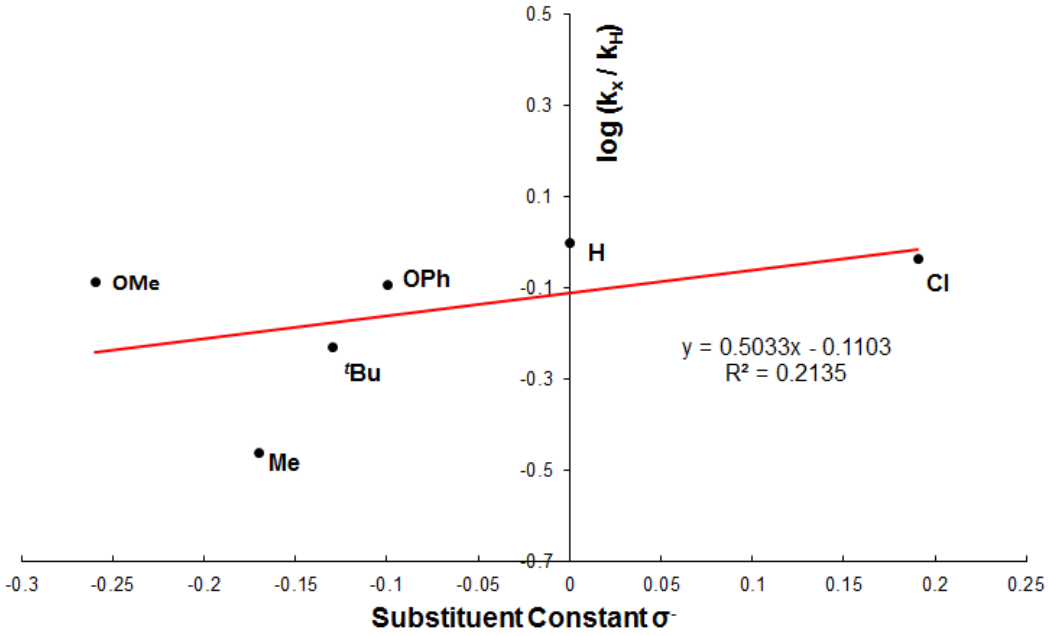

Figure S18. Hammett plot (σ^-) for reaction between **1b** and 4-X-PhC≡CH at 25 ºC.

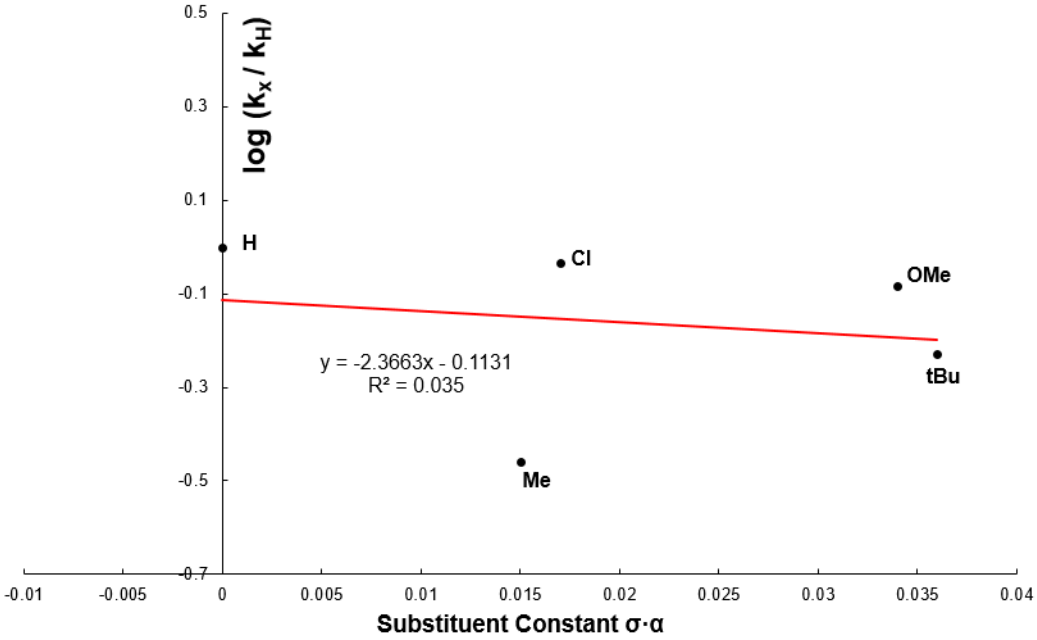

Figure S19. Hammett plot (σ^{α}) for reaction between **1b** and 4-X-PhC≡CH at 25 ºC.

3. NMR Spectra for Isolated Compounds

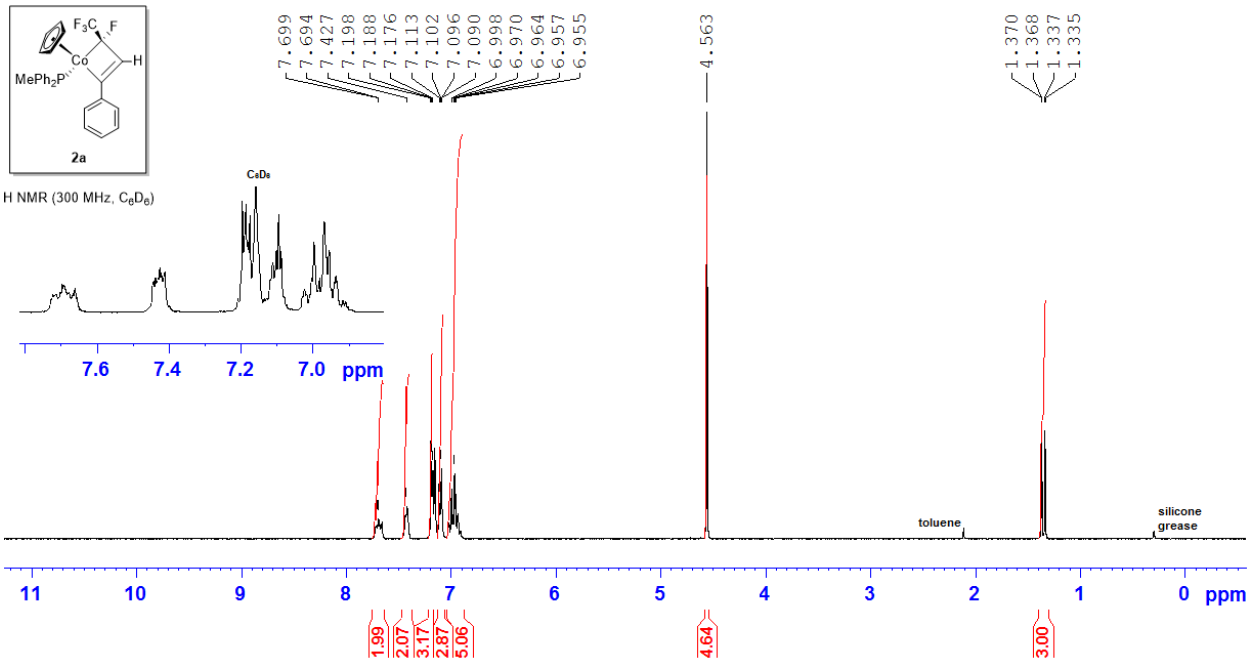

Figure S20. ^{1}H NMR (300 MHz, C_6D_6) spectrum of **2a**.

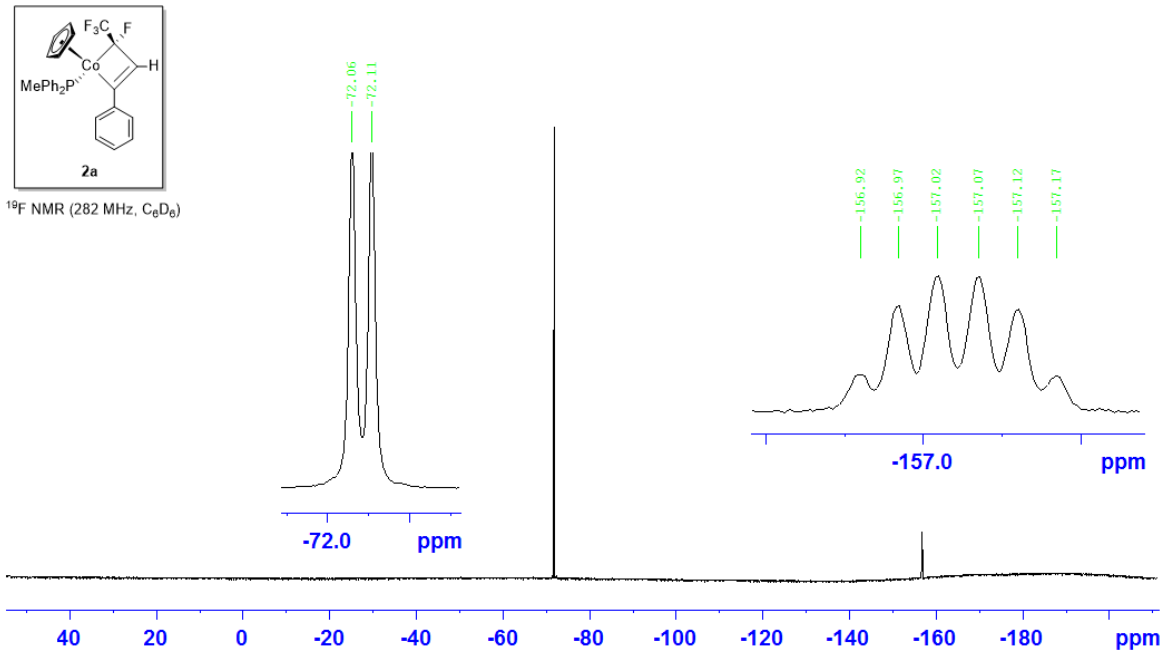

Figure S21. ^{19}F NMR (282 MHz, C_6D_6) spectrum of **2a**.

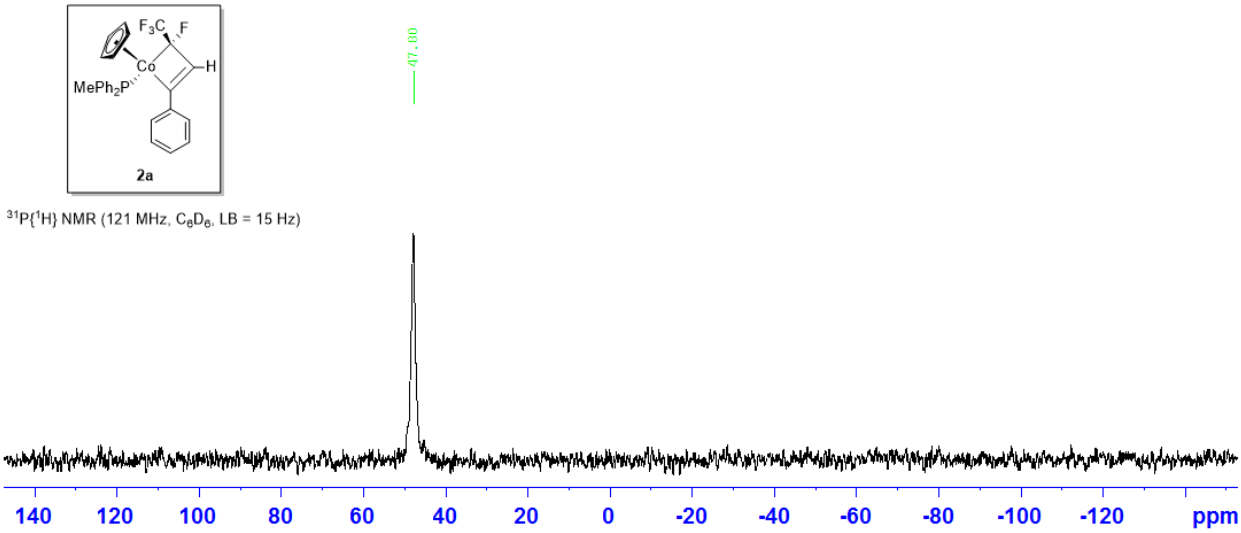

Figure S22. $^{31}P\{^{1}H\}$ NMR (121 MHz, C_6D_6) spectrum of **2a**.

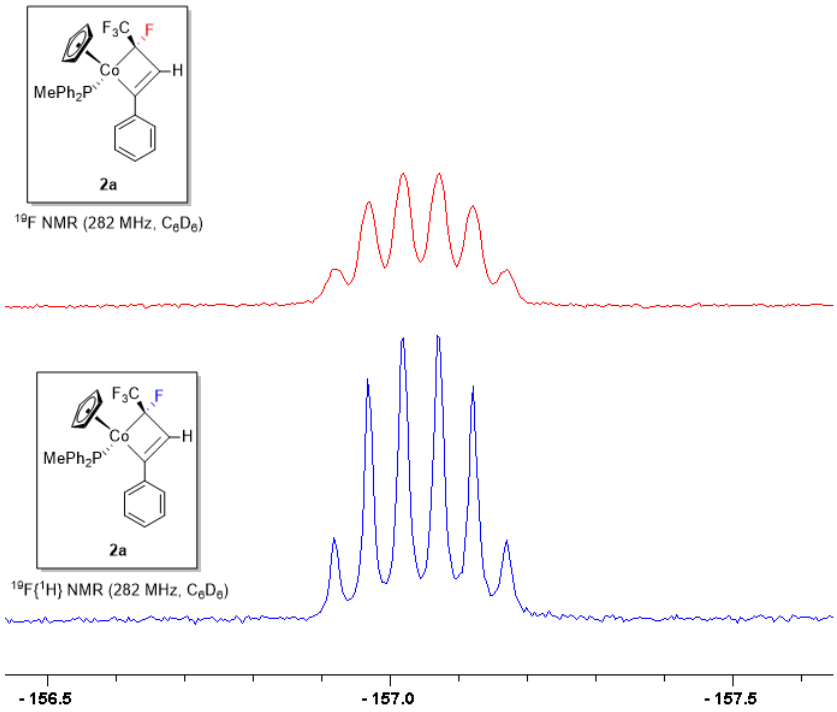

Figure S23. Overlay of the signals for the α fluorine in the ^{19}F and $^{19}F\{^{1}H\}$ NMR spectra of **2a**.

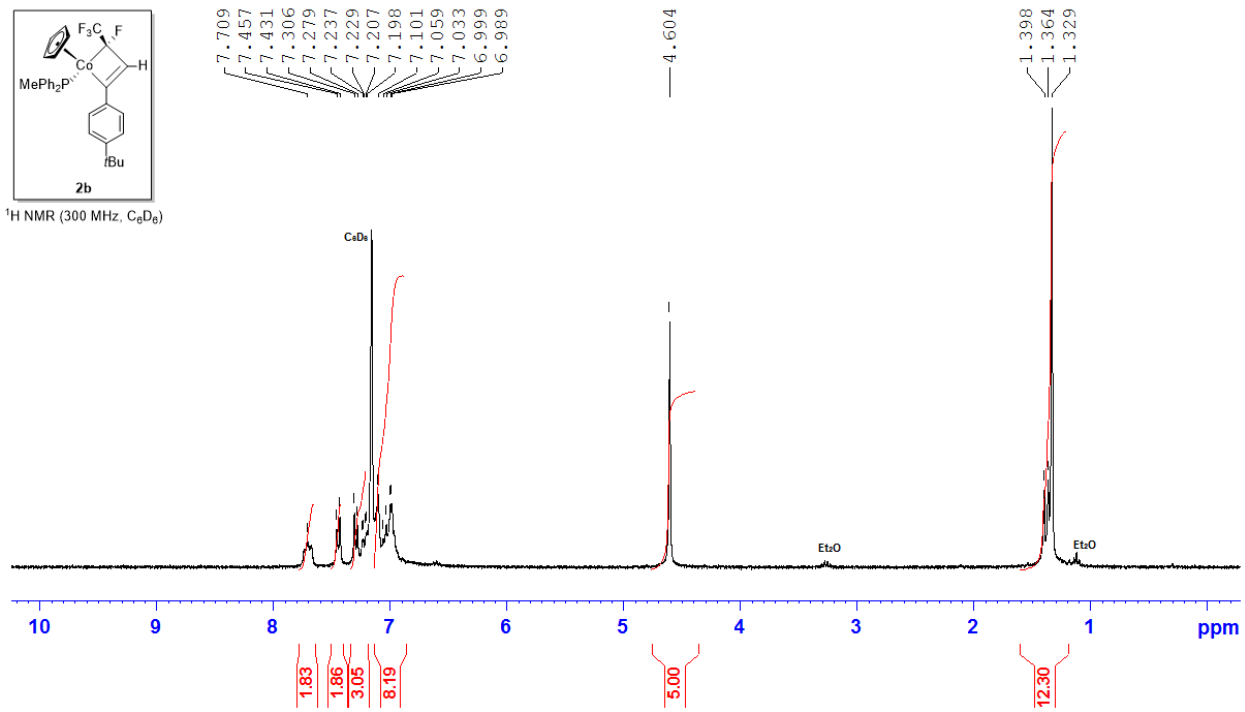

Figure S24. ^{1}H NMR (300 MHz, C_6D_6) spectrum of **2b**

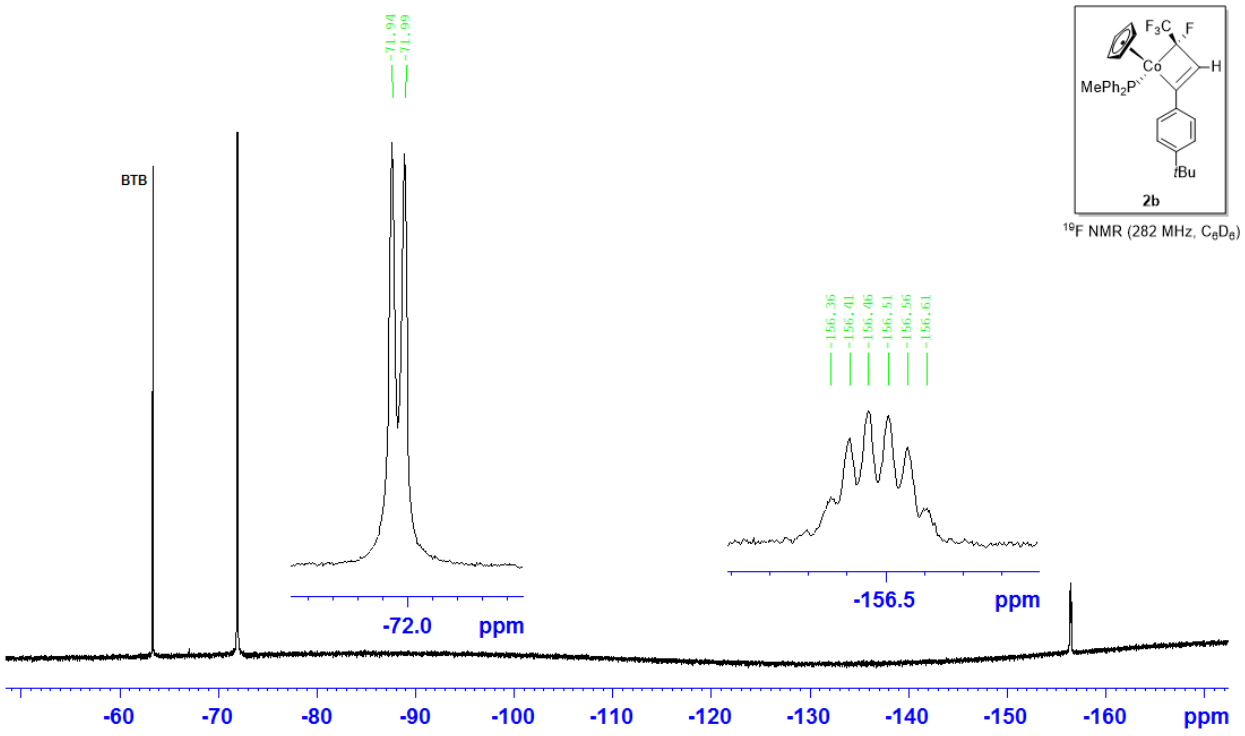

Figure S25. ^{19}F NMR (282 MHz, C_6D_6) spectrum of **2b**.

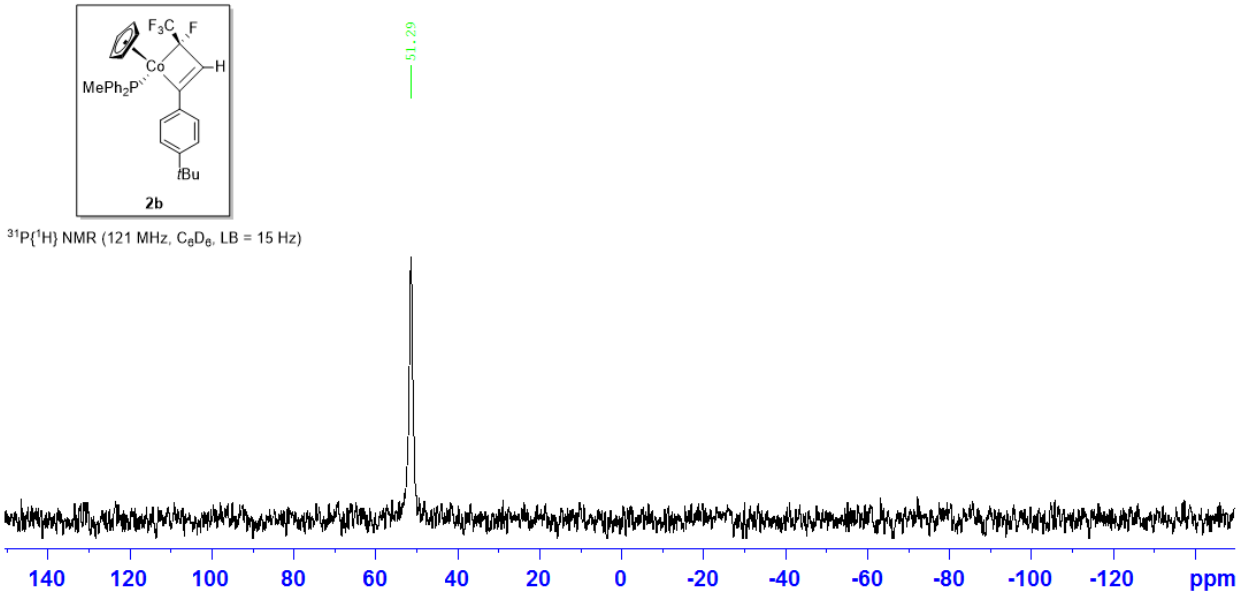

Figure S26. $^{31}P\{^{1}H\}$ NMR (121 MHz, C_6D_6) spectrum of **2b**.

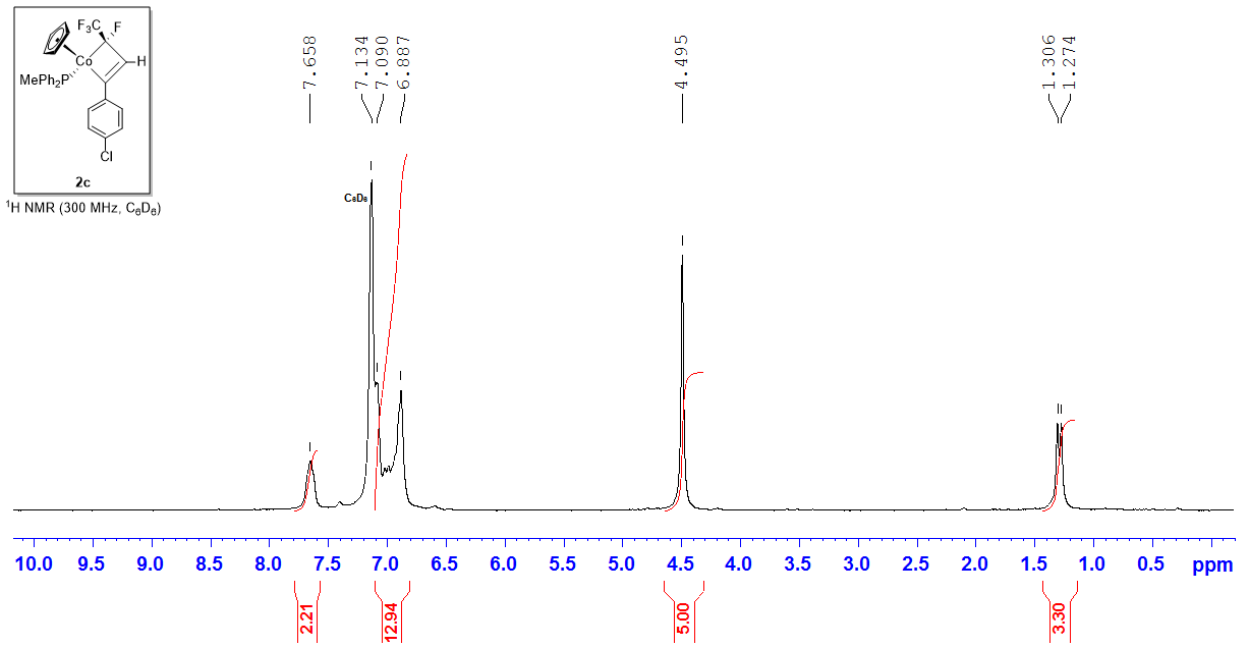

Figure S27. ^{1}H NMR (300 MHz, C_6D_6) spectrum of **2c**.

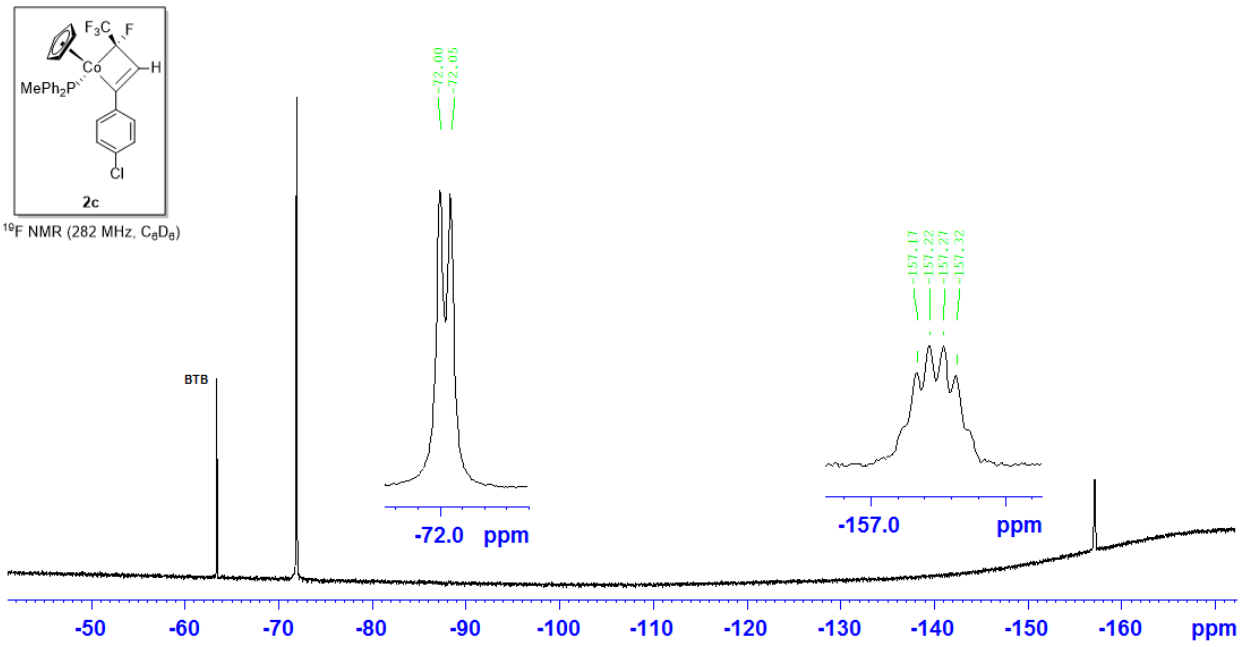

Figure S28. ^{19}F NMR (282 MHz, C_6D_6) spectrum of **2c**.

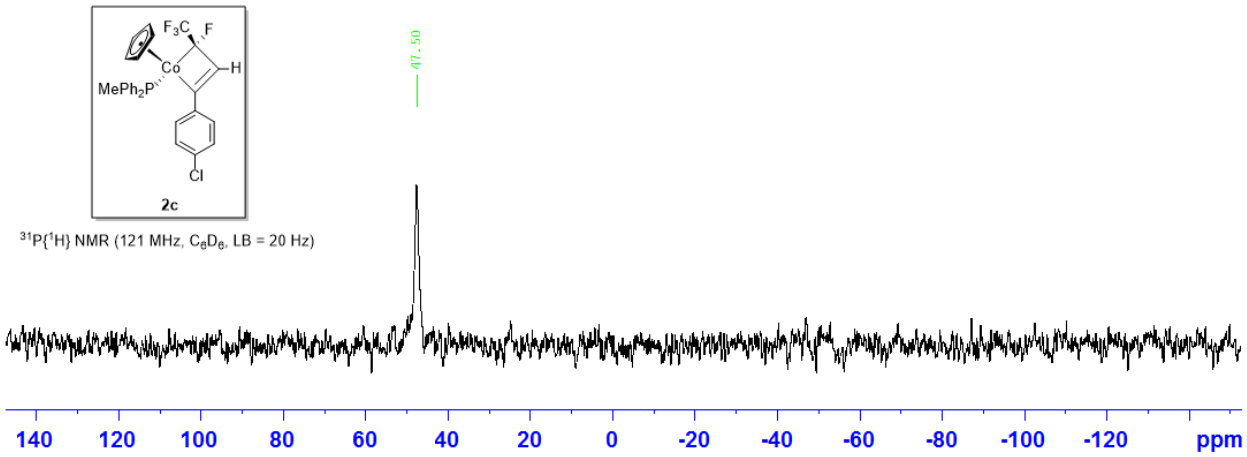

Figure S29. $^{31}P\{^1H\}$ NMR (121 MHz, C_6D_6) spectrum of **2c**.

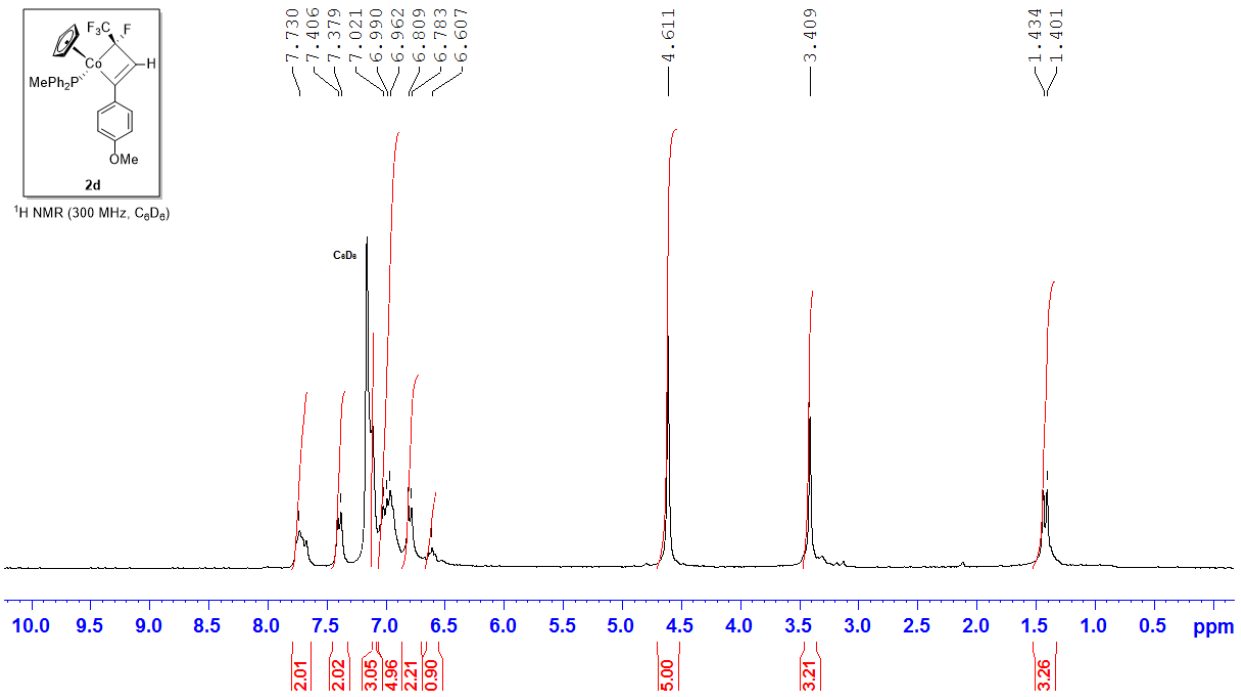

Figure S30. ^{1}H NMR (300 MHz, C_6D_6) spectrum of **2d**.

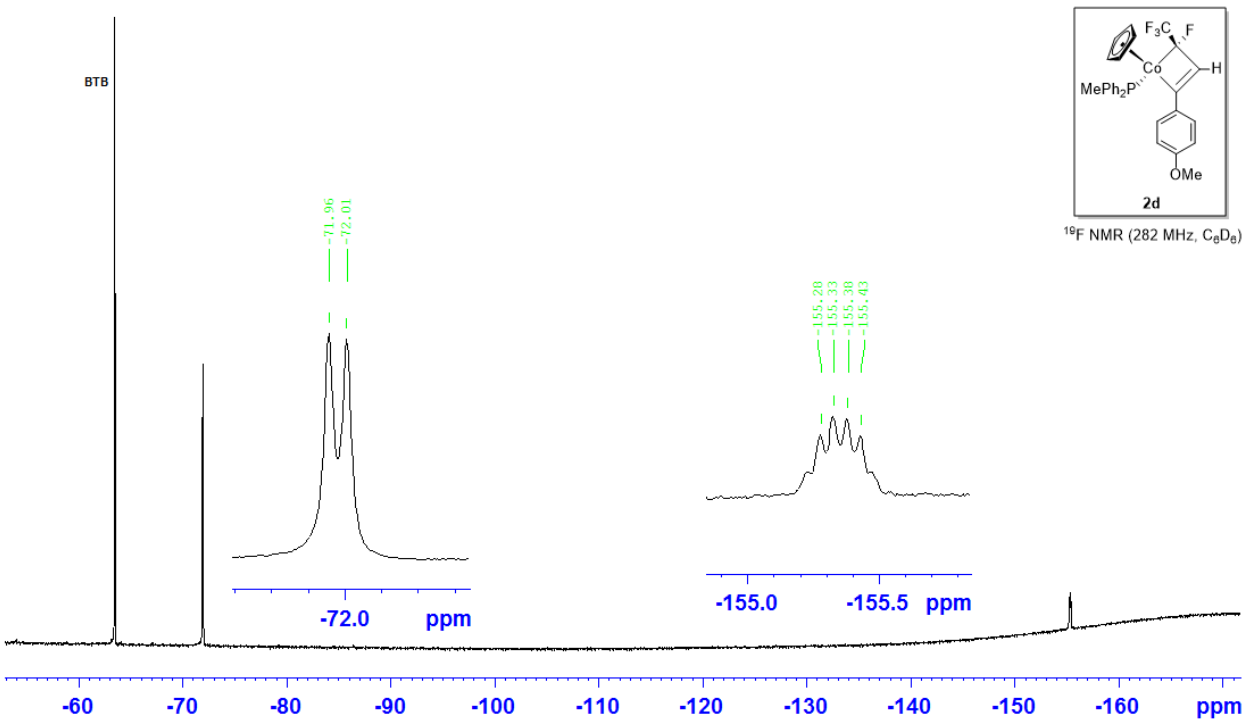

Figure S31. ^{19}F NMR (282 MHz, C_6D_6) spectrum of **2d**.

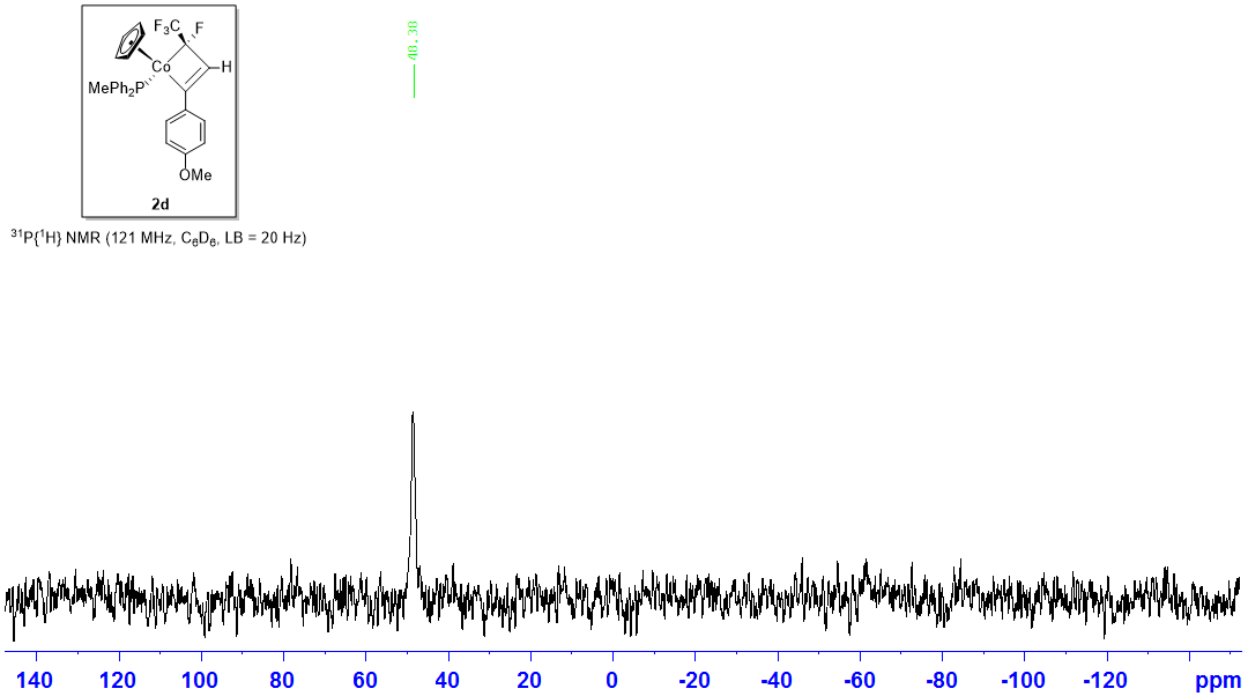

Figure S32. $^{31}P\{^{1}H\}$ NMR (121 MHz, C_6D_6) spectrum of **2d**.

4. UV-Vis Spectra

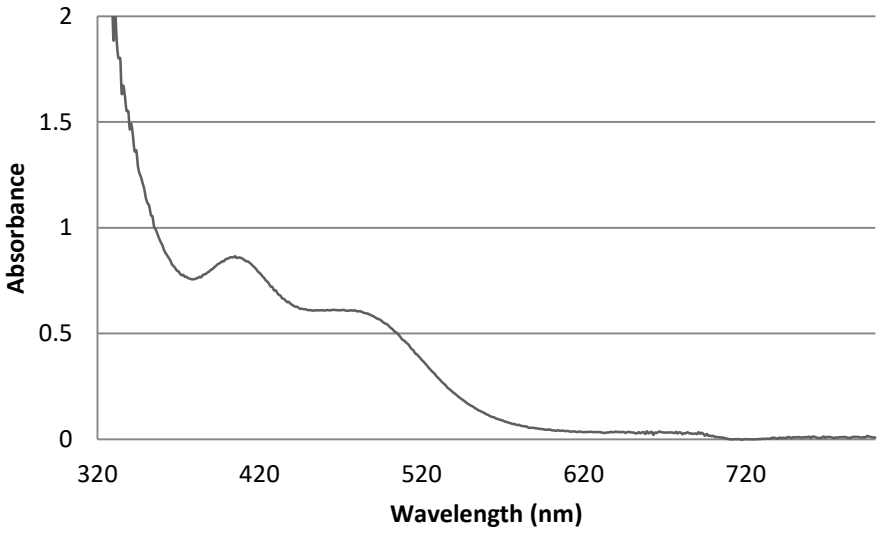

Figure S33. UV-Vis (1.0 mM in hexanes) spectrum of **2a.**

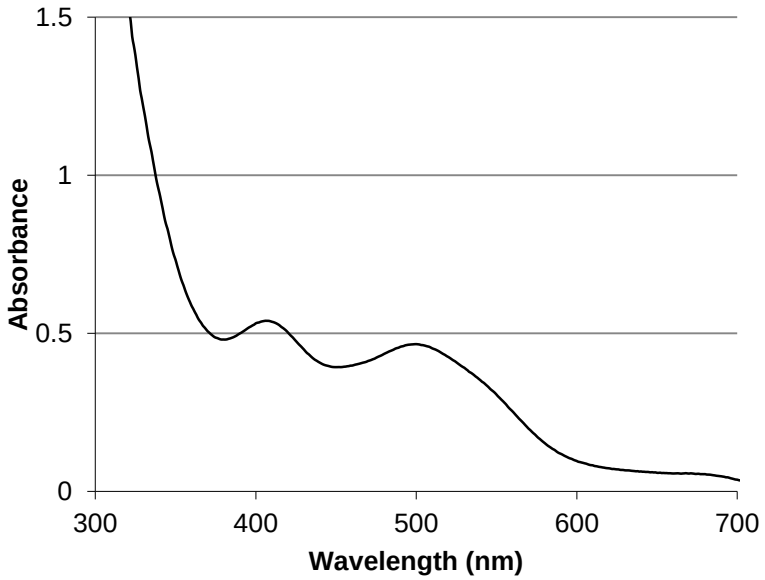

Figure S34. UV-Vis (0.25 mM in hexanes) spectrum of **2b.**

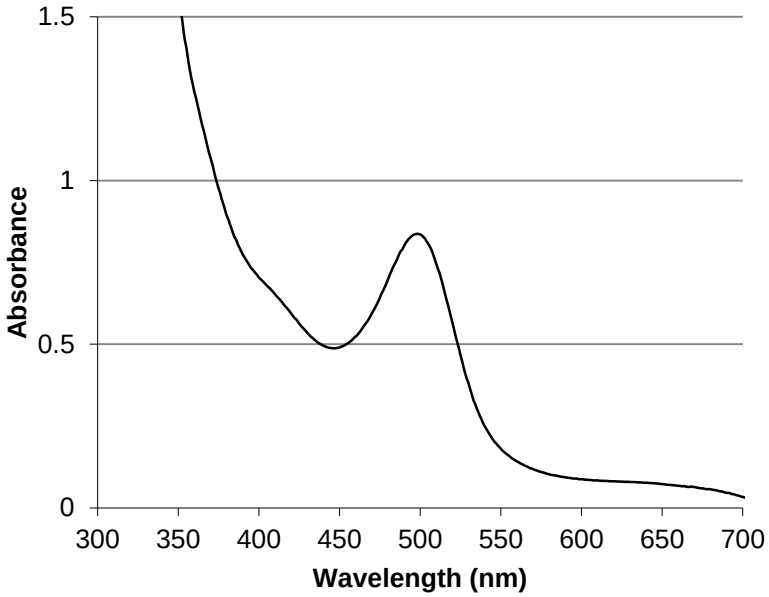

Figure S35. UV-Vis (0.25 mM in CH_2Cl_2) spectrum of **2c.**

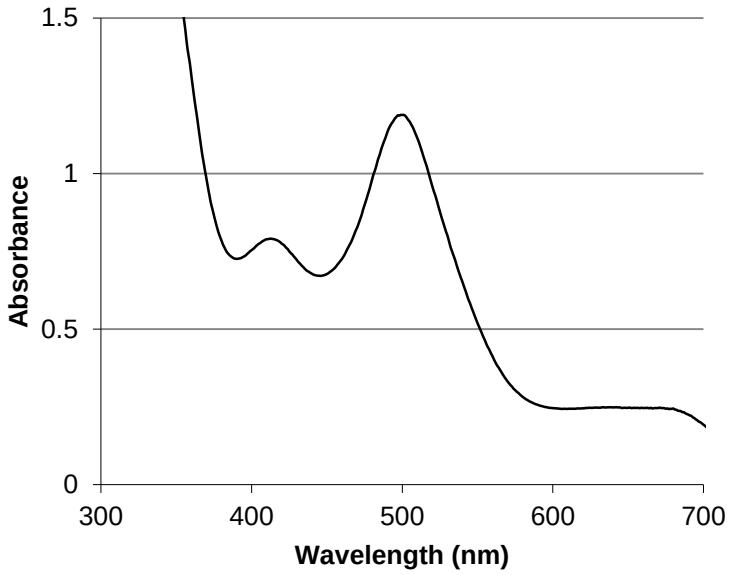

Figure S36. UV-Vis (0.25 mM in CH_2Cl_2) spectrum of **2d.**

5. X-ray Structure Data and Characterization

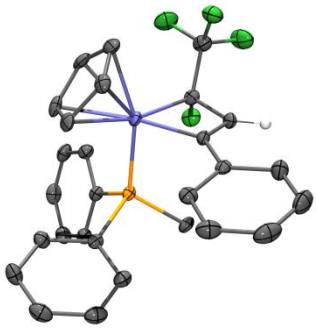

Table S1. Crystal data and structure refinement for tb074 (**2a**).

CCDC - 1544594

Identification code	tb074	
Empirical formula	C28 H24 Co F4 P	
Formula weight	526.37	
Temperature	200(2) K	
Wavelength	0.71073 A	
Crystal system, space group	Orthorhombic, P2(1)2(1)2(1)	
Unit cell dimensions	a = 10.9132(4) A	alpha = 90 deg.
	b = 14.5445(5) A	beta = 90 deg.
	c = 14.7938(5) A	gamma = 90 deg.
Volume	2348.18(14) A^3	
Z, Calculated density	4, 1.489 Mg/m^3	
Absorption coefficient	0.845 mm^-1	
F(000)	1080	
Crystal size	0.11 x 0.07 x 0.05 mm	
Theta range for data collection	1.96 to 28.33 deg.	
Limiting indices	-14<=h<=14, -18<=k<=19, -19<=l<=19	
Reflections collected / unique	41930 / 5816 [R(int) = 0.0671]	
Completeness to theta = 28.33	99.4 %	
Absorption correction	Semi-empirical from equivalents	
Max. and min. transmission	0.9589 and 0.9127	

Refinement method	Full-matrix least-squares on F^2
Data / restraints / parameters	5816 / 0 / 307
Goodness-of-fit on F^2	1.003
Final R indices [I>2sigma(I)]	R1 = 0.0423, wR2 = 0.0735
R indices (all data)	R1 = 0.0754, wR2 = 0.0826
Absolute structure parameter	-0.002(13)
Largest diff. peak and hole	0.579 and -0.689 e.A^-3

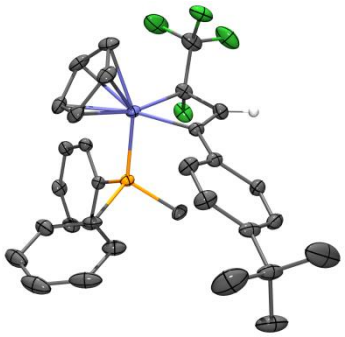

Table S2. Crystal data and structure refinement for tb103_5 (**2b**).

CCDC - 1544591		
Identification code	tb103_5	
Empirical formula	C32 H32 Co F4 P	
Formula weight	582.47	
Temperature	200(2) K	
Wavelength	0.71073 Å	
Crystal system	Monoclinic	
Space group	P 21/c	
Unit cell dimensions	a = 8.8048(2) Å	a= 90°.
	b = 23.3553(6) Å	b= 92.9792(13)°.
	c = 13.4791(3) Å	g = 90°.
Volume	2768.08(11) $Å^3$	
Z	4	
Density (calculated)	1.398 Mg/m^3	

Absorption coefficient	0.725 mm^{-1}
F(000)	1208
Crystal size	0.260 x 0.160 x 0.040 mm^3
Theta range for data collection	1.744 to 26.385°.
Index ranges	-11<=h<=10, 0<=k<=29, 0<=l<=16
Reflections collected	6691
Independent reflections	5611 [R(int) = ?]
Completeness to theta = 25.242°	99.1 %
Absorption correction	Semi-empirical from equivalents
Max. and min. transmission	0.972 and 0.834
Refinement method	Full-matrix least-squares on F^2
Data / restraints / parameters	5611 / 0 / 344
Goodness-of-fit on F^2	1.006
Final R indices [I>2sigma(I)]	R1 = 0.0409, wR2 = 0.0963
R indices (all data)	R1 = 0.0613, wR2 = 0.1085
Extinction coefficient	n/a
Largest diff. peak and hole	0.679 and -0.297 e.$Å^{-3}$

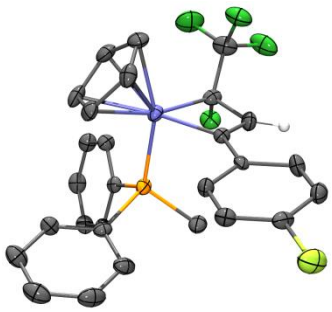

Table S3. Crystal data and structure refinement for tb112 (**2c**).

CCDC - 1544592

Identification code	tb112
Empirical formula	C28 H23 Cl Co F4 P

Formula weight	560.81	
Temperature	200(2) K	
Wavelength	0.71073 Å	
Crystal system	Orthorhombic	
Space group	P 21 21 21	
Unit cell dimensions	a = 10.7277(4) Å	a= 90°.
	b = 14.6920(5) Å	b= 90°.
	c = 15.5616(5) Å	g = 90°.
Volume	2452.69(15) $Å^3$	
Z	4	
Density (calculated)	1.519 Mg/m^3	
Absorption coefficient	0.920 mm^{-1}	
F(000)	1144	
Crystal size	0.350 x 0.250 x 0.120 mm^3	
Theta range for data collection	1.906 to 24.745°.	
Index ranges	-12<=h<=12, -15<=k<=17, -18<=l<=18	
Reflections collected	15833	
Independent reflections	4154 [R(int) = 0.0500]	
Completeness to theta = 25.242°	94.5 %	
Absorption correction	Semi-empirical from equivalents	
Max. and min. transmission	0.7451 and 0.6565	
Refinement method	Full-matrix least-squares on F^2	
Data / restraints / parameters	4154 / 0 / 317	
Goodness-of-fit on F^2	1.019	
Final R indices [I>2sigma(I)]	R1 = 0.0396, wR2 = 0.0621	
R indices (all data)	R1 = 0.0661, wR2 = 0.0692	
Absolute structure parameter	0.19(2)	
Extinction coefficient	n/a	
Largest diff. peak and hole	0.326 and -0.250 $e.Å^{-3}$	

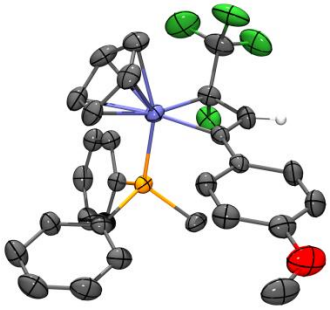

Table S4. Crystal data and structure refinement for tb118 (**2d**).

CCDC - 1544593		
Identification code	tb118	
Empirical formula	C29 H26 Co F4 O P	
Formula weight	556.40	
Temperature	200(2) K	
Wavelength	0.71073 Å	
Crystal system	Orthorhombic	
Space group	P 21 21 21	
Unit cell dimensions	a = 11.0059(15) Å	a= 90°.
	b = 14.572(2) Å	b= 90°.
	c = 16.051(2) Å	g = 90°.
Volume	2574.2(6) $Å^3$	
Z	4	
Density (calculated)	1.436 Mg/m^3	
Absorption coefficient	0.778 mm^{-1}	
F(000)	1144	
Crystal size	0.144 x 0.080 x 0.070 mm^3	
Theta range for data collection	1.888 to 28.395°.	
Index ranges	-13<=h<=14, -19<=k<=19, -21<=l<=21	
Reflections collected	40833	
Independent reflections	6391 [R(int) = 0.0608]	
Completeness to theta = 25.242°	99.7 %	

Absorption correction	Semi-empirical from equivalents
Max. and min. transmission	0.7457 and 0.6850
Refinement method	Full-matrix least-squares on F^2
Data / restraints / parameters	6391 / 2 / 335
Goodness-of-fit on F^2	0.982
Final R indices [I>2sigma(I)]	R1 = 0.0379, wR2 = 0.0744
R indices (all data)	R1 = 0.0769, wR2 = 0.0879
Absolute structure parameter	0.361(18)
Extinction coefficient	n/a
Largest diff. peak and hole	0.284 and -0.200 e.$Å^{-3}$

6. Computational Methods

All calculations were carried out using the Jaguar quantum mechanical program from Schrodinger.[1] Structures were optimized with the M06 functional[2] combined with the LACVP** basis set. For open-shell species, unrestricted UM06 was used. Solvation corrections were made using the Poisson-Boltzmann method[3] as implemented in Jaguar. Stationary point structures were confirmed to be minima or first-order saddle points by calculating the vibrational frequencies using analytical second derivatives.

Reported free energies are:

(U)M06/def2-TZVP(THF)//(U)M06/LACVP**(gas) at 298 K and 1 atm

$\Delta G = \Delta E_{(\text{def2-TZVP})} + \Delta G_{\text{solv(def2-TZVP)}} + \Delta E_{\text{ZPE(LACVP**)}} + \Delta U_{(\text{LACVP**})} + \text{nRT} - \text{T}\Delta S_{(\text{gas phase})}$.

$\Delta G_{\text{solv(def2-TZVP)}}$ free energy corrections were determined using the Poisson-Boltzmann implicit THF solvent model implemented in Jaguar.

For open-shell singlet species the Jaguar keyword IOSS=1 option was used to converge on a spin-polarized singlet energy. For the open-shell singlet intermediates the S^2 values were very close to 1.0. For transition states the S^2 values ranged from 0.5 to 0.8.

(U)M06/def2-TZVP(THF) spin-projected energies were found by

$E^{\text{SP}}_{\text{singlet}} = E_{\text{singlet}} + \varkappa(E_{\text{singlet}} - E_{\text{triplet}})$

$\varkappa = (\langle S^2\rangle \text{ and Energies}_{\text{singlet}}/\langle S^2\rangle_{\text{triplet}})/[1 - (\langle S^2\rangle_{\text{singlet}}/\langle S^2\rangle_{\text{triplet}})]$

Images were produced using CYLView.[4]

References.

(1) *Jaguar, versions 7.0-9.3*, Schrödinger, LLC, New York, NY: 2007-2016.

(2) (a) Zhao, Y.; Truhlar, D. G. *Theor. Chem. Acc.* 2008, *120*, 215-241; (b) Zhao, Y.; Truhlar, D. G. *Acc. Chem. Res.* 2008, *41*, 157-167.

(3) (a) Tannor, D. J.; Marten, B.; Murphy, R.; Friesner, R. A.; Sitkoff, D.; Nicholls, A.; Honig, B.; Ringnalda, M.; Goddard, W. A. *J. Am. Chem. Soc.* 1994, *116*, 11875-11882; (b) Marten, B.; Kim, K.; Cortis, C.; Friesner, R. A.; Murphy, R. B.; Ringnalda, M. N.; Sitkoff, D.; Honig, B. *J. Phys. Chem.* 1996, *100*, 11775-11788.

(4) Legault, C. Y. *CYLview, 1.0b*, Université de Sherbrooke: Université de Sherbrooke, 2009

Appendix B – Supplementary Information for Chapter 6

Table of Contents

I. Supplementary High-Throughput Experiment Data

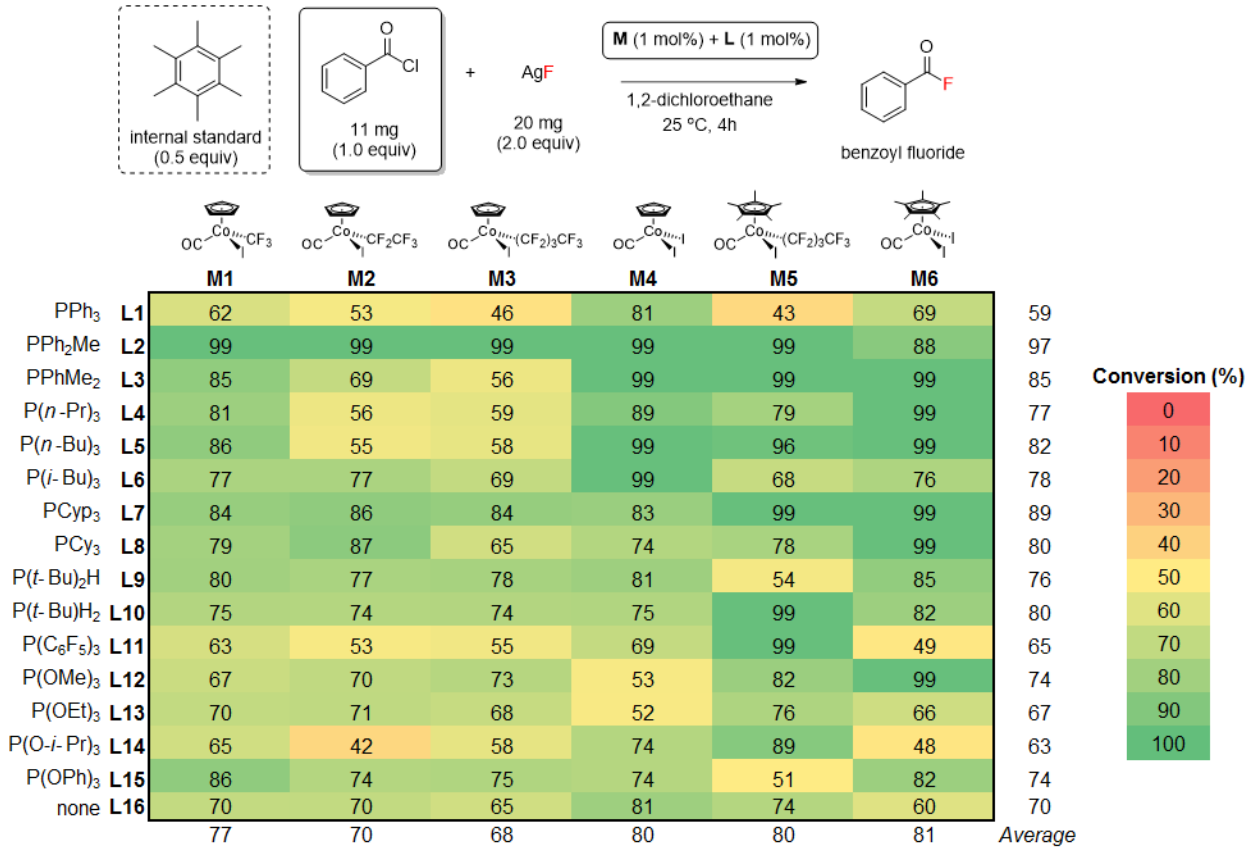

Figure S1. Conversion of **1a** during high-throughput experiment.

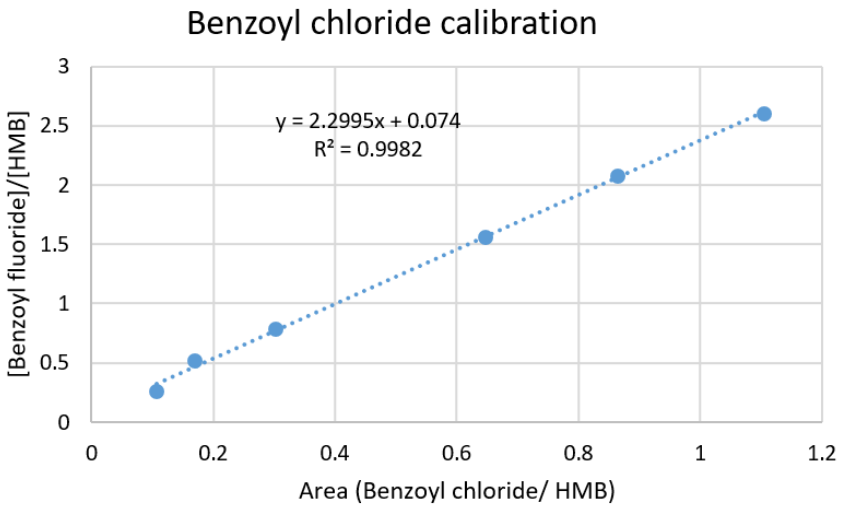

Figure S2. GC-FID calibration curve for **1a** and HMB.

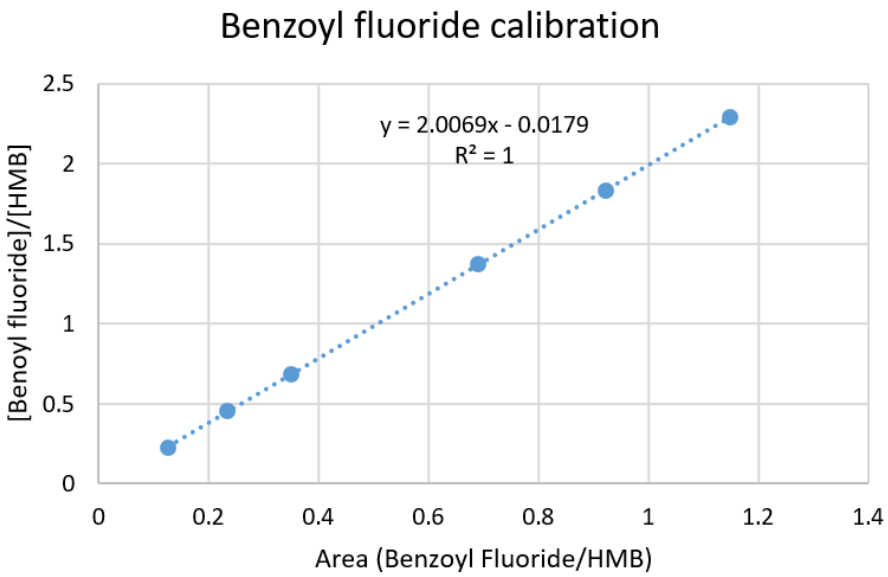

Figure S3. GC-FID calibration curve for **2a** and HMB.

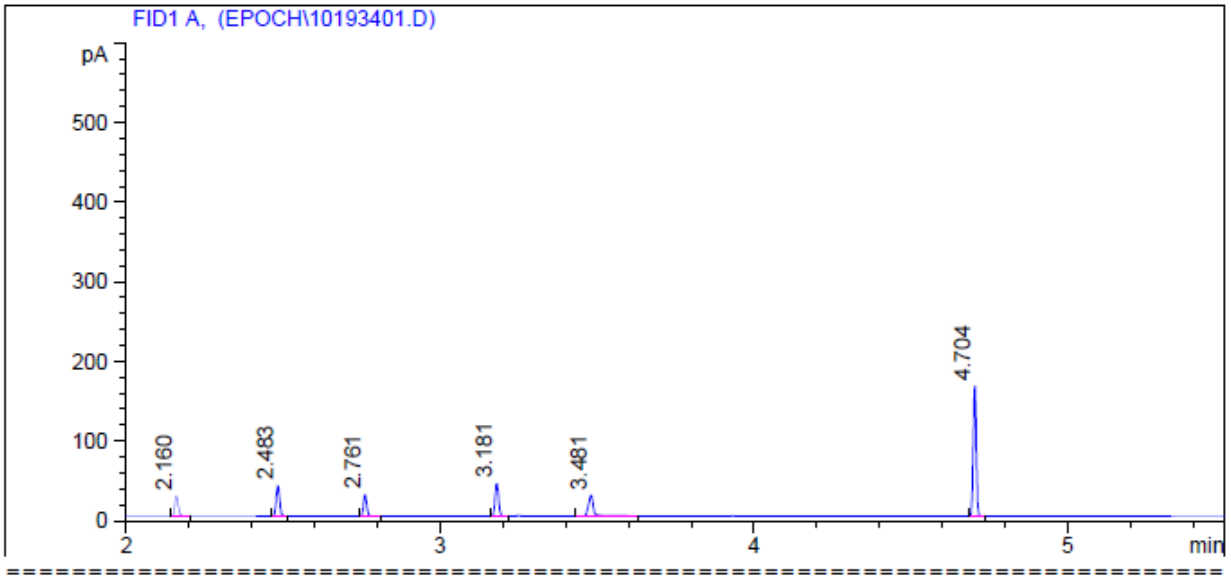

Signal 1: FID1 A,

Peak #	RT [min]	Name	Area	Area %	Amount
1	2.160		20.516	15.358	0.00000
2	2.483	Benzoyl fluoride	29.667	22.208	0.00000
3	2.761		19.730	14.770	0.00000
4	3.181	Benzoyl chloride	32.971	24.681	0.00228
5	3.481		30.704	22.984	0.00000
6	0.000	Hexamethylbenzene_BF	0.000	0.000	0.00000
7	4.704	Hexamethylbenzene_BC	111.573	83.520	0.00315

Figure S4. Example of GC-FID chromatogram for high-throughput experiment.

II. NMR/IR Spectra of Isolated Compounds

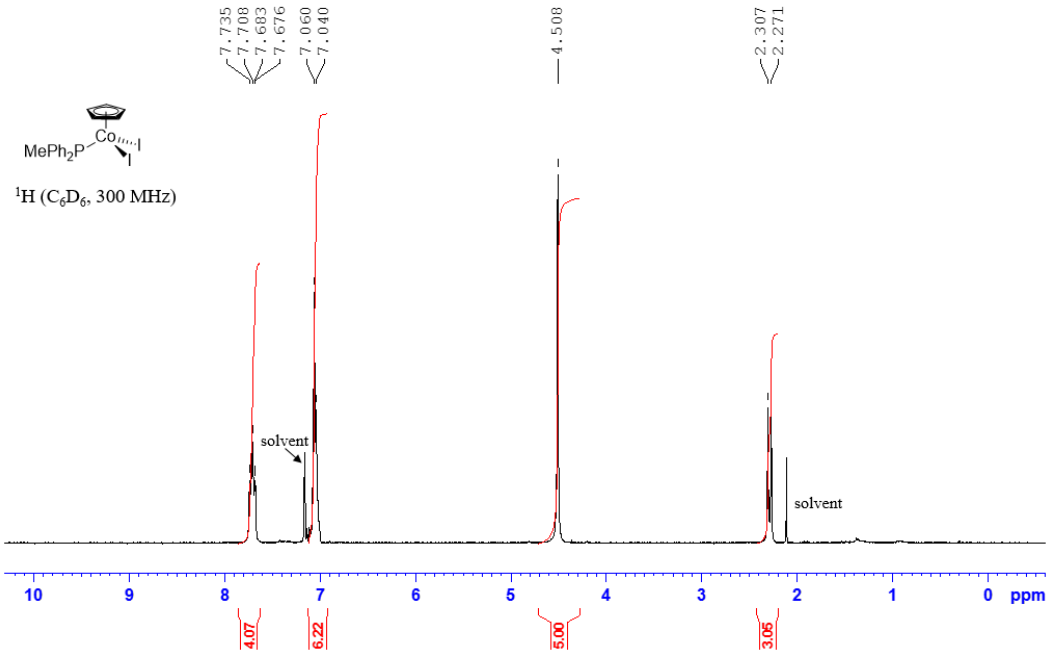

Figure S5. ^{1}H NMR spectrum of $CpCo(I)_2(PPh_2Me)$.

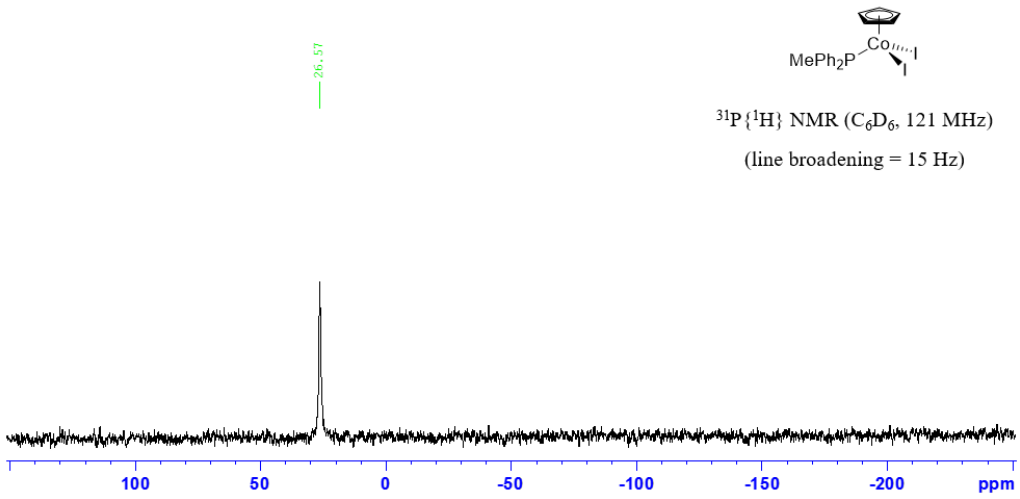

Figure S6. $^{31}P\{^{1}H\}$ NMR spectrum of $CpCo(I)_2(PPh_2Me)$.

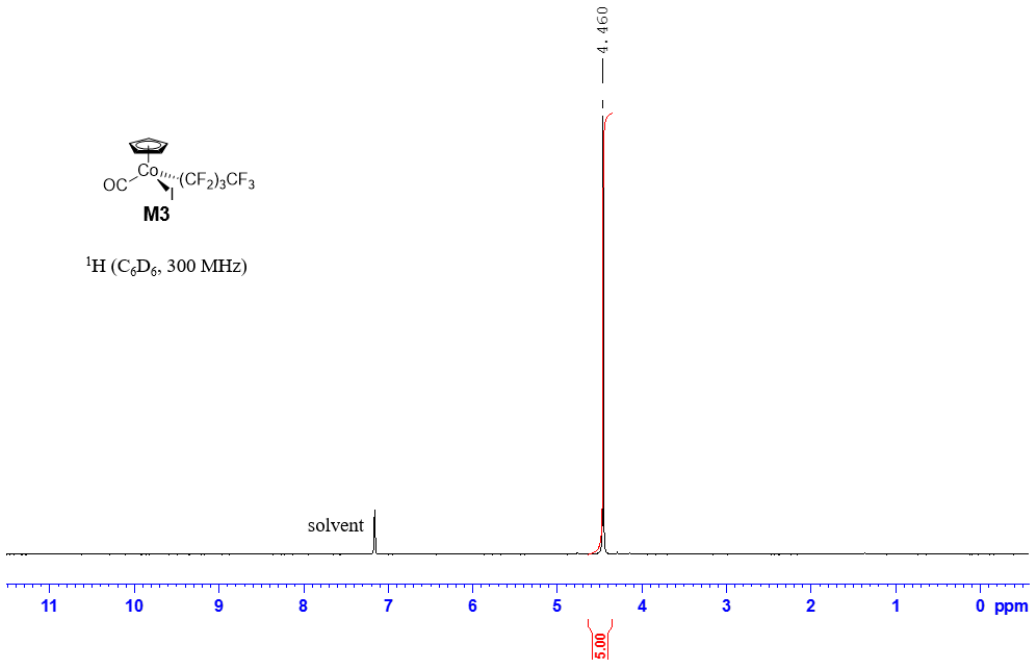

Figure S7. ^{1}H NMR spectrum of CpCo(I)(CO)($CF_2CF_2CF_2CF_3$) (**M3**).

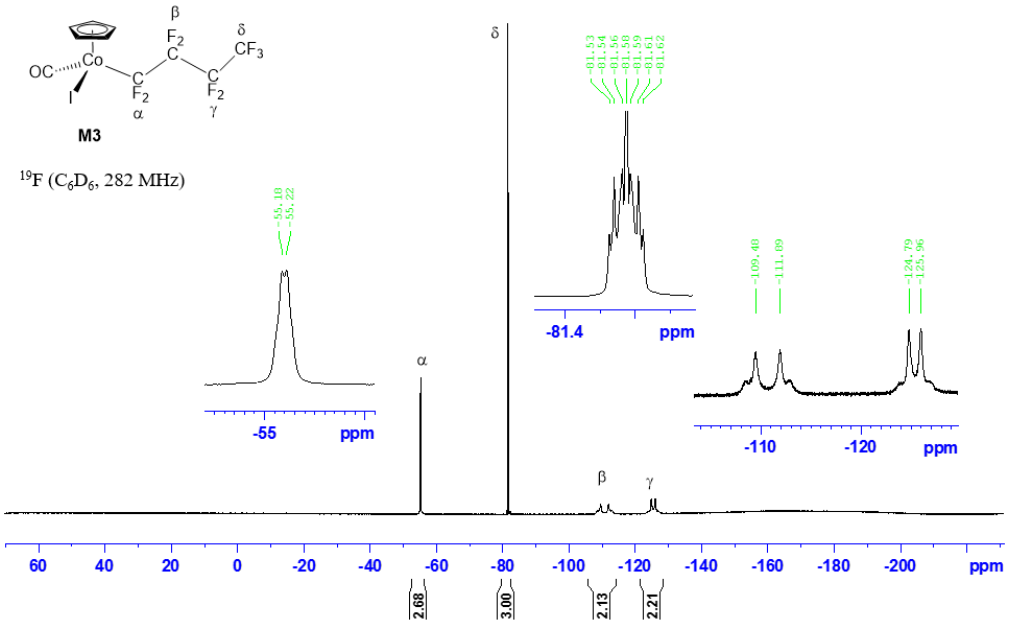

Figure S8. ^{19}F NMR spectrum of CpCo(I)(CO)($CF_2CF_2CF_2CF_3$) (**M3**).

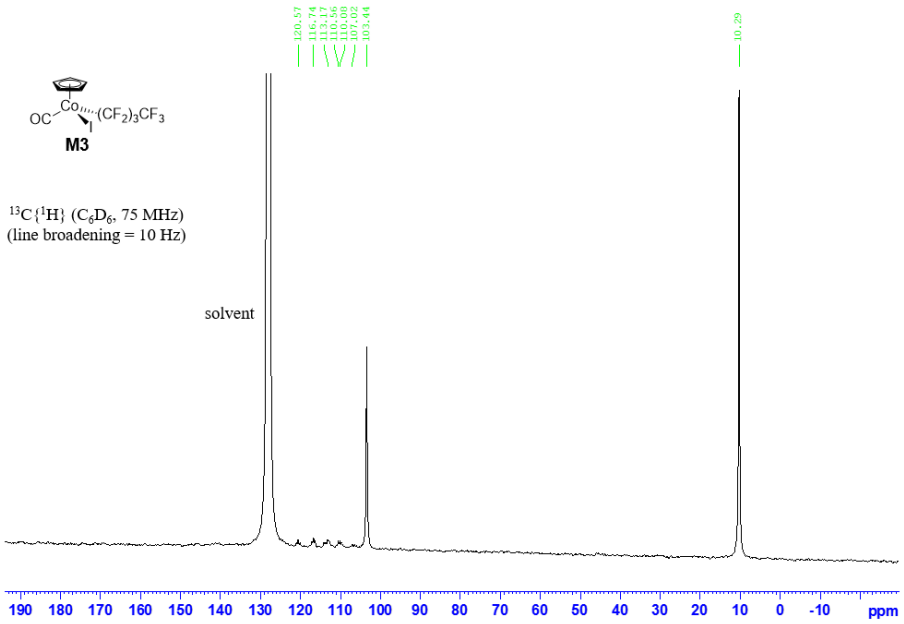

Figure S9. $^{13}C\{^{1}H\}$ NMR spectrum of $CpCo(I)(CO)(CF_2CF_2CF_2CF_3)$ (**M3**).

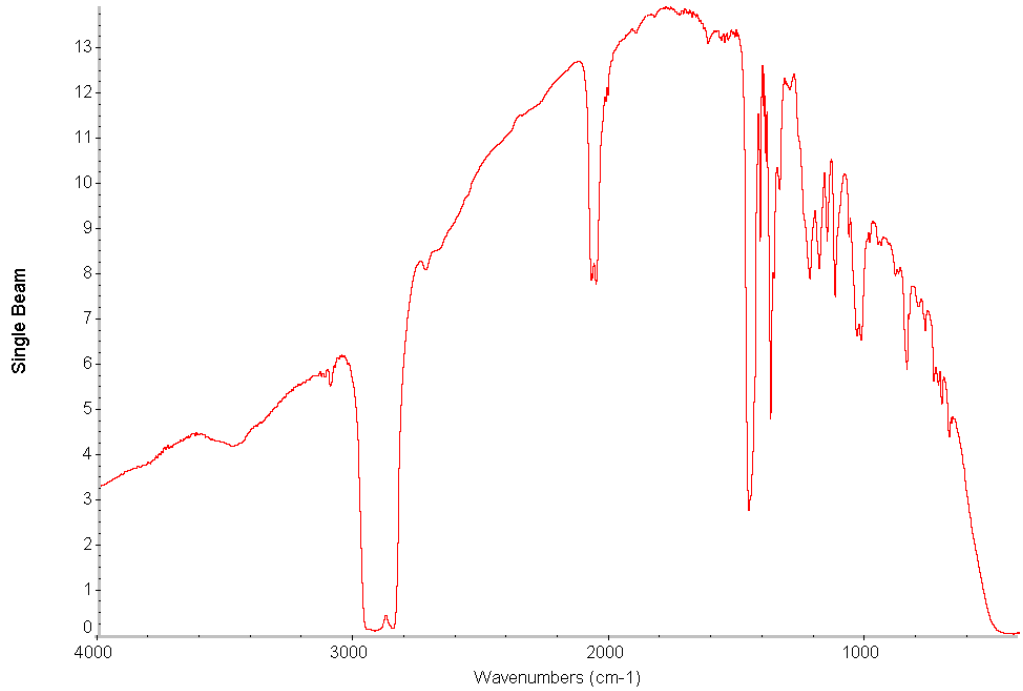

Fig S10. IR spectrum of $CpCo(I)(CO)(CF_2CF_2CF_2CF_3)$ (**M3**).

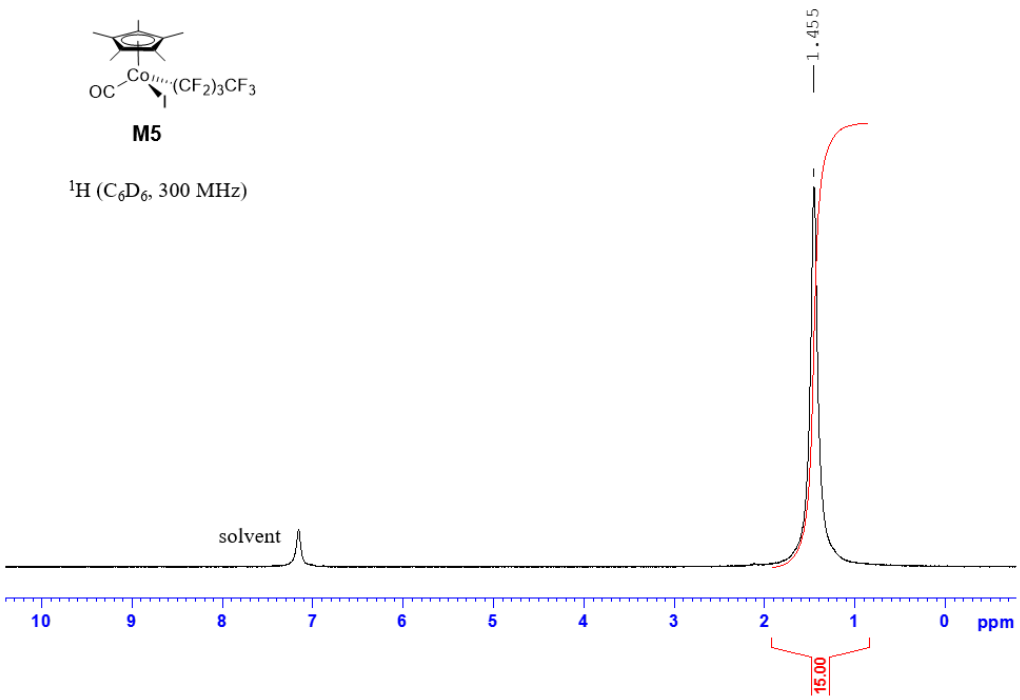

Figure S11. ^{1}H NMR spectrum of Cp*Co(I)(CO)($CF_2CF_2CF_2CF_3$) (**M5**).

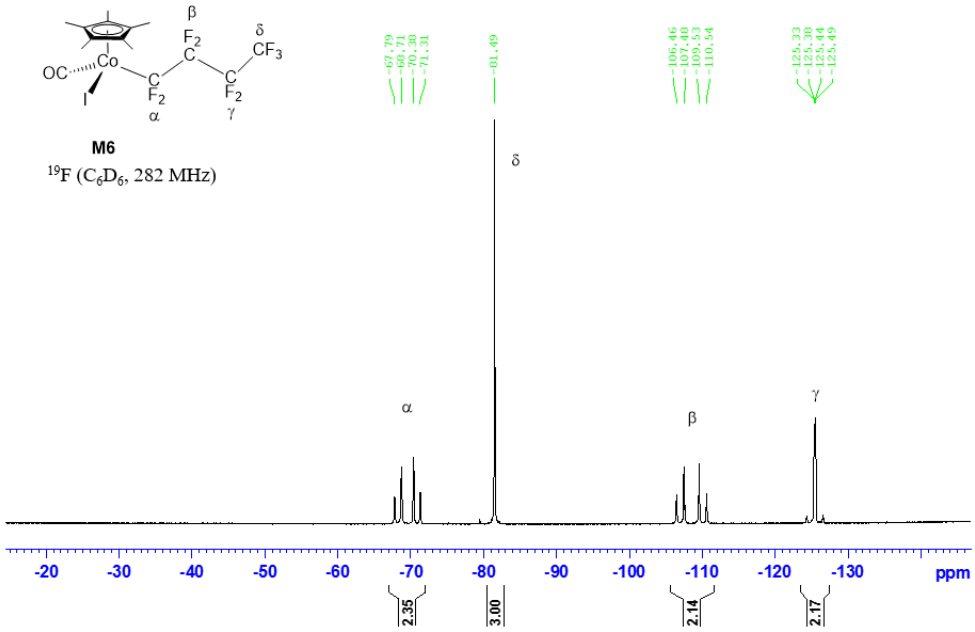

Figure S12. ^{19}F NMR spectrum of Cp*Co(I)(CO)($CF_2CF_2CF_2CF_3$) (**M5**).

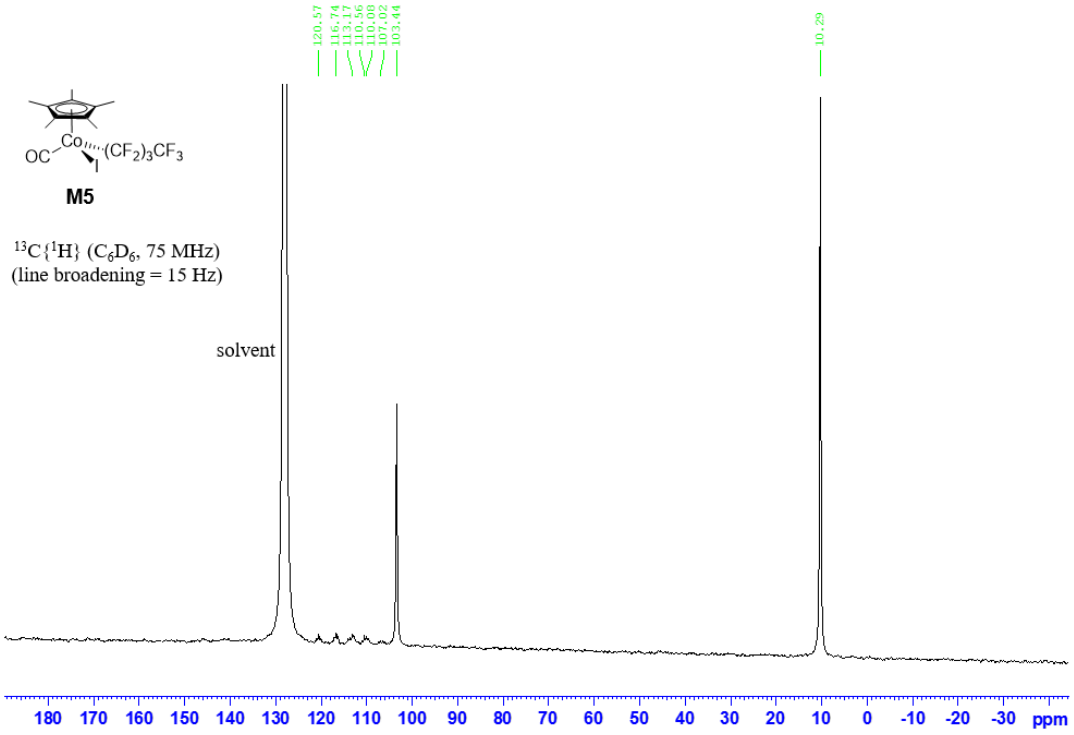

Figure S13. $^{13}C\{^{1}H\}$ NMR spectrum of Cp*Co(I)(CO)($CF_2CF_2CF_2CF_3$) (**M5**).

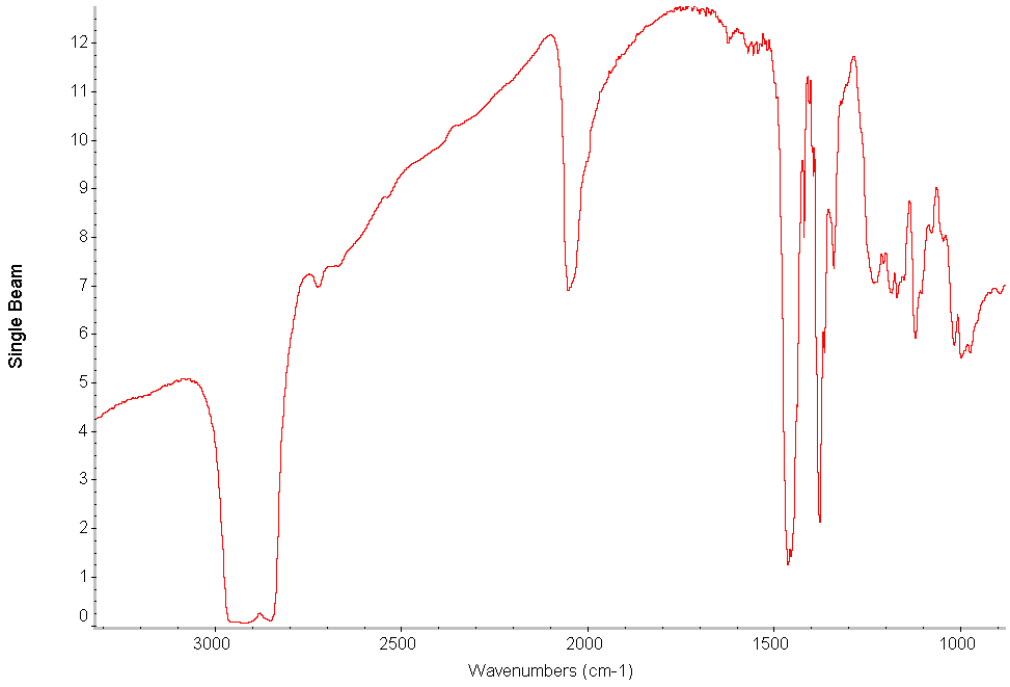

Fig S14. IR spectrum of Cp*Co(I)(CO)($CF_2CF_2CF_2CF_3$) (**M5**).

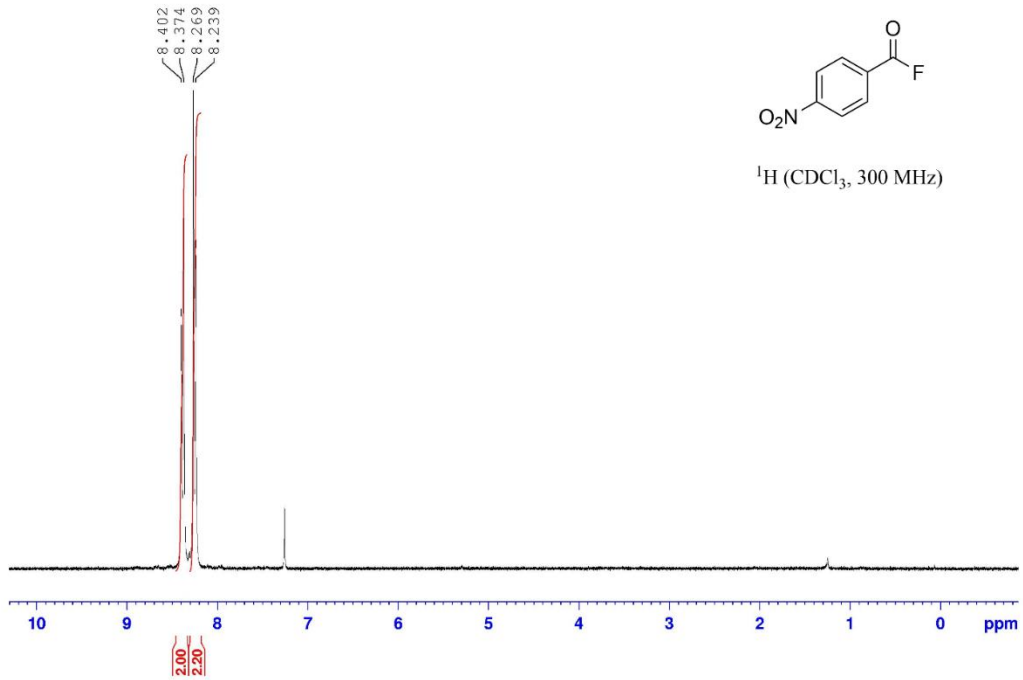

Figure S15. ^{1}H NMR spectrum of 4-nitrobenzoyl fluoride (**2b**).

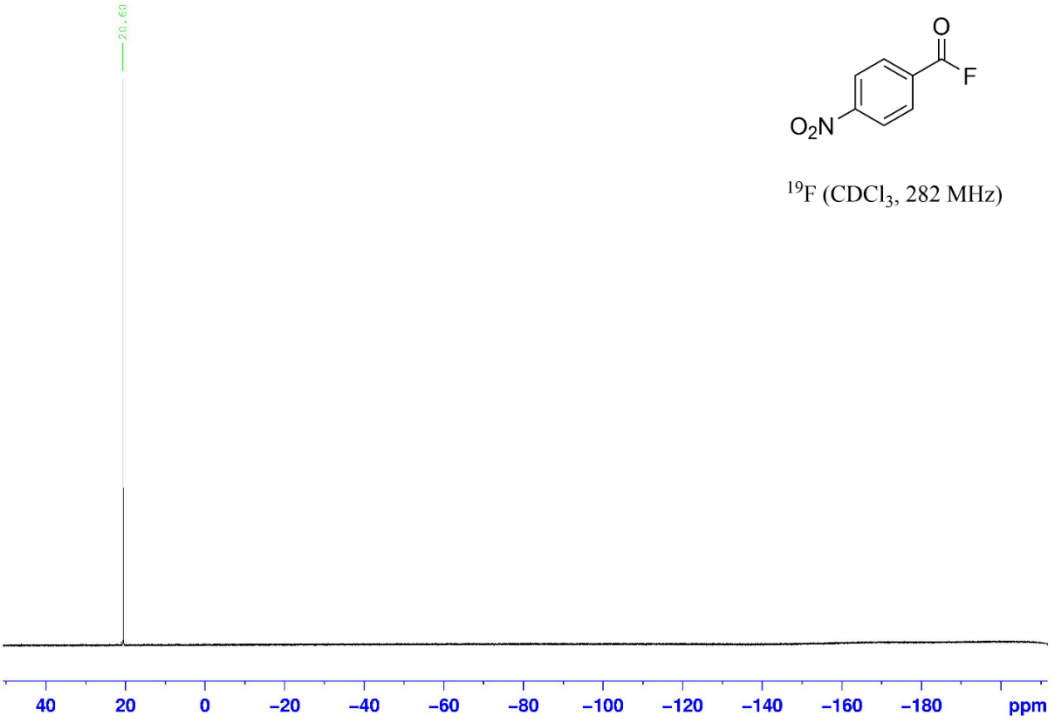

Figure S16. ^{19}F NMR spectrum of 4-nitrobenzoyl fluoride (**2b**).

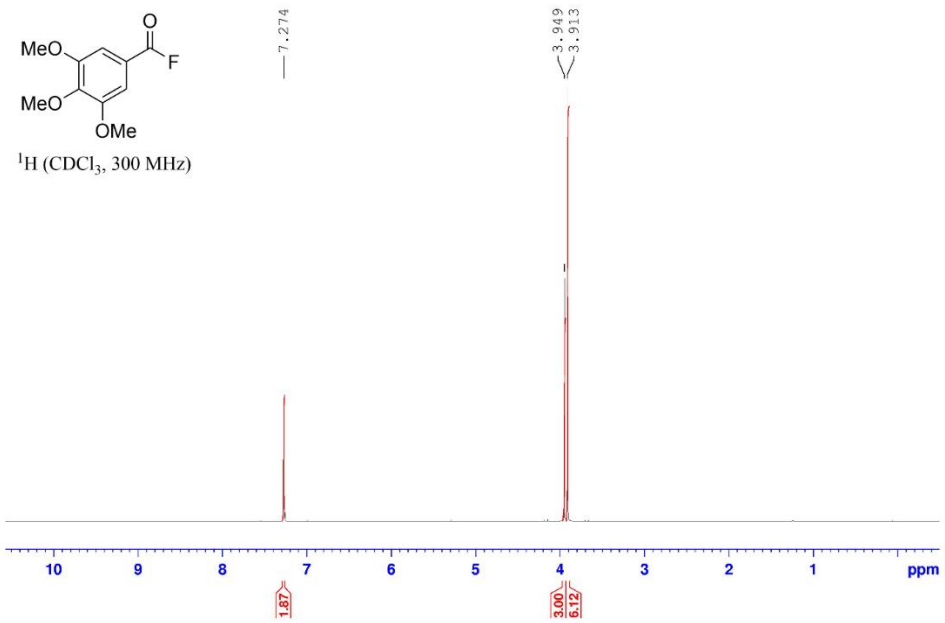

Figure S17. ^{1}H NMR spectrum of 3,4,5-tris(methoxy)benzoyl fluoride (**2k**).

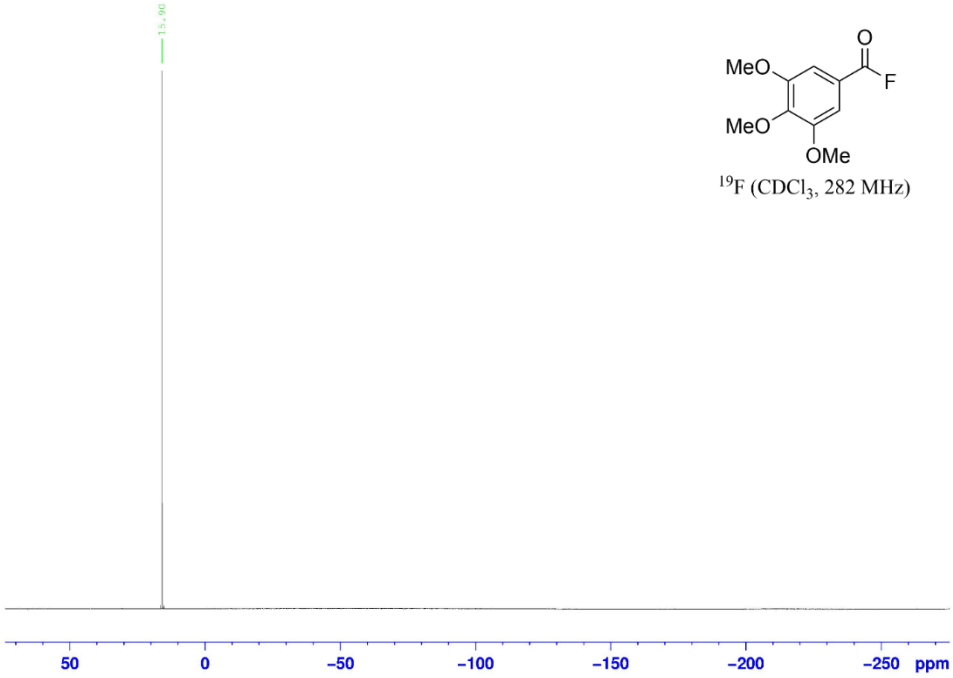

Figure S18. ^{19}F NMR spectrum of 3,4,5-tris(methoxy)benzoyl fluoride (**2k**).

III. Crude ^{19}F NMR Spectra of Acyl Fluorides

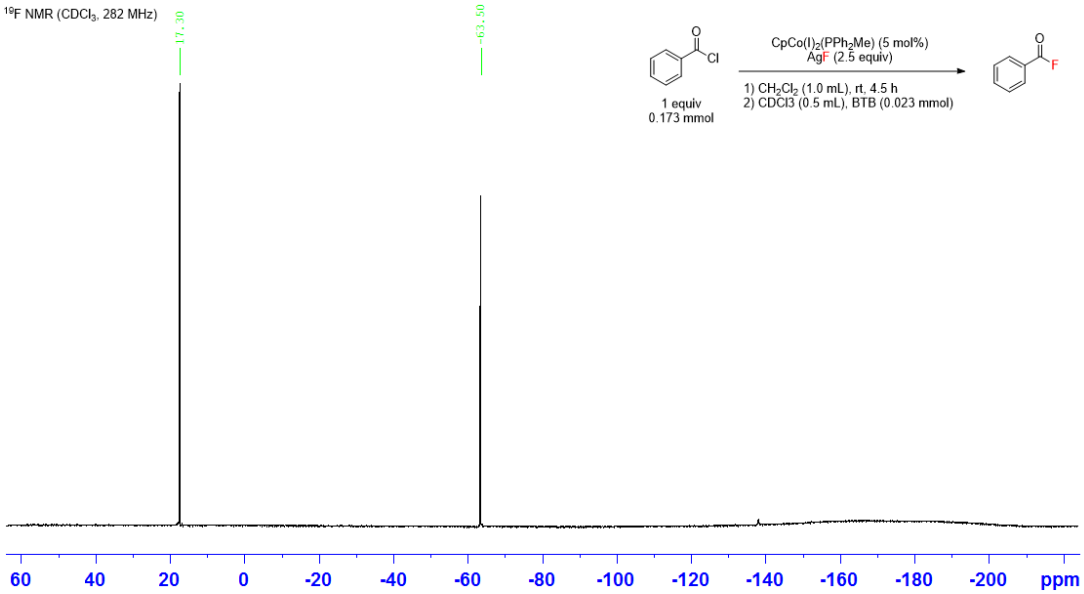

Figure S19. Crude ^{19}F NMR spectrum of **2a**.

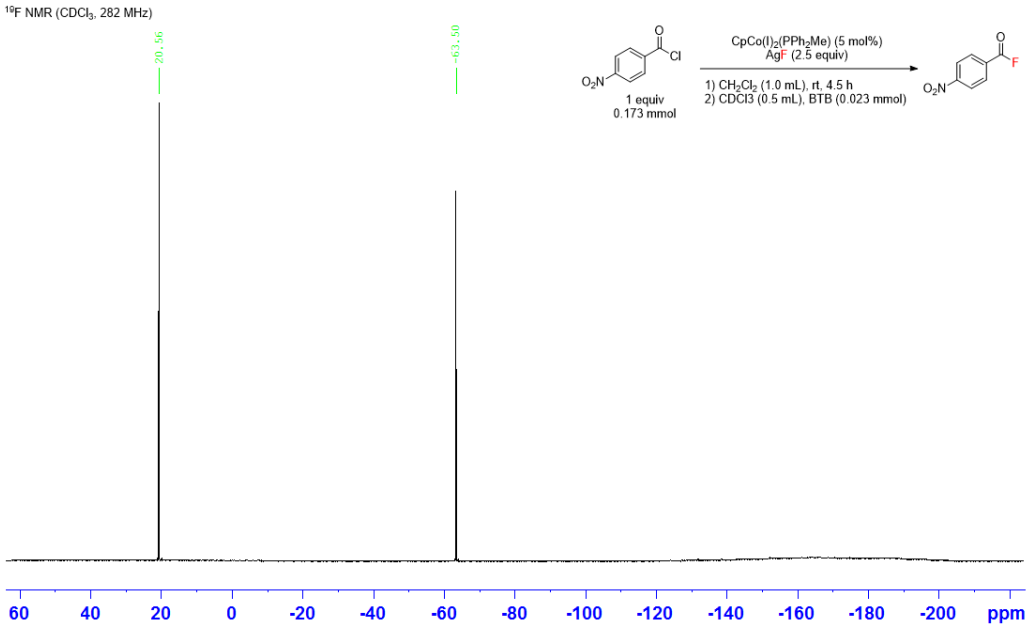

Figure S20. Crude ^{19}F NMR spectrum of **2b**.

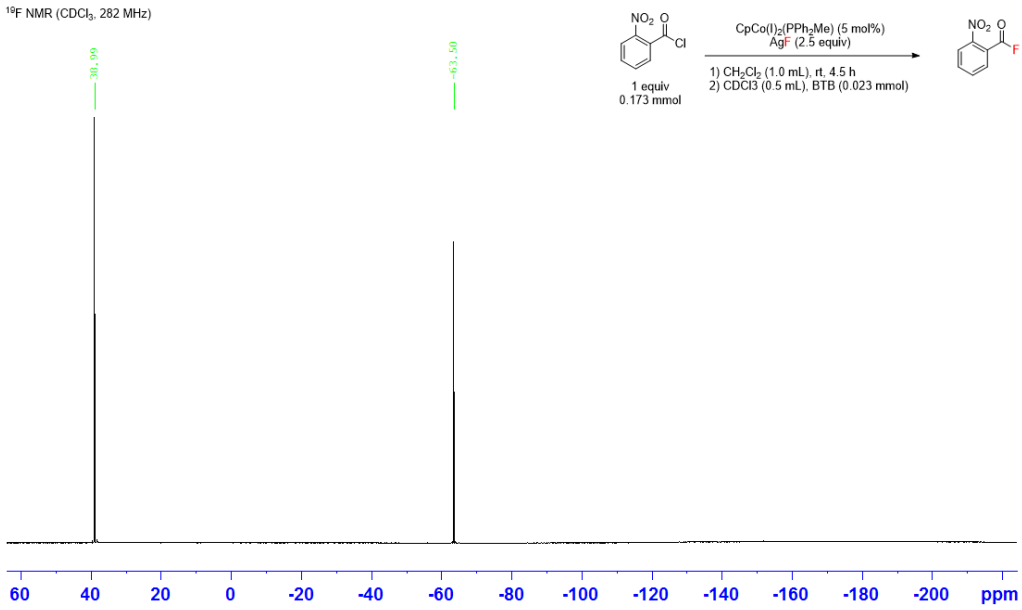

Figure S21. Crude ^{19}F NMR spectrum of **2c**.

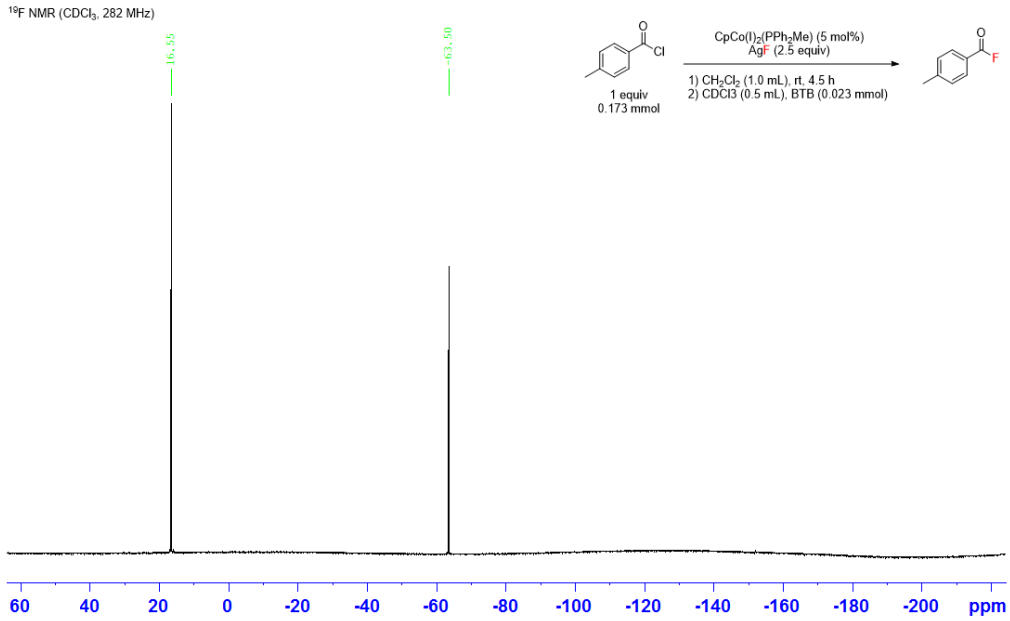

Figure S22. Crude ^{19}F NMR spectrum of **2d**.

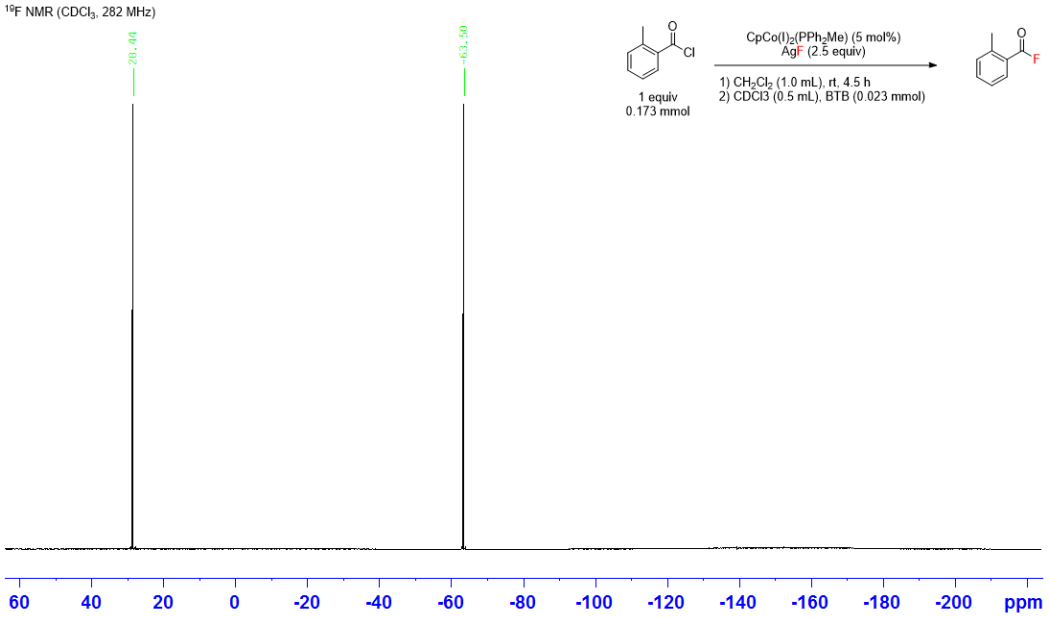

Figure S23. Crude ^{19}F NMR spectrum of **2e**.

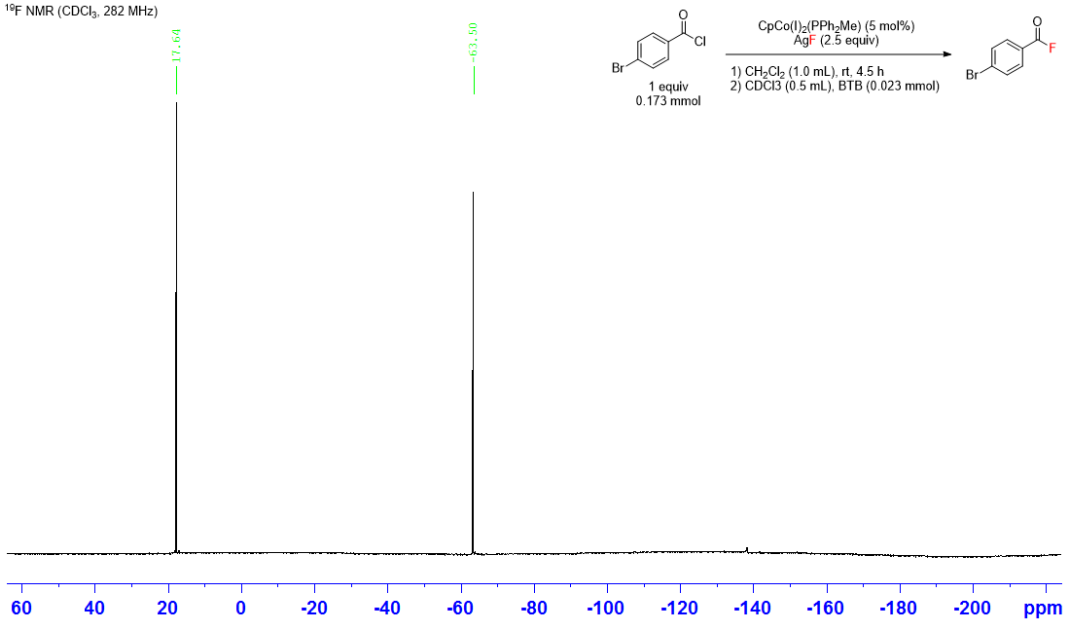

Figure S24. Crude ^{19}F NMR spectrum of **2f**.

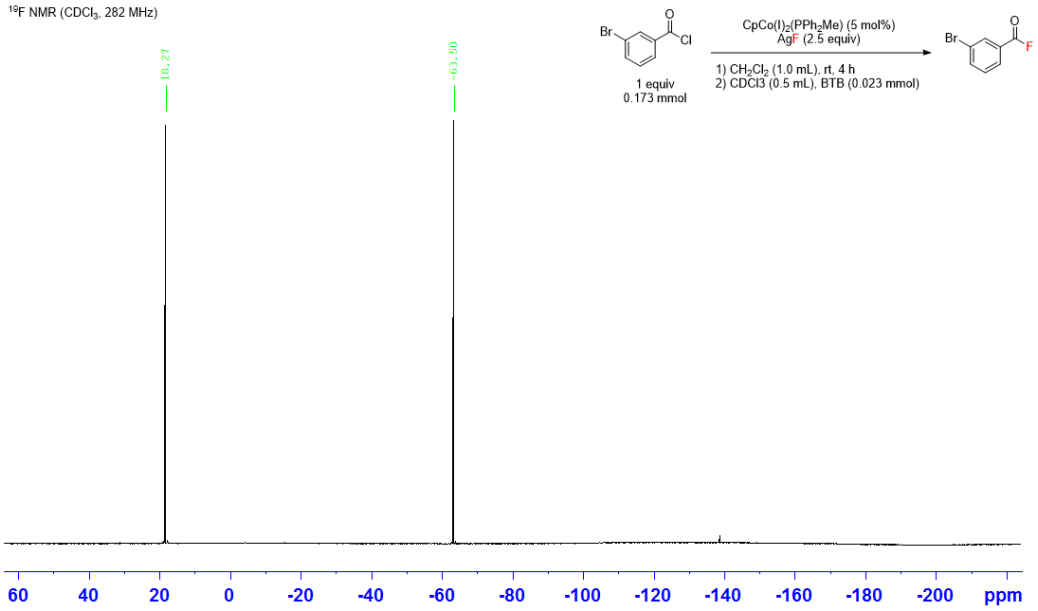

Figure S25. Crude ^{19}F NMR spectrum of **2g**.

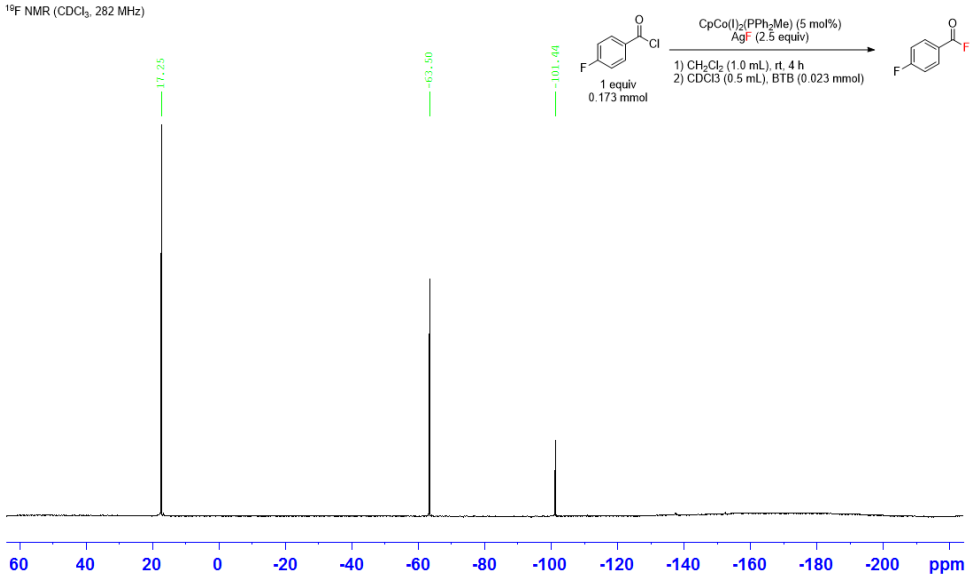

Figure S29. Crude ^{19}F NMR spectrum of **2h**.

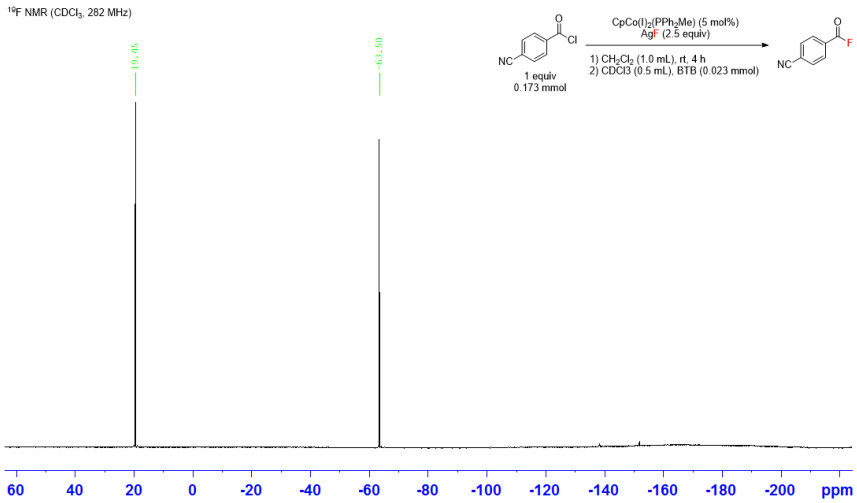

Figure S30. Crude ^{19}F NMR spectrum of **2i**.

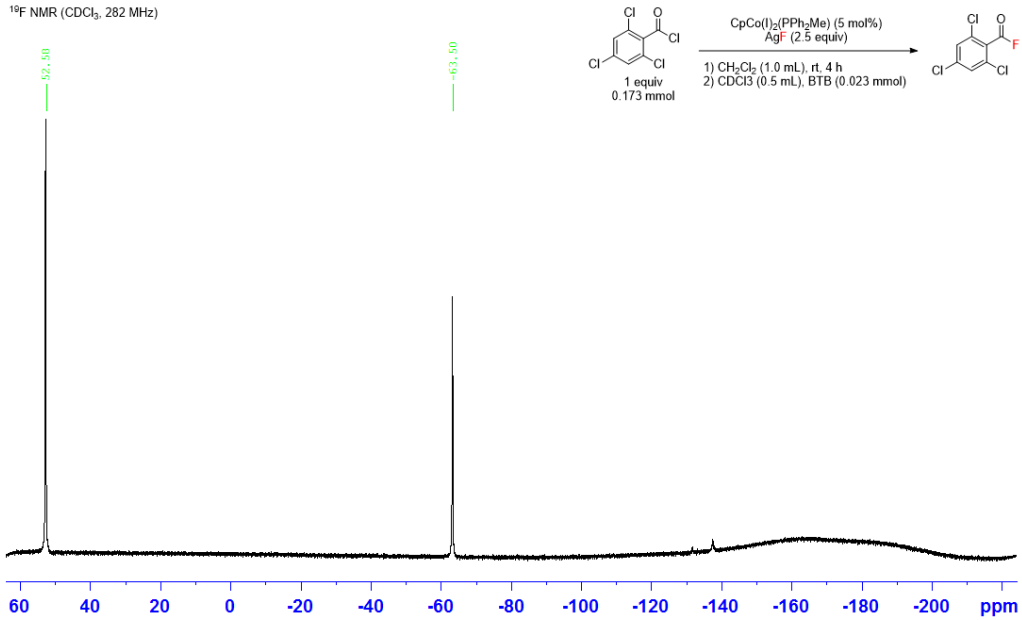

Figure S26. Crude ^{19}F NMR spectrum of **2j**.

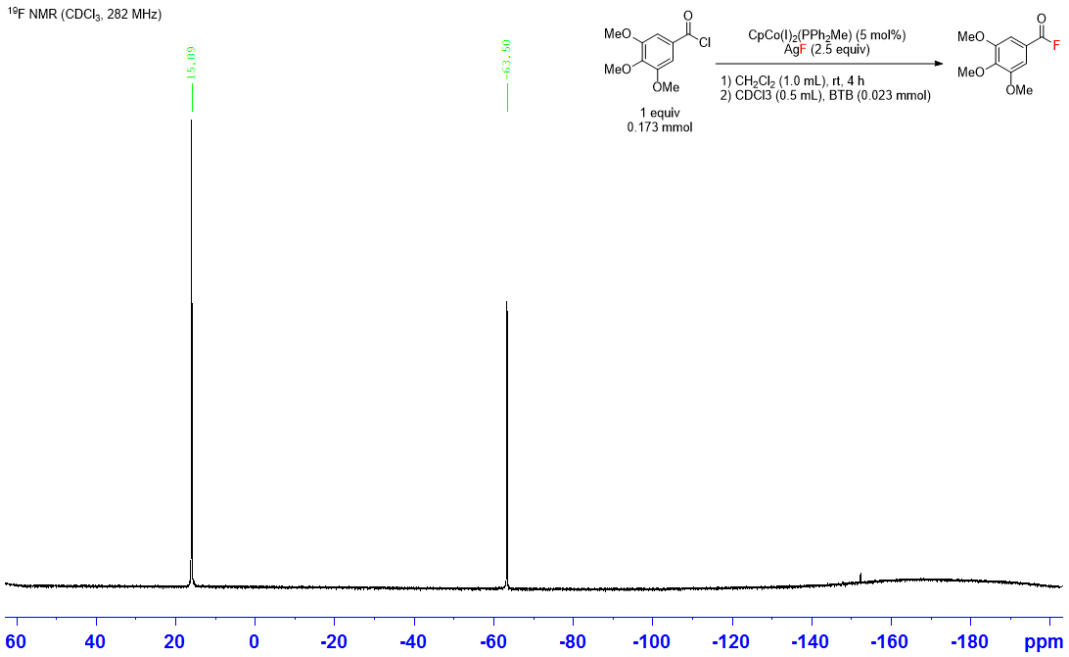

Figure S31. Crude ^{19}F NMR spectrum of **2k**.

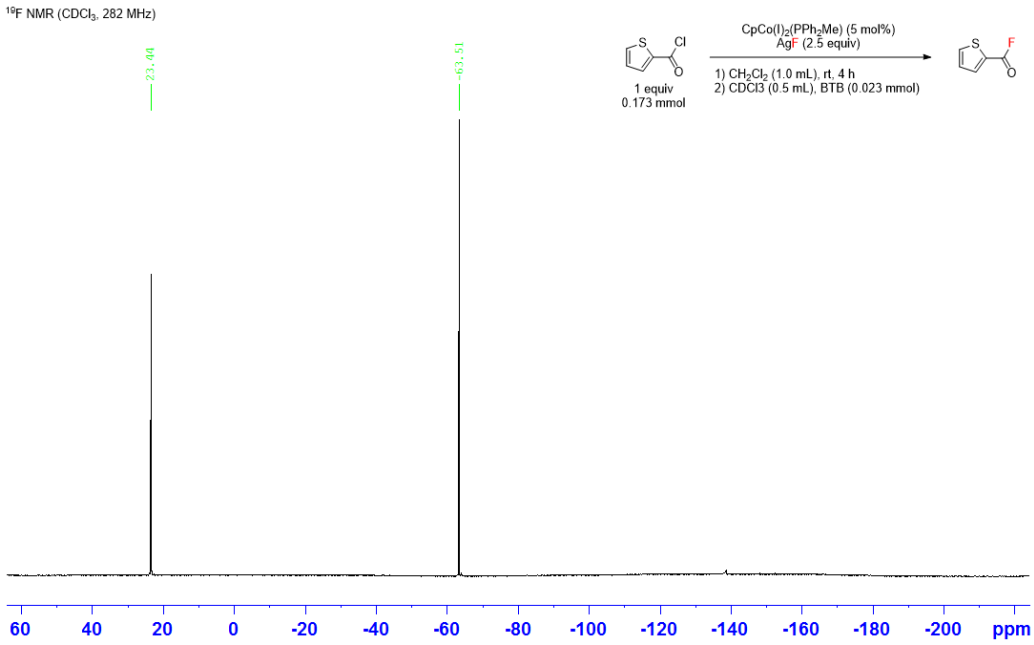

Figure S27. Crude ^{19}F NMR spectrum of **2l**.

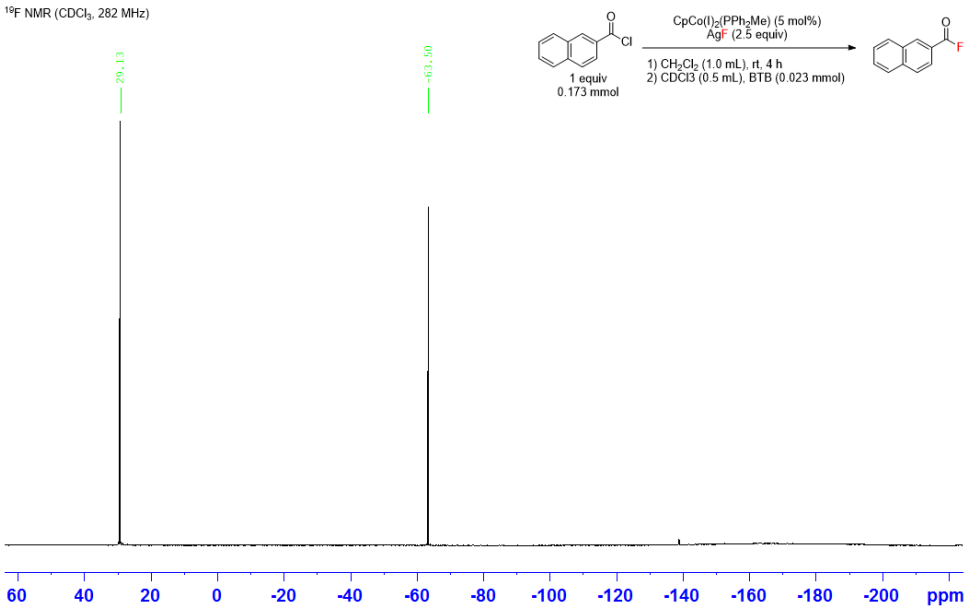

Figure S28. Crude ^{19}F NMR spectrum of **2m**.

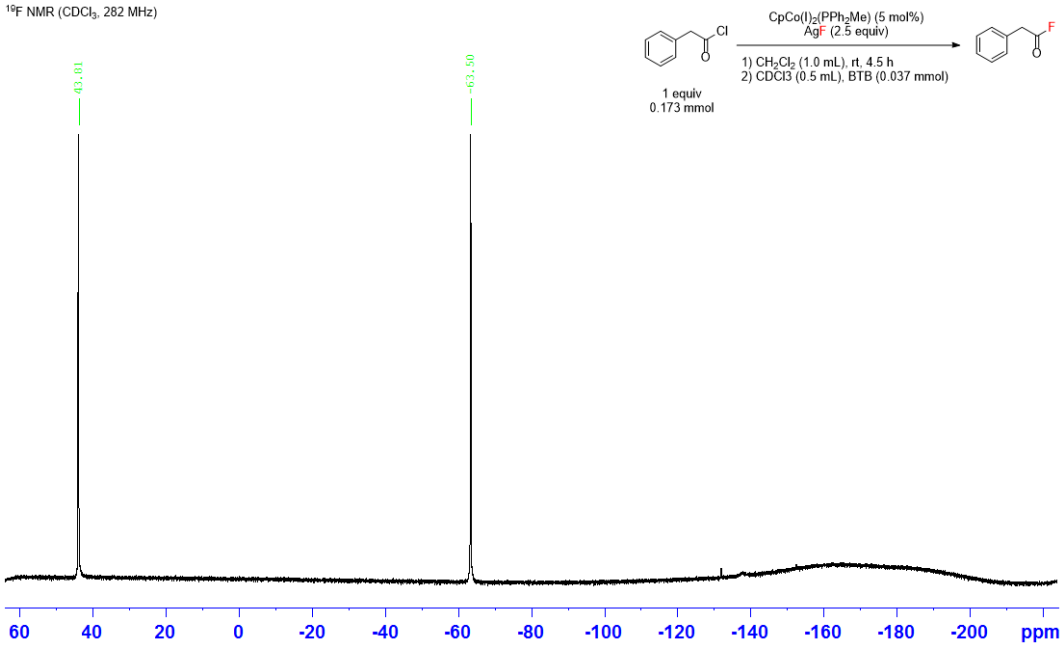

Figure S32. Crude ^{19}F NMR spectrum of **2n**.